# Final Report

## Autonomous Space Traffic Management

AE3200 Design Synthesis

DSE Group 06

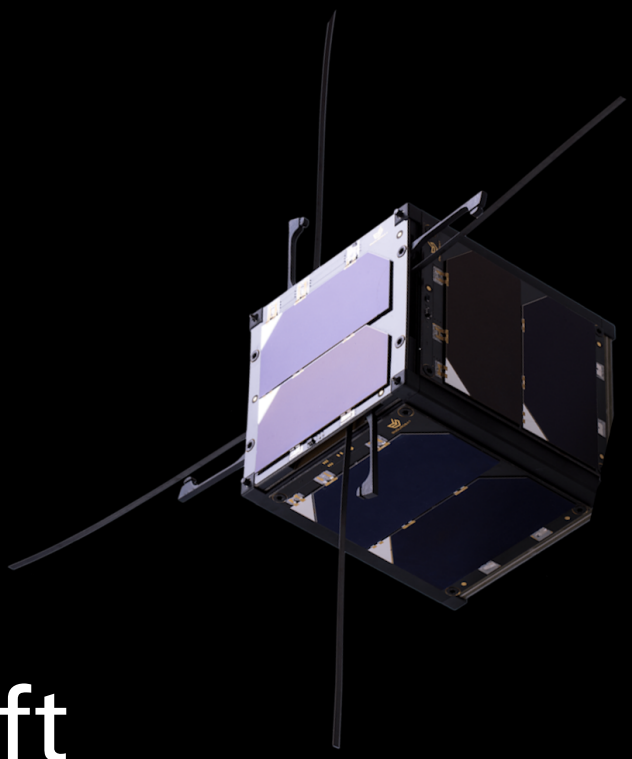

Delft University of Technology

TU Delft

# Final Report

## Autonomous Space Traffic Management

by

## DSE Group 06


| Student Names | Student Nr |
|---|---|
| Wout Barrez | 5533678 |
| Maximilian Hübner | 5447984 |
| Tjalling Huson | 5109698 |
| Sabin Ilegitim | 5734037 |
| Yann Tapiero | 5681383 |
| Robbe Truyts | 5224551 |
| Efe Uğurlu | 5810728 |
| Cas van Mierlo | 4351495 |
| Richard Xu | 5109442 |
| Serdar Yazıcı | 5688612 |



| | |
|---|---|
| Principal Tutor: | E. Gill |
| Coaches: | K. Mesman |
| | V. Pallichadath |
| Project Duration: | 04, 2025 - 06, 2025 |
| Faculty: | Faculty of Aerospace Engineering, TU Delft |

| | |
|---|---|
| Cover: | 1U CubeSat Platform By: EnduroSat |
| Style: | TU Delft Report Style |


TU Delft

# Executive Summary

This chapter presents an executive overview of the final report for the Bachelor of Aerospace Engineering end project, the Design Synthesis Exercise. The project is performed by 10 students in 10 weeks time.

## Introduction and Motivation

The near-Earth space environment is getting more and more crowded, and this growth in satellite numbers is not expected to slow down. Forecasts report an average of over 3700 satellites to be launched annually [1]. Due to this ever-increasing number of objects in Low-Earth Orbit (LEO), there is a need to improve the accuracy of the positional estimates of spacecraft to better predict close approaches and avoid collisions between operational spacecraft and space debris alike. However, current technologies do not allow global Space Situational Awareness (SSA). This report concerns the design of a small, lightweight, power-efficient and low-cost standardized payload for space traffic management based on a snapshot Global Navigation Satellite System (GNSS) receiver. This standardized payload could then be easily integrated in virtually any LEO spacecraft and provide accurate position fixes for it. This gathered position data would then also enable the improvement of upper atmospheric density models, increasing the precision of LEO object orbit propagation and supporting SSA. From this the team developed the following mission statement:

> *"Design a standardized payload for space traffic management, based on a snapshot GNSS receiver, and an associated technology demonstration mission and satellite to validate this payload."*

The Autonomous Space Traffic Management (ASTM) would achieve its autonomy due to the independence of ground stations after initialization of the receiver.

Within the design synthesis exercise, the group acted as a research/design group or student team at the faculty, rather than as a group of engineers at a company or startup. This proved important in many aspects of the mission architecture such as the logistics, operations and budgeting.

At the core of the standardized payload is a snapshot GNSS receiver, capable of acquiring position data through millisecond-scale signal captures of GNSS signals. This mode of operation enables intermittent, ultra-low power consumption, making it suitable even for power-constrained platforms such as CubeSats or PocketQubes. To initialize the snapshot processing, a standard GNSS receiver with a band processor is also added as part of the standardized payload. This allows for minimal power consumption whilst remaining it to self initialize. The implementation of this technology for in-orbit applications is a novel approach.

To validate the functionality and performance of the Standardized Payload (SP) in orbit, a dedicated technology demonstration mission is proposed. This mission will host the SP on a compact satellite platform, designed to verify the viability of this technology. The demonstration satellite will operate in orbit for 6 to 12 months, collecting and downlinking position fixes generated onboard. These position solutions will be independently validated using other satellite tracking technologies, such as Doppler ranging, Satellite Laser Ranging (SLR) and conventional GNSS receivers. The mission is to be realized under a strict cost cap of €10 million and a total mass below 10 kg, launched piggyback. In compliance with space debris mitigation guidelines, the satellite will be designed to de-orbit within five years of orbit injection epoch, ensuring responsible operations throughout the mission lifecycle.

## Design Foundations

The market analysis and regulations and policies investigation lead to requirements, these then form the foundation for the design.

### Market Analysis

The current standard for globally tracking LEO objects larger than ~10 cm are the Two-Line Element (TLE) sets provided by North American Aerospace Defense Command (NORAD). With an accuracy of ~1 km [2], the position predictions these TLE enable through orbital propagation are too inaccurate to reliably monitor close approaches and potential collisions. Traditional ground-based radiometric ranging and Doppler measurements provide an accuracy of ~10 m [3], but are limited to specific tracking arcs, and they can only simultaneously track a few satellites. SLR has an accuracy in the order of only centimeters [4], but in addition to a direct line-of-sight, this technique requires retroreflector arrays to be fitted to the satellite. Another well-established

technique is spaceborne tracking through the use of onboard GNSS receivers, but these systems are specifically designed and produced for space applications, typically making them relatively large, heavy, expensive (~€10 k to 20 k[(1)(2)]), and power-hungry.

A small (~36 mm × 44 mm × 6 mm), lightweight (~32 g), power-efficient (~0.85 mW), and inexpensive (€250) standardized snapshot GNSS receiver payload could fill this gap by providing position measurements accurate to ~20 m [5] at much more appealing Size, Weight, Power and Cost (SWaP-C) values.

Furthermore, the accuracy of position prediction is limited by current upper atmospheric density models, so there is a need to improve these models. As a standardized module, the SP fits on any satellite. Furthermore, by designing the standardized payload such that it is the smallest, most lightweight, most power-efficient, and least expensive spacecraft-tracking module on the market, it becomes desirable to include on any mission. The gathered positional data of the many satellites would then enable the improvement of upper atmospheric density models, increasing the precision of LEO object orbit propagation and enabling Space Situational Awareness. In the future, once virtually every LEO satellite is equipped with the standardized payload and the authorities have regulated the rules-of-the-road for space, a distributed autonomous infrastructure for space traffic management could remove the need for human involvement in avoiding spacecraft collisions, enabling true autonomous space traffic management and thereby ensuring the LEO environment as well as its critical infrastructure remains sustainable and available.

The key stakeholders identified in the stakeholder analysis are:

- **TU Delft College van Bestuur:** As the project group will be acting as a research and design group within TU Delft, they are a key stakeholder. The standardized payload and technical demonstration satellite are developed under the sponsorship of the university. Therefore, the university is the "customer."
- **Scientific Community:** Scientists across the globe may be interested in the raw data the standardized payload generates on the demonstration satellite as well as on future satellites it may be integrated on. This data should be easily accessible such that scientists can use it to perform their research, for example, on upper atmospheric density modeling.
- **Royal Netherlands Air Force:** This is a stakeholder interested in aiding and advising in the development of the standardized payload and potentially using snapshot GNSS receiver technology on their satellites in the future.
- **Spacecraft Developers:** Spacecraft operators may want or even need to integrate a standardized snapshot GNSS receiver payload into their spacecraft for power-efficient, inexpensive position tracking. They would have to reserve space within the spacecraft as well as allocate a certain power and downlink budget to allow the payload to function.

## Regulations and Policies Investigation

The regulatory landscape governing the use of satellite payloads with GNSS receivers is shaped by international, regional, and national space laws. These laws impose legal and technical constraints that influence the design, deployment, and operation of such systems, ensuring compliance with both current and emerging regulations.

At the international level, GNSS receiver regulations are heavily influenced by export control laws. In the United States of America (USA), the International Traffic in Arms Regulations (ITAR) Regulations and the USA Munitions List govern the export and use of satellite navigation equipment with military capability. The possible consequence is the receiver being switched off without notice during operations. Export restrictions also apply to certain European GNSS technologies under European Union (EU) Regulation and the Wassenaar Arrangement [6, 7]. Access to certain GNSS signals, such as Galileo's Public Regulated Service (PRS), is also restricted. For spacecraft radio frequency usage, telecommunications regulations involve strict coordination of frequencies and orbital slots via national spectrum regulators and the International Telecommunication Union (ITU).

At the regional level, the EU is progressing toward a unified regulatory framework. The upcoming EU Space Act aims to set mandatory standards for satellite sustainability and collision avoidance, shifting away from previously voluntary guidelines. The current voluntary guidelines are influential, like the space debris and collision mitigation policies that are guided by frameworks such as the United Nation (UN) Committee on

[(1)]GNSS Receiver Module, Pumpkinspace, 2025. [Online]. Date of Last Access (DoLA): May 7, 2025. Available: https://www.pumpkinspace.com/store/p58/GNSS_Receiver_Module_%28GPSRM_1%29_Kit.html

[(2)]Onboard Computer with GNSS, Endurosat, 2025. [Online]. DoLA: May 7, 2025. Available: https://www.endurosat.com/products/onboard-computer-with-gnss

the Peaceful Uses of Outer Space (COPUOS) Long-Term Sustainability (LTS) Guidelines, the International Standardization Organization (ISO) 24113 standard, and European Space Administration (ESA)'s internal mitigation requirements. These focus on spacecraft passivation, collision avoidance, and post mission de-orbiting , especially for LEO missions.

Nationally, EU member states implement these international agreements through domestic laws. In the Netherlands, the Dutch Space Activities Act mandates licensing through the Nederlands Space Office (NSO), aligning national oversight with international obligations. For example, the Rijksinspectie Digitale Infrastructuur (RDI) manages the coordination for missions operating varying radio frequency bands. Launch regulations impose liability on launching states per the 1972 Liability Convention. If launch occurs outside the EU, for New Zealand, operators must comply to the Outer Space and High-Altitude Activities Act.

Looking ahead, the standardization of GNSS based space payloads akin to maritime Automatic Identification System (AIS) faces both technical and legal hurdles. Implementing a mandatory GNSS snapshot payload will require: International consensus via COPUOS and International Committee on Global Navigation Satellite Systems (ICG), technical specification development through ISO and Consultative Committee for Space Data Systems (CCSDS), licensing law amendments by national regulators like the Federal Communications Commission (FCC) and Federal Aviation Administration (FAA) and ESA. Only after endorsement, standardization, and legal adaptation will payload integration into launch and satellite systems become enforceable. This long and complex process is worthwhile due to the growing momentum for universal space traffic management and safety compliance.

## Requirements

The determination of the requirements for the project follows a structured top-down approach. First, a subset of stakeholder requirements were obtained from the stakeholder analysis. Then, from the system requirements the driving and key requirements were determined.

### Driving & Key Requirements

From the full list of system requirements listed in Table 2.4, the driving (⚠) and key (🔑) requirements were identified. The driving requirements dominate the overall design and strongly affect system performance, cost, risk, and/or schedule [8]. They directly shape engineering trade-offs and design decisions. Whereas the key requirements are of primary importance to the customer and represent known/expected risk items. They ensure alignment with mission goals and compliance expectations [8]. The following requirements were identified as the driving and key requirements:

**Table 1:** Driving and Key Requirements

| ID | Driving/Key | Requirement |
|---|---|---|
| | | **Standardized Payload (SP)** |
| **STM-SYS-SP-1** | ⚠ \| 🔑 | The SP shall have a mass of at most 0.1 kg. |
| **STM-SYS-SP-2** | ⚠ \| 🔑 | The SP shall have a power consumption below 100 mW. |
| **STM-SYS-SP-3** | ⚠ \| 🔑 | The SP shall have a volume envelope of at most 5 cm × 5 cm × 1 cm. |
| **STM-SYS-SP-5** | ⚠ | The SP shall comply with PC104 and PQ60 integration standards. |
| **STM-SYS-SP-8** | 🔑 | The SP shall provide position fixes with an accuracy of 20 meters (3D r.m.s.). |
| **STM-SYS-SP-10** | ⚠ \| 🔑 | The SP shall have a maximum manufacturing cost of at most 10 k€. |
| **STM-SYS-SP-11** | ⚠ | The SP shall be able to operate in orbit for at least 5 years. |
| | | **Demonstration Spacecraft (S/C)** |
| **STM-SYS-SC-5** | ⚠ | The S/C shall have a mass of at most 10 kg. |
| **STM-SYS-SC-8** | ⚠ | The S/C shall be able to transmit all the on-board generated data to the ground station. |
| | | **Technology Demonstration Mission** |
| **STM-SYS-M-1** | ⚠ \| 🔑 | The S/C shall be inserted into a LEO with an altitude between 300 km and 800 km. |
| **STM-SYS-M-3** | ⚠ | The S/C shall deorbit within 5 years after EOL. |
| **STM-SYS-M-4** | ⚠ \| 🔑 | The accuracy of the SP stated in STM-SYS-SP-8 shall be validated in orbit. |
| **STM-SYS-M-6** | ⚠ \| 🔑 | The S/C shall remain operational for at least 6 months. |
| **STM-SYS-M-8** | ⚠ \| 🔑 | The Technology Demonstration Mission shall cost no more than 10 M€. |

# Mission Architecture

The main mission of the project is to design a standardized payload for space traffic management. Then, to demonstrate this payload and validate its performance a technology demonstration satellite carrying the payload must be launched to LEO.

## Logistical and Operational Overview

The logistics and operational overview of the mission is divided into three main blocks: Qualification and Production, Launch, and Mission Operations, each adapted from standard industry definitions but tailored to the specific logistical requirements of the satellite project.

During the Qualification and Production block, the focus is on validating the spacecraft and payload. Most components are commercial off-the-shelf and only require performance verification, but custom parts like the payload require more rigorous testing. While some tests can be performed at TU Delft others must be outsourced to specialized facilities. Industry standards, notably from Ariane 6, were used as reference to determine acceptance testing needs, as there were none mentioned by Rocket Lab. Cleanroom handling and contamination control are essential, particularly for ride-share missions. Once qualified, the spacecraft is shipped to the nearest Rocket Lab processing facility.

In the Launch phase, the satellite leaves the production facility about 30 days prior to launch, transported in a specialized container alongside the integration team. Final verifications, software uploads, and battery charging are conducted on site. Integration with the launch vehicle occurs about two weeks before launch, after which the spacecraft becomes physically inaccessible. Following launch, Rocket Lab provides the CubeSat's state vector within 90 minutes. A radio silence period of at least 30 minutes is maintained before the satellite begins emitting signals.

The Mission Operations phase begins with satellite separation and automatic entry into Boot Up Mode. After confirming safe separation, the satellite deploys its antenna and aligns passively with Earth's magnetic field. Communication is then established with a primary ground station located at TU Delft. Given the mission's simplicity, operations can be run from a basic laptop without a dedicated control center. The spacecraft cycles between idle, communications, and software update modes as it transmits data and receives new instructions. In case of anomalies, it switches to safe mode via an onboard watchdog system. Once mission objectives are completed, the spacecraft transitions to End of Life Mode, during which it continues to be monitored until atmospheric drag causes natural deorbiting.

Throughout these phases, operational and logistical implications tied to specific system and stakeholder requirements, such as secure data transfer, power constraints, ground communication access, and legal compliance are managed with reference to established engineering handbooks and standards.

## Mission Orbit and Launch

To design the spacecraft (S/C), the orbit has to determined first. This is due to the fact that multiple subsystems depend on it. For example, the sizing of the solar arrays and strength of the transmitters depend on the orbital altitude. The orbit is mainly governed by requirement **STM-SYS-M-3**, which states that the S/C shall de-orbit within five years after its injection into orbit and is based on the ESA Space Debris Mitigation Requirement. Thus, an altitude must be chosen that ensures an orbital lifetime of less than five years without using de-orbit devices as the size constraints of the S/C can not accommodate these devices.

After a simulation was ran using General Mission Analysis Tool (GMAT), a high fidelity orbital simulation modeling software created by National Aeronautics and Space Administration (NASA), an altitude of 500 km was found to be suitable and, is a common altitude such that an available piggy-back mission can be reliably found. Piggy-back launch indicates that the S/C will not be the primary payload and will be launched along side other satellites. Using this approach, the costs are expected to be €80,000.[(1)]

After the orbital altitude was chosen, the orbital inclination is determined. It was assumed that the eccentricity is zero i.e. the orbit is perfectly circular. The chosen launch provider ensures an orbit injection accuracy of 15 km thus it is deemed justified[9]. The orbital inclination was chosen as to optimize the contact time between the ground station and the S/C. The ground station is the TU Delft, since the mission is performed by a student team at the TU Delft and the needed infrastructure is already available on the top of the Electrical Engineering, Math and Computer Science (EEMCS) building. With the minimum elevation angle taken as 10° as a conservative value, GMAT was run again to simulate the amount of contacts and duration of said contacts between the ground station and satellite. It was found that an inclination of 60° is optimal and will result in around 20 hours of contact in $\sim$ 185 visitations in a month, or about 40 minutes each day. This will most likely be even more since the communication systems at the TU Delft have a clear line of sight and are located on a high-rise building with no other skyscrapers nearby.

With the orbit is determined, other parameters can be derived. Mainly, the eclipse duration since this is of great importance when sizing the battery. However, this varies over time due to the drift of the Right Ascension of

[(1)] CubeSat Tables, Nanosats, 03/04/25, [Online]. DoLA: 18 June, 2025. Available: https://www.nanosats.eu/tables#launch-providers

the Ascending Node (RAAN) caused by the oblateness of the Earth. The eclipse varies from being exposed to the sun for the full orbit to a maximum eclipse fraction of 37.79 %.

All used mission parameters can now be derived from these values and are listed in the Table 2

**Table 2:** Mission parameters.

| Parameter | Symbol | Value | Unit |
|---|---|---|---|
| Altitude | $h$ | 500 | km |
| Inclination | $i$ | 60 | ° |
| Initial Right Ascension of the Ascending Node (RAAN) | Ω | −180 | ° |
| Eccentricity | $e$ | ~ 0 | - |
| Initial ecliptic true solar longitude | Γ | 0 | ° |
| Orbital period | T | 5668 | s |
| Average time between passes | $\Delta t_{avg}$ | 14 022 | s |
| Orbital velocity | v | 7.61 | $\mathrm{km\,s^{-1}}$ |

A launch broker tailored to the missions needs was then found. Multiple promising options presented themselves but the chosen one is Rocket Lab due to the low cost and Rocket Lab already having performed multiple launches with similar characteristics. It must be said that due to the ride-share construction used, it is advised to inquire other launch brokers aside from Rocket Lab to increase the chance of an optimal launch date.

Rocket Lab was chosen as it had already targeted altitudes around 500 km multiple time and has low launch costs. The launch vehicle used is the Electron rocket and it launches from the Rocket Lab Launch Complex 1 in the Mahia Peninsula in New Zealand.

# Standardized Payload Design

The SP is a compact, low-mass, ultra-low-power GNSS add-on designed to broadcast precise position fixes from any LEO satellite. A key aspect of the design process is to make this payload a 'plug-and-play' module, putting standardization at the forefront of design choices. Seven commonly used intra-satellite communication protocols on satellites were identified and implemented.

The SP is fully designed and production-ready: every detail, resistor and capacitor values, PCB trace widths, component placement, and stack-up, has been defined and the board layout has been verified. Production requirements have been factored in, and a complete bill of materials down to the smallest passives is provided for one unit, showing a parts cost of €250. The subsequent phase would then consist of the fabrication.

Additionally, easy mechanical adaptation into PocketQubes, CubeSats, and larger satellites has been implemented by adding adapter Printed Circuit Board (PCB)s and standard connectors. In order to accommodate for these needs, a dual receiver configuration with the following hardware is used: a lightweight small GNSS antenna, an Radio Frequency (RF) switch, a GNSS receiver module acting as an Ephemerides Acquisition Receiver (EAR), a snapshot GNSS, an Microcontroller Unit (MCU), a non-volatile memory unit, a power management unit and a PCB. Additionally, the payload is enclosed in an aluminum envelope which leads to the final dimension of 4 mm × 36 mm × 6 mm and a total mass of **33 g**. This includes 2 GNSS antennas on the exterior of the satellite which have an area of 15 mm × 10 mm. Snapshot duration is 20 ms with an average of **0.94 mW** and a peak power consumption of 77 mW.

# Technology Demonstration Satellite Subsystem Design

The S/C consists of the SP, Validation Payload (VP), and the subsystems. In the previous part, the detailed design of the SP was discussed as it is the primary payload. In this part, the secondary payload, the VP, and the rest of the subsystems are designed. For each system, the detailed design approach, part selection, and final budgets are presented.

## Validation Payload

Now that the SP has been designed, a way to validate it is considered through the VP. After performing a trade-off, two suitable options presented themselves. The first is a conventional GNSS receiver, which works by constantly listening to the GNSS constellations in Medium Earth Orbit, and the second is the use of SLR.

The primary option that will be included in the design is that of a conventional CubeSat GNSS receiver, the Celeste GNSS of SpaceManic. Using a GNSS receiver it is possible to validate the SP for the entire orbit and see whether GNSS broadcast data is received and processed well. The chosen receiver has the least amount of power while still providing a sufficient accuracy of 2 m Circular Error Probable (CEP), which means that there

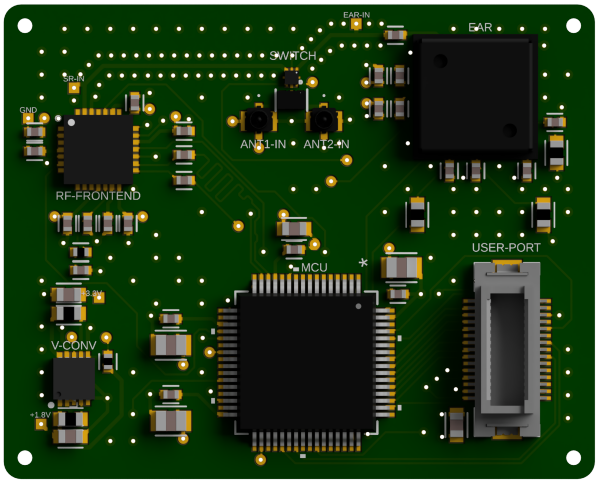


**Figure 1:** Main electronics board of SP.

is a 50 % chance that the satellite's position lies within a circle with a radius of 2 m. This radius is increased to 6 m to ensure a higher detection probability of 99.8 % to check if it would always ensure a higher accuracy than that of the SP. It will use the same antennas as the SP as this does not increase complexity and is a way to validate the antennas as well as check if the data of the GNSS constellations are correctly received.

The secondary option is using SLR. It works by emitting laser pulses to the S/C, which itself is fitted with retroreflectors. Retroreflectors are mirror like devices that reflect light back to a source with minimum scattering. Thus, the laser pulse is reflected back from the body-mounted retroreflectors and is detected by the ground station. Due to the highly stable laser, fast pulse rate, and the laser traveling at the speed of light, it is possible to determine the location of the S/C to centimeter-level accuracy. The TU Delft has SLR facilities present at the campus, however, it was determined that the infrastructure does not support a laser strong enough to close the link budget for this S/C. This is due to the retroreflectors being size constraint to only having a diameter of 12.7 mm. To increase detection chance and considering that the S/C will tumble, two retroreflectors are added on the ± X, Y sides and only one on the ± Z sides, due to space constraints. This does still not enable the closure of the link budget for TU Delft. Luckily, an International Laser Ranging Service (ILRS) exists with stations hosted globally. The closest promising ILRS stations identified that were able to close the link budget were those in Potsdam (Germany), Matera (Italy) and the TU Graz in Austria. A simulation was ran with GMAT to identify the average time per visitation of the S/C for each station. All three times are long enough to find the S/C and acquire enough data points for the ranging.

Summarizing, on board the S/C are two systems for validating the SP. One is the Celeste GNSS receiver, which consumes an average of **100 mW**, and the other are ten ∅12.7 mm retroreflectors for SLR. The whole system weighs, including margins, **84.8 g** and is estimated to cost **€10.2 k** for one S/C.

## Structural

Based on payload sizing, the technology demonstration satellite can be designed as a 1U CubeSat. Designing the satellite as a CubeSat [10] is the ideal way to efficiently come to a good standardized structural design that is certain to integrate with a deployer. The chosen CubeSat structure is the 1U CubeSat structure by EnduroSat[(1)]. This structure adheres to the CubeSat design specifications and uses Aluminum Alloy (AA)6061-T651 or AA6082-T6. This structure has a mass of **120 g** and costs **€1700**.

## Command and Data Handling

The Command and Data Handling (C&DH) subsystem comprises the On-Board Computer (OBC) and the communication link of the satellite to the ground station.

Preliminary design ruled out directional antennas operating in the low gain bands due to size incompatibility with a 1U LEO satellite. Given the mission's aim to demonstrate snapshot GNSS with minimal downlink, pointing and power constraints, an omni-directional UHF antenna was selected.

From the preliminary design concept, the finalized concept is derived. The selected C&DH architecture

[(1)]1U CubeSat Structure, EnduroSat, 2025. [Online]. DoLA: 10 June, 2025. Available: https://www.endurosat.com/products/1u-cubesat-structure/

includes a selection of Commercial off-the-shelf (COTS) components by ISISPACE, Spacemanic and Gomspace with flight heritage. The selected components are evaluated based on average power consumption, operating temperature range, peak power, SWaC: resulting in:

- Antenna: NanoCom ANT430 - a deployable, rigid, omni-directional antenna with circular polarization.
- Transceiver: NanoCom AX100 - a half duplex, UHF transceiver with Gaussian Minimum Shift Keying (GMSK) or Gaussian Frequency-Shift Keying (GFSK) modulation.
- On Board Computer: NanoMind A3200 - includes a 3-axis magnetometer, gyroscope, RTC, temperature sensor, and watchdog.
- Motherboard: NanoDock DMC-3 - support four daughterboards with Inter-Integrated Circuit (I2C) and Controller Area Network (CAN) communication interfaces.

For system architecture, the communication between the OBC and other subsystems will occur over an I2C bus in multi-master mode, as required by the NanoCom AX100 transceiver. For data downlink, GMSK modulation is selected due to its constant envelope, which is ideal for non-linear power amplifiers. The system implements CCSDS standards for encryption (SDLS), compression (POCKET+), and Forward Error Correction (FEC) using a convolutional and Reed-Solomon scheme. A Single Poly Dual Throw (SPDT) switch allows dual transceiver control of the antenna. A debug port (Molex PicoBlade 53261-0471 on the OBC) doubles as the Arming Plug port, activating the Electric Power System (EPS) post-separation.

The downlink performance of the C&DH with a total data rate of 298.5 bit/s of which 262.5 bit/s for housekeeping and 33.3 bit/s for Payload (PL) data. The Signal to Noise Ratio (SNR) is 11.37 dB for downlink and 28.65 dB for uplink, with link margin after applying GMSK being 5.03 dB for downlink and 22.30 dB for uplink. The margin remains larger than 3 dB at a distance of 2500 km with the Ground Station (GS) and orbit altitude of 500 km. The system budgets with 5 % margin for the C&DH subsystem are: mass: **169.05 g**, average power: **737 mW**, operating temperature **−30 °C** to **85 °C**, and a cost of **€43.5 k**.

## Attitude Determination and Control

The design of the Attitude Determination and Control System (ADCS) was driven by three main aspects: SP, C&DH, EPS needs and the mission design. All communication systems on the spacecraft as well as the electric power generation were designed such that they can work in all orientations. For this reason, an active attitude control system was deemed unnecessary. Nevertheless, external conditions such as disturbance torques or the deployment mechanism could cause cause high rotation rates that would reduce the performance of the C&DH antenna and the SP antenna. Because of these reasons, it is important to control the tumbling rate of the spacecraft. The most common way of achieving this is through a Passive Magnetic Attitude Control (PMAC) system. A passive control system requires no sensors to operate; nevertheless, the placement of the SP antennas means that broadcast words could be missed depending on the tumbling rate. In order to quantify the performance of the SP depending on the tumbling rate, a suite of attitude sensors was deemed to be necessary. The design process of these two sides of ADCS will now be summarized.

The PMAC system comprises two main parts. First, a permanent magnet needs to provide a control torque. This permanent magnet will interact with the Earth's magnetic field in order to provide a control torque that will align the spacecraft in the same manner a compass needle points north. A study was done to guarantee the that control torque would be 15 times larger than the worst case disturbance torques. To achieve this a COTS magnet was found which would provide the necessary control torque. The second part of the PMAC system are the hysteresis rods. These rods are made of a material with a low magnetic coercivity. As the spacecraft rotates, the Earth's magnetic field works to align the atomic dipoles inside the hysteresis rods. The energy required to align the atomic dipoles is dissipated as heat, thereby damping the motion. The design was inspired by other satellites such as Quetzal-1 [11], Colorado Student Space Weather Experiment (CSSWE) [12] and UNISAT-4 [13]. An empirical method was used to evaluate the performance of the system and it validated by comparing to data from CSSWE [12] and Quetzal-1 [11]. This analysis estimated that the spacecraft would reach a stable tumbling rate of 0.1 rad/s within 5 to 12 days.

Subsequently, the attitude determination system was designed. Since the control system is passive the attitude determination is not needed for control, nevertheless attitude measurements are important for evaluating the performance of the SP. For this reason, the simplicity of the system was considered the most important aspect. A suite of six sun sensors was chosen because of their flight heritage and reliability. During the eclipse period of the orbit, an attitude estimation can be done using a gyroscope. The gyroscope is only used for a maximum continuous time of ~30 min meaning the attitude error will remain below 1°. Additionally, the chosen OBC also includes a magnetometer, which can be used as a backup. The magnetometer was not chosen as the main mode of attitude determination due to possible interferences with the PMAC system, causing

errors and requiring careful calibration. These two systems combine to form the ADCS. ADCS has a mass of 25 g, an average power consumption of 60 mW and a cost of €12.3 k.

## Electrical Power

The EPS design followed a structured process. Fuel cells, rigid solar panels, and deployable solar panels were evaluated through a weighted trade-off analysis, with reliability, SWaP-C, sustainability, and impact on other subsystems as criteria. Rigid panels were selected for their simplicity and high reliability.

Triple-junction gallium-arsenide (TJ GaAs) solar cells and lithium-ion batteries were selected for preliminary design based on space heritage, their high power/energy densities, and specific power/energy. Peak power tracking was selected to size EPS based on average rather than peak power, reducing overall mass and volume. The power budget analysis showed that the EPS must deliver 0.98 W of average power during all mission phases (with system-level and subsystem-level margins), and a usable battery capacity of 1.08 W h was required to provide enough power in eclipse. A centralized EPS architecture was adopted to combine the Power Conditioning Unit (PCU), Power Distribution Unit (PDU), and battery into a single unit. This integrated approach, common in CubeSats and PocketQubes, minimizes harness complexity and saves mass and volume.

Based on the preliminary sizing, the selected components include the AAC Clyde Space Starbuck Nano-Pico Power Conditioning & Distribution Unit (PCDU) and the AAC Clyde Space PHOTON rigid solar panels. The Starbuck Nano-Pico PCDU was chosen for its compact design, integrated 10 Wh battery, and multiple regulated outputs [14]. The PHOTON solar panels were selected for their compatibility with the PCDU and their high Beginning-of-Life (BOL) efficiency [15]. To have a reliable architecture, solar arrays are mounted on all six S/C surfaces. The PCDU provides 3.3 V, 5 V, and 12 V power lines to the respective subsystems [14]. Harnessing was implemented using Spec44 cables and a Glenair Nano connector for testing and pre-launch charging [16, 17].

A sensitivity analysis demonstrated the robustness of the design. The EPS can support eclipse durations up to 330 min, eclipse fractions up to 51.9 %, average power demands up to 1.32 W, and mission durations up to 18 years. The final EPS configuration achieves a total mass of **379 g**, including the 5 % subsystem-level margin recommended for COTS components, and an estimated cost of **€20.9 k**.

## Thermal

The thermal subsystem design was primarily driven by a single requirement: all components must remain within their specified operating temperature ranges. To establish clear boundaries, these ranges were gathered from the selected COTS components and then translated into more specific and detailed thermal requirements. Compliance with these requirements will be verified through a thermal vacuum test performed on the fully assembled system.

Preliminary analyses identified the antenna and solar panels as critical components, particularly during eclipse phases. While solar panels can quickly recover upon re-exposure to sunlight, the antenna may be required to operate during the eclipse, making it a key focus of the thermal analysis. To improve the accuracy of the predictions, a multi-node thermal model was developed. In this model, each spacecraft component is represented as an individual thermal node, accounting for its interconnections, exposure to space, material properties, and environmental radiation sources. A total of 16 nodes were defined, each assigned realistic thermal characteristics, with particular attention to emissivity, absorptivity, and conductivity.

The spacecraft (S/C) was assumed to maintain a fixed orientation throughout the analysis. A worst-case scenario was identified, where one face of the S/C remained continuously shadowed, receiving no direct sunlight. The antenna was placed on this coldest face to assess whether it could survive the extreme conditions. If it could endure this case, it would also be capable of surviving a tumbling scenario, where heat input is more evenly distributed.

Simulation results showed that the internal subsystems would remain within a safe temperature range of approximately $-$**5.4 °C to 3.0 °C**, while the external subsystems experienced more significant variation, ranging from $-$**31.25 °C to 24.8 °C**. To account for modeling uncertainty and simplifications, a design margin of ± 8 °C was applied, as recommended by the European Cooperation for Space Standardization (ECSS). For the antenna, this resulted in approximately **2 °C** of margin between the simulated minimum temperature and the specified operational limit.

Thermal component selection was minimal, relying primarily on temperature sensors already embedded on the PCBs. No dedicated thermocouples were included for structural monitoring; instead, the thermal behavior of structural elements was inferred based on the performance of nearby components.

# Final Design of the Technology Demonstration Satellite

## Budgets

Table 3 summarizes the power, mass, and data rate budgets of the S/C, while the cost breakdown of the technology demonstration mission is highlighted in Table 4.

**Table 3:** Subsystem power, mass, and data rate budgets.

| Subsystem | Power [mW] | Mass [g] | Data Rate [bps] |
|---|---|---|---|
| SP | < 1 | 33 | 36.7 |
| VP | 110 | 85 | 36.7 |
| C&DH | 737 | 169 | 102.4 |
| ADCS[(1)] | 59 | 26 | 20.0 |
| Thermal[(2)] | 25 | 0 | 0 |
| Structures | 0 | 126 | 0 |
| EPS | 0 | 379 | 100.0 |
| *Margin* | 10% | 10% | 10% |
| **Total** | **982** | **900** | **325.4** |

**Table 4:** Cost breakdown of mission segments.

| Cost Segment | Cost [k€] |
|---|---|
| Travel Expenses | 8.2 |
| Launch | 82.5 |
| TT&C | *50.6 |
| ADCS | 5.8 |
| OBC | *36.4 |
| Structure | 3.4 |
| EPS | 41.8 |
| VP | *21.8 |
| SP | 0.4 |
| Integration | *1.0 |
| **Total** | **251.9** |

Values indicated by an asterisk, $*$, are estimates based on prices of similar products.

The average power requirement of the S/C is **982 mW**, its total mass is **900 g**, and its total data rate is **325.4 bit s$^{-1}$**. These values contain a 10 % system-level safety margin in addition to the subsystem-level margins imposed on the mass and power budgets. The total cost of the mission is estimated at **€251.9 k**, with the highest contributions from launch (€82.5 k). Labor, testing, integration, and ground segment costs are assumed to be zero due to institutional support from TU Delft. All component costs include necessary margins and **duplication** for both qualification and flight models.

## Technical Risk Assessment

Every scientific project that is planned to be realized needs to be assessed on possible risks. The risks were identified and labeled based on their probability of occurring and severity when occurring. For each of the risks a probability mitigation and severity mitigation plan was constructed to maximize the likelihood of not encountering them. For critical risks, a risk map was constructed to visualize how the mitigation plans reduce the severity and likelihood of the risk occurring. The principal project risk identified prior to mitigation is faulty testing equipment, which is addressed through regular maintenance and redundant test set-ups to ensure measurement accuracy. Furthermore, almost every subsystem has redundancy options integrated into it. For example, the validation payload consists of two separate systems, and the EPS has 28% more solar array area than needed.

## Sustainable Development Strategy

Designing with sustainability in mind for a space mission poses challenges compared to aircraft design. The main challenge is that there are two different environments to take into account: The earth environment, and the space environment.

For the Earth environment, the identified driving parameters are pollution of the atmosphere, natural resource usage, material toxicity, manufacturing energy usage, and human sustainability. For the space environment, the identified driving parameters are space debris, RF congestion, and RF pollution. The last two parameters have to do with the increasing congestion in the RF bands. Similarly to the space debris, the RF usage is increasing exponentially, causing issues in the RF usage of other operators.

Preliminary design decisions were based on a qualitative approach using these parameters. Even though it wasn't possible to quantify the environmental impact yet, including sustainability in the design decisions was especially important, as the early design decisions usually have the largest sustainability impact.

In the detailed design, each subsystem had the specific parts chosen. This meant a Life Cycle Assessment (LCA) could be performed. A LCA means that, for each part of the project the environmental impact is assessed. For a battery for example, the delving of lithium needs to be taken into account, as well as manufacturing and assembling of the battery. This was performed for all parts of all subsystems, to arrive at an environmental impact figure for the spacecraft. The Carbon Footprint (CF) for the SP and the S/C are **1.99 kg** and **17.68 kg**

[(1)] Magnetometer and gyroscope power are not accounted in the total, as they are already accounted for in OBC.
[(2)] Power is not accounted in the total, as they are already accounted for in other subsystems.

respectively. More design iterations should be performed on the SP to bring the CF down, since the SP is designed to be mass produced - any contributions to environmental impact will be multiplied for each unit produced.

For a complete environmental assessment, the launch and other environmental impacts also needed to be assessed. The launcher impact was assessed based on existing analyses of launchers, but other environmental impacts was hard to assess, because it is not clear what to include, and what not to include. It was decided that the travel to the launch site is included, but other factors aren't. The CF of the launch is **185.6 kg** and the CF of the travel to the launch site is $\mathbf{4.2 \times 10^3}$ **kg**. Interestingly enough, the impact of the travel to the launch site far outweighs the impact of the S/C or the launch. This highlights that even though Earth sustainability is an important aspect to consider in spacecraft design, more focus could go towards space sustainability when considering nanosatellite design. The CF of the entire mission is $\mathbf{4.4 \times 10^3}$ **kg**.

# Next Steps

The Next Steps Chapter provides an overview of the necessary tasks and plans to manufacture, assemble, integrate, and verify all subsystems as well as the complete system. Additionally, detailed explanations of testing and modeling methods are provided in this section.

## Post DSE Plan

The post-DSE plan presents the next steps that will be taken to fully develop, test, and integrate all subsystems, including the SP, after the DSE concludes. This section also explains the current state of the subsystems, including the standardized payload in terms of the phase structuring used by ESA [(1)]. Furthermore, this section also includes a Gantt chart that provides an overview of the post-DSE tasks and provides a timeline for them with a sufficient buffer.

## Manufacturing, Assembly and Integration

The Manufacturing, Assembly, Integration (MAI) plan details how to produce and acquire all the components (Manufacturing), how to put them together and connect them (Assembly), and how to test that everything works (Integration). In detail, manufacturing entails a Manufacturing Readiness Check, procurement, production, and Quality Control. The assembly phase consists of Connecting Parts of PCBs, Intra-Subsystem Harnessing, Mounting Subsystems into the CubeSat Structure, and Final Satellite Harnessing. Lastly, the Integration phase requires Unit-level Functional tests, System Environmental Qualification, Full System Verification, and a Flight Readiness check.

## System Verification and Validation

A model philosophy analysis has been conducted in order to choose the number and kinds of models for both the S/C and the SP. The S/C will have an Engineering Qualification Model for all tests, excluding Acceptance Testing, and a Flight Model, which will undergo Acceptance Testing. The SP will have multiple Development Models for design iterations, Integration Models mostly for software development, and also an Engineering Qualification Model and a Flight Model. The S/C has fewer models compared to the SP due to the fact that most S/C components are COTS, whereas the SP is designed in-house.

Development, Qualification, Acceptance and Pre-launch Testing will be conducted. Under Qualification Testing fall Single-unit Testing, FlatSat Testing, Integrated Testing, day-in-the-life Testing and Environmental Testing. The following Environmental Tests will be done: Dynamic (vibration and shock), thermal-vacuum cycling, and radiation for the SP.

## Logistic and Operations

The logistics and operations plan begins with engaging the launch provider to clarify requirements, acceptance testing, and ground station needs during early operations. This informs a detailed test plan and the booking of appropriate facilities. Parallel coordination with the TU Delft Space Institute assesses the use of their ground station, while ground segment software is developed or acquired. These interactions guide the development of a detailed mission operations plan that aligns ground station availability and capabilities with the satellite's communication needs. Once the launch date is set, a logistical plan coordinates the integration team's deployment, site access, accommodation, and communication with the Delft support team, including contingencies for potential delays to ensure uninterrupted mission readiness.

[(1)] Building and Testing Spacecraft - ESA, 2025. [Online]. DoLA: June 18, 2025. Available: https://www.esa.int/Science_Exploration/Space_Science/Building_and_testing_spacecraft

# Contents

# Nomenclature

| | |
|---|---|
| **AA** | Aluminum Alloy |
| **ABF** | Apply Before Flight |
| **AD** | Analog to Digital |
| **ADCS** | Attitude Determination and Control System |
| **AIS** | Automatic Identification System |
| **API** | Application Programming Interface |
| **ASTM** | Autonomous Space Traffic Management |
| **AU** | Astronomical Unit |
| **BER** | Bit Error Rate |
| **BOL** | Beginning-of-Life |
| **BOM** | Bill of Materials |
| **CAD** | Computer Aided Design |
| **CAN** | Controller Area Network |
| **CCSDS** | Consultative Committee for Space Data Systems |
| **C&DH** | Command and Data Handling |
| **CEP** | Circular Error Probable |
| **CEPT** | European Conference of Postal and Telecommunications Administrations |
| **CF** | Carbon Footprint |
| **COPUOS** | Committee on the Peaceful Uses of Outer Space |
| **COTS** | Commercial off-the-shelf |
| **CRS** | Carrier Recovery System |
| **CSKB** | CubeSat Kit Bus |
| **CSSWE** | Colorado Student Space Weather Experiment |
| **DA** | Digital to Analog |
| **DoLA** | Date of Last Access |
| **DPS** | Degree Per Second |
| **DSE** | Design Synthesis Exercise |
| **EAR** | Ephemerides Acquisition Receiver |
| **ECC** | Electronic Communications Committee |
| **ECCN** | Export Control Classification Number |
| **ECEF** | Earth Centered Earth Fixed |
| **ECSL** | European Centre for Space Law |
| **ECSS** | European Cooperation for Space Standardization |
| **EEMCS** | Electrical Engineering, Math and Computer Science |
| **EGSE** | Electrical Ground Support Equipment |
| **EMC** | Electromagnetic compatibility |
| **EOL** | End-of-Life |
| **EPS** | Electric Power System |
| **ESA** | European Space Administration |
| **EU** | European Union |
| **FAA** | Federal Aviation Administration |
| **FBD** | Functional Breakdown Structure |
| **FCC** | Federal Communications Commission |
| **FEC** | Forward Error Correction |
| **FFD** | Functional Flow Diagram |
| **FFT** | Fast Fourier Transform |
| **FOV** | Field Of View |
| **GFSK** | Gaussian Frequency-Shift Keying |
| **GMAT** | General Mission Analysis Tool |
| **GMSK** | Gaussian Minimum Shift Keying |
| **GND** | Ground |
| **GNSS** | Global Navigation Satellite System |
| **GPIO** | General Purpose Input Output |
| **GPS** | Global Positioning System |
| **GS** | Ground Station |
| **HK** | Housekeeping |
| **I2C** | Inter-Integrated Circuit |
| **IADC** | Inter-Agency Space Debris Coordination |
| **IARU** | International Amateur Radio Union |
| **IC** | Integrated Circuit |
| **ICG** | International Committee on Global Navigation Satellite Systems |
| **IF** | Intermediate Frequency |
| **IISL** | International Institute of Space Law |
| **ILRS** | International Laser Ranging Service |
| **IR** | Infrared Radiation |
| **ISO** | International Standardization Organization |
| **ITAR** | International Traffic in Arms Regulations |
| **ITU** | International Telecommunication Union |
| **LCA** | Life Cycle Assessment |
| **LCI** | Life Cycle Inventory |
| **LEAT** | Launch Emission Assessment Tool |
| **LEO** | Low-Earth Orbit |
| **LEOP** | Launch and Early Orbit Phase |
| **LOS** | Line of sight |
| **LPUART** | Low-Power Universal Asynchronous Receiver/Transmitter |
| **LTS** | Long-Term Sustainability |
| **LV** | Launch Vehicle |
| **MAI** | Manufacturing, Assembly, Integration |
| **MCU** | Microcontroller Unit |
| **MIL-STD** | Military Standard |
| **NASA** | National Aeronautics and Space Administration |
| **NORAD** | North American Aerospace Defense Command |
| **NSO** | Nederlands Space Office |
| **NZ** | New Zealand |
| **OBC** | On-Board Computer |
| **OS** | Operating System |
| **PCB** | Printed Circuit Board |
| **PCDU** | Power Conditioning & Distribution Unit |
| **PCU** | Power Conditioning Unit |
| **PDU** | Power Distribution Unit |
| **PL** | Payload |
| **PLL** | Phase-Locked Loop |
| **PMAC** | Passive Magnetic Attitude Control |
| **PNT** | Position, Navigation and Timing |
| **PPS** | Precise Positioning Service |
| **PRN** | Pseudo-Random Noise |
| **PRS** | Public Regulated Service |
| **QUADSPI** | Quad Serial Peripheral Interface |
| **RAAN** | Right Ascension of the Ascending Node |
| **RDI** | Rijksinspectie Digitale Infrastructuur |
| **RF** | Radio Frequency |
| **RILDOS** | Radio with Identity and Location Data for Operations and Space Situational Awareness |
| **RMS** | Root Mean Square |
| **RR** | Radio Regulation |
| **RS-232** | Recommended Standard 232 |
| **RS-485** | Recommended Standard 485 |
| **RTC** | Real-Time Clock |
| **S/C** | spacecraft |
| **SAI** | Serial Audio Interface |
| **SDLS** | Space Data Link Security |
| **SDMMC** | Secure Digital/MultiMediaCard Interface |
| **SIDLOC** | Spacecraft Identification and Localization |
| **SLR** | Satellite Laser Ranging |
| **SNR** | Signal to Noise Ratio |
| **SP** | Standardized Payload |
| **SPDT** | Single Poly Dual Throw |
| **SPI** | Serial Peripheral Interface |
| **SSA** | Space Situational Awareness |
| **SSO** | Sun-Synchronous Orbit |
| **SST** | Space Surveillance and Tracking |
| **STM** | Space Traffic Management |
| **SWaP-C** | Size, Weight, Power and Cost |
| **TADI** | Testing, Analysis, Demonstration and Inspection |
| **TBD** | To Be Determined |
| **TCXO** | Temperature Compensated Crystal Oscillator |
| **TJ GaAs** | Triple-junction gallium-arsenide |
| **TLE** | Two-Line Element |
| **TRL** | Technology Readiness Level |
| **TVAC** | Thermal Vacuum |
| **UART** | Universal Asynchronous Receiver/Transmitter |
| **UHF** | Ultra High Frequency |
| **UN** | United Nation |
| **UNOOSA** | United Nations Office for Outer Space Affairs |

**USA** United States of America
**USART** Universal Synchronous/Asynchronous Receiver/Transmitter
**USB** Universal Serial Bus
**USML** US Munitions List
**VERON** Vereniging voor Experimenteel Radio Onderzoek in Nederland
**VHF** Very High Frequency
**VP** Validation Payload

# 1. Introduction and Motivation

The near-Earth space environment is getting more and more crowded, and this growth in satellite numbers is not expected to slow down. Forecasts report an average of over 3700 satellites to be launched annually [1]. Specifically, four major constellations: Starlink, Kuiper, G60, and GuoWang will make up 65% of the satellite demand quantity [1]. With all four of these constellations in low-Earth orbit, the risk of collisions is becoming ever greater. To avoid the Kessler effect [18], losing access to the Low-Earth Orbit (LEO) environment and its vital space infrastructure such as telecommunications, navigation and weather prediction, there is a need to improve the accuracy of the positional estimates of spacecraft to better predict close approaches and avoid collisions between operational spacecraft and space debris alike. However, current technologies do not allow global Space Situational Awareness (SSA) as Two-Line Element (TLE) do not provide sufficient accuracy [2], traditional ground-based ranging and Satellite Laser Ranging (SLR) are unsuitable to track many satellites simultaneously [3, 4] and conventional spacecraft Global Navigation Satellite System (GNSS) receivers' Size, Weight, Power and Cost (SWaP-C) makes them unable to be used on all satellites. This report concerns the design of an innovative, small, lightweight, power-efficient and inexpensive standardized payload for Space Traffic Management (STM) based on a snapshot GNSS receiver. This standardized payload could then be easily integrated in virtually any LEO spacecraft and provide accurate position fixes for it. This gathered position data would then enable the improvement of upper atmospheric density models, increasing the precision of LEO object orbit propagation and enabling space situational awareness.

## Scope

This project encompasses the development of a standardized payload and a technology demonstration satellite for autonomous space traffic management, which is described as:

> "STM encompasses the means and the rules to access, conduct activities in, and return from outer space safely, sustainably, and securely." [(1)]

Within the design synthesis exercise the group will act as a student team at the faculty. The aim of this project is as follows:

> *"Design a standardized payload for space traffic management, based on a snapshot GNSS receiver, and an associated technology demonstration mission and satellite to validate this payload."*

### Standardized Payload

The idea behind standardizing this snapshot GNSS receiver payload is to allow it to easily be integrated into virtually any host spacecraft. This ease of integration, combined with its greatly superior SWaP-C costs compared to conventional GNSS receiver payloads, makes the standardized payload a highly compelling module to include when designing a LEO satellite. As space is not governed by any single nation, union, or organization, imposing regulatory mandates is inherently complex, and requiring the inclusion of a standardized payload on all satellites poses a substantial challenge. However, by making the Standardized Payload (SP) so exceptionally small, lightweight, power-efficient and inexpensive that it becomes the default choice for satellite operators, the hurdle towards regulatory enforcement diminishes, perhaps even to a point where it is no longer a hurdle at all.

Then, due to its ease of integration, large numbers of satellites can be equipped with this SP and enable a distributed autonomous infrastructure for real-time orbital state reporting to be established. Each satellite periodically broadcasts its GNSS-derived position to ground stations (or, in the future, even to neighboring satellites), creating a collaborative framework for autonomous space traffic management and collision avoidance.

At the core of the standardized payload is a snapshot GNSS receiver, capable of acquiring position data through millisecond-scale signal captures. This mode of operation enables intermittent, ultra-low power consumption, making it suitable even for power-constrained platforms such as CubeSats or PocketQubes. To initialize the snapshot processing, a standard GNSS receiver with a band processor is also added as part of the standardized

[(1)] Space Traffic Management, European Commission, 2025. [Online]. Date of Last Access (DoLA): April 28, 2025. Available: https://defence-industry-space.ec.europa.eu/eu-space/space-traffic-management_en

payload. This allows a hybrid use and minimizes energy consumption throughout an orbit. Although the hybrid GNSS receiver technology exists and has been patented [19], the implementation of this technology for in-orbit applications is a novel approach.

In addition to positioning data, the SP can be configured to sense and relay in-situ environmental parameters, most notably, atmospheric density. Variations in atmospheric density are the primary source of uncertainty in orbit propagation models. A network of SP-equipped satellites would provide a dynamic global dataset of atmospheric conditions in LEO, significantly enhancing predictive capabilities for orbit evolution and close-approach risk assessment.

The SP concept offers a scalable and efficient path toward improving LEO operational safety through a combination of low-power GNSS positioning, cooperative localization, and real-time environmental monitoring.

### Technology Demonstration Mission

To validate the functionality and performance of the SP in orbit, a dedicated technology demonstration mission is proposed. This mission will host the SP and Validation Payload (VP) on a compact satellite platform, designed to verify the viability of snapshot GNSS receiver technology. The demonstration satellite will operate in orbit for 6 months, collecting and downlinking position fixes generated onboard. These position solutions will be independently validated using other satellite tracking technologies, such as Doppler ranging, SLR or a conventional GNSS receiver payload. The mission will be realized under a strict cost requirement of €10 million and a total satellite mass below 10 kg, both these requirements are satisfied very well as the mission cost is less than €300 k and the satellite mass less than 1 kg. In compliance with space debris mitigation guidelines, the satellite will be designed to de-orbit within five years of orbit injection epoch, ensuring responsible operations throughout the mission life-cycle.

## Report Structure

The report first lays the foundations of the design process in Chapter 2, which includes a market analysis, a literature study on relevant laws and regulations, as well as a requirement generation. Chapter 3 defines the mission architecture, presenting the functional flow, an overview of the logistics and operations and defining the mission orbit and launch. With the groundwork laid, Chapter 4 then explains the design of the standardized payload. With the main payload designed, Chapter 5 shows the subsystem design performed for the technology demonstration satellite. Building onto the subsystem design, Chapter 6 provides an overview of the final spacecraft design, including the final budgets and costs, the satellite architecture, a risk analysis, the sustainability and requirement compliance. Chapter 7 presents the road map for future work, discussing the next steps to be taken, especially with regards Manufacturing, Assembly, Integration (MAI) and testing. Finally, Chapter 8 concludes the report, reflects on the Design Synthesis Exercise (DSE) and gives recommendations.

This report was created without any text written using A.I. assistance.

# 2. Design Foundations

This chapter lays the foundations for the design of the standardized payload for space traffic management as well as the technology demonstration satellite and mission. Section 2.1 performs a market analysis, describing the current market landscape and market gap as well as provides a stakeholder analysis. Section 2.2 continues by thoroughly investigating the regulations and policies relevant to the project. Finally, the requirements gathered in the market analysis and regulations investigation are listed in Section 2.3.

## 2.1. Market Analysis

This section analyses the market for an autonomous space traffic management system, providing the motivation for its development. First, the market landscape is explored in Subsection 2.1.1. Then Subsection 2.1.2 discusses the gaps and unmet needs in the market as well as the potential impact of the project as a solution. Finally, Subsection 2.1.3 performs an analysis of potential stakeholders.

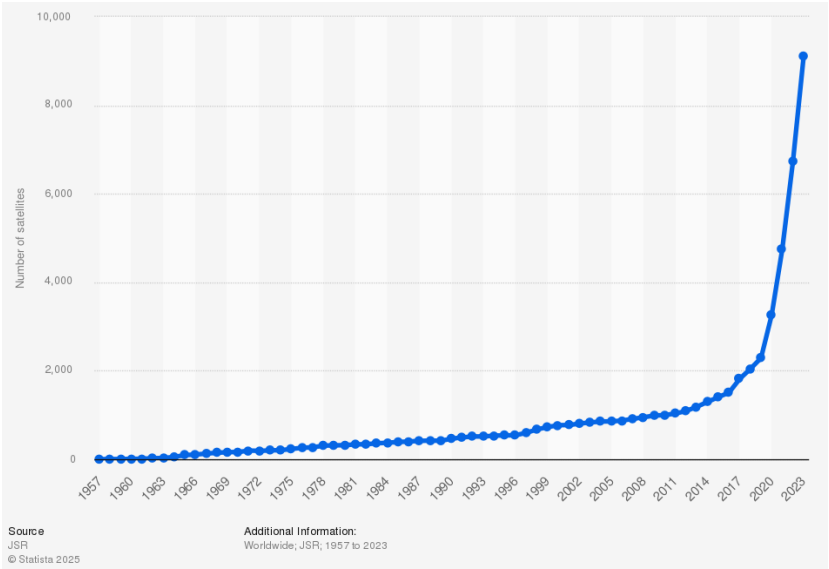


**Figure 2.1:** Number of active satellites from 1957 to 2023.[(1)]

### 2.1.1. Market Landscape

The near-Earth space environment is getting more and more crowded. Figure 2.1 clearly shows this. This growth in satellite numbers is not expected to slow down. Novaspace's latest "*Satellites to be Built and Launched*" report forecasts an average of over 3700 satellites to be launched annually [1]. Specifically, four major constellations: Starlink, Kuiper, G60, and GuoWang will make up 65 % of the satellite demand quantity. With all four of these constellations in Low-Earth Orbit (LEO), the risk of collisions is increasing.

The current standard for globally tracking LEO objects larger than ~10 cm is the Two-Line Element (TLE) sets set provided by North American Aerospace Defense Command (NORAD). With an accuracy of ~1 km [2], the position predictions these TLE sets enable through orbital propagation are too inaccurate to reliably monitor close approaches and potential collisions. This TLE data is accessible for free through space-track.org[(2)], which averages over a quarter million Application Programming Interface (API) queries per day by more than 180,000 users from over 180 different countries [20]. Traditional ground-based radiometric ranging and Doppler measurements provide an accuracy of ~10 m [3], but are limited to specific tracking arcs and can only simultaneously track a few satellites. Satellite Laser Ranging (SLR) has an accuracy in the order of only centimeters [4], but in addition to a direct line-of-sight, this technique requires retroreflector arrays to be fitted

[(1)] Number of active satellites from 1957 to 2023 [Graph], JSR, January 15, 2024. [Online]. Date of Last Access (DoLA): April 24, 2025. Available: https://www.statista.com/statistics/897719/number-of-active-satellites-by-year/

[(2)] space-track.org, 2025. [Online]. DoLA: 12 June, 2025. Available: https://www.space-track.org/

to the satellite. Another well-established technique is spaceborne tracking through the use of onboard Global Navigation Satellite System (GNSS) receivers. However, these systems are specifically designed and produced for space applications, making them relatively large, heavy, expensive (~€10 k to 20 k[(1)(2)]), and power-hungry.

### 2.1.2. Market Gap Analysis

Due to the ever-increasing number of objects in LEO, there is a need to improve the accuracy of positional estimates to better predict close approaches and avoid collisions between operational spacecraft and space debris alike. However, current techniques do not allow global space situational awareness as TLE do not provide sufficient accuracy, traditional ground-based ranging and SLR are unsuitable for global satellite tracking and conventional spacecraft GNSS receivers' Size, Weight, Power and Cost (SWaP-C) makes them unable to be used on all satellites. A small (~36 mm × 44 mm × 6 mm), lightweight (~33 g), power-efficient (~0.94 mW), and inexpensive (€275) standardized snapshot GNSS receiver payload could fill this gap by providing position measurements accurate to ~20 m [5] at much more appealing SWaP-C values.

Furthermore, current upper atmospheric density models do not allow accurate position prediction, so there is a need to improve these models. As a standardized module, the Standardized Payload (SP) fits on any satellite. Furthermore, by designing the standardized payload such that it is the smallest, most lightweight, most power-efficient, and least expensive spacecraft-tracking module on the market, it becomes desirable to include on any mission. The gathered positional data of the many satellites would then enable the improvement of upper atmospheric density models, increasing the precision of LEO object orbit propagation and enabling Space Situational Awareness. Then in the future, once virtually every LEO satellite is equipped with the standardized payload and the authorities have regulated the rules-of-the-road for space, a distributed autonomous infrastructure for space traffic management could remove the need for human involvement in avoiding spacecraft collisions, enabling true autonomous space traffic management and thereby ensuring the LEO environment as well as its critical infrastructure remains sustainable and available.

### 2.1.3. Stakeholder Analysis

Various stakeholders can influence or be impacted by the project. These stakeholders are identified as well as categorized into key and non-key stakeholders in Table 2.1. Figure 2.2 then analyzes them by putting them in a stakeholder interest-influence graph.

**Table 2.1:** Identified stakeholders for the standardized payload.

| Stakeholder | Description |
|---|---|
| | **Key Stakeholders** |
| **TU Delft College van Bestuur** | As the project group will be acting as a student team within TU Delft, a key stakeholder is the Delft University of Technology. The standardized payload and technical demonstration satellite are developed as a research project under the sponsorship of the university, therefore, the university is the "customer." |
| **Scientific Community** | The scientific community is an important stakeholder. Scientists across the globe may be interested in the raw data the standardized payload generates on the demonstration satellite as well as on future satellites it may be integrated on. This data should be easily accessible such that scientists can use it to perform their research, for example, on upper atmospheric density modeling. |
| **Royal Netherlands Air Force** | The Royal Netherlands Air Force is a stakeholder interested in aiding and advising in the development of the standardized payload and potentially using snapshot GNSS receiver technology on their satellites in the future. |
| | **Non-key Stakeholders** |
| **Space Agencies** | Space agencies such as European Space Administration (ESA) and National Aeronautics and Space Administration (NASA) are highly connected to the scientific community, and they may also be interested in the raw data for research purposes. Furthermore, they may be interested in the integrated payload itself to integrate it on their future spacecraft to replace or add to existing tracking methods. |
| **Regulatory Agencies** | Regulatory agencies such as United Nations Office for Outer Space Affairs (UNOOSA), European Centre for Space Law (ECSL), and International Institute of Space Law (IISL) may choose to make it mandatory for all future LEO spacecraft to have the standardized payload for Space Traffic Management (STM) integrated in order to enable space traffic management. |
| **Spacecraft Developers** | Spacecraft operators may want or even need to integrate a standardized snapshot GNSS receiver payload into their spacecraft for power-efficient, inexpensive position tracking. They would have to reserve space within the spacecraft as well as allocate a certain power and downlink budget to allow the payload to function. |
| **Spacecraft Operators** | Ground stations will be needed to receive the data from the standardized payloads on Earth and either send it to data processing facilities or make it directly available to the users. |
| **Launch Vehicle Providers** | The launch vehicle provider will set requirements, for example, the launch loads the standardized payload, and the technical demonstration satellite must survive. |
| **Launch Brokers** | The launch broker will set requirements such as the launch and orbit insertion cost. |

Continued on next page.

[(1)]GNSS Receiver Module, Pumpkinspace, 2025. [Online]. DoLA: May 7, 2025. Available: https://www.pumpkinspace.com/store/p58/GNSS_Receiver_Module_%28GPSRM_1%29_Kit.html

[(2)]Onboard Computer with GNSS, Endurosat, 2025. [Online]. DoLA: May 7, 2025. Available: https://www.endurosat.com/products/onboard-computer-with-gnss

| Stakeholder | Description |
|---|---|
| **Manufacturers** | Manufacturers will provide all the necessary parts for the standardized payload as well as the technical demonstration satellite. This standardized payload may also be manufactured externally by subcontractors to allow it to be made in bulk and enable space traffic management. As off-the-shelf parts will be used for the standardized payload, the manufacturers of these parts may be able to sell components in large quantities. |

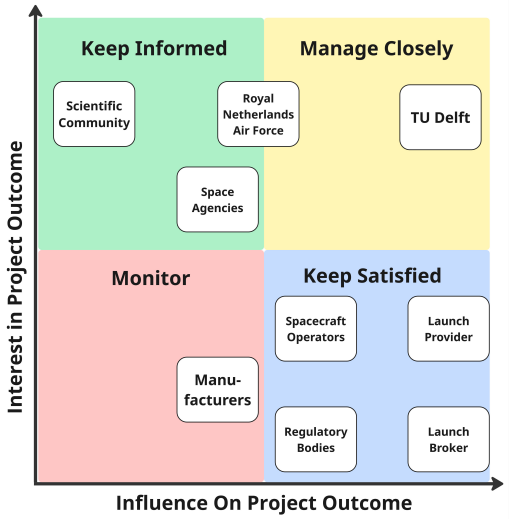


**Figure 2.2:** Stakeholder interest-influence graph.

## 2.2. Regulations and Policies Investigation

The outer space cannot be claimed by any sovereignty, by means of use or occupation, or by any other means under UNOOSA, United Nations treaties Article II [21]. Beyond the Outer Space Treaty, all space-faring nations must carry out their activities "for the benefit of all countries." under Article I of the 1967 Treaty [21]. Even though no state may claim sovereignty in outer space, each launch and spacecraft operator falls under a national licensing regime. This ensures adherence to international obligations on spacecraft, payloads, and mission design. These requirements mandate that states authorize and supervise all space operations under their jurisdiction from the United Nations treaties Article VI [21].

At the regional level, the European Union (EU) has been working toward a unified space regulatory framework. From the proposed timeline, the EU is expected to finalize the first draft of the EU Space Act in 2025, which will establish EU-wide minimum requirements for collision avoidance and long-term sustainability of satellites operating or providing services within member states [22]. Although details of the draft regulation remain confidential, the industry anticipates a shift from voluntary guidelines toward enforcing mandatory standards for the space industry [(1)].

Within individual EU nations, national licensing frameworks translate the Outer Space Treaty. In the Netherlands, the Dutch Space Activities Act of 2007 governs all space-related endeavors [(2)]. Under this law, any person established in the Netherlands must notify the Nederlands Space Office (NSO) when conducting space operations. The NSO represents the Netherlands inside ESA and operates under the Ministry of Economic Affairs and Climate Policy on the launch of a space object [23].

Consequently, compliance with both the international and the national regulations places clear technical constraints on satellite design, launch processes, and operational practices. The analysis that follows aims to identify and navigate these constraints to prevent any violations of existing legal frameworks.

### GNSS Receiver Regulations

In order to make use of a GNSS receiver, depending on where it is manufactured, there may be requirements and regulations to be complied with.

[(1)]Europe's far-reaching space act nears launch, SpaceNews, 2025. [Online]. DoLA: June 6, 2025. Available: https://spacenews.com/europes-far-reaching-space-act-nears-launch/

[(2)]Wet ruimtevaartactiviteiten en satellietcommunicatie, Government of the Netherlands, January 1, 2019. [Online]. DoLA: June 6, 2025. Available: https://wetten.overheid.nl/BWBR0021418/2019-01-01/

For the United States of America (USA), if the subject is deemed to be in US Munitions List (USML), International Traffic in Arms Regulations (ITAR) applies [24]. For spacecraft and related articles, it falls under USML category XV. If the use of the satellite has a military purpose it then directly concerns ITAR regarding "Significant Military Equipment" with the extent specified in §120.7. The spacecraft will require an ITAR license if it falls under the USML XV subcategory c-2, Global Positioning System (GPS) receiving designed for producing navigation results above 60 000 ft altitude and at 1852 km $h^{-1}$ velocity or greater. The possible consequence is if the receiver uses the GPS P-Code signal, which, by USA policy, the receiver will be switched off without notice [25].

For the GNSS receivers, USML category XII d-2 applies to GNSS receiving equipment that is specially designed for military applications that are capable of providing navigation information at speeds in excess of 600 m $s^{-1}$. In addition, it mentions GPS receiving equipment specially designed for encryption or decryption of GPS Precise Positioning Service (PPS) signals [24]. The acquisition of space-grade GNSS receivers is controlled by the Export Control Classification Number (ECCN) 9A515.x [24].

Meanwhile, the EU Space Program is governed by specific EU Regulations. A passive GNSS receiver is generally unregulated as it only receives global navigation signals and does not emit. For Galileo GNSS data access, the EU decided in 1104/2011/EU that the public regulated service from Galileo requires no special license [26]. By contrast, operating an USA GNSS receiver system, acquiring Galileo signals requires licensing of receive-only equipment for non USA GNSS signals, according to the the Federal Communications Commission (FCC), under 47 CFR §25.115(b)(9)(i) unless duly approved [(1)].

## Telecommunication Regulations

For orbital slot, uplink and downlink frequencies, the operators must apply to their national spectrum regulator. For the EU, the mandates are managed by the European Conference of Postal and Telecommunications Administrations (CEPT)[(2)] and Electronic Communications Committee (ECC)[(3)].

The regulator handles the International Telecommunication Union (ITU) Radio Regulation (RR) 2020 that governs all spectrum use and satellite orbits globally. This radio link must be coordinated through national administrations to the ITU RR Article 7 before operations, ensuring no harmful interference per Article 15 [27]. The ITU states in 4.10 "Member States recognize that the safety aspects of radio navigation and other safety services require special measures to ensure their freedom from harmful interference; it is necessary therefore to take this factor into account in the assignment and use of frequencies." However, as mentioned previously, the new EU initiatives may affect spectrum availability and priority.

The national regulator in the Netherlands is the Rijksinspectie Digitale Infrastructuur (RDI)[(4)]. With the mission design for a LEO telemetry payload operating in Ultra High Frequency (UHF)/Very High Frequency (VHF), the national frequency authorization will be managed by the RDI. This includes handling the ITU coordination under RR Article 11, Article 11 procedure and satellite telemetry are recorded in the Master International Frequency Register via ITU's International Frequency Information Circular process[(5)]. In case of amateur bands, administration allows license exemption as coordination is done via the International Amateur Radio Union (IARU)[(6)]. For the Netherlands it is the Vereniging voor Experimenteel Radio Onderzoek in Nederland (VERON)[(7)]. Utilizing amateur bands limits the use of data encryption from the regulation by the FCC 97.309[(8)].

## Space Debris and Collision Mitigation Regulations

For sustainability, United Nation (UN)'s Committee on the Peaceful Uses of Outer Space (COPUOS) Long-Term Sustainability (LTS) Guidelines urge limiting debris release, spacecraft passivation, and sharing collision-

[(1)] 47 CFR § 25.115(b)(9)(i), Electronic Code of Federal Regulations (eCFR), 2025. [Online]. DoLA: June 6, 2025. Available: https://www.ecfr.gov/current/title-47/section-25.115#p-25.115(b)(9)(i)

[(2)] CEPT - European Conference of Postal and Telecommunications Administrations, CEPT, [Online]. DoLA: June 6, 2025. Available: https://cept.org/cept

[(3)] ECC - Electronic Communications Committee, CEPT, [Online]. DoLA: June 6, 2025. Available: https://cept.org/ecc

[(3)] RNSS and the ITU Radio Regulations, Ingo Baumann, January 1, 2018. [Online]. DoLA: June 10, 2025. Available: https://insidegnss.com/rnss-and-the-itu-radio-regulations/

[(4)] Ruimtevaart, Radiocommunications Agency Netherlands (RDI), [Online]. DoLA: June 6, 2025. Available: https://www.rdi.nl/onderwerpen/ruimtevaart

[(5)] Master International Frequency Register (MIFR), International Telecommunication Union (ITU), [Online]. DoLA: June 6, 2025. Available: https://www.itu.int/en/ITU-R/terrestrial/broadcast/Pages/MIFR.aspx

[(6)] International Amateur Radio Union, IARU, [Online]. DoLA: June 6, 2025. Available: https://www.iaru.org/

[(7)] VERON - Vereniging voor Experimenteel Radio Onderzoek in Nederland, VERON, [Online]. DoLA: June 6, 2025. Available: https://www.veron.nl/

[(8)] 47 CFR § 97.309, Electronic Code of Federal Regulations (eCFR), 2025. [Online]. DoLA: June 6, 2025. Available: https://www.ecfr.gov/current/title-47/section-97.309

avoidance data, albeit voluntarily [28]. For debris, the Inter-Agency Space Debris Coordination (IADC) debris mitigation guidelines and International Standardization Organization (ISO) 24113:2023 standard classify best practices on passivation, minimized debris release, and post-mission disposal [29][(1)]. These require measures such as on-board passivation, no leftover fuel or energy that could cause explosions, minimizing mission-related debris, and post-mission disposal.

The ESA Space Debris Mitigation Requirements [30] for all ESA programs and projects define the space debris mitigation requirements applicable to all elements of systems launched into, or passing through, Earth and Lunar space. This includes launch vehicle orbital stages, spacecraft and any parts released. The standard aims at meeting and exceeding the relevant international standards on space debris mitigation and space traffic coordination.

An important requirement for the technical demonstration satellite is that described by *5.4.2.3 LEO protected region clearance* [30], which describes that the orbit lifetime for a LEO spacecraft with no recurrent maneuver capability shall be less than 5 years starting from the orbit injection epoch.

For collision, the EU sets up Space Surveillance and Tracking (SST) to detect and warn for EU assets for collision, re-entry, and fragmentation[(2)].

### Launch Safety Regulation

For liability, the UNOOSA Article VII makes the launching state "absolutely liable" for any damage caused by its space objects. This falls in line with the Liability Convention of 1972; the launching state is liable for damage on Earth or in airspace. This article puts emphasis on regulations from the launching state [21].

For launch site outside of the EU, the transportation imposes regulations on acquired EU components. Due to EU Regulation 2021/821 imposing export controls on “dual-use” items, this covers advanced Category 5 satellite components like GNSS receivers [6, 31].

Launching in other States involves their regulatory restrictions. For Rocket Lab’s primary pad, it is in New Zealand (NZ). Under NZ Outer Space and High-Altitude Activities Act 2017, any payload launched from NZ requires a payload permit and a launch license issued by the NZ Space Agency [32]. These licenses require safety analysis, insurance, compliance with debris mitigation, and international obligations. Additionally, local environmental and airspace clearances from NZ Civil Aviation and hazardous materials approvals are typically required for launch. These will be managed by the launch provider, while the operator should coordinate with the launch provider on all safety cases and insurance requirements.

### Export Control Regulation

From Section 2.2 regulations on GNSS receiver are described for satellite or ground station hardware that contains USA origin technology, requiring export licenses due to ITAR/Ephemerides Acquisition Receiver (EAR) rules.

Other than the regulations from the USA, the Wassenaar arrangements also control the export of GNSS receivers requiring an export license on an international level [7]. For EU Member States regulation 2021/821 is enforced, for example, under Part VII 5A101, high-precision GNSS receivers and encryption modules may require export licenses for sales to non EU countries [6].

Although not regulated, it is important to note that EU funded data like Galileo have usage rules. GNSS data are open to the public per EU Galileo policies; certain Galileo signals Public Regulated Service (PRS) are restricted to government use [(3)].

### Looking Towards the Future

Many authors have performed studies on the form and overarching structure a future space traffic management regime should have, yet no actual universal rules-of-the-road will be agreed upon [33]. With the new draft of the EU Space Act being published in June of 2025, universal rules-of-the-road will be set in place [22].

In order to standardize the Snapshot GNSS payload, the regulatory process is arduous. The standardized payload needs to be approved by many regulatory bodies:

[(1)] ISO 24113: Space systems - Space debris mitigation requirements, International Organization for Standardization (ISO), [Online]. DoLA: June 6, 2025. Available: https://www.iso.org/obp/ui/en/#iso:std:iso:24113:ed-4:v1:en

[(2)] EU SST Services, European Union Space Surveillance and Tracking (EUSST), [Online]. DoLA: June 6, 2025. Available: https://www.eusst.eu/services

[(3)] Galileo Services, European Union Agency for the Space Program (EUSPA), [Online]. DoLA: June 6, 2025. Available: https://www.euspa.europa.eu/eu-space-programme/galileo/services

- ITU and FCC for radio frequency allocation.
- UN COPUOS for space object registration.
- IADC for collision and debris avoidance: end-of-life disposal, passivation.
- ISO for voluntary space hardware standards, ease of compatibility adoption.
- Consultative Committee for Space Data Systems (CCSDS) for navigation data message formats and tracking interfaces. Facilitating interoperability of a GNSS payload across agencies.
- International Committee on Global Navigation Satellite Systems International Committee on Global Navigation Satellite Systems (ICG) helps resolve legal/licensing issues for GNSS signal utilizationDoLA[(1)].

There is precedence on the implementation of equipment on a global scale for a specific industry. In Maritime, it is the Automatic Identification System (AIS) enforced by the International Maritime Organization. For aviation, the International Civil Aviation Organization mandated GNSS based navigation and ADS-B for aircraft [34]. Introducing a mandatory space payload requires both technical justification and international consensus. The typical policy path is to propose at international fora such as the COPUOS, ICG, and ITU. Then build technical standards and secure regulatory adoption for treaties or national laws, finally, implement via licensing conditions. ESA has proposed beacon standards like Radio with Identity and Location Data for Operations and Space Situational Awareness (RILDOS)[(2)] and Spacecraft Identification and Localization (SIDLOC) to tag satellites[(3)].

These highlight the interest from industry in standardization. For the passive use of GNSS signals, it does require a license according to international regulatory bodies; national rules may apply. CCSDS could define a "Spacecraft Tag Message" analogously to AIS's standardized VHF data link.

The implementation starts by developing a prototype snapshot GNSS payload. A technical working group on CCSDS or ISO drafts specifications for message formats and interface standards. ISO or CCSDS committees propose formal standards every 2 to 3 years for balloting. For international policy, proposals are through a coalition of states and agencies presenting the concept to COPUOS. Then GNSS provider countries via ICG agree on signal use. For new frequencies, a proposal is submitted to an ITU World Radiocommunication Conference cycle, the preparation and decision will take over 4 to 8 years.

Afterwards, through UN endorsement and adopting non-binding guidelines recommending the standardized payload, much like the application of the 2019 LTS Guidelines. UN Member States might then push for a UN General Assembly resolution endorsing its adoption, similarly to the endorsement of the debris and sustainability guidelines. Following international endorsement, each country or region would amend its licensing rules. In the USA, the Federal Aviation Administration (FAA) and FCC would undertake law makings to add the GNSS payload to launch or satellite license requirements. In Europe, national space launch regulations or the future EU space traffic rules would be updated. This process can take 1 to 2 years in each jurisdiction.

Once in law, each launch license and satellite would be conditioned on carrying a compliant GNSS snapshot payload. Launch/service providers would include it in design reviews and tests. Certification would involve verifying the device meets the agreed standards e.g. ISO/CCSDS specifications, and does not interfere with other systems.

## 2.3. Requirements

This section presents the high-level requirements for the project. The stakeholder requirements derived from the stakeholder analysis in Subsection 2.1.3 and the regulations investigation in Section 2.2 encapsulate the needs and expectations of all stakeholders involved, Table 2.2 lists these requirements organized by stakeholder for clarity and traceability. Table 2.3 then tabulates the top-level requirements as given by the project guide [35].

[(1)] International Committee on Global Navigation Satellite Systems (ICG), United Nations Office for Outer Space Affairs (UNOOSA), [Online]. DoLA: June 6, 2025. Available: https://www.unoosa.org/oosa/en/ourwork/icg/icg.html

[(2)] RILDOS-Based Operations Telecom Missions ARTES, European Space Agency (ESA), [Online]. DoLA: June 6, 2025. Available: https://connectivity.esa.int/funding/rildosbased-operations-telecom-missions-artes-3a119

[(3)] SIDLOC Secure and Intelligent Positioning, SIDLOC, [Online]. DoLA: June 6, 2025. Available: https://sidloc.org/

**Table 2.2:** Stakeholder requirements.

| ID | Requirement |
|---|---|
| | **Royal Netherlands Air Force** |
| STM-SH-ML-1 | The SP shall provide accurate data for space threat monitoring. |
| STM-SH-ML-2 | The SP shall provide reliable data transfer. |
| STM-SH-ML-3 | The SP shall contribute to reducing reliance on foreign space navigation services. |
| STM-SH-ML-4 | The SP shall provide accurate data that can improve the SSA. |
| STM-SH-ML-5 | The operation of the SP shall require minimal personnel involvement. |
| | **Scientific Community** |
| STM-SH-SCC-1 | The SP shall provide data to improve atmospheric density models. |
| | **Space Agencies** |
| STM-SH-SA-1 | The SP shall aid in SSA and collision avoidance. |
| STM-SH-SA-2 | The technology demonstration satellite shall comply with applicable international space debris mitigation guidelines. |
| | **Regulatory Agencies** |
| STM-SH-RA-1 | The S/C shall have an End-of-Life (EOL) disposal procedure. |
| STM-SH-RA-2 | The SP and S/C shall comply with the ITU-R legal regulations. |
| STM-SH-RA-3 | The SP and S/C shall operate within allocated frequency bands to avoid interference. |
| | **Manufacturers** |
| STM-SH-MF-1 | Both the SP and the S/C design shall follow standard mechanical interface requirements. |
| STM-SH-MF-2 | Both the SP and the S/C design shall follow standard electrical interface requirements. |
| STM-SH-MF-3 | Both the SP and the S/C shall be designed to meet all applicable safety requirements. |
| STM-SH-MF-4 | The SP shall be mass manufacturable. |
| STM-SH-MF-5 | The S/C and SP shall come with complete documentation for manufacturing. |
| | **Launch Brokers** |
| STM-SH-LB-1 | The S/C shall fit within the predetermined mass budget. |
| STM-SH-LB-2 | The S/C shall fit within the predetermined volume budget. |
| STM-SH-LB-3 | The S/C shall comply with safety requirements during Launch and Early Orbit Phase (LEOP). |
| | **Launch Vehicle Providers** |
| STM-SH-LVP-1 | The S/C shall be compatible with standard launch interfaces. |
| STM-SH-LVP-2 | The S/C shall comply with LEOP safety requirements as defined by the launch vehicle. |
| | **Satellite Developers** |
| STM-SH-SD-1 | The SP shall be easy to integrate as a plug-and-play module. |
| STM-SH-SD-2 | The SP shall have low power consumption. |
| STM-SH-SD-3 | The SP shall have low mass. |
| STM-SH-SD-4 | The SP shall have a low volume envelope. |
| STM-SH-SD-5 | The SP shall come with complete documentation for operation. |
| STM-SH-SD-6 | The SP shall interface with the other satellite system. |
| STM-SH-SD-7 | The SP shall not interfere with the other satellite operations. |
| STM-SH-SD-8 | The SP shall be safe to handle during assembly, integration, and testing. |
| STM-SH-SD-9 | The SP shall come with complete documentation for integration and testing. |
| | **Satellite Operators** |
| STM-SH-SO-1 | The S/C shall be able to send telemetry to ground stations. |
| STM-SH-SO-2 | The S/C shall be able to receive telecommands from ground stations. |
| | **TU Delft College van Bestuur** |
| STM-SH-TUD-1 | The SP and S/C shall be developed at TU Delft. |

Together with the requirements listed above in Table 2.2, the requirements in Table 2.3 form the basis for the design of both the standardized payload and the technology demonstration satellite. With these requirements as a foundation, Section 3.3 can define the mission architecture. For clarity, throughout Chapter 4 and Chapter 5, the system-level requirements required to begin the design of the standardized payload or technology demonstration satellite subsystems are always listed before the beginning of the design.

**Table 2.3:** Top-level requirements.

| ID | Requirement |
|---|---|
| | **Performance** |
| PF1 | The payload shall use a snapshot GNSS receiver to determine the satellite position with 20 m (3D r.m.s.). |
| PF2 | The technology demonstration satellite shall demonstrate autonomous Space Traffic Management using the payload under P1. |
| | **Safety and reliability** |
| SR1 | The payload shall not cause mechanical, electrical, or thermal problems when flown as a compulsory unit on future satellites. |

Continued on next page.

| ID | Requirement |
|---|---|
| SR2 | The payload shall withstand all conditions during LEOP including nominal operations and decommissioning. |
| SR3 | The payload shall be able to operate in space for at least five years. |
| | **Sustainability** |
| SU1 | The technology demonstration satellite shall be removed from space according to international regulations. |
| SU2 | The payload shall be usable as a standardized compulsory unit on LEO satellites. |
| | **Engineering budgets** |
| EB1 | The total mass of the payload shall be not more than 0.1 kg. |
| EB2 | The total mass of the technology demonstration satellite shall be not more than 10 kg. |
| EB3 | The payload shall be ready to be implemented as a compulsory unit on LEO satellites by 2030. |
| | **Cost** |
| CO1 | The total mission cost of the technology demonstration satellite shall be less than 10 Million Euros, including manufacturing, launching, and five years of operation. |
| CO2 | The development cost of the standardized payload shall be determined with associated uncertainty margins. |
| | **Legal/Regulatory** |
| LR1 | The payload and its usage as a compulsory unit on LEO satellites shall to comply with the international laws and regulations. If this is not possible, a roadmap shall be presented, how such compliance can be achieved. |
| LR2 | The technology demonstration mission shall comply with international laws and regulations. |

These top-level and stakeholder requirements are then translated into the system requirements, which are summarized in Table 2.4. In the detailed design these will then be assigned to their relevant subsystems and any remaining To Be Determined (TBD) values will be worked out there. In Table 2.4 a (⚠) indicates a driving requirement and a (🔑) indicates a key one.

**Table 2.4:** System Requirements

| ID | Driving/Key | Requirement |
|---|---|---|
| | | **Standardized Payload (SP)** |
| **STM-SYS-SP-1** | ⚠ \| 🔑 | The SP shall have a mass of at most 0.1 kg. |
| **STM-SYS-SP-2** | ⚠ \| 🔑 | The SP shall have a power consumption below 100 mW. |
| **STM-SYS-SP-3** | ⚠ \| 🔑 | The SP shall have a volume envelope of at most 5 cm × 5 cm × 1 cm. |
| **STM-SYS-SP-4** | | The SP shall not cause mechanical, electrical, or thermal problems or interference when flown on satellites. |
| **STM-SYS-SP-5** | ⚠ | The SP shall comply with PC104 and PQ60 integration standards. |
| **STM-SYS-SP-5.1** | | The SP design shall follow standard mechanical interface conventions as described in ECSS-E-ST-32C. |
| **STM-SYS-SP-5.2** | | The SP design shall follow standard electrical interface conventions as described in ECSS-E-ST-20C. |
| **STM-SYS-SP-5.3** | | The SP design shall support software integration. |
| **STM-SYS-SP-6** | | The data gathered by SP shall be transmitted to the ground station. |
| **STM-SYS-SP-7** | | The SP shall have a bandwidth requirement below <TBD>. |
| **STM-SYS-SP-8** | 🔑 | The SP shall provide position fixes with an accuracy of 20 meters (3D r.m.s.). |
| **STM-SYS-SP-9** | | The SP shall have a maximum development cost of at most 5 k€. |
| **STM-SYS-SP-10** | ⚠ \| 🔑 | The SP shall have a maximum manufacturing cost of at most 10 k€. |
| **STM-SYS-SP-11** | ⚠ | The SP shall be able to operate in orbit for at least 5 years. |
| **STM-SYS-SP-12** | | The SP shall be ready to be implemented as a compulsory unit on LEO satellites by 2040. |
| **STM-SYS-SP-13** | | The SP shall withstand all conditions during LEOP. |
| **STM-SYS-SP-13.1** | | The SP shall operate within a temperature range of -40 to +85 °C during LEOP. |
| **STM-SYS-SP-13.2** | | The SP shall withstand vibration levels up to 9 g RMS during LEOP. |
| **STM-SYS-SP-13.3** | | The SP shall withstand a vacuum pressure of $10 \times 10^{-5}$ mbar during LEOP. |
| **STM-SYS-SP-14** | | The SP and its usage as a compulsory unit on LEO satellites shall comply with <TBD> international laws and regulations. |
| **STM-SYS-SP-15** | | The SP shall operate within radio frequency bands allocated by the ITU and relevant national regulatory bodies, ensuring non-interference with existing space and ground systems. |
| **STM-SYS-SP-16** | | The integration and testing of the SP shall be safe. |
| **STM-SYS-SP-17** | | The SP shall be capable of performing autonomous PNT functions with European GNSS infrastructure. |
| **STM-SYS-SP-18** | | The SP shall have a reliability of 0.95. |
| **STM-SYS-SP-19** | | The SP shall come with complete documentation for manufacturing. |
| **STM-SYS-SP-20** | | The SP shall come with complete documentation for integration and testing. |
| **STM-SYS-SP-21** | | The SP shall provide secure data transfer. |
| | | **Demonstration Spacecraft (S/C)** |
| **STM-SYS-SC-1** | | The S/C shall host the SP. |
| **STM-SYS-SC-2** | | The S/C shall provide power to the SP. |
| **STM-SYS-SC-3** | | The S/C shall be compatible with CP-CDS-R14.1 [36] launch interfaces. |
| **STM-SYS-SC-4** | | The S/C shall meet all safety and operational requirements defined for the LEOP, including non-interference with the launch vehicle and co-passengers. |

Continued on next page.

| ID | Driving/Key | Requirement |
|---|---|---|
| **STM-SYS-SC-5** | ⚠ | The S/C shall have a mass of at most 10 kg. |
| **STM-SYS-SC-6** | | The S/C shall have a volume envelope of at most 11 cm × 11 cm × 11 cm. |
| **STM-SYS-SC-7** | | The S/C shall comply with ESA international laws and regulations. |
| **STM-SYS-SC-8** | ⚠ | The S/C shall be able to transmit all the on-board generated data to the ground station. |
| **STM-SYS-SC-9** | | The S/C shall support the reception of telecommands from ground stations. |
| **STM-SYS-SC-10** | | The S/C shall operate within radio frequency bands allocated by the ITU and relevant national regulatory bodies, ensuring non-interference with existing space and ground systems. |
| **STM-SYS-SC-11** | | The S/C shall be able to determine its attitude with pointing accuracy <TBD>. |
| **STM-SYS-SC-12** | | The S/C shall be able to control its attitude with pointing accuracy <TBD>. |
| **STM-SYS-SC-13** | | The integration and testing of the S/C shall be safe. |
| **STM-SYS-SC-14** | | The S/C shall have a reliability of <TBD>. |
| **STM-SYS-SC-15** | | The S/C shall have complete documentation for integration and testing. |
| **STM-SYS-SC-16** | | The S/C shall have complete documentation for manufacturing. |
| | | **Technology Demonstration Mission** |
| **STM-SYS-M-1** | ⚠ \| 🔑 | The S/C shall be inserted into a LEO with an altitude between 300 km and 800 km. |
| **STM-SYS-M-2** | | The S/C shall be launched piggyback. |
| **STM-SYS-M-3** | ⚠ | The S/C shall deorbit within 5 years after EOL. |
| **STM-SYS-M-4** | ⚠ \| 🔑 | The accuracy of the SP stated in STM-SYS-SP-8 shall be validated in orbit. |
| **STM-SYS-M-5** | | <TBD> portion of the data processing shall be done onboard. |
| **STM-SYS-M-6** | ⚠ \| 🔑 | The S/C shall remain operational for at least 6 months. |
| **STM-SYS-M-7** | | The Technology Demonstration Mission shall comply with UN international laws and regulations. |
| **STM-SYS-M-8** | ⚠ \| 🔑 | The Technology Demonstration Mission shall cost no more than 10 M€. |

# 3. Mission Architecture

The main mission of the project is to design a standardized payload for space traffic management. Then, to demonstrate this payload and validate its performance a technology demonstration satellite carrying the payload must be launched to LEO. With the requirements presented in Chapter 2 in mind, this chapter presents the mission architecture for the project. Section 3.1 provides the functional breakdown and functional flow. Section 3.2 then explains the logistics and operations concepts for the mission. Finally, Section 3.3 finishes the mission architecture by defining the orbit and launch parameters.

## 3.1. Functional Breakdown Structure & Functional Flow Diagram

Two diagrams were developed to support the mission analysis: the Functional Breakdown Structure (FBD) and the Functional Flow Diagram (FFD). The FBD, presented in Appendix A, gives a detailed hierarchical view of the spacecraft's functions. The FFD, presented in Appendix B, outlines the sequential timeline of mission activities.

## 3.2. Logistics and Operational Overview

The following section provides a closer examination of the inherent logistical and operational requirements of a satellite mission. As shown in Figure 3.1, the mission is divided into three primary phases, in accordance with industry standards[(1)]. However, these predefined phases do not fully align with the logistical time frame of the mission. Therefore, the timeline has been restructured into three distinct blocks, each with its own specific logistical and operational requirements, which will be discussed in more detail later. Despite these distinctions, the overall support infrastructure for the mission remains relatively simple, comprising a production facility, a single ground station for communication, a mission control center and a launch complex with its corresponding launch vehicle.

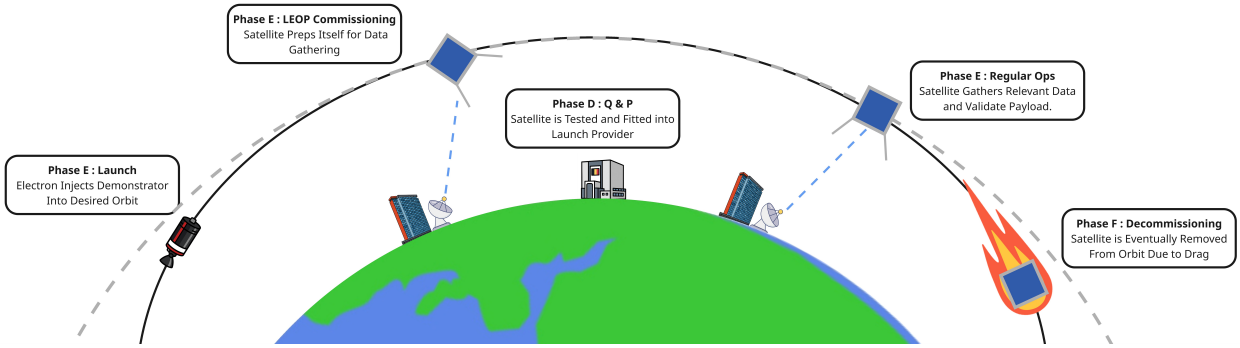


**Figure 3.1:** Concept of operations.

### Qualification and Production (Phase D)

Phase D as kept as it is defined by industry. It can be divided into two main parts: the first focuses on validating the demonstrator and the SP, while the second concerns the procedures required to safely hand over the spacecraft to the launch broker and complete all associated pre-launch steps.

Most spacecraft components will be Commercial off-the-shelf (COTS), which have already undergone a certain degree of testing. This reduces the need for additional testing, aside from verifying their performance parameters. The only components requiring comprehensive testing are the custom-made parts, such as the SP. Some tests can be performed using infrastructure available at TU Delft. However, for certain specialized tests, external companies such as ALTER[(2)] and SPACEMANIC[(3)] may need to be contacted to gain access to

[(1)]Building and Testing Spacecraft - ESA, 2025. [Online]. DoLA: June 18, 2025. Available: https://www.esa.int/Science_Exploration/Space_Science/Building_and_testing_spacecraft

[(2)]Small Sats Testing, doEEET, -, 2021. [Online]. DoLA: June 10, 2025. Available: `https://www.doeeet.com/content/small-satellites/`

[(3)]Our Services: Testing, SPACEMANIC, -, 2025. [Online]. DoLA: June 13, 2025. Available: `https://www.spacemanic.com/services/`

specialized testing facilities, such as a thermal vacuum testing.

The Rocket Lab User's Guide does not specify the acceptance testing required for payloads launching with them. Therefore, the Ariane 6 User's Manual was referenced to gain insight into the typical testing requirements for CubeSats [9]. According to the Ariane 6 guidelines, it is recommended that CubeSats undergo Static, Random Vibration, and Shock testing on both the Engineering Qualification Model and the Flight Model prior to integration with the launcher. Additionally, CubeSats must remain completely dormant during launch and must not interfere with any aspect of the launch vehicle's operation [37].

For certain tests, the spacecraft (S/C) must be fully assembled and integrated. To avoid contamination, the satellite must be baked prior to assembly and subsequently handled in an ISO Class 8 clean room. Such procedures are especially necessary for ride-share missions to avoid contaminating other spacecraft onboard the same launch vehicle [38].

Once all tests are completed and the satellite is validated, it will be shipped to the Rocket Lab processing facility closest to the chosen launch site.

### Launch (Phase E)

Deviating from the standard the next logical block defined is the launch block. It includes all activities between the satellite leaving the production facility up until its separation with the launcher.

The spacecraft is typically transported to the processing facility approximately 30 days before launch. It will be carried in a specialized transport case designed specifically to house CubeSats and will accompany the integration team on their flight to the processing facility [39]. Rocket Lab offers various support facilities for final preparations, although accommodations for the integration crew are not included [9].

During this period, final verification tests are conducted, the onboard battery is charged, and the final version of the software is uploaded and verified. The satellite is powered up and thoroughly checked. Once these steps are complete, the S/C is officially handed over to the launch provider and integrated onto the payload plate of the launcher. After integration, the entire payload is encapsulated, making it physically inaccessible. This typically occurs two weeks before launch [9].

Following a successful launch, there is a post-launch window of up to 90 min in which the CubeSat's state vector is provided by Rocket Lab to the costumer. This state vector includes the position of the launcher and the departure vector of the CubeSat [9]. While Rocket Lab does not specify when the S/C is allowed to emit Radio Frequency (RF) signals, a waiting period of 30 min is adopted, in accordance with the guidelines outlined in the Ariane 6 and Falcon 9 user guides [37, 38]. At this point, the S/C should be ready to begin the commissioning phase.

### Mission Operations (Phase E & F)

The last logistical block is the mission operations block. It begins once the satellite separates from the launcher, triggering its Boot Up Mode, and can start to operate independently in orbit. After a safe clearance from the launcher is confirmed, it performs a health check and initiates antenna deployment, while the passive stabilization starts immediately aligning the satellite with the Earth magnetic field.

The satellite will then begin to establish communication with the ground station. The primary candidate is the station atop the Electrical Engineering, Math and Computer Science (EEMCS) faculty building. However, depending on the satellite's initial orbit, it may not be in immediate contact with this station. Since commissioning is mission-critical additional ground stations may be required, along the path of the launcher. These services can be procured from external partners if necessary.

Due to the simple nature of the mission, no dedicated physical space is required for missions control, as the amount of data generated and the the commands send will be minimal. In fact, mission control can be located virtually anywhere, as a laptop could be sufficient to perform all necessary operations.

During regular operations, the spacecraft will operate itself in idle mode , where it simply conducts its mission and takes the snapshots at the specified rate. It will then switch to communications mode when it is expected to be in a contact window and then will wait till contact is established. When this happens, it will transmit down the gathered data and in return receive new mission parameters or even trigger software Update mode etc...

Then it will switch back to idle mission and it repeats this process until mission completeness. If it were to encounter any abnormality in its housekeeping data it will trigger a watchdog that will transition the spacecraft

into safe mode, until the issue can be resolved. For more explanation on how the mentioned mode works please refer to Figure 6.3

Once the mission objectives have been fulfilled, the logistical demands will decrease but will not disappear entirely. Since the spacecraft lacks the capability to actively de-orbit , it must instead rely on external forces, such as atmospheric drag, for orbital decay.As a result, continued monitoring is required until the spacecraft has lost sufficient energy to begin de-orbiting naturally. During this interim period, the spacecraft will transition into End of Life Mode and the primary operational focus will be on tracking the spacecraft's position to prevent potential collisions.

## Requirements Related Operations and Logistics

Only those requirements whose fulfillment results in substantive operational procedures or distinct logistics activities are listed below. Design-driven or commercial requirements that can be satisfied off-line during development have been omitted to shorten this section. For generating the operations and logistics implications for the mission phases and requirements, the operations and logistics sections of SMAD [40], The New SMAD [41], ECSS Space Engineering guides [42], and the NASA Systems Engineering Handbook [43] were used. Table 3.1 present the stakeholder requirements, Table 3.2 the SP ones and Table 3.3 those that relate to the S/C and mission.

**Table 3.1:** Stakeholder requirements: Operations and logistics implications.

| Req ID | Requirement (abridged) | Operations implications | Logistics implications |
|---|---|---|---|
| STM-SH-PB-1 | Launch success | Launch countdown; Go/No-Go procedures | Transport to pad; schedule buffer for unexpected circumstances |
| STM-SH-PB-4 | Safe de-orbit | Disposal timeline; alert preperations | - |
| STM-SH-U-1 | Orbital-prediction support | Bulk downlink windows | Data-sharing agreements |
| STM-SH-U-2 | Reliable data transfer | Link-margin, ground station access | Link budget tests |
| STM-SH-U-3 | Secure data transfer | Encryption protocol | Encryption modules; ITAR compliance |
| STM-SH-U-5 | Improve SSA | Real-time data transfer to the SSA network | Cloud-based information sharing |
| STM-SH-SA-1 | Aid collision avoidance | Daily orbital prediction updates | Software patches and upgrades |
| STM-SH-SA-2 | Debris-mitigation compliance | End-of-life checklist in the ops. plan | Checklist and compliance documentation |
| STM-SH-RA-1 | EOL disposal procedure | EOL ops. | Legal notifications |
| STM-SH-RA-3 | Operate within bands | Spectrum monitoring ops. | Band-pass filters; RF license |
| STM-SH-LV-1 | Launch-interface compatibility | Connection checks; compatibility tests | - |
| STM-SH-SO-6 | Full ops. documentation | ops. guide, procedure checklists | Operator training |
| STM-SH-GS-1 | Ground-station comms. | Contact plan; Doppler windows | Station contracts; link budget |
| STM-SH-ENG-1 | Easy AIT debugging | Convenient interface; diagnostics | Break-out harnesses; debug ports |

**Table 3.2:** System requirements: Standardized payload.

| Req ID | Requirement (abridged) | Operations implications | Logistics implications |
|---|---|---|---|
| STM-SYS-SP-2 | ≤40 mW average power | Power budgeting; | Low-power parts; Power supply units for tests |
| STM-SYS-SP-4 | No mech./elec./thermal interference | Compatibility checklist; thermal evaluation | Safety equipment |
| STM-SYS-SP-6 | Transmit data to GS | Communication channel allocation | Antenna coupons; RF front-end |
| STM-SYS-SP-8 | 20 m (3D r.m.s.) accuracy | Snapshot-GNSS ops.; in-orbit calibration | Flight GNSS chipset procurement |
| STM-SYS-SP-11 | Operate ≥ 5 y | Radiation monitoring; Health inspections | Radiation tolerant parts; warranties; |
| STM-SYS-SP-13 | Survive Launch/LEOP | Safe-mode ops.; safe-mode limits | Vibration & pyro-shock tests |
| STM-SYS-SP-17 | Autonomous PNT | Self-test routines; ephemeris cache | - |
| STM-SYS-SP-21 | Secure data transfer | Encryption key handling in ops. | Secure ground links |
| STM-SYS-SP-23 | ≤10 kB telecommand/day | Command budget; Data flow | Key distribution logistics |

**Table 3.3:** System requirements: Spacecraft and mission.

| Req ID | Requirement (abridged) | Operations implications | Logistics implications |
|---|---|---|---|
| STM-SYS-SC-1 | Host the SP | Allocate volume, harness, power, thermal | Harness kit |
| STM-SYS-SC-2 | Provide power | EPS power cycle tables, safe budgets | EPS board; solar panel documentation |
| STM-SYS-SC-8 | Comply with laws | ITAR/ECCN checks | Approvals; customs documents |
| STM-SYS-SC-12 | Determine attitude | ADCS calibration passes | - |
| STM-SYS-SC-13 | Control attitude | Reaction-wheel tables; safe-mode rules | Torque-rod spares; wheel spare |
| STM-SYS-M-1 | Insert into 300–800 km LEO | Orbit insertion ops. | Launch contract; |
| STM-SYS-M-4 | Verify SP accuracy | Dedicated verification phase | Additional verification payload |
| STM-SYS-M-6 | Operate ≥ 6 months | Operations staff, consumable goods tracking | Ground station contracts; warranties |

| Req ID | Requirement (abridged) | Operations implications | Logistics implications |
|---|---|---|---|
| STM-SYS-M-7 | Mission legal compliance | Legal considerations; procedure updates | Compliance archive |

## 3.3. Mission Orbit and Launch

This section will outline the orbital parameters and launch characteristics of the mission. In Subsection 3.3.1 the requirements are listed that drive the preliminary design, in Subsection 3.3.2, and detailed design, in Subsection 3.3.3. Having finished the design, the characteristics are reiterated for clarity in Subsection 3.3.4.

### 3.3.1. Requirements

The requirements regarding the validation system for the standardized payload are given in Table 3.4 and were generated in the previous report [44]. An overview of the all the requirements and if the mission complies can be found at the end of the report in Table 4.17.

**Table 3.4:** Requirements that drive the mission design.

| ID | Requirement |
|---|---|
| STM-SYS-M-1 | The S/C shall be inserted into a LEO with an altitude between 300 km and 800 km. |
| STM-SYS-M-3 | The S/C shall deorbit within 5 years after EOL. |
| STM-SYS-M-6 | The S/C shall remain operational for at least 6 months. |
| STM-SYS-SP-12 | The SP shall be ready to be implemented as a compulsory unit on LEO satellites by 2040. |

Requirement STM-SYS-M-3 was a constraint by ESA Space Debris Mitigation Requirements [30], which states that spacecraft without recurrent maneuver capabilities shall have an orbital lifetime of less than 5 years starting from the orbit injection epoch. Requirement STM-SYS-M-6 was decided upon since the reliability of components is still above 75 % for S/C in the first six months [45]. It should be noted that a longer mission duration is preferred as it provides more data but 6 months still provides large enough time frame for all the scheduled tests.

### 3.3.2. Preliminary Design Results

In the previous report [46], two launch options were determined using a rudimentary analytical model that ensure that the S/C would de-orbit within a time frame of 5 years. The early launch option would launch between 2028 and 2030 to an altitude of 400 km using the Electron launch vehicle from RocketLab. The other option would be a later launch in 2032 to 2034 to a higher altitude of 500 km. The higher altitude was possible due the mission being closer to the solar maximum of the solar cycle. The solar cycle is an 11-year cycle where the solar activity fluctuates. Near the solar maxima, higher solar activity and flux are observed which cause the atmospheric density to increase in LEO. The higher density creates more drag on the S/C which results in a shorter orbital lifetime. If an even later launch is favored, an even higher altitude needs to be chosen as the solar maximum is around 2035/2036. The two preliminary options are shown in Table 3.5.

**Table 3.5:** Preliminary launch parameter options.

| Parameter | Launch 1 | Launch 2 |
|---|---|---|
| Altitude [km] | 400 | 500 |
| Launch year | 2028-2030 | 2032-2034 |
| Launch provider | Rocket Lab | SpaceX |
| Launch location | New Zealand | USA |

### 3.3.3. Detailed Design

Now that a foundation has ben laid by the preliminary design, the detailed design can commence. First the orbit is evaluated in detail, then the rest of the mission architecture is discussed in Figure 3.3.3.

#### Determining optimal orbit

For the orbit it was decided that the eccentricity is assumed to be close to zero. This is deemed to be justifiable as the launch provider provides an orbit injection accuracy of ±15 km[9]. This simplifies calculations and is justified since most LEO are near circular. A circular orbit is also preferred for this mission as this provides consistent ground contact time compared to elliptical orbits.

**Orbital Altitude**

The preliminary altitudes that were determined to be 400 km and 500 km were found via analytical models. For the detailed design a semi-empirical model was created with as inputs the altitude, mass, surface area, solar 10 cm radio flux and geomagnetic index. The latter two were derived for 2029 using data from the last decades [47]. The model numerically integrates using a very coarse density model without any other perturbations. This resulted in an orbital lifetime of 3.43 years for 400 km.

However, after having ran a simulation in General Mission Analysis Tool (GMAT) for 400 km starting from 1st January 2029 it was found that this resulted in an orbital lifetime of 4 months. This large difference is due to simplified model not accounting for seasons, solar extremes or variations in the density. Since such a large discrepancy between the models exist, the semi-empirical model was dismissed and only the high-fidelity model is used.

An orbital lifetime of 4 months is too short to accomplish the mission as a settling time for tumbling has to be happen and varying snapshot rates will be tested with varying tumbling speeds. Thus, the altitude was increased to 500 km to lengthen the orbital lifetime of the S/C. After running the simulation with the new altitude, a lifetime of about 2.2 years was found. The altitude can vary by some kilometers around this range depending on the mission requirements set by the main payload satellite that the S/C would ride-share with.

The earlier launch option, between 2028 and 2030, is chosen as it is enough time for the construction and testing of the S/C. It also helps to achieve requirement **STM-SYS-SP-12** which states; *"The SP shall be ready to be implemented as a compulsory unit on LEO satellites by 2040"*.

**Orbital Inclination**

The orbital inclination is chosen to optimize the satellite's communication window with the ground station. The TU Delft's ground station was preliminary chosen to be the primary one. It is possible to transfer all data between the ground station and S/C when only using Delft. Thus, it will be the only ground station used, which additionally minimizes the cost of the mission.

The preliminary inclination was determined to be 55° which is refined in this section using GMAT. Some variables still need to be established before running the simulation. One variable is the minimum elevation angle. The common minimum elevation angle taken for CubeSats is between 2° and 10° [48]. For this specific mission, the ground station is at TU Delft with the communication systems being on top of the EWI-building, which is 90 m tall[(1)], without any other high-rise buildings present. Thus, the minimum elevation angle would probably fall on the lower end. However, to guarantee communication a conservative estimate is taken of 10 degrees. This angle is also taken in Delfi-n3Xt's design [49].

Lastly, the launch date is chosen such that the ecliptic true solar longitude, $\Gamma$, is zero to ease calculations. The launch date causes the Right Ascension of the Ascending Node (RAAN) to begin at $-180°$ and it shifts throughtout the mission duration by around $-3.825°$ per day due to nodal precession caused by the J2 perturbation.

With these variables, GMAT was used to model the communication windows between the S/C and the Ground Station (GS) for a month. The amount of times the S/C came into contact range of Delft, the visitation frequency, and contact time during each pass were graphed with different inclinations to optimize inclination. These are shown in Figure 3.2 and Figure 3.3 respectively.

The reason for the significant drop in visitation frequency after 64 ° can be explained by the S/C being just outside of the communication cone of the TU Delft created by the minimum elevation angle.

The optimal inclination angle maximizes the amount of time the S/C and GS can communicate on average, which Figure 3.3 is shown to be 60°. With this inclination it can communicate, on average, for around 9.5 % of the orbit. It should be noted that the initial inclination of the launch vehicle will not exactly be 60°. However, RocketLab guarantees the preferred inclination even if the main payload satellite will be inserted in another inclination [50]. Furthermore, it has been checked that communication with the TU Delft is possible as long as the inclination is at least 52°, as TU Delft lies on 52° latitude. A lower inclination would result in a trajectory that does not extend sufficiently northward to communicate with Delft.

**Eclipse Duration**

Both the power and thermal subsystem design iterations require knowledge of the eclipse period for the chosen orbit, as it directly influences the amount of solar radiation received. However, due to the drift of the RAAN, the actual eclipse duration will vary over time [51]. The eclipse period of an orbit depends on its $\beta$ angle, which

[(1)]EWI TU Delft, Dylunio, [Online]. DoLA: 04/06/2025, url:https://www.dylunio.nl/projecten#/ewi-tu-delft/

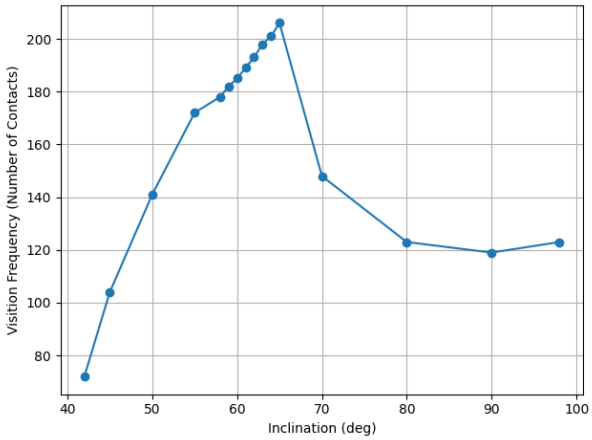


**Figure 3.2:** Number of contact moments between TU Delft and a LEO satellite at 500 km in one month for a 10 ° minimum elevation angle.

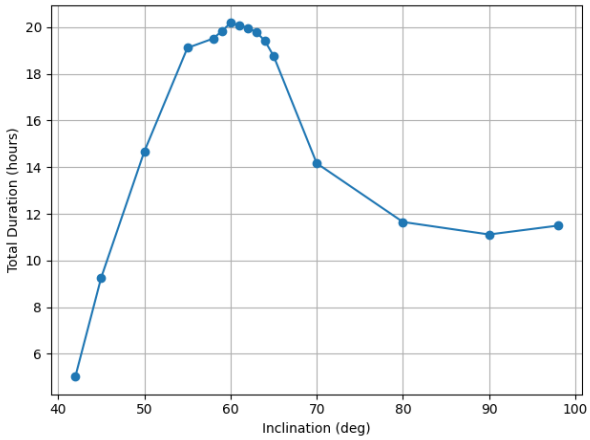


**Figure 3.3:** Amount of contact time between TU Delft and a LEO satellite at 500 km in one month for a 10 ° minimum elevation angle

is defined as the angle between the orbital plane and the Sun vector. The drift of the $\beta$ can be estimated by considering the drift of the RAAN and the Sun vector, its exact value can be determined using Equation 3.1 [52].

$$\beta = \sin^{-1}\left[\cos(\Gamma)\sin(\Omega)\sin(i) - \sin(\Gamma)\cos(\epsilon)\cos(\Omega)\sin(i) + \sin(\Gamma)\sin(\epsilon)\cos(i)\right] \tag{3.1}$$

Here, $\Gamma$ is the ecliptic true solar longitude and drifts by $0.986\,^\circ\,\mathrm{d}^{-1}$ [52]. $i$ is the orbit's inclination, and $\epsilon$ is the obliquity of the ecliptic, which has a value of 23.45° and does not change. $\Omega$ is the RAAN, who's drift can be calculated using Equation 3.2 [51].

$$\dot{\Omega} = \frac{-3}{2} J_2 \left(\frac{R_E}{h}\right)^2 \sqrt{\frac{\mu}{h^3}} \cos i \tag{3.2}$$

In this equation, $\mu$ is the standard gravitational parameter, $R_E$ the radius of the Earth, $h$ the orbital altitude and $J_2$ is a parameter that account for the oblateness of the earth. Equation 3.3 [53] is used to finally attain an estimate for the eclipse duration over the whole six month mission duration and is given as a percentage.

$$f_E = \begin{cases} \frac{1}{\pi}\arccos\left(\frac{\sqrt{2R_E h + h^2}}{(R_E + h)\cos\beta}\right) & |\beta| < \beta^* \\ 0 & |\beta| \geq \beta^* \end{cases} \tag{3.3}$$

Here $\beta^*$ is called the critical $\beta$ angle. It is the value of $\beta$ after which eclipse periods will no longer occur and the S/C will remain in continuous sunlight, which is determined using Equation 3.4 [53].

$$\beta^* = \arcsin\left(\frac{R_E}{R_E + h}\right) \tag{3.4}$$

Using the previously determined orbital parameters, a critical $\beta$ angle of approximately 68° was calculated. With all relevant orbital elements and their interrelationships established, the expected $\beta$ angle can be computed for each day of the mission by propagating the necessary parameters accordingly. This results in a $\beta$ range from $-40.84°$ to 83.43° over the six-month mission duration, as illustrated in Figure 3.4a. The corresponding eclipse fraction is shown in Figure 3.4b.

Examining Figure 3.4b, it was concluded that the longest eclipse period will be when the $\beta$ angle is equal to zero. A $\beta$ angle of 0 results in a eclipse fraction of 37.79 %.

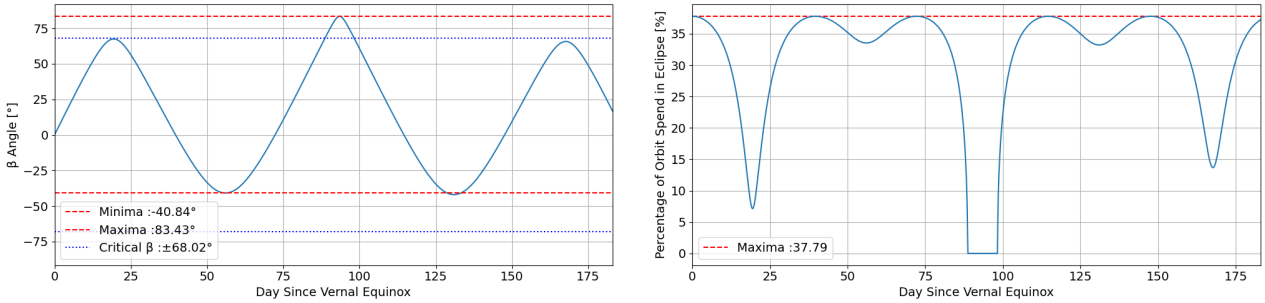


**(a)** $\beta$ angle variation over the six month mission duration.

**(b)** Fraction of orbital period spent in eclipse over the six month mission duration.

**Figure 3.4:** Comparison of mission parameters over the six-month duration.

### Determining the launch

Having determined the orbit, a launch segment can be found that best suits the mission. First, the launch provider will be decided on which will result in the launch site. Finally, the launch site can be used to calculate a suitable launch angle called the launch azimuth.

**Launch Provider** More than twelve launch providers and brokers were considered with the constraints consisting of their ability to launch at the desired orbit and rideshare capabilities. Other launch brokers seemed promising but were ruled out for not disclosing the cost of their services. Further research may send inquiries to launch brokers to determine if a more suitable option exists.

Three remaining options remained: SpaceX, RocketLab and Nanoracks. SpaceX mainly launches at 500 km due to the injection of the Starlink constellation [54]. The Nanoracks option only deploys at an inclination of 51.8 ° which is too close to the lower limit of visibility between GS and S/C [55]. SpaceX is a more affordable option but mainly launches in a Sun-Synchronous Orbit (SSO) and is an American company which is not preferred due to the geopolitical developments. That leaves RocketLab as the most suitable option. It should be noted that a revision may occur when actual inquiries are sent to launch brokers/providers.

**Launch Location** With the Rocket Lab being selected as launch provider, the launch location needs to be selected. Possible launch locations are the Rocket Lab Launch Complex 1, Mahia-LC-1, in the Mahia Peninsula, New Zealand or Mid-Atlantic Regional Spaceport Launch Complex 2, MARS-LC-2 on Wallops Island in Virginia[(1)]. The MARS-LC-2 is mainly used for their hypersonic suborbital rocket. With this information, the Mahia-LC-1 will be the assumed launch site.

**Launch Date** The launch window was set to be between 2028 and 2030. Preferably, the launch is at the end of March in 2029 as this is when the ecliptic true solar longitude, $\Gamma$, is around zero. In reality, a launch date somewhere around this date will be chosen based of the availability of the piggy-back launches but this would not significantly alter the values.

**Launch Azimuth** The launch azimuth is the angle at the launch site between true north and the orbital plane in which the launch vehicle launches. To simplify, it is the compass heading one heads for. It is most efficient to launch eastwards to utilize the rotation of the Earth for a velocity boost.

The azimuth angle, $\beta$, can be determined by using spherical trigonometry using the desired inclination, $i$, and the given latitude of the launch site, $\phi$ using Equation 3.5.

$$\cos(i) = \cos(\phi) \cdot \cos(\beta) \tag{3.5}$$

Now solving for the launch azimuth angle results in:

$$\beta = \arcsin(\frac{\cos(i)}{\cos(\phi)})$$

With an inclination of 60°, the launch site being the Mahia Peninsula in New Zealand, having a latitude of −39.2609°, the resulting azimuth angle is 40.22° northeast trajectory, or 139.78° southeast trajectory.

Both options will result in the same orbit but 40.22° would be preferred considering the safety concerns due to the distance the Electron rocket travels downrange.

[(1)]Launch Experience, RocketLab, [Online]. DoLA: 02/06/2025. URL: https://rocketlabcorp.com/launch/launch-with-us/

### 3.3.4. Mission Characteristics

This section summarizes all the determined parameters as to give an overview of the chosen orbit and launch architecture. Some values were calculated from the previously determined values and are used later on in the report for sizing. The first of these parameters is the orbital period which is calculated via Equation 3.6.

$$T = 2\pi\sqrt{\frac{a^3}{GM_E}} \tag{3.6}$$

Where $a$ is the semi-major axis. However, due to the assumption of a circular orbit this is equal to the radius of the Earth plus the altitude, $R_E + h$, and is 6871 km. Lastly, $GM_E$ is the gravitational coefficient of the earth and often shown as $\mu_E$. The drag coefficient is taken as the standard for CubeSats at 2.2 [41].

**Table 3.6:** Mission parameters.

| Parameter | Symbol | Value | Unit |
|---|---|---|---|
| Altitude | $h$ | 500 | km |
| Inclination | $i$ | 60 | ° |
| RAAN | $\Omega$ | $-180$ | ° |
| Eccentricity | $e$ | 0 | - |
| Ecliptic true solar longitude | $\Gamma$ | 0 | ° |
| Orbital period | T | 5668 | s |
| Average time between passes | $\Delta t_{avg}$ | 14 022 | s |
| Drag Coefficient | $C_d$ | 2.2 | - |
| Orbital velocity | v | 7.61 | $\mathrm{km\,s^{-1}}$ |

**Table 3.7:** Launch parameters.

| Launch site | Launch date | Launch provider | Launch vehicle | Ground station |
|---|---|---|---|---|
| Rocket Lab Launch Complex 1 | 2028/2030 | RocketLab | Electron | TU Delft |

### 3.3.5. Conclusion and next steps

Now that the mission architecture has been decided, the design of the SP and the rest of the S/C can commence. First, the SP is worked out in Chapter 4. The rest of the S/C is then created to accommodate the SP in Chapter 5.

For future research and to realize the mission the following steps need to be taken:

1. **Establish a launch date:** Inquire about the planned ride-share missions with Rocket Lab to see if a suitable options exists. If not, reach out to other launch brokers. ISISpace is a valid options with the added benefit of being a long-time partner of the TU Delft.
2. **Finalize final orbital parameters:** Rerun the simulations with the finalized data now that the launch date is known using the steps laid out in this chapter.
3. **Document findings:** Update and document the final parameters.

# 4. Standardized Payload Design

The Standardized Payload is an accurate, low-power GNSS payload that can be taken on any LEO satellite. It has been decided that a fully autonomous payload, capable of calculating a position fix without any external support from ground stations or host S/C, is the most attractive option. To achieve this, a dual receiver configuration was found to be effective during the preliminary design phase.

This chapter describes the complete design of the Standardized Payload, emphasizing the electronics and the Printed Circuit Board (PCB) used to turn it into a fully functional product. The SP is composed of three sub-assemblies: one main electronics board covered by an aluminum enclosure that houses the GNSS receivers, Microcontroller Unit (MCU), and other supporting Integrated Circuit (IC)s; and two antenna sub-assemblies composed of a PCB acting as a ground plane (to improve antenna coverage), with a GNSS patch antenna soldered on top, connected to the SP PCB within the satellite by using coaxial cables.

Section 4.1 explains how the GNSS signals work and how the SP can generate position fixes by using these signals. Furthermore, Section 4.2 lists the requirements on which the detailed design process was based. These have been taken from the midterm report [46], and some have been adapted based on updated data. Section 4.3 describes the standardization aspects of electrical and mechanical interfaces. These are vital in the pursuit of making the SP a standardized and 'plug-and-play' module. Section 4.4 describes all the components the SP is comprised of, down to the resistors and capacitors, presenting the bill of materials for building one SP. Then, Section 4.5 describes each of the main components in detail, presents their pinout, and then explains how they are all connected. The section ends with Subsection 4.5.4, which shows a complete design of the PCB used as the heart of the SP.

Section 4.6 introduces how to about GNSS antenna placement on the host satellite in relation to ephemerides acquisition and offers the rationale for a second antenna while also narrowing down the required ephemerides update frequency. Section 4.7 then evaluates and describes where on the host spacecraft they could be placed.

Section 4.8 follows next, in which the power consumption of the SP is treated, then Section 4.9 circles back to the requirements and displays if all of them are met. The chapter concludes with Section 4.10 where an overview of the complete design is given.

## 4.1. Design Context

To provide a high-level overview of how this payload can utilise the GNSS signals to reach position fixes, the GNSS signal structure and the concept of the SP will be explained in this section.

### GNSS Signal Structure

The navigation message transmitted by the GNSS satellites is a 12.5 min long combination of 25 frames. Each frame is 30 s long and is divided into 5 equally large sub-frames [(1)]. The most important part of these signals for the SP is ephemerides and almanac data, as they are fundamental to computing GNSS position fixes.

- **Ephemerides:** centimeter to meter-level accurate Keplerian orbit parameters for the individual transmitting satellite
- **Almanac:** coarse orbital parameters for the entire constellation.

Commonly, the first three sub-frames contain information about the ephemerides. These subframes are repeated every 30 s until the ephemerides reaches the end of its validity period. The last two sub-frames contain information about the almanac, and this changes after the 5 sub-frames are completed. Therefore, it takes 12.5 min to acquire a full set of almanac data [(2)].

Once the recorded almanac provides a newly powered receiver with the coarse positions of all GNSS satellites for the first time, it can now concentrate on the correct Pseudo-Random Noise (PRN)s. These PRNs are unique identifiers used by satellites to distinguish their signals from others. Therefore, they allow the GNSS receiver to understand which satellite ephemerides they are acquiring and storing. After recording the first three

[(1)]GPS Navigation Message - Navipedia (ESA GNSS Science Support Centre), 2011. [Online]. Accessed: June 23, 2025. Available: https://gssc.esa.int/navipedia/index.php/GPS_Navigation_Message

[(2)]GPS Navigation Message - Navipedia (ESA GNSS Science Support Centre), 2011. [Online]. Accessed: June 23, 2025. Available: https://gssc.esa.int/navipedia/index.php/GPS_Navigation_Message

sub-frames to acquire ephemerides, the SP now has to take snapshots of these GNSS signals to solve for position fixes.

## Standardized Payload Concept

Generating a position fix implies solving for position unknowns, which are classified as $x, y, z$, time unknown $t$, and receiver clock bias $b$ [56]. Therefore, there are 5 unknowns to be determined.

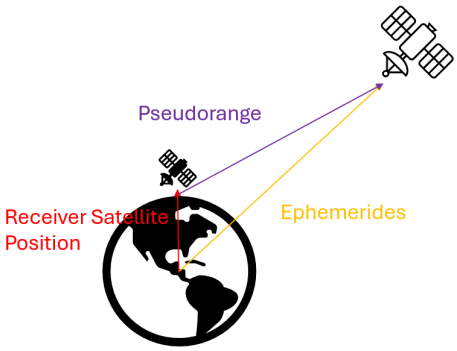


**Figure 4.1:** Schematic for generating position fixes from snapshots

As Figure 4.1 shows, acquiring ephemerides provides the receiver with the position of a specific GNSS satellite with respect to the Earth. Without ephemerides, the receiver satellite position cannot be solved due to the number of unknowns. Once the ephemerides is available, the SP records a snapshot of the GNSS signal, which is used to determine the relative distance between the receiver and the GNSS satellite, the pseudorange, by evaluating the clock information. This is shown by the purple vector in Figure 4.1.

With 5 unknowns to be determined, snapshot processing requires 5 equations. Therefore, the SP will record 5 different pseudoranges from 5 different GNSS satellites to iteratively solve for the unknowns [56]. The solution will provide the receiver satellite position, as shown by the red vector.

## Operational Concept - Dual Receiver, All Processing Internal

1. **Commissioning:** Before launch, ground uploads an initial almanac; MCU stores it in flash and pushes it to the ephemerides acquisition receiver Ephemerides Acquisition Receiver (EAR). Alternatively, the almanac can also be uplinked from the ground or acquired by EAR by turning the RF front-end on for 15 min.
2. **Ephemerides upkeep:** Three times every 2 orbits, the EAR is powered for ~50 s, obtains an ephemerides set before returning to Real-Time Clock (RTC) sleep.
3. **Snapshot loop:** Every 10 min:
   (a) MCU enables Temperature Compensated Crystal Oscillator (TCXO) & MAX2769 snapshot receiver; waits 3 ms for frequency lock
   (b) Records a 20 ms Intermediate Frequency (IF) burst, also named as **snapshot** (~16 kB),
   (c) Baseband processor in MCU runs Fast Fourier Transform (FFT)-based acquisition  tracking, decodes navigation data and computes Earth Centered Earth Fixed (ECEF) position (~750 ms of MCU time),
   (d) packages position, velocity, time, and housekeeping data for the host,
   (e) powers down RF, TCXO, and returns MCU to Stop-mode.

A high-level overview of how the components are connected for this operational concept is provided in Figure 4.2

As the figure shows, the antenna captures the signal and feeds it either into the EAR or the snapshot receiver. Then, the snapshots are processed in the MCU to generate position fixes. This data is stored in the non-volatile memory and then transferred to the OBC. The system is powered by the EPS, which provides voltages that are regulated by the power management unit.

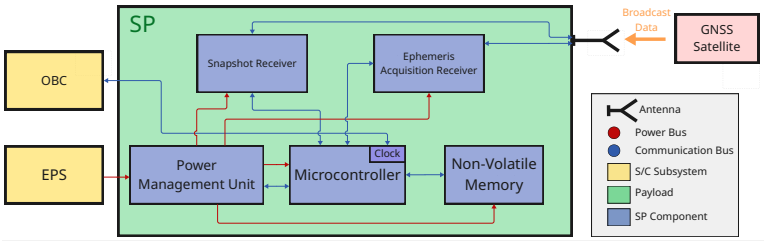


**Figure 4.2:** High Level SP Electric Block Diagram. [57]

### Frequency Band Considerations

Ionospheric refraction is a significant source of error for signal acquisition and position calculation [(1)]. Therefore, to minimize this error, a dual-frequency approach was chosen. By measuring the difference in delay between two frequencies, the refraction can be corrected. As L1 is the most commonly used frequency band for GNSS receivers [58], one of the frequencies was chosen as L1, and due to the high power transmission capabilities of L5 that result in higher gain and precision [58], L5 was chosen as the second one.

## 4.2. Requirements

This section presents the requirements for the standardized payload as shown in Table 4.1. This serves as the starting point for the detailed design. These are based on the final requirements from the preliminary design [46]. Requirements marked with an asterisk (*) have been updated, and a rationale for the update is provided.

**Table 4.1:** SP final requirements. Requirements marked with an asterisk (*) have been updated from their previous (midterm) versions.

| ID | Requirement |
|---|---|
| **STM-SYS-SP-1** | The SP shall have a mass of at most 0.1 kg |
| **STM-SYS-SP-2*** | The SP shall have an average power consumption below 1 mW. |
| **Rationale:** | The SP average power consumption found in the previous design phase was 0.26 mW. Aiming for below 1 mW average power is a reasonable goal for detailed design. |
| **STM-SYS-SP-3*** | The SP shall have a board area of at most 48 mm × 48 mm. |
| **Rationale:** | PocketQubes, which are the smallest satellites that this standardized payload is expected to accommodate, have an available area of 25 $cm^2$. Leaving a small margin at the sides, the maximum area of the SP board should not exceed 4.8 cm × 4.8 cm = 23.04 $cm^2$. |
| **STM-SYS-SP-4** | The SP shall not cause mechanical, electrical, or thermal problems or interference when flown on satellites. |
| **STM-SYS-SP-5.1** | The SP design shall follow standard mechanical interface conventions as described in ECSS-E-ST-32C. |
| **STM-SYS-SP-5.2** | The SP design shall follow standard electrical interface conventions as described in ECSS-E-ST-20C. |
| **STM-SYS-SP-5.3*** | The SP shall expose a documented Universal Asynchronous Receiver/Transmitter (UART), Serial Peripheral Interface (SPI), Inter-Integrated Circuit (I2C) API for command, control, and data telemetry integration with the host spacecraft. |
| **Rationale:** | More communications protocols have been added to the requirement. |
| **STM-SYS-SP-6** | The data gathered by the SP shall be transmitted to the ground. |
| **STM-SYS-SP-7*** | The SP's GNSS front-end shall support a minimum RF sampling bandwidth of 4.092 MHz. |
| **STM-SYS-SP-8** | The SP shall provide position fixes with an accuracy of 20 m (3-D r.m.s.). |
| **STM-SYS-SP-9** | The SP shall have a maximum development cost of at most 5 k€. |
| **STM-SYS-SP-10*** | The SP shall have a maximum manufacturing cost of at most €1000. |
| **Rationale:** | The unit cost has been narrowed down in the previous design phase, and a maximum cap of €1000 is imposed in order to keep the design low-cost. |
| **STM-SYS-SP-11** | The SP shall be able to operate in orbit for at least 5 years. |
| **STM-SYS-SP-12** | The SP shall be ready to be implemented as a compulsory unit on LEO satellites by 2040. |
| **STM-SYS-SP-13** | The SP shall withstand all conditions during LEOP. |
| **STM-SYS-SP-13.1** | The SP shall operate within a temperature range of −40 °C to 85 °C during LEOP. |
| **STM-SYS-SP-13.2*** | The SP shall withstand vibration levels up to 9 g RMS during LEOP. |
| **Rationale:** | Falon 9 user guide states the maximum vibration level is 8.5 g [38]. |
| **STM-SYS-SP-13.3** | The SP The SP shall withstand a vacuum pressure of $10 \times 10^{-5}$ mbar during LEOP. |
| **STM-SYS-SP-14** | The SP and its usage as a compulsory unit on LEO satellites shall comply with <TBD> international laws and regulations. |
| **Note:** | A rigorous review of applicable international space laws and regulations will be completed post Design Synthesis Exercise (DSE). |

*Continued on next page.*

[(1)] Why multi-frequency and multi-constellation matters for GPS/GNSS receivers – Septentrio, 2025. [Online]. DoLA: June 23, 2025. Available: https://www.septentrio.com/en/learn-more/about-GNSS/why-multi-frequency-and-multi-constellation-matters

| ID | Requirement |
|---|---|
| **STM-SYS-SP-15** | The SP shall operate within radio-frequency bands allocated by the ITU and relevant national regulatory bodies, ensuring non-interference with existing space and ground systems. |
| **STM-SYS-SP-16** | The integration and testing of the SP shall be safe. |
| **STM-SYS-SP-17** | The SP shall be capable of performing autonomous Position, Navigation and Timing (PNT) functions with European GNSS infrastructure. |
| **STM-SYS-SP-18** | The SP shall have a reliability of 0.95. |
| **STM-SYS-SP-19** | The SP shall come with complete documentation for manufacturing. |
| **STM-SYS-SP-20** | The SP shall come with complete documentation for integration and testing. |
| **STM-SYS-SP-21** | The SP shall provide secure data transfer. |
| **STM-SYS-SP-25** | The SP shall have a maximum volume of 10 $cm^3$. |
| **STM-SYS-SP-26** | The SP shall have an antenna capable of receiving signals in the L1 and L5 frequency bands. |

## 4.3. Standardization

One goal of this payload is to design it as a plug-and-play module for as many LEO satellites as possible. This requires compatible electrical and physical interfaces which most spacecraft have. For this analysis, PocketQubes and CubeSats in particular have been analyzed as this payload was designed to reduce mass and power, which becomes crucial the smaller the satellites gets. However, larger satellites have also been analyzed.

### Electrical Interfaces

One important factor to consider is how the SP will communicate with the satellite. Most likely, it will communicate primarily with the On-Board Computer (OBC). In order to make it as easy as possible for the satellite designer to integrate the SP, the aim is accommodate for the most commonly used communication protocols within the satellite. This will allow for the desginer not needing to adjust for new communication protocols and the SP can simply be connected to the already existing communication bus. Some of the most common intra-satellite communication protocols are: I2C, SPI, Recommended Standard 485 (RS-485), Recommended Standard 232 (RS-232), Military Standard (MIL-STD)-1553, Controller Area Network (CAN), Universal Synchronous/Asynchronous Receiver/Transmitter (USART), Low-Power Universal Asynchronous Receiver/Transmitter (LPUART), Serial Audio Interface (SAI), Secure Digital/MultiMediaCard Interface (SDMMC), Carrier Recovery System (CRS), Universal Serial Bus (USB) and Quad Serial Peripheral Interface (QUADSPI). In Table 4.2, one can find all these standards in addition to a 'Commonly Used in S/C' column which is based on whether the data bus communication type is commonly used in satellites [59–61] and deemed necessary. The compatibility column is based on whether the chosen MCU (STM32L452) offers the capability of communication via the electrical data bus communication type [62].

**Table 4.2:** MCU data bus compatibility.

| Data Bus Communication Type | Commonly Used in S/C | MCU Compatiblility |
|---|---|---|
| I2C | Yes | Yes |
| SPI | Yes | Yes |
| RS-485 | Yes | via USART |
| RS-232 | Yes | via USART |
| MIL-STD-1553 | Yes | No |
| CAN | Yes | Yes |
| USART | Yes | Yes |
| LPUART | Yes | Yes |
| SAI | No | No |
| SDMMC | No | No |
| CRS | No | No |
| USB | No | Yes |
| QUADSPI | No | Yes |

As can be seen in Table 4.2, the MIL-STD-1553 data bus communication type is deemed necessary but not compatible with the SP MCU. In order for these communication types to work one needs a protocol controller and transformers for the MIL-STD-1553 communication standard [63], which will be implemented into the PCB design.

Considering the desired data bus communication types certain aspects of the design have to be considered in addition to the number of pins required when designing the SP. This is summarized in Table 4.3.

**Table 4.3:** Satellite bus communication protocol pins and external components.

| Protocol | Pins Used | External Components |
|---|---|---|
| I2C [64] | SCL, SDA | Pull-up resistors (typically 4.7 kΩ) |
| SPI [65] | SCLK, SIMO, SOMI, CE (per device) | Optional series resistors (33 Ω to 100 Ω) |
| USART, LPUART [66] | TX, RX | Level shifter (e.g., MAX232 for RS-232) |
| RS-485 [67] | TxD+, TxD- | RS-485 transceiver (e.g., SN65HVD) |
| RS-232 [68] | TX, RX (optional RTS, CTS) | Level shifter (e.g., MAX232), 4-5 capacitors |
| CAN [69] | CAN_H, CAN_L | CAN transceiver (e.g., TJA1050), 120Ω termination |
| MIL-STD-1553 [63] | Custom interface via transceiver | Transformer, transceiver, controller (e.g., BU-64863) |

In addition to the communication pins one also needs at least one power pin and one Ground (GND) pin in order to power the SP. Considering all the pins seen in Table 4.3, a minimum of 14 pins is needed to allow for most of the communication buses wanted. In case additional power, ground, or unaccounted-for pins (like for the MIL1552 standard) are needed, 4 extra pins are added as a safety margin. Thus, a minimum of 20 pins (2 for power and ground, 14 for communication and 4 for redundancy) are needed in total.

## Mechanical Interfaces

Again, the Standardized Payload's mechanical interface design should also reflect the 'plug-and-play' philosophy. As three main satellite types are considered (PocketQubes, CubeSats and larger), the mechanical design needs to be easily integrable for all three. Thanks to the standardization of SmallSats, a large pin allocation can easily be implemented using standard satellite communication bus hardware like the PQ60 for PocketQubes (Figure 4.3a) or the PC/104 for CubeSats (Figure 4.3b).

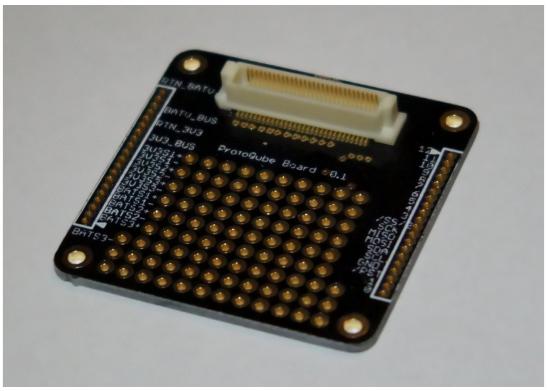


**(a)** Picture of the female PQ60 connector.

**(b)** Picture of the PC/104 connector (gray) in a satellite stack.

**Figure 4.3:** Standard SmallSat electrical interfaces.

Despite the ease of standardization mentioned, designing a one-size fits all PCB was deemed impossible as if one were to design a PCB for a PocketQube with the PQ60, this standard would not fit onto a CubeSat with the PC/104 and vice versa. A solution to this was to design the smaller PCB (5 x 5 mm) for the PocketQube and have an adapter PCB which 'docks' onto the PocketQube PCB in order to form a PCB which fits the CubeSat standard (10 x 10 mm). However, this does not accommodate larger satellites. Therefore, the following solution was chosen: producing the smallest PCB possible in addition to one adapter PCB for the CubeSats and a different adapter PCB for PocketQubes. A standard connector will be used to connect the SP to these adapter PCBs. The adapter PCBs have the standard connectors (PQ60 and PC/104) and can therefore easily integrate into PocketQube and CubeSats. For larger satellites, the satellite designer has to introduce the mating connector of the standard connector on the SP and ensure it is connected to the satellite bus. Overall, this allows for more freedom of the larger satellite manufacturer as the size of the SP is smaller than the PocketQube standard.

## 4.4. Component Selection

This section lists the standardized payload's main components based on the operational concept described in Figure 4.1 and the standardization considerations described in Section 4.3. The final bill of materials is presented in Table 4.4 as a preview of all of the components used in the design. A detailed description of all of the parts listed in the Bill of Materials (BOM) will then follow in Section 4.5.

### Hardware Building Blocks

- **Antenna:** Two 5.2 mm × 3.7 mm × 0.7 mm ceramic loop antenna (2JL67) mounted on 10 mm × 15 mm PCBs on the host's S/C surface.
- **RF switch:** RF switch (Skyworks SKY13351-378LF) routes the signal from the antenna either to the EAR or the SR.
- **Ephemeris Acquisition Receiver (EAR):** Antenova M20071 GNSSNOVA module; Universal Asynchronous Receiver/Transmitter (UART) interface, real-time clock (RTC) backup domain.
- **Snapshot Receiver:** Analog Devices MAX2769C L1 front-end (2-bit IF), a 26 MHz TCXO (SiT8021).
- **Microcontroller Unit (MCU):** 64-pin STM32L452RE MCU (sleep <2 µA, active 80 µA $MHz^{-1}$).
- **Non-volatile memory:** 256 kB flash memory holds firmware, almanac, ephemeris, and a rolling buffer of raw snapshots; integrated in the MCU.
- **Power management:** 3.3 V and 1.8 V bucks in the form of a dual voltage converter (LTC3407EDD-3#PBF); always-on 1.8 V LDO feeds the RTC crystal in the MCU.
- **Printed Circuit Board:** 6-layer PCB with 3 data layers and dedicated ground, 1.8 V and 3.3 V layers.
- **Antenna Printed Circuit Board:** 15 mm × 10 mm PCB with TBD layers.
- **User Connector:** 30-pin DF17 connector accommodating many common communication protocols, including a 5 V power supply pin.
- **Mechanical envelope:** Electronics card 34 mm × 43 mm × 5 mm; antennas add 10 mm × 15 mm on two sides of host S/C.

### Bill Of Materials

Apart from the main components, some capacitors and inductors are also required in order to connect all of the elements listed above correctly. Thus, the bill of materials listing every component needed for the Standardized Payload is shown in Table 4.4. All costs and masses (except for the PCB) were taken from `https://eu.mouser.com/`. If an exact mass was not provided, it has been estimated from the masses of similar parts. The cost of components available in multiple versions from different manufacturers is shown as an average and marked with an asterisk. Estimated masses and costs are marked with an asterisk (*). PCB cost is based on the price quoted by `https://be.eurocircuits.com/` for a 37 mm × 44 mm 6-layer board. The carbon footprint (CF), expressed in kilograms of CO2 per kilogram of each component type, is also shown. The total carbon footprint of the electronics board is calculated, with further details provided in Section 6.5.

**Table 4.4:** Standardized payload bill of materials. Values marked with an asterisk (*) are estimates.

| Part | Part ID | Value | Number | Mass | Part Cost [€] | CF [kg/kg] |
|---|---|---|---|---|---|---|
| Voltage Regulator | LTC3407EDD-3#PBF [70] | N/A | 1 | 12 mg | 7.78 | 65.84 |
| EAR | M20071 [57] | N/A | 1 | 0.8 g | 15.85 | 1312.82 |
| SR | MAX2769CETI+ [71] | N/A | 1 | 63 mg | 6.44 | 1312.82 |
| RF Switch | SKY13351-378LF [72] | N/A | 1 | 0.75 g | 0.75 | 65.84 |
| Power Combiner | PD1722J5050S2HF [73] | N/A | 1 | 5.5 g | 0.95 | 65.85 |
| MCU | STM32L452RET6PLQFP64 [74] | N/A | 1 | 49 mg | 6.66 | 1667.24 |
| Antenna | 2JL67 [75] | L1/L5 | 2 | 1 g* | 7.0* | 77.11 |
| Antenna Connector | A-2JA [76] | N/A | 2 | 0.3 g | 1.09 | 65.84 |
| SP Connector | DF17_3.0_-30DS-0.5V_57 [77] | N/A | 1 | 2 g | 1.82 | 65.84 |
| Main PCB | N/A | N/A | 1 | 5 g* | 110* | 77.11 |
| Antenna PCB | N/A | N/A | 2 | 2 g* | 20* | 77.11 |
| Capacitor | c_CHIP-0402 | 22 pF-2.2 µF | 24 | 1.5 mg | 0.5* | 66.29 |
| Capacitor | C_CHIP-0603 | 1 µF-10 µF | 4 | 7 mg* | 2.0* | 66.29 |
| Capacitor | C_CHIP-0805 | 47 µF | 3 | 20 mg* | 2.0* | 66.29 |
| Inductor | L_CHIP-0603 | 47 nH | 3 | 4 mg* | 1.5* | 43.60 |
| Resistor | R_CHIP-0402 | 20 kΩ | 1 | 0.7 mg | 2.4* | 32.00 |
| Aluminium Enclosure | N/A | N/A | 1 | 11 g | 10* | 8.16 |
| **Total** | | | | **30 g** | **250** | **2.92 kg** |

## 4.5. Electronics Board

This section describes the design of the PCB used for the standardized payload, including all the components soldered on it. First, the pinouts of the main components will be described, and then some connection schematics are shown. Finally, the layout and routing processes are shown. All components used are described in Table 4.4.

### 4.5.1. Components Pinout and Connection Schematics

The components of the standardized payload contain pins that enable them to perform various functions, like connecting to power, and also facilitating communication. All pins have a dedicated purpose, and therefore, they must be connected meticulously for proper functionality.

For this subsection, the pin functions will be directly provided as a table from the datasheet when possible. For descriptions that are either too large or unclear, the description will be provided in text. Furthermore, the pin descriptions include a variety of abbreviations that will not be explained for conciseness. For further details about these abbreviations or pin functions, the reader is encouraged to refer to the corresponding datasheet.

#### GNSS Module

The full GNSS Module, Antenova M20071, is used to decode the almanac during the orbit insertion and then acquire ephemerides once every 3 h for position. Having a separate GNSS module instead of relying on ground transmission of ephemerides and almanac allows this payload to function significantly more independently, enhancing its standardization capabilities. Figure 4.4 shows the footprint of this GNSS module and Table 4.5 provides the specific functions of all pins on the component.

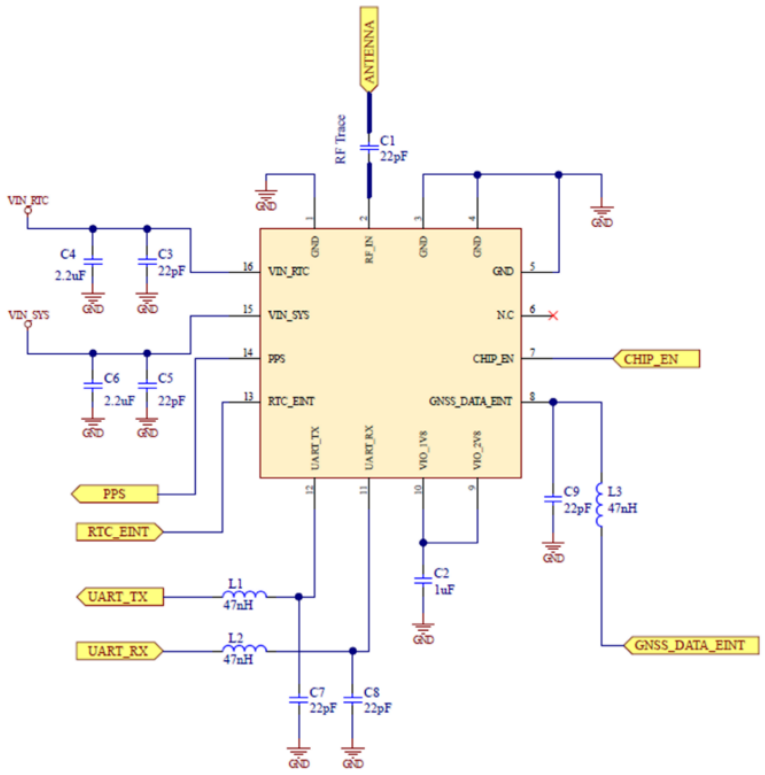


**Figure 4.4:** M20071 connection schematic. [57]

Figure 4.4 additionally shows the capacitors, inductors, and the ground connections necessary for the pin connections to function properly. These additional components are mainly used for filtering, decoupling, and matching [57]. For example, the capacitors placed near the power pins are used to transfer high-frequency noise to ground and stabilize the 1.8 V supply rails. On the other hand, the capacitor near the RF_IN pin prevents any DC bias from the antenna feed from entering the module's RF front-end. Although more components can be explained in further detail for the GNSS module and also for the remaining SP components, they will not be included as part of the report. More information can be found on the datasheet referenced for each part [57, 70–72, 74, 75, 78].

**Table 4.5:** M20071 GNSS module pinout. [57]

| Pin | Name | Description |
|---|---|---|
| 1 | GND | Ground connection (Round pad) |
| 2 | RF_IN | RF connection from antenna (50 Ω) |
| 3 | GND | Ground connection |
| 4 | GND | Ground connection |
| 5 | GND | Ground connection |
| 6 | N.C | No connect |
| 7 | CHIP_EN | System reset, active low |
| 8 | GNSS_DATA_EINT | Handshaking with host |
| 9 | VIO_2V8 | 2.8 V input for 2.8 V I/O support |
| 10 | VIO_1V8 | 1.8 V output for 1.8 V I/O support |
| 11 | UART_RX | UART receive data line |
| 12 | UART_TX | UART transmit data line |
| 13 | RTC_EINT | Wake module from RTC mode |
| 14 | PPS | Pulse-per-second output |
| 15 | VIN_SYS | Main supply voltage (1.8 V typ) |
| 16 | VIN_RTC | RTC supply voltage (1.8 V typ) |

### Microcontroller Unit (MCU)

In the proposed dual receiver architecture, the MCU is responsible for processing the snapshots, generating position fixes, coordinating the system, and handling data.

As described in Section 4.3, the standardized payload should accommodate a variety of communication types. Therefore, different configurations of the chosen microcontroller unit STM32L452 were evaluated. Based on the datasheet [74], the LQFP64, a 64-pin version, was determined to support all necessary functions and was therefore chosen for the final design.

The pins on the MCU can be separated into two types: voltage pins and communication pins. As Figure 4.5 shows, the voltage pins such as VBAT, VDD, or VSS either supply power to different parts of the MCU or connect to the ground as a reference. For example, the VDD pins power the core and digital I/O circuits. VDDA pins, on the other hand, power the analog peripherals such as ADC (Analog-to-Digital Converter) and DAC (Digital-to-Analog Converter).

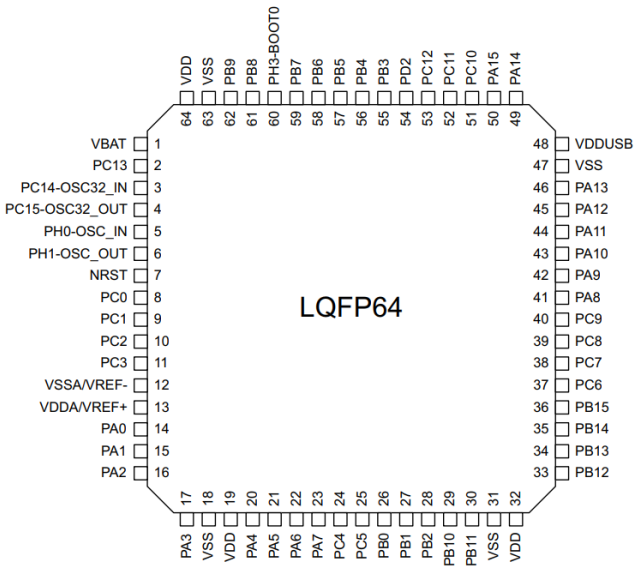


**Figure 4.5:** LQFP64 footprint. [74]

The remaining pins, labelled such as PA0, PB10, PC6, can provide and receive information from the OBC and also communicate with the other components on the board. Therefore, they either function as general-purpose input and output (GPIO) or are allocated communication pins. The type of communication they support depends on their specific alternative function. Thus, all pins were evaluated in detail before initiating the allocation process.

Similar to the GNSS module, several pins for the MCU also require additional capacitors and decoupling connections. For example, capacitors placed close to the MCU's VDD pins shunt high-frequency noise to

ground, preventing supply glitches. Additionally, ferrite beads placed on the power lines prevent voltage spikes. Specifications about the placement and purposes of more subcomponents of the MCU can be found in the datasheet [74].

### RF Front-end

The RF front end is the component that allows the acquisition of snapshots within this dual receiver architecture. It takes the weak, high-frequency signals picked up by the antenna and converts them into usable intermediate signals by filtering, amplifying, and down-converting. This forms an intermediate frequency (IF), which is then transferred to the analog-to-digital converter (ADC). Finally, the digital signal is sent to the MCU for further processing to generate position fixes. Figure 4.6 shows the footprint of this component.

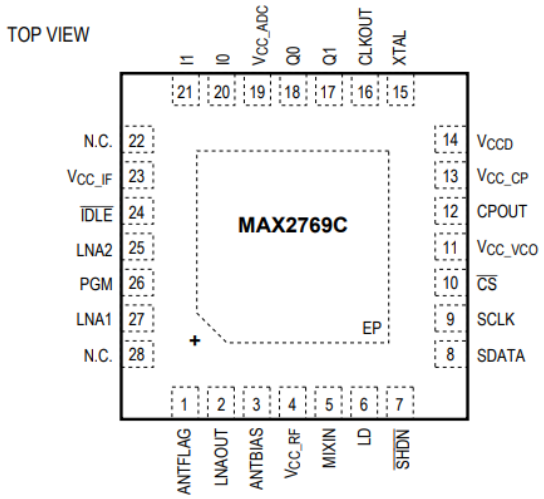


**Figure 4.6:** MAX2769C footprint. [71]

As the figure shows, the component has 28 pins with discrete functions, and their connections to other components depend on these functions. Therefore, Table 4.6 provides the descriptions of the pins for this component and the additional components, such as capacitors or resistors, that the pins might need for connections.

**Table 4.6:** MAX2769C pinout. [71]

| Pin | Name | Function |
|---|---|---|
| 1 | ANTFLAG | Active Antenna Flag Logic Output. A logic-high indicates that an active antenna is connected to the ANTBIAS pin. |
| 2 | LNAOUT | LNA Output. The LNA output is internally matched to 50 Ω. |
| 3 | ANTBIAS | Buffered Supply Voltage Output. Provides a supply voltage bias for an external active antenna. |
| 4 | VCC_RF | RF Section Supply Voltage. Bypass to ground with 100 nF and 100 pF capacitors in parallel as close as possible to the pin. |
| 5 | MIXIN | Mixer Input. The mixer input is internally matched to 50 Ω. |
| 6 | LD | Lock-Detector CMOS Logic Output. A logic-high indicates the PLL is locked. |
| 7 | SHDN | Operation Control Logic Input. A logic-low shuts off the entire device. |
| 8 | SDATA | Data Digital Input of 3-Wire Serial Interface. |
| 9 | SCLK | Clock Digital Input of 3-Wire Serial Interface. Active when CS is low. Data is clocked in on the rising edge of the SCLK. |
| 10 | CS | Chip-Select Logic Input of 3-Wire Serial Interface. Set CS low to allow serial data to shift in. Set CS high when the loading action is completed. |
| 11 | VCC_VCO | VCO Supply Voltage. Bypass to ground with a 100 nF capacitor as close as possible to the pin. |
| 12 | CPOUT | Charge-Pump Output. Connect a PLL loop filter as a shunt C and a shunt combination of series R and C (see the Typical Application Circuit). |
| 13 | VCC_CP | PLL Charge-Pump Supply Voltage. Bypass to ground with a 100 nF capacitor as close as possible to the pin. |
| 14 | VCCD | Digital Circuitry Supply Voltage. Bypass to ground with a 100 nF capacitor as close as possible to the pin. |
| 15 | XTAL | XTAL or Reference Oscillator Input. Connect to XTAL or a DC-blocking capacitor if TCXO is used. |
| 16 | CLKOUT | Reference Clock Output. |
| 17 | Q1 | Q-Channel Voltage Outputs. Bits 0 and 1 of the Q-channel ADC output or analog differential voltage output. |
| 18 | Q0 | Q-Channel Voltage Outputs. Bits 0 and 1 of the Q-channel ADC output or analog differential voltage output. |
| 19 | VCC_ADC | ADC Supply Voltage. Bypass to ground with a 100 nF capacitor as close as possible to the pin. |
| 20 | I0 | I-Channel Voltage Outputs. Bits 0 and 1 of the I-channel ADC output or analog differential voltage output. |
| 21 | I1 | I-Channel Voltage Outputs. Bits 0 and 1 of the I-channel ADC output or analog differential voltage output. |

*Continued on next page.*

| Pin | Name | Function |
|---|---|---|
| 22 | N.C. | No Connection. Leave this pin unconnected. |
| 23 | VCC_IF | IF Section Supply Voltage. Bypass to ground with a 100 nF capacitor as close as possible to the pin. |
| 24 | IDLE | Operation Control Logic Input. A logic-low enables idle mode, in which the XTAL oscillator is active and all other blocks are off. |
| 25 | LNA2 | LNA Input Port 2. Typically used with an active antenna. Internally matched to 50 Ω. |
| 26 | PGM | Logic Input. Connect to ground to use the serial interface. A logic-high allows programming via states of SDATA, CS, and SCLK (see Table 19). |
| 27 | LNA1 | LNA Input Port 1. Typically used with a passive antenna. Internally matched to 50 Ω (see the Typical Application Circuit). |
| 28 | N.C. | No Connect. |
| — | EP | Exposed Pad. Ultra-low-inductance connection to ground. Place several vias to the PCB ground plane. |

### RF Switch

In the dual receiver architecture, the signal captured by the passive antenna must either be transmitted to the RF front-end for the snapshot mode or to the GNSS module for ephemeris acquisition. Therefore, an RF switch is necessary to route this signal to the correct component. Figure 4.7 shows how the pins are placed on the chosen RF switch, and Table 4.7 provides the descriptions for these pins.

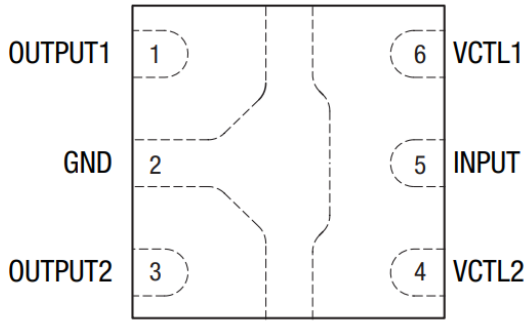


**Figure 4.7:** SKY13351-378LF footprint. [72]

**Table 4.7:** SKY13351-378LF pinout. [72]

| Pin | Name | Description |
|---|---|---|
| 1 | OUTPUT1 | RF port. Must be DC-blocked. |
| 2 | GND | Ground. |
| 3 | OUTPUT2 | RF port. Must be DC-blocked. |
| 4 | VCTL2 | DC control voltage. |
| 5 | INPUT | RF port. Must be DC-blocked. |
| 6 | VCTL1 | DC control voltage. |

The datasheet [72] does not mandate the use of capacitors for the voltage pins, unlike other component. However, it requires the addition of DC blocking capacitors for OUTPUT1, OUTPUT2, and INPUT pins in the stated magnitude.

### SP Antenna

For ceramic antennas to function, they must be placed on a specific size ground plane that determines their radiation pattern and gain characteristics [79]. The antenna proposed in the preliminary design was tested by the manufacturer on an 80 mm × 40 mm ground plane [80]. As there was no information provided about the minimum size, a different and smaller antenna is now proposed as part of the standardized payload. 2JL67 is also a surface-mounted ceramic passive antenna [75]. On a similarly sized ground plane, it has similar characteristics to the Antenova Raptor. However, it is stated to have a minimum ground plane size of 15 mm × 10 mm [75]. As this ground plane PCB is going to be placed on the exterior of the spacecraft, more convenient ground plane requirements make this antenna an attractive option. Figure 4.8 shows the pins of the antenna and how they must be connected to the ground plane. This description also includes the capacitors required for these connections. As there is only an input pin other than the 4 ground connection pins, the pin description table will be omitted.

### Wilkinson Combiner

The Wilkinson combiner is a tool that combines the outputs of two antennas by blocking the flow between them. Currently, single or dual antenna configurations are being considered as a part of the SP. Therefore, in case a two-antenna configuration is chosen, a Wilkinson combiner is required.

Other than the use of the combiner, gathering one output from two antennas requires several considerations. In Section 4.6, the simulation shows it is possible to have more than 20 GNSS satellites in view at any given instance. Acquiring signals from different GNSS satellites poses no issues as each signal is equipped with a unique PRN code that is orthogonal to all other PRN codes from different satellites. Therefore, when two or more of these signals are combined, they can be processed without destructive interference.

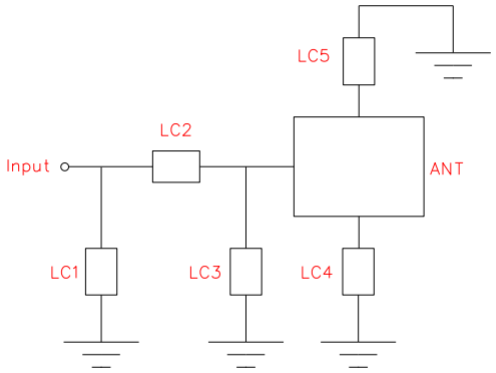


**Figure 4.8:** 2JL67 connection schematic. [75]

The structure of the Wilkinson combiner and the pin descriptions are provided in Figure 4.9 and Table 4.8.

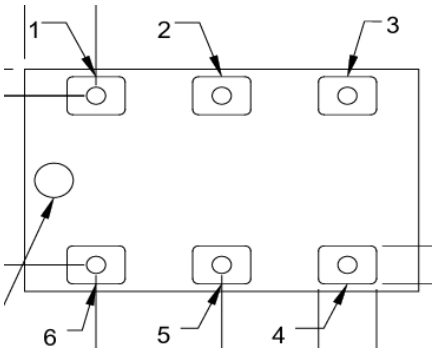


**Figure 4.9:** Wilkinson combiner schematic. [73]

**Table 4.8:** Wilkinson combiner pin descriptions [73]

| Pin | Designation |
|---|---|
| 1 | GND |
| 2 | Input |
| 3 | GND |
| 4 | Output 1 |
| 5 | GND |
| 6 | Output 2 |

### Voltage Converter

The voltage converter is a component on the PCB that takes a range of voltages as input and provides certain voltages based on user requirements. This is a crucial component for standardization as spacecraft have varying voltage outputs coming from their EPS subsystem. Additionally, several components on the SP work with 1.8 V, which is not a standard EPS output voltage. Therefore, it requires a regulator.

To accomplish these requirements, LTC3407-3 is determined to be the best component due to it's compact size and dual voltage output properties [70]. The component, and the capacitor, inductor, and resistor requirements for its pins are provided in Figure 4.10.

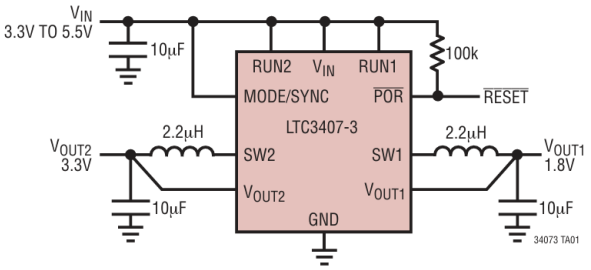


**Figure 4.10:** LTC3407-3 connection schematic. [70]

Additionally, the pin descriptions in Table 4.9 are taken from the datasheet directly to provide an overview of pin functions.

**Table 4.9:** LTC3407-3 pin description. [70]

| Pin | Name | Description |
|---|---|---|
| 1 | $V_{OUT1}$ | Output Voltage Feedback Pin for Channel 1. An internal resistive divider divides the output voltage down for comparison to the internal reference voltage. |
| 2 | RUN1 | Regulator 1 Enable. Forcing this pin to $V_{IN}$ enables regulator 1, while forcing it to GND causes regulator 1 to shut down. Do not float this pin. |
| 3 | $V_{IN}$ | Main Power Supply. Must be closely decoupled to GND. |
| 4 | SW1 | Regulator 1 Switch Node Connection to the Inductor. This pin swings from $V_{IN}$ to GND. |
| 5 | GND | Ground. This pin is not connected internally. Connect to PCB ground for shielding. |
| 6 | MODE/SYNC | Combination Mode Selection and Oscillator Synchronization. Controls the operation of the device. When tied to $V_{IN}$ or GND, Burst Mode or pulse-skipping mode is selected, respectively. The oscillation frequency can be synchronized to an external oscillator. Do not float this pin. |
| 7 | SW2 | Regulator 2 Switch Node Connection to the Inductor. This pin swings from $V_{IN}$ to GND. |
| 8 | POR | Power-On Reset. This common-drain logic output is pulled to GND when the output voltage falls below -8.5% of regulation and goes high after 117ms when both channels are within regulation. |
| 9 | RUN2 | Regulator 2 Enable. Forcing this pin to $V_{IN}$ enables regulator 2, while forcing it to GND causes regulator 2 to shut down. Do not float this pin. |
| 10 | $V_{OUT2}$ | Output Voltage Feedback Pin for Channel 2. An internal resistive divider divides the output voltage down for comparison to the internal reference voltage. |
| 11 | Exposed Pad (GND) | Power Ground. Connect to the (-) terminal of $C_{OUT}$, (-) terminal of $C_{IN}$. Must be connected to electrical ground on PCB. |

### TCXO

As previously explained, one of the main purposes of the RF front-end is downconverting the incoming signal. Although the component has an internal clock, it also requires an external clock to have a stable and low-noise reference for the Phase-Locked Loop (PLL) [78]. Initially, the clock in SiT8021 was chosen, especially due to its small size. However, due to its relatively high power consumption, it was removed from the design. Therefore, the internal clock of the MCU was connected to the RF front-end as the reference clock for downconverting.

In order for the position error to be within the 20 m desired range, a clock with a high enough frequency should be used in the position determination. To translate a desired range error $\Delta p$ into a timing error $\Delta t$, use

$$\Delta p = c\,\Delta t, \qquad c = 299\,792\,458\,\mathrm{m\,s^{-1}}.$$

**Table 4.10:** Timing budget for 20 m GNSS range accuracy.

| Quantity | Value | Reasoning |
|---|---|---|
| Desired range error $\Delta p$ | 20 m | Requirement |
| Allowable time error $\Delta t$ | $\frac{20\ \mathrm{m}}{c} = 6.7 \times 10^{-8}\ \mathrm{s}$ | $\Delta t = \Delta p / c$ |
| Required clock frequency $f$ | $f = \frac{1}{\Delta t} \approx 15\ \mathrm{MHz}$ | $f = 1/\Delta t$ |

A sampling or local-oscillator frequency of roughly 15 MHz yields one time tick every 66.7 ns, which limits the raw range error to 20 m. Commercial GNSS front-ends typically use higher multiples (e.g. 16.368, 24, or 26 MHz) and refine the result further through code phase interpolation and continuous disciplining of the receiver's oscillator. Thus, a clock frequency of at least 15 MHz should be used for calculating the position fixes.

### SP User Connector

The SP user connector is the component that connects the standardized payload to the adapter PCB, allowing the user to connect . The pin allocation of the SP connector is arbitrary, as these will be rerouted on the adapter PCB to align with the standardized pin allocations for PocketQubes and CubeSats. However, to accommodate larger satellites, this pin allocation on the adapter PCB needs to be provided to the operator for connections. Figure 4.11 shows the SP connector [77], where the pins on this component are dedicated based on PCB routing convenience. Based on the pin function, these pins are then either routed to dedicated communication pins on the MCU or the power layers on the PCB board.

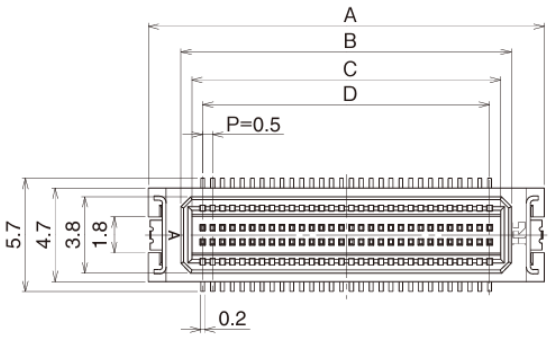


**Figure 4.11:** DF17(3.0)-50DS-0.5V(57) Footprint [77]

### 4.5.2. Pin Allocation

The MCU works by getting information from the components and commands from the OBC. This flow of information is facilitated by pin connections. The pins on the MCU, indicated by the pin number up to 64 and a label such as "PB0", can be separated into two main sections: power pins and input/output channels. Power pins begin with the letter "V", and they are either used as a reference voltage input, power input, or ground connection. The input channels, on the other hand, start with the letter "P" and they are General Purpose Input Output (GPIO) pins with a variety of Alternate Functions (AFs). These AFs mainly include different communication types, timers, clocks, and secondary connections. As not all communication types are available on all input channels, the pins on the PCB must be connected by considering the limiting pins on the MCU. These AFs are especially important for communication connections, as different AFs relate to different communication types. Therefore, communication pins will be connected first to ensure that the pins necessary for communication are not unnecessarily occupied by other functions. This is given in Table 4.11:

**Table 4.11:** Communication pin assignments.

| # | Interface | Pin on the MCU | AF # |
|---|---|---|---|
| 1 | Generic USART2 | PA2 (16), PA3 (17) | 7 |
| 2 | RS-232 via LPUART1 | PC0 (8), PC1 (9) | 8 |
| 3 | RS-485 via USART3 | PC10 (50), PC11 (51), PC12 (52) | 7 |
| 4 | SPI1 | PB3 (54), PB4 (55), PB5 (56), PB6 (57) | 5 |
| 5 | $I^2C2$ | PB10 (47), PB11 (48) | 4 |
| 6 | CAN1 | PB8 (45), PB9 (46) | 9 |
| 7 | MIL-STD-1553 via SPI3 + DIR (GPIO) | PC6 (37), PC7 (38), PC8 (39), PA15 (5), PC2 (10) | 6 |

After the allocation of these communication pins on the MCU, the remaining connections are made with voltage and input channels. As the majority of these connections can be handled by the GPIO functions, the pin selection is made based on the empty pins and routing convenience on the PCB. This is shown by Figure 4.13 and Figure 4.12, which provide the pin connections on the SP connector and the MCU, respectively. The labels placed on the green extensions next to the pins show the pin name on the other components that they are connected to.

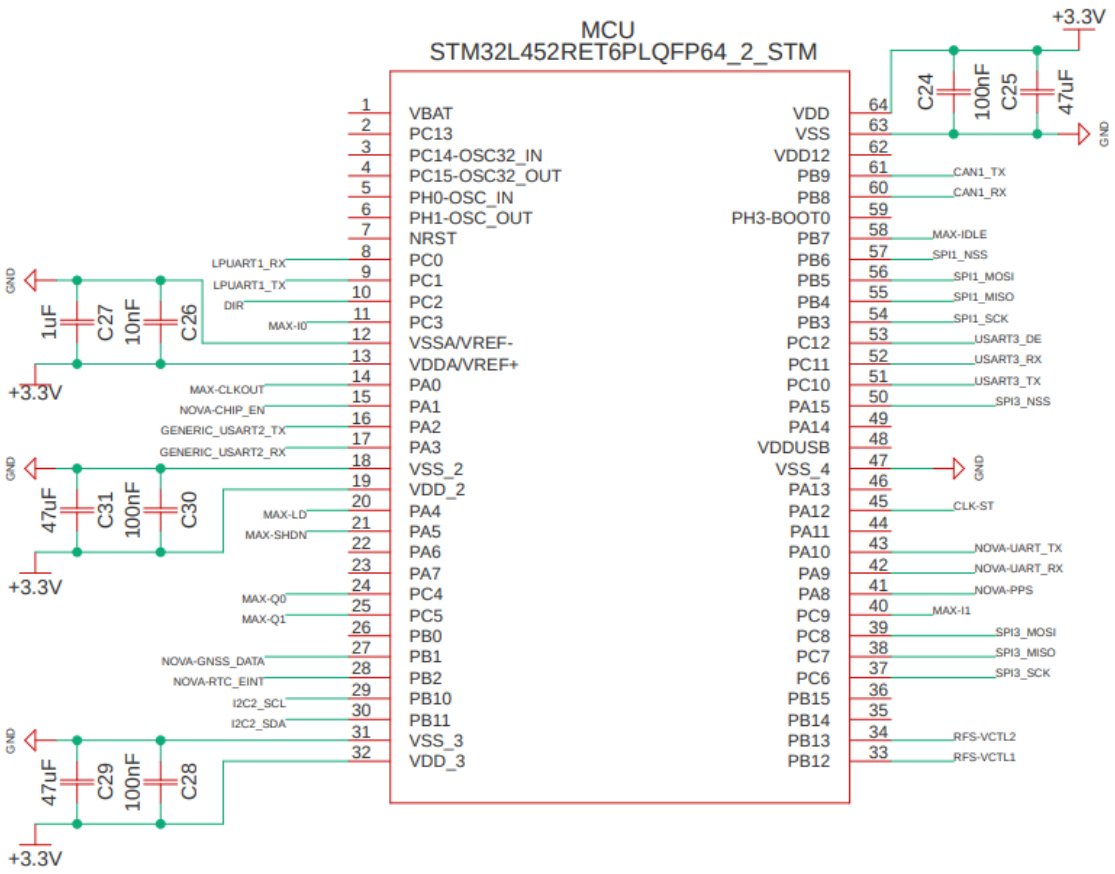


**Figure 4.12:** MCU pin allocation.

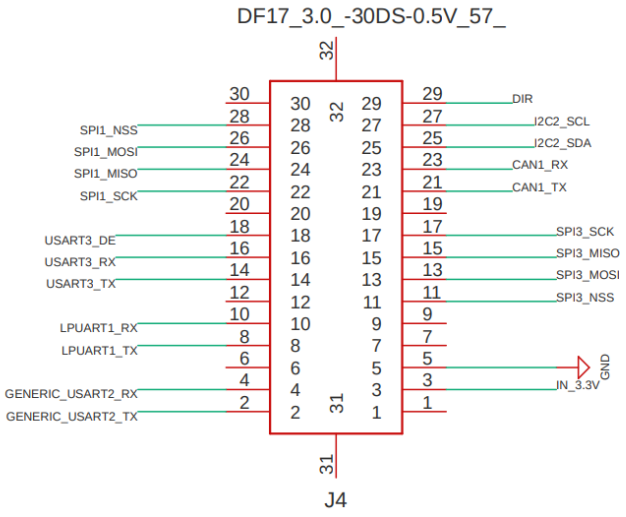


**Figure 4.13:** SP user connector pin allocation.

The connection names on the pins are given based on a specific labeling convention. NOVA indicates the pins on the Antenova GNSS module, MAX belongs to the RF front-end, RFS belongs to the RF switch, and the remaining connection names are provided based on the communication type.

The SP connector schematic, Figure 4.13 shows how specific functions are allocated to various pins on this component. As previously mentioned, this selection is arbitrary and the important consideration is how this is transferred to the satellite connector on the adapter PCB for standardization.

As the connections on the MCU demonstrate, the GPIO pins are connected to other components on the PCB with regard to their specific AFs, and voltage pins are connected to the appropriate power rails through the

proper capacitor loops and ground connections. It is sufficient to only show the connections on the MCU alongside the SP connector, as every other component is connected to the MCU, and there are no additional interconnections. The only exception is the RF switch, which is connected to the antenna and therefore shown in Figure 4.14.

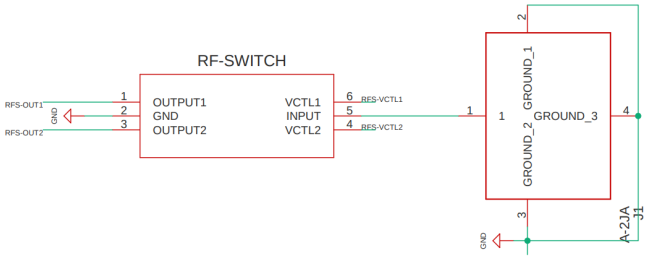


**Figure 4.14:** RF switch pin connections.

Additionally, the ground connections and the power connections of the pins are made based on the guides provided in the datasheet [71]. For example, the datasheet for the MCU provides the necessary components for decoupling in the power pins as shown in Figure 4.12, pin 13. A similar approach is followed for all components on the PCB, where they are connected to the proper power rails and to the ground based on their specifications. These connections will be visible in a CAD design of the PCB in Chapter 4.

### 4.5.3. Radiation Hardening

The majority of the components on the PCB are not space-grade or flight-proven. Therefore, hardware modifications are required to ensure that the radiation in LEO will not result in equipment failure throughout the mission duration. As various components require additional measures, various methods of radiation hardening will be highlighted in this subsection.

#### Aliminium Housing

The payload is going to be placed in a housing for protective and convenience purposes. Based on NASA's Mission Radiation Environment Modeling and Analysis guide [81], a 2 mm thick Al housing almost completely eliminates trapped electron dose and significantly reduces trapped proton doses. However, high-energy protons and ions are still able to penetrate. Therefore, additional protective measures are still required.

#### Local Spot Shielding

Components on the PCB can be protected against radiation by local covering of the structure with certain materials. According to "Multilayer radiation shield for satellite electronic components protection" by Daneshvar, covering critical components with Tantalum (Ta) or Tungsten (W) can have up to 72% shielding effectiveness [82]. Additionally, research has also proven that epoxy-resin composites such as silica are also effective for radiation shielding [83]. Such composites will be used to cover the areas concentrated on power, such as the LDO or the supply rails, as they are especially sensitive to radiation.

#### Ceramic Capacitors

Finally, the radiation also impacts the ceramic capacitors by causing leakages and reducing capacitance [84]. As these capacitors are a crucial part of the payload design, they are selected as X7R grade, which is determined to be resistant against radiation and temperature changes by NASA [85].

### 4.5.4. PCB Layering and Layout

A 6-layer design is used for the SP PCB, with a total thickness of 1.06 mm. There are three signal layers, dedicated 1.8 V and 3.3 V layers for components that require different voltages, and one ground layer. The signal layers are spread apart in order to minimize interference between signals. The layer stack is shown in Figure 4.15a.

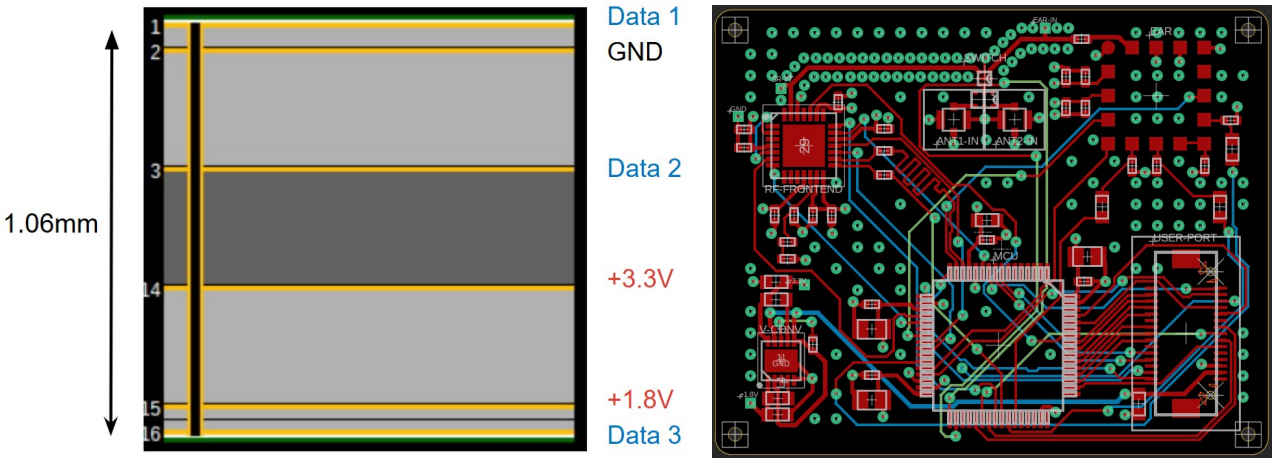


**(a)** 6-layer stack.

**(b)** Component layout.

**Figure 4.15:** PCB Layout.

The layout and routing were performed in Fusion 360 using the complete connection scheme. Important design considerations are highlighted in Table 4.12.

**Table 4.12:** Layout and routing considerations.

| Aspect | Implementation | Purpose |
|---|---|---|
| Inductor placement | Inductors are sufficiently spaced apart | Minimize magnetic coupling |
| Capacitor placement | Capacitors are placed close to their corresponding pins to maximize effectiveness | Improved decoupling |
| Antenna traces | Traces from the antenna connectors are impedance-matched to avoid path-loss differences between the two signals | Preserve signal integrity |
| Clock traces | Clock traces in and out of the MCU are length-matched | Maintain synchronous timing |
| Low-impedance return path | Every signal on an adjacent layer has a short, uniformly low-inductance loop back to its source | Reduce ringing, overshoot, and crosstalk |
| EMI suppression & shielding | The ground plane forms a broad Faraday shield that confines switching fields inside the board | Reduce radiated emissions and sensitivity to external noise |
| RF Signal Integrity | Line stitching in the form of periodic ground vias along a trace edge | Protects low power RF signal traveling from antenna port to RF switch |
| Trace Ampacity | Optimize power trace thickness | Insure power traces carry the intended amperes without excessive heating |

### PCB Design Verification

Fusion 360 includes two verification tools: Electrical Rule Check (ERC) and Design Rule Check (DRC). ERC confirms that all nets are consistent and that the schematic contains no electrical errors. DRC checks the PCB layout to ensure the design is manufacturable and complies with the predefined design rules, such as wire clearance, copper width, and trace angles. The proposed design passed both checks, confirming that its connections and layout are correct. Future work should focus on implementing the ECSS-Q-ST-70-12C[86] standard into the DRC tool.

## 4.5.5. Link Budget

Link budget for the receiving passive patch antenna of the payload is crucial as it directly impacts whether the acquired signal is within the acceptable dBm range for GNSS receivers. The minimum C/No ratio requirement for GNSS receivers is stated to be 28 dB-Hz [87]. To determine whether the current SP setup is sufficient to reach this value, the link budget tool described in Table 5.4.4 was utilized. After the necessary changes in the code, such as updating atmospheric losses, the final values for the signal-to-noise ratio for L1 and L5 bands are 29.87 dB-Hz and 32.81 dB-Hz, respectively. These values also take into account an 8dB loss due to the reduced PCB size [88], which is the maximum value that does not consider the improvements suggested on the antenna PCB in Section 4.6. Therefore, even with the conservative approach, the SP satisfies the link budget requirements.

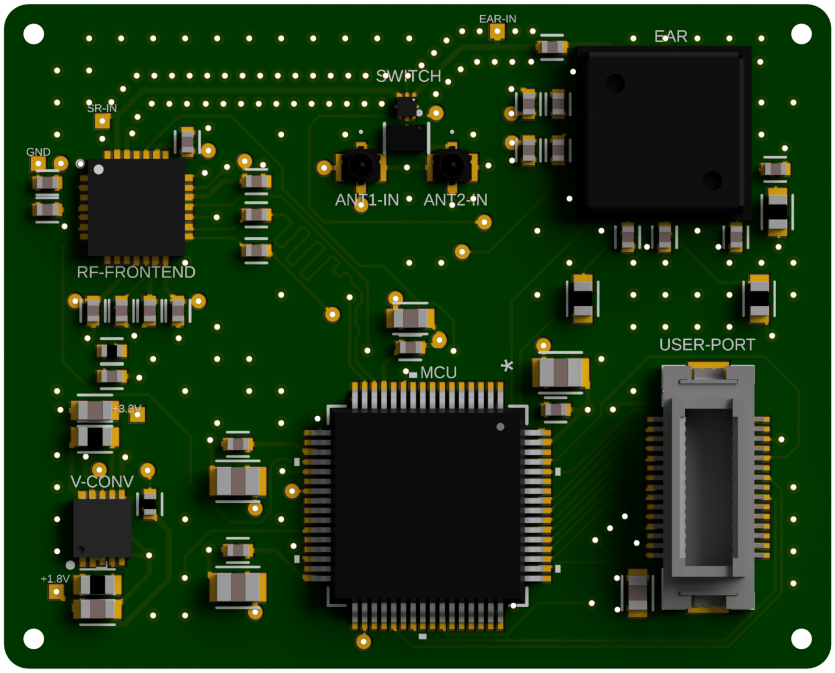


**Figure 4.16:** Enclosed SP unit.

## 4.6. Standardized Payload Antenna Considerations

As mentioned before the antenna for the payload (2JL67 [75]) requires a minimum ground plane of 15 mm × 10 mm. The radiation pattern, and therefore the view range of the antenna, is directly dependent on the ground plane size. The tests of 2JL67 are performed on a ground plane of 80 mm × 40 mm. Therefore, the 15 mm × 10 mm ground plane size will result in a significant reduction in the view range, which is reported to be approximately 180° in the datasheet [75].

In the "Small Ground-Plane Size Effects on Microstrip Patch Antennas Revisited" research paper by Peixeiro [88], a ground plane size reduction from 75 mm × 75 mm to 25 mm × 25 mm resulted in an approximate 40 % view range reduction [88]. As the reduction in the ground plane size is similar for the SP antenna, a similar drop is expected. Without any mitigation measures, the approximate reduction in the view range would likely be around 50 %, although this cannot be calculated without further experiments. However, several methods allow enhancing the radiation pattern without enlarging the ground plane size. For example, capacitive via-fence loading, which is placing rows of closely-spaced, plated vias around the surface currents [89], increases the view range. Additionally, dielectric superstrates, which are thin, lightly loaded superstrates or flat meta-lenses over the patch [90], also serve a similar purpose. Therefore, an ultimate reduction of 45 % for the SP antenna is estimated for the calculations, which results in a total view angle of 100°. This will be tested, and the calculations will be adjusted in the verification phase.

The significant reduction in the view range will have implications on the antenna placement and the antenna number, as the power consumption is aimed to be kept as small as possible.

As explained in Section 4.1, GNSS signals are composed of sub-frames, of which the first three include the ephemerides. These sub-frames are 18 s long in total, and they repeat every 30 s. The pieces of information, known as "words," inside these signals are sequential, meaning that every word is unique. If a word is missed, the receiver must wait 30 seconds for that specific information to repeat to capture it. Therefore, if a set of ephemerides cannot be captured within the first 18 seconds of the signal, it will require at least 30 seconds to acquire it due to waiting time for the repeating broadcast.

This situation is critical for the SP due to the limited range of the antenna's view. If, due to tumbling or relative motion between the satellites, a signal momentarily drops out of the view range, the time required to acquire ephemerides will increase, as additional time will be needed to catch the missed words after the signal broadcast repeats. The ability of the SP to acquire ephemerides conveniently depends on the view range, which depends on the number of antennas. This is crucial as needing a longer time to acquire ephemerides would result in an increased duty cycle and power consumption. Therefore, it is crucial to simulate tumbling with the antenna configurations being considered. This is shown in Subsection 4.6.1

Furthermore, snapshot processing for position fixes [56] requires at least 5 snapshots taken from 5 distinct GNSS satellite signals. This implies that to have the capability to reach position fixes at every point around the orbit, the antenna needs at least 5 GNSS satellites in view. More crucially, to process these 5 snapshots, the ephemerides of these GNSS satellites are required.

As the relative velocity of the SP compared to the GNSS satellites is significantly higher, GNSS satellites drop out of view throughout the orbit. Therefore, even though the SP initially acquires ephemerides for the set of GNSS satellites it has in range, these satellites will be unfit for snapshot processing after a given time as the antenna will not capture their signal. Thus, the number of ephemerides acquisitions per orbit directly correlates with the view range of the antenna, which depends on the number of antennas. Due to this situation, it is crucial to simulate the ephemerides acquisitions required per orbit with different antenna configurations. More acquisitions per orbit would result in increased duty cycle and, therefore, a higher power consumption for the SP. This is further explained in Subsection 4.6.2

### 4.6.1. Monte Carlo Simulation for Tumbling

For the tumbling simulation, the body-fixed reference frame is utilized. The Z-axis of the satellite is assumed to point at the center of Earth initially, and the X and Y axes are considered to be tangent to the surface. For the current mission, the X-axis includes the surface on which the spacecraft antenna is placed. At t = 0, a Line of sight (LOS) vector is randomly placed within the view range of the antenna. This means that the signal might make contact with the antenna anywhere within the 100-degree view. After this initial lock, the satellite starts being rotated with respect to X, Y, Z, XY, YZ, XZ, and XYZ axes. For every rotation axis, the satellite is subjected to a range of angular velocities from 0.5 Degree Per Second (DPS) to 8 DPS. For the one antenna configuration, the antenna is placed on the +X surface as for the technology demonstration mission, this surface will not be rotating. In the two-antenna configuration, however, the second antenna is placed on the +Z surface, as this proved to be the most efficient after several trials.

The GNSS signal is composed of words as described in the chapter intro for Section 4.6. Therefore, he simulation defines 0.6-second-long words and stores the words that are captured before the LOS vector leaves the view range of the antenna. As the satellite continues tumbling, the LOS re-enters the view range of the antenna after some time. The simulation ends when all 30 words required for ephemerides are decoded.

This simulation is run over 1000 trials for each tumbling rate. This number was determined to be the optimal for both tumbling and re-acquisition simulations, as a smaller number of trials resulted in inconsistent results and a larger number of trials required excessive computational power. The decoding time, or even the feasibility of decoding, depends on the initial location of the LOS vector within the antenna's view range. If the simulation begins with an undesirable LOS vector placement or a problematic tumbling rate, the satellite may miss the same words in every rotation, resulting in some trials where ephemerides are never decoded. Therefore, alongside the average time for decoding, the 95th percentile and the success rate are also provided for every DPS value.

Performing this simulation will also provide valuable information about the number of patch antennas that must be placed on the host satellites, as the average time for decoding ephemerides will depend on the total view range and, thus, the number of antennas.

**Table 4.13:** Monte Carlo results for tumbling about the +X-axis with one antenna.

| dps | Average Time (s) | 95th Percentile (s) | Success Rate |
|---|---|---|---|
| 0.50 | 45.28 | 18.00 | 1.000 |
| 1.00 | 41.53 | 288.00 | 0.998 |
| 1.50 | 43.02 | 217.44 | 0.993 |
| 2.00 | 48.89 | 168.00 | 0.990 |
| 2.50 | 45.67 | 138.00 | 1.000 |
| 3.00 | 34.88 | 108.00 | 0.885 |
| 3.50 | 57.12 | 198.00 | 1.000 |
| 4.00 | 18.00 | 18.00 | 0.616 |
| 4.50 | 54.92 | 162.78 | 0.995 |
| 5.00 | 54.49 | 138.00 | 0.997 |
| 5.50 | 82.62 | 198.00 | 1.000 |
| 6.00 | 18.00 | 18.00 | 0.540 |
| 6.50 | 126.05 | 226.20 | 1.000 |
| 7.00 | 71.15 | 160.80 | 0.995 |
| 7.50 | 74.57 | 195.60 | 0.996 |
| 8.00 | 18.00 | 18.00 | 0.529 |

**Table 4.14:** Monte Carlo results for tumbling about the +X-axis with two antennas.

| dps | Average Time (s) | 95th Percentile (s) | Success Rate |
|---|---|---|---|
| 0.50 | 74.84 | 558.00 | 0.999 |
| 1.00 | 71.79 | 318.00 | 0.996 |
| 1.50 | 79.19 | 228.00 | 0.979 |
| 2.00 | 72.03 | 168.00 | 0.956 |
| 2.50 | 91.62 | 273.84 | 0.999 |
| 3.00 | 58.28 | 108.00 | 0.753 |
| 3.50 | 103.47 | 198.00 | 1.000 |
| 4.00 | 18.00 | 18.00 | 0.224 |
| 4.50 | 96.38 | 167.40 | 0.982 |
| 5.00 | 101.00 | 217.32 | 0.997 |
| 5.50 | 152.79 | 258.00 | 0.999 |
| 6.00 | NaN | NaN | 0.000 |
| 6.50 | 227.08 | 278.40 | 0.998 |
| 7.00 | 131.22 | 307.80 | 0.997 |
| 7.50 | 132.57 | 196.20 | 0.981 |
| 8.00 | NaN | NaN | 0.000 |

These two tables provide the ephemerides acquisition envelope for the two different antenna configurations. As the technology demonstration satellite is projected to rotate with respect to the X-axis as it is aligned with the magnetic fields, the X-axis tumbling envelopes are provided as examples. However, for the operators who place this payload on their satellites, the full envelope will be provided for precise power calculations.

As previously mentioned, the first three sub-frames of the GNSS signal that include ephemerides are 18 s in total. Ultimately, this leads to two crucial dps values on both tables. When dps = $6\,^{\circ}\,s^{-1}$, the minimum required view range for the antenna to decode in one rotation is 108° with the 18 s ephemerides sub-frame time.

As the view range for one antenna is approximately 100°, it is impossible for one antenna to acquire ephemerides in one rotation as it requires at least 18 s. Additionally, 6 dps means one rotation takes 60 seconds. As the signal repeats every 30 seconds, the same part of the signal will be caught at every rotation. Therefore, it will be impossible to decode ephemerides with one antenna, resulting in a success rate of 0.

The same situation makes decoding with two antennas either perfect at 18 s or impossible. If the initial LOS vector has more than 108° available before the signal leaves the view range, it will decode in 18 seconds. If less than this amount is available, the missed words will not be caught in the next rotations due to the synchronization of the signal and rotation.

The same situation is also observed for 8 dps. However, the difference is that the signal will repeat at the same word every two rotations instead of one. Therefore, the same resonance is still valid.

The comparison between the simulation results of one antenna and two antennas shows that having two antennas provides a significant advantage for ephemerides acquisition time and the success rate over different angular velocities. However, the final consensus on the antenna number also depends on its impact on the ephemerides acquisition frequency.

### 4.6.2. Monte Carlo Simulation for Ephemerides Acquisition Frequency

For this simulation, the orbital planes and the satellites of Galileo, GPS, Beidu-I, and Beidu-M are placed on a simulated orbit around Earth with each GNSS satellite having a unique ID. Either one antenna is placed on the +X surface or two antennas on the +X and +Z surfaces of the satellite, which is on a circular orbit at 500 km. The positions of the GNSS satellites and the position of the antenna are randomized, and 1000 trials are performed. With the pre-defined view range of the antenna, the GNSS satellites in view are recorded, and their IDs are saved, implying that the ephemerides are acquired from these satellites. Solving for snapshots requires the ephemerides from preferably 5 GNSS satellites, and as the snapshot frequency can be as high as once per minute, ephemerides from at least 5 satellites must be known at every point in the orbit. Therefore, when the number of saved satellites from the initial ephemerides acquisition drops below 5, another ephemerides acquisition is performed. Ultimately, the number of ephemerides acquisitions required per orbit is calculated for each trial. Ultimately, a frequency versus re-acquisitions per orbit plot is made.

One important consideration with this ephemerides acquisition frequency is the validity time of the information. As ephemerides are valid for a minimum of two hours, they do not have to be decoded at every orbit. Once the acquisitions are made at one orbit, no new acquisitions are necessary for the next one. Therefore, the number of re-acquisitions per orbit is valid once every two orbits.

Figure 4.17 presents an example of how the re-acquisitions are calculated. From the initial 26 satellites, when 5 of these satellites remain in view, the ephemerides are acquired. This is repeated throughout the orbit.

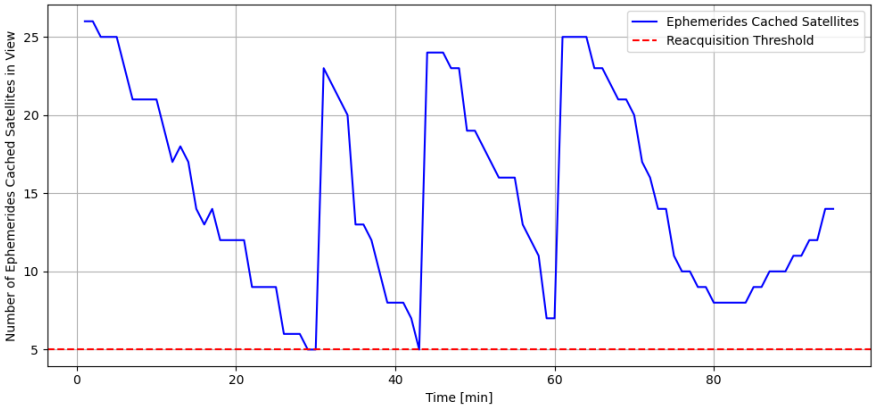


**Figure 4.17:** One trial for ephemerides saved satellites vs time with two antennas.

Figure 4.18a and Figure 4.18b show the frequency versus re-acquisitions per orbit results of the Monte Carlo simulation. As the plots show, the majority of the cases require 7-8 re-acquisitions per orbit for a single antenna configuration and 2-3 re-acquisitions for a dual antenna configuration. This is caused by the extended view range that results from the use of multiple antennas.

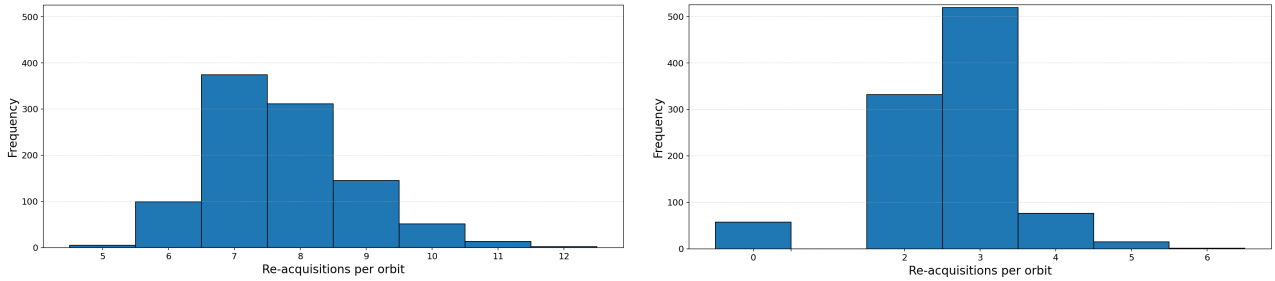


**(a)** One antenna

**(b)** Two antennas

**Figure 4.18:** Monte Carlo simulations (1000 trials) for ephemerides re-acquisitions per orbit using one vs. two antennas

### Chosen SP Antenna Configuration

The Monte Carlo simulations show that including two antennas in the payload significantly reduces the duty cycle and enhances user convenience. However, putting a second antenna on the spacecraft results in an additional 1.5 $cm^2$ of required surface area. If this surface area is taken away from the solar panel surface area, approximately 20 mW of additional power will be lost in the spacecraft. This results in the payload taking away more power with the second antenna compared to the power saved by reducing the duty cycle. However, PocketQubes and CubeSats commonly have small empty spaces on their surfaces that are not covered by solar panels. With meticulous placement, the area taken away from solar panels can be minimized. Additionally, the convenience benefits of reduced duty cycle and reduced risk of unfeasible ephemerides acquisition make the second antenna a better option. Furthermore, considering that the number of CubeSats is significantly larger than the number of PocketQubes [(1)] , the solar panel surface area taken will likely not pose any issues due to the availability of larger spaces for CubeSats. Therefore, the final decision for the SP antenna configuration includes a dual antenna architecture.

## 4.7. GNSS Antenna Placement on Host Spacecraft

The previously selected Antenova Raptor SR4G053 GNSS antenna is still an option for this mission [46]. However, another smaller 2JL67 GNSS antenna has been identified and selected. The antenna previously selected has a size of 16 mm × 8.0 mm × 1.7 mm [46] and the chosen antenna has a size of 5.2 mm × 3.7 mm × 0.7 mm [91] without a compromise of functionality. The 2JL67 GNSS antenna requires a 10 mm × 15 mm PCB to accommodate for extra electrical components in order to work. A size comparison can be seen in Figure 4.19.

[(1)]Nanosats Database - Nanosats.eu, 2025.[Online]. DoLA: June 16, 2025. Available: https://www.nanosats.eu

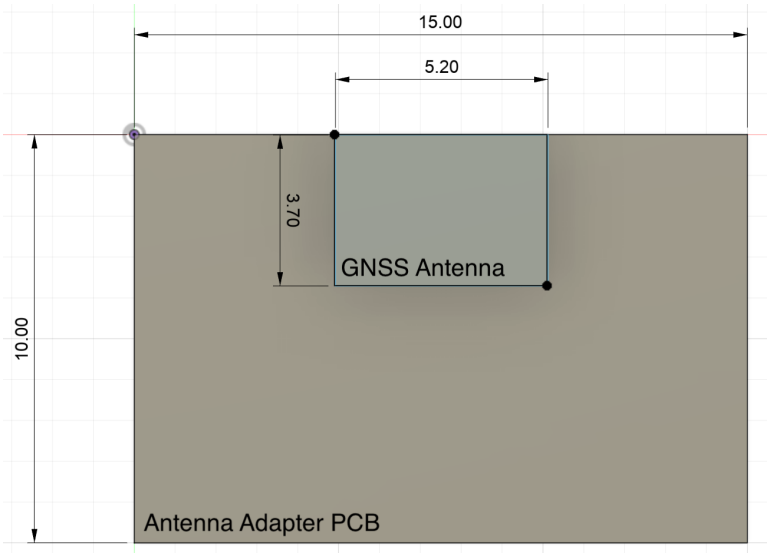


**Figure 4.19:** Relative scale of GNSS antenna and accommodating PCB (units in mm.)

The antenna and the adapter PCB will be placed on 2 sides of the satellite (which are not opposite to each other) with a wire attached to it that connects to the SP. In order to determine where to place the antenna one has to consider the exterior of the satellite and the wiring path within the satellite. In the future this will have to be done in the design process of all the satellites this standardized payload is supposed to be integrated on. An example of how to do so will be done on the technology demonstration satellite.

When considering the location on the exterior of the satellite one has to ensure that

- it does not cause destructive interference when the signals are combined;
- it does not overlap with the solar cells;
- that part of the PCB is not above the satellite structure such that a wire can be connected (otherwise one would have need a hole in the structure);
- that it does not overlap with any screws.

In terms of the first point of consideration, the GNSS signal travels different distances to reach the SP antennas due to the relative distance between the antennas. Therefore, when the signals are combined, they might interfere destructively if the path difference due to distance traveled equals half of the wavelength. The schematic for this interference is shown in Figure 4.20, where the same GNSS signal is being acquired by two different antennas on the satellite.

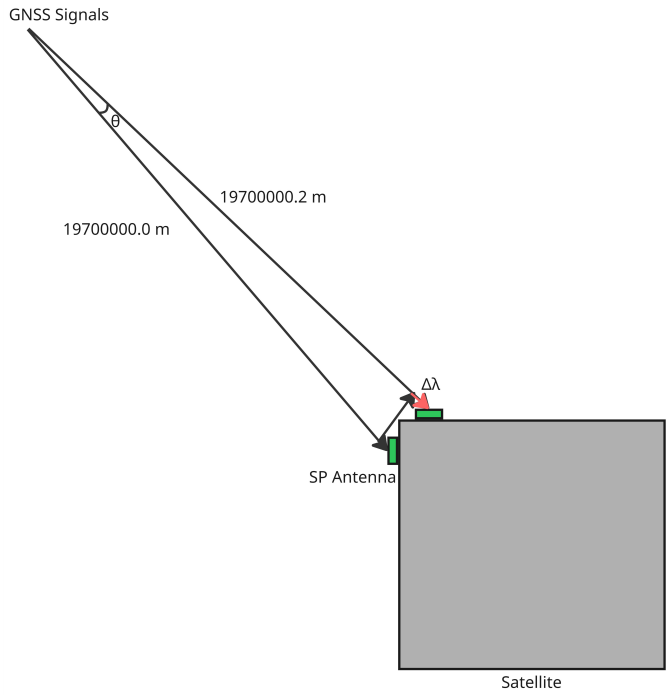


**Figure 4.20:** GNSS signal interference schematic.

At L1 and L5 frequencies, the half wavelength is approximately equal to 20 cm. As the path difference between the distance covered by the two LOS vectors from the GNSS satellites, indicated by $\Delta\lambda$, must be equal to an odd multiple of 20 cm for destructive interference to occur, the limiting scenario is considered at 20 cm. In this scenario, the distance between the GNSS satellite and the antenna is assumed to be 19 700 000 m, which is the closest possible distance by orbital geometry. Furthermore, $\theta$ is defined as the angle between the two LOS vectors. Thus, the smallest possible distance between the antennas for destructive interference can be written as $\approx 19700000 \cdot \sin\theta$. Therefore, by using the cosine rule,

$$19700000^2 + 19700000.2^2 - 2 \cdot 19700000 \cdot 19700000.2 \cdot \cos\theta = (19700000 \cdot \sin\theta)^2. \tag{4.1}$$

As this equation does not have any real solutions for $\theta$, destructive interference will never occur. Therefore, signal interference does not have additional implications with regard to antenna placement.

In terms of the remaining antenna placement considerations, options A and B are evaluated, as shown in Figure 4.21, where option A considers the possibility of placing the GNSS antenna closer to the shorter side of the solar cells, and option B considers placing it closer to the longer side. In both cases, the PCB is big enough such that it does not cover the structure and does not obstruct cabling as seen in Figure 4.22. However, in Option B, the antenna is closer to the solar panel overall, increasing the probability of shadow, thus option A is chosen. Please note that the figures may contain an outdated Computer Aided Design (CAD) model, however the procedure of how to attain a viable GNSS antenna location remains the same.

Within option A, there are still multiple possibilities of where to put the antenna. Therefore, the ease harness design will dictate the choice. Considering the curvatures of the PCBs of the different subsystem, one can identify a path of least resistance. One needs to be able to feed a wire all the way through the satellite as the payload is located very close to one side of the satellite (as opposed to the middle). Therefore if the side furthest away from the satellite is chosen, the wire needs to almost reach from one end of the satellite to another. Figure 4.23 shows the possible locations of with the structure and solar panels hidden. Clearly it can be seen that in order to feed a wire all the way one has choose the top hole as the bottom hole is being obstructed by the green PCB.

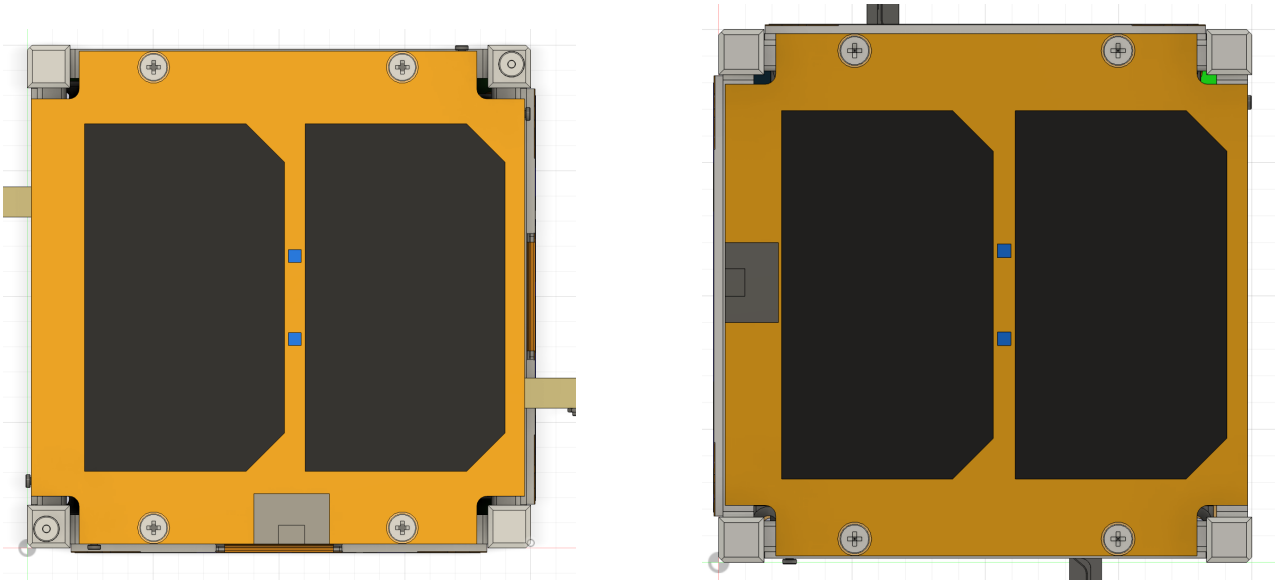

**(a)** GNSS antenna placement, Option A.

**(b)** GNSS antenna placement, Option B.

**Figure 4.21:** GNSS antenna placement options.

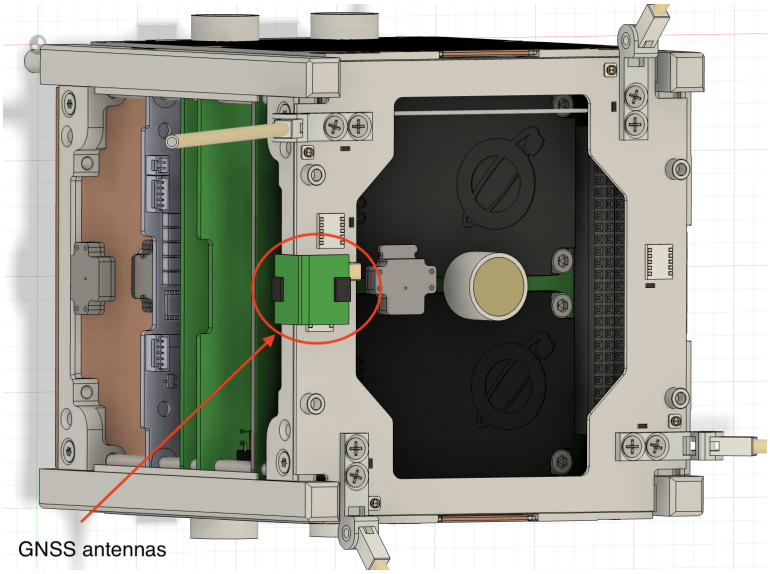


**Figure 4.22:** Location of GNSS antennas on satellite.

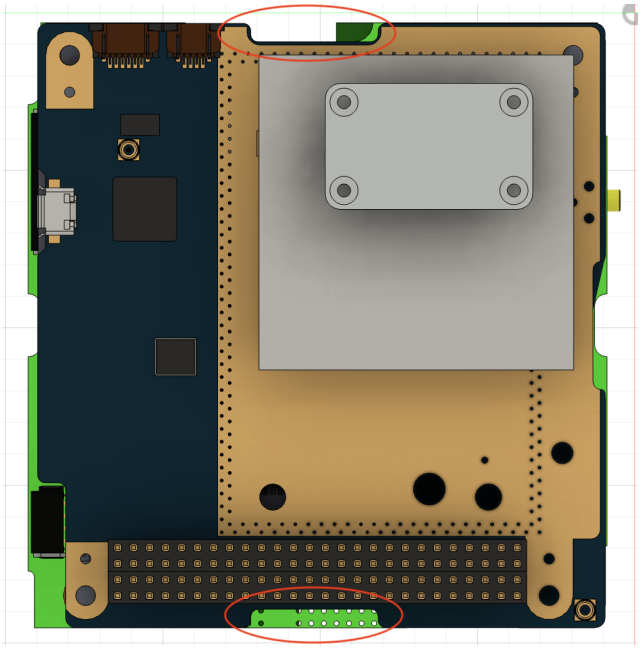

**Figure 4.23:** Possible locations to feed GNSS antenna wire through.

The last design choice to make is the choice of wire and type connection to both the GNSS antenna adapter PCB (seen in Figure 4.19) and the SP. For the connection to the PCBs one has to choose between

- putting a connector on the PCB, allowing for connecting and disconnecting the wire;
- producing the PCB with a built-in wire, thus not allowing for connecting and disconnecting the wire.

At least one of the PCBs (i.e. the SP or the GNSS adapter PCB) has to have the connector option otherwise integrating the satellite becomes very challenging. The GNSS antenna adapter is the limiting factor here due to the fact that one will have to find a spot on the outside of the satellite, where there is already limited space - thus one aims to make this placement as easy as possible. Therefore, the cable will be directly integrated to the GNSS adapter PCB and the SP will have a connector to which this cable can connect to. Due to the high frequencies used in GNSS signal reception and due to the fact that the 2JL67 antenna is designed with a 50 Ω impedance, a coaxial cable is used [92]. A viable coaxial cable is the 1.3 mm Low Loss Coaxial Cable from GradConn due to its small radius, 50 Ω impedance and lightweight design [93]. A small connector for this cable that is to be placed on the SP is the A-2JA from Amphenol RF [94].

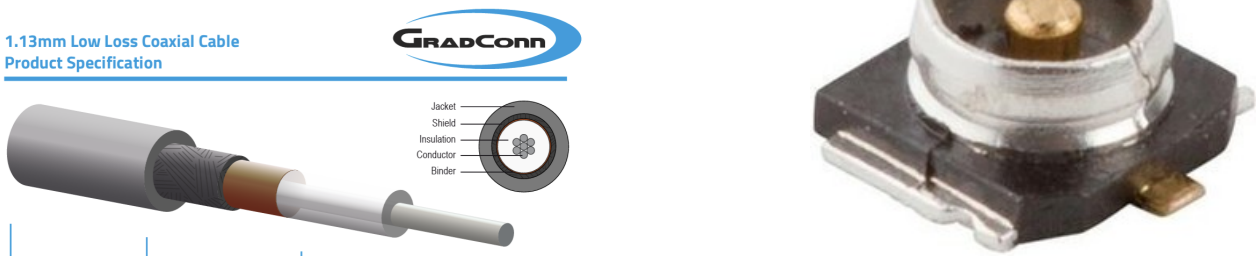


**(a)** 1.3 mm Low Loss Coaxial Cable from GradConn

**(b)** A-2JA connector from Amphenol.

**Figure 4.24:** GNSS antenna wire and connector.[(1)]

## 4.8. Standardized Payload Power Budget

The total power used by the standardized payload can be calculated based on the final design presented in the previous sections and the components in Table 4.4. This section presents the exact power used by the SP considering different snapshot rates and the ephemerides update frequency described in Subsection 4.6.2. Subsection 4.8.1 calculates the required snapshot rate needed in order to get the desired accuracy and the power required for such a snapshot rate. Subsection 4.8.2 then shows a in-depth breakdown of the total power used by the SP.

### 4.8.1. Varying Snapshot Rate

Varying the rate of snapshots can increase the accuracy, but at the cost of higher power consumption. However, as can be seen in Figure 4.26, the main power draw of the SP is created by the EAR. When the snapshot rate is increased, both the snapshot receiver and the MCU will have a higher duty cycle.

To test the capabilities of SP in terms of generating position fixes with snapshots at various frequencies, the SP will have a varying snapshot rate throughout the mission. Various snapshot frequencies, specifically once per minute, 5 minutes, 10 minutes, 30 minutes, and once per orbit, will be tested. As each user might prefer a different frequency of position fixes for their satellites, having an envelope of tested snapshot frequencies, with their corresponding accuracy, will ensure that the SP can accommodate all users' requirements.

The decision to test the payload once per minute is not a strict restriction. The payload is capable of computing position fixes as frequently as possible, as long as there is sufficient time between snapshots that allows the components to wake up and function properly. However, orbit propagation on the scale of several minutes is accurate, especially since the error grows exponentially with time [95]. Figure 4.25 shows the variation of the total average power of the SP as a function of the time intervals between the snapshots.

### 4.8.2. Standardized Payload Final Power Budget

The power budget estimate is shown in Table 4.16. Snapshots were assumed to be 20 ms long, and based on the estimations in Subsection 4.8.1, a frequency of once per minute was chosen. One of the main functions of the

[(1)] Amphenol RF A-1JB, Mouser Electronics, 2025. [Online]. DoLA: June 6, 2025. Available: https://www.digikey.nl/en/products/detail/amphenol-rf/A-2JA/5029285

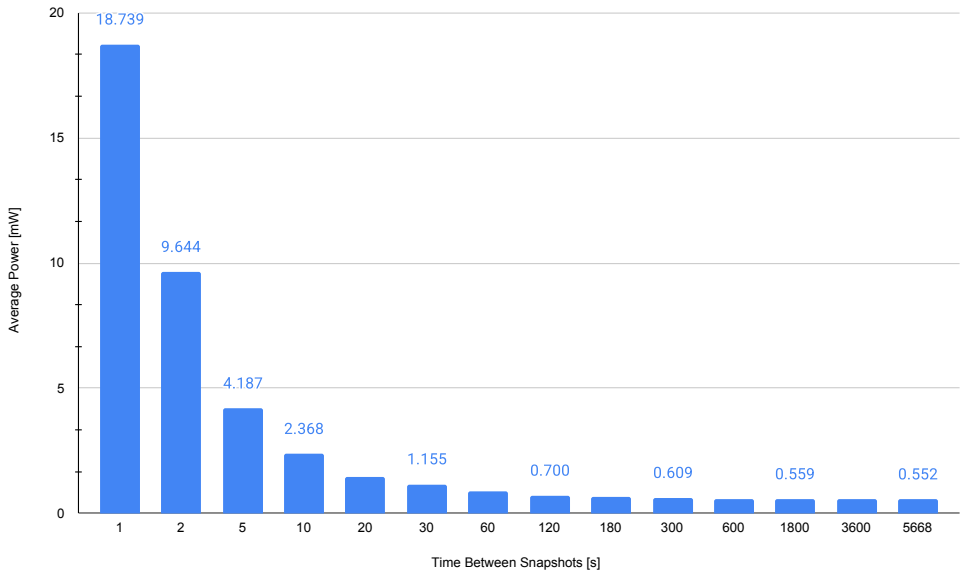


**Figure 4.25:** Average SP power as function of time interval between snapshots.

SP is computing the position onboard. Thus, the MCU run time needs to be calculated in order to estimate the average power consumption.

**MCU Run Time**

Snapshots are initially down-converted to an IF and digitized by the RF front-end. After this process, the signal is now in binary format. As explained in Section 4.1, this digitalized signal include PRNs, the are satellite-specific information that allows the receiver to determine which satellite the signal is coming from. Acquiring this information is necessary as ephemerides are stored per satellite and to process snapshots, they must be matched with the correct ephemerides. Therefore, the PRNs must be decoded, and this is accomplished with a Fast Fourier Transform [56]. According to the spec sheet of the MCU [96], FFT is performed by binning - the signal is stored with certain size frequency steps. These frequency steps are called FFT points. Note that this spec sheet does not belong to the specific model that was chosen for the SP, but to an MCU version from the same family, with the same core and sampling rate. Smaller steps result in more detailed processing and therefore can capture more information. However, this has power consumption implications as the MCU has to iterate more in order to acquire information from the smaller frequency steps. These iterations are called cycles, and the spec sheet contains information about the processing time for various cycle values. For a 1024-point FFT with Q15 fixed point format (15-bit data), approximately 77 000 cycles are required to perform one FFT [96]. This requires $\approx 0.9$ ms. However, since the GNSS signal is stored in two bits for the current SP configuration, the FFT can be performed by using the minimum fixed-point format, Q7 (only 7-bit data). According to the spec sheet, this reduces the number of cycles to approximately half. Therefore, the FFT time is reduced to $\approx 0.45$ ms.

This is crucial as the ADC samples the 20 ms snapshot at approximately 16 MHz. This results in 320 000 raw samples, which are divided into FFT batches of size 1024, specified by the FFT points. Ultimately, there are $320000/1024 = 313$ batches, and these batches are renamed as blocks for convenience. Since the snapshot solving requires five satellites to generate position fixes, the FFT has to be performed five times for each block to acquire the 5 PRNs. Therefore, the MCU has to perform $313 \cdot 5 = 1565$ FFTs. Since each FFT takes 0.45 ms, processing snapshots from 5 GNSS satellites requires approximately 700 ms. Table 4.15 summarizes this process step by step.

**Table 4.15:** MCU time for computing position fix.

| Quantity | Value | Reasoning |
|---|---|---|
| ADC Sampling Rate | $f_s$ =16.368 MHz | 16 × chip-rate |
| Snapshot Length | $T_s$ =20 ms | Fixed in preliminary design |
| Raw Samples | $N \approx 320\,000$ | $N = f_s \cdot T_s$ |
| FFT Points | $N_{FFT} = 1024$ | Use 1024-point FFT [97] |
| Number of Blocks | $B = 313$ | $B = N/N_{FFT}$ |
| Satellites (PRNs) Computed | $N_{PRN}$ =5 | 5 pseudo-ranges needed |
| CPU Time/FFT | $C \approx 450\,\mu s$ | From spec. sheet [96] |
| **Total MCU Time** | $t$ =**704 ms** | $t = C \cdot B \cdot N_{PRN}$ |

Ephemerides updates were considered 50 s long, taken 3 times every two orbits (worst case scenario from circumstances described in Subsection 4.6.2); time required for MCU to load the ephemerides was assumed 3 s. The MCU time required for the position solver was rounded up to 750 ms. A more detailed view of the snapshot rate can be found in Subsection 4.8.1 and one on the ephemerides refresh rate in Subsection 4.6.2. Power consumed by processing commands from the host OBC and by sending telemetry to the host OBC has not been taken into account but should be considered in future power calculations.

**Table 4.16:** Average power budget of the standardized payload.

| Role | Device | Duty | Active[mW] | Avg. [mW] | Notes |
|---|---|---|---|---|---|
| GNSS Antennas | 2JL67 | 1.78 % | - | - | Listens to the signal broadcast on L1 and L5 frequency bands. |
| Ephemeris Acquisition | Antenova M20071 | 1.32 % | 32 | 0.423 | 3 acquisitions every other orbit; 50 s per acquisition for Galileo. |
| Snapshot capture | MAX2769C | 0.03 % | 77 | 0.026 | 20 ms burst every 60 s; 27 mW at 2.85 V. |
| Position solver | STM32L452 | 1.25 % | 22.2 | 0.278 | 84 µA $MHz^{-1}$ (LDO Mode) clock running at 80 MHz on 3.3 V. |
| Loading ephemerides | STM322L452 | 0.08 % | 22.2 | 0.018 | 3 s load time for ephemerides |
| Always-on RTC | 32 kHz XO (part of MCU) | 100 % | 0.008 | 0.008 | Schedules wake-ups. |
| Voltage regulator & leakage | LTC3407EDD-3#PBF | — | — | 0.1 | Inefficiencies and off-state leakage margin. |
| | | **Total average power** | | **0.852** | **<1 mW average** |

The average power consumption of the SP processes is shown as a pie chart in Figure 4.26 for easy visualization. It is observed that the main power draw comes from the ephemerides acquisition process. The second most power-hungry operation is calculating the position fixes using the GNSS data.

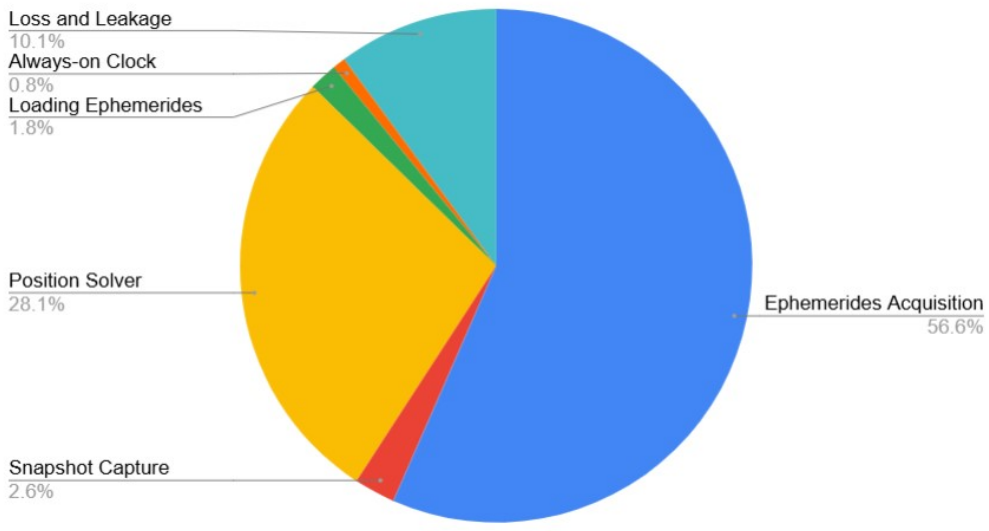


**Figure 4.26:** SP average power consumption breakdown.

## 4.9. Requirement Verification and Compliance Matrix

Table 4.17 cross-references the finalized SP requirements against the proposed final design. For each item, it records whether the requirement is met, the measured or assumed value where applicable, and a brief note on any pending verification or validation. The verification method is also listed for each requirement. The following abbreviations are used in the "Verification Method" column:

- **Inspection (I):** Inspect the design documentation or the product to show compliance with the requirement.
- **Analysis (A):** Establish by mathematical or other analysis techniques that the product complies with the requirement.
- **Demonstration (D):** Establish by operation, adjustment, or reconsideration of a test article its compliance with the requirement.
- **Test (T):** Test (a representative model of) the product's compliance with the requirement under representative conditions.

**Table 4.17:** Requirement compliance matrix. *N/A* indicates requirements deferred to the post DSE phase, while *TBD* marks parameters still under analysis.

| Requirement | Met | Value | Comment | Verification Method (TADI) |
|---|---|---|---|---|
| STM-SYS-SP-1 | Yes | 33 g | Meets requirement, large margin still available. | A/I: CAD and BOM cross-checked with the mass budget. T: Weigh the payload |
| STM-SYS-SP-2 | Yes | 0.94 mW | < 1 mW average power budget | A/T: Test power consumption by simulating ephemerides acquisition, snapshots, and generating position fixes on ground with GNSS simulators. |
| STM-SYS-SP-3 | Yes | 16.02 $mm^2$ | 36 mm × 44.5 mm PCB < 23.04 $cm^2$ | I: Dimensions of the PCB inspected |
| STM-SYS-SP-4 | Yes | – | Low-power COTS, negligible EMI/heat | T/I: Functional testing and EMI evaluation |
| STM-SYS-SP-5.1 | N/A | – | To be implemented post DSE | – |
| STM-SYS-SP-5.2 | N/A | – | To be implemented post DSE | – |
| STM-SYS-SP-5.3 | Yes | – | All protocols accomodated | D/I: Demonstrate host communication and inspect API documentation |
| STM-SYS-SP-6 | Yes | – | Position packets sent to C&DH via chosen communication channels | D/T: Ground communication simulation and tests |
| STM-SYS-SP-7 | Yes | Both L1, L5 | Meets 4x chip-rate criterion | A: RF bandwith measured |
| STM-SYS-SP-8 | Yes | High clock frequency, L1 and L5 used | Verified post DSE | T: Test with on-ground GNSS simulator |
| STM-SYS-SP-9 | TBD | €4M | Being a student team results in reduced labor and development costs | A: Detailed budget breakdowns, regular spending checks and budget updates |
| STM-SYS-SP-10 | Yes | €275 | BOM indicates €250, 10% margin component costs for one unit; will benefit from economies of scale if mass-produced. Manufacturing will not exceed €750. | A/D: Cost can be further analysed, prototype can be produced |
| STM-SYS-SP-11 | TBD | – | Radiation hardening and temperature cycles considered | T: Radiation and thermal vacuum testing should pe performed post DSE |
| STM-SYS-SP-12 | Yes | 2040 | TRL ≥ 8; schedule fits roadmap | A: Analyse the roadmap timeline with additional margins |
| STM-SYS-SP-13.1 | Yes | −40 °C to 85 °C | Component ratings cover range | A/T: Component analysis and thermal cycling test in vacuum chamber |
| STM-SYS-SP-13.2 | TBD | – | To be verified post DSE | T: Vibration test on shaker table |
| STM-SYS-SP-13.3 | Yes | Space-tailored components | No vacuum sensitive parts | A/T: Vacuum chamber tests and material analysis |
| STM-SYS-SP-14 | TBD | – | Comply with laws and regulations highlighted in Section 2.2 | A: Legal review of applicable space laws |
| STM-SYS-SP-15 | Yes | – | SP does not transmit signals | – |
| STM-SYS-SP-16 | Yes | – | No hazardous assembly/test steps | I: Review of AIT procedure and safety measures |
| STM-SYS-SP-17 | Yes | – | Supports autonomous Galileo PNT | A/T: Receivers compatible with Galileo, on-ground testing post DSE |
| STM-SYS-SP-18 | TBD | – | To be tested post DSE | A/T: Calculate reliability, test failure modes, heavy duty-cycling and radiation resistance |
| STM-SYS-SP-19 | N/A | – | Manufacturing documentation to be generated | I: Documentation review |
| STM-SYS-SP-20 | N/A | – | Integration/test documentation pending | I: Review of test plans and integration checklist |

*Continued on next page.*

| Requirement | Met | Value | Comment | Verification Method |
|---|---|---|---|---|
| STM-SYS-SP-21 | N/A | – | Encryption methods evaluated in software development post DSE phase | T: Test with cryptanalytic attacks |
| STM-SYS-SP-25 | Yes | 9.5 $cm^3$ | Current CAD envelope | A/I: CAD volume calculations and physical inspection of the assembled SP |
| STM-SYS-SP-26 | Yes | – | Chosen antenna covers L1 and L5 | T/A: Antenna performance test and datasheet analysis |

## 4.10. Standardized Payload Configuration Overview

The SP is fully designed and production-ready: every detail, resistor and capacitor values, PCB trace widths, component placement, and stack-up, has been defined and the board layout is verified. Production requirements have been factored in, and a complete bill of materials down to the smallest passives is provided for one unit, showing a parts cost of €275. The next step is fabrication.

Additionally, easy mechanical adaptation into PocketQubes, CubeSats, and larger satellites has been implemented by adding adapter PCBs and standard connectors. In order to accommodate for these needs, a dual receiver configuration with the following hardware is used: a lightweight small GNSS antenna, an RF switch, a GNSS receiver module acting as an EAR, a snapshot GNSS, an MCU, a non-volatile memory unit, a power management unit and a PCB. Additionally, the payload is enclosed in an aluminum envelope which leads to the final dimension of 4 mm × 36 mm × 6 mm and a total mass of 33 g. This includes 2 GNSS antennas on the exterior of the satellite which have an area of 15 mm × 10 mm. Snapshot duration is 20 ms with an average of 0.94 mW and a peak power consumption of 77 mW. Table 4.18 shows the final budgets with a 10 % margin on mass, cost and mass.

**Table 4.18:** Standardized payload final budgets. Margins applied.

| Component | Margin [%] | Number | Mass [g] | Size [mm] | Cost [€] | Power [mW] | Operational Temp. [°C] |
|---|---|---|---|---|---|---|---|
| Main Electronics Box | 10 | 1 | 24 | 45 × 36 × 6 | 223 | 0.852 | −40 to 85 |
| Antenna PCB | 10 | 2 | 3 | 15 × 10 × 1 | 27 | 0 | −40 to 85 |
| **Total** | - | - | **33** | **45 × 36 × 6** | **275** | **0.94** | **−40 to 85** |

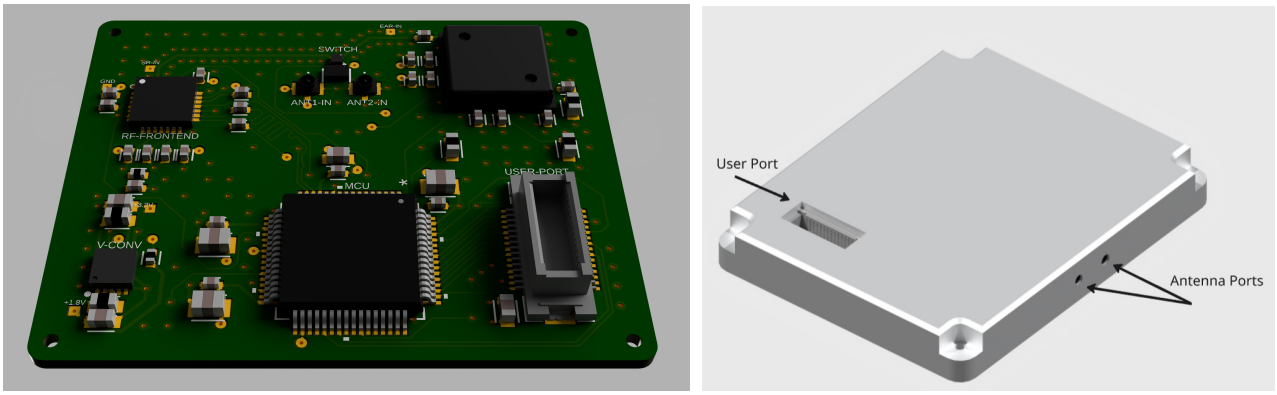


**(a)** SP main electronics board.

**(b)** Enclosed SP unit.

**Figure 4.27:** SP hardware: (a) assembled PCB and (b) final boxed unit.

# 5. Technology Demonstration Satellite Subsystem Design

The S/C consists of the SP, the Validation Payload (VP) and the subsystems. In the previous chapter the detailed design of the SP was discussed; in this chapter, the VP and the subsystems of the S/C are highlighted. First a general overview of what each subsystem structure looks like will be highlighted in Section 5.1, after that the subsystems are shown. The Validation Payload will be reported on in Section 5.2. The validation payload is the system that will ensure the SP is functioning as intended. Since the mission is to demonstrate the SP technology, a way to validate it is essential. The structural design of the S/C is reported on in Section 5.3. It highlights the chosen size of the S/C, and verifies it meets the strength requirements. Command and Data Handling will be reported on in Section 5.4. It consists of both the on-board processing, and the communication link of the S/C. The Attitude Determination and Control System (ADCS) is reported on in Section 5.5. It ensures the S/C doesn't enter an unrecoverable tumbling scenario, and provides attitude determination for Payload (PL) data processing. The Electric Power System (EPS) is reported on in Section 5.6. The EPS is about power generation, and how this power is distributed to other subsystems. Finally, the thermal design will be discussed in Section 5.7. The thermal design discusses simulation methods to verify the S/C subsystems temperature constraints are met.

## 5.1. Design Approach

In this chapter, multiple subsystems shall present their detailed design. Each subsystem has reported the detailed design in the same basic structure. First the requirements were shown. After that, the preliminary design results from the midterm report [46] were re-stated. From both the requirements and the preliminary design results, the detailed design could be performed. For each subsystem, a part selection was made, and the budgets per subsystem were determined. Finally, the future steps for each subsystem were explored.

### Sustainability Design Strategy for Subsystems

Sustainability hasn't been taken into account extensively in the design process. Large wins in sustainability were chosen to be taken in the preliminary steps of the design rather than the detailed design. By making sustainability a criterion in the preliminary trade-off process, the preliminary design decisions were made with sustainability in mind. With the subsystems' final parts being chosen, the sustainability of the project was able to be assessed, and will be discussed in Section 6.5.

## 5.2. Validation of Standardized Payload

The standardized payload needs to be verified. For this, two systems will be evaluated and specified. First the subsystem requirements are reiterated in Subsection 5.2.1. Then the preliminary design decisions are explained in Subsection 5.2.2. Then, the finalized design is created in Subsection 5.2.3. Lastly, the system is summarized and next steps are laid out in Subsection 5.2.4.

### 5.2.1. Requirements

In this section, the requirements for the validation payload of the payload are further derived and/or changed from the following high-level system and payload requirements:

- **STM-STM-SYS-SP-8:** The SP shall provide position fixes with an accuracy of 20 m (3D r.m.s.).
- **STM-STM-SYS-SP-17:** The SP shall be capable of performing autonomous Positioning, Navigation, and Timing functions with European GNSS infrastructure.
- **STM-STM-SYS-M-4:** The accuracy of the SP stated in STM-STM-SYS-SP-8 shall be validated in orbit.

The subsystem requirements for the VP are summarized in Table 5.1. To demonstrate compliance, each requirement has its method of verification written after it. The way of verification is one of four; Testing, Analysis, Demonstration and Inspection (TADI).

**Table 5.1:** Subsystem requirements for the validation payload.

| ID | Requirement | Verification Method (TADI) |
|---|---|---|
| STM-SYS-VP-1: | The validation payload shall provide position accuracy that is always better than **10 m** (3D r.m.s.) | **T:** Perform ground testing using a GNSS Signal Simulator that has high-fidelity LEO trajectories, including ±35 kHz Doppler, realistic signal dynamics, and representative ionospheric delays for both L1 and L5 |
| STM-SYS-VP-2: | The validation payload shall fit within a **1U** cubesat, **10 cm × 10 cm × 10 cm** | **I/D:** Visually inspect and verify that it can fit inside the structure |
| STM-SYS-VP-3: | The validation payload shall have a mass of less than **980 g** | **T/D:** Weigh the systems |
| STM-SYS-VP-4: | The validation payload shall deliver the position accuracy specified in **VP-1** for the **6 months** nominal mission duration. | **T/A:** Mission lifetime VP performance analysis based on obtained data and perform tests to verify ECSS compliance via e.g. thermal-vacuum tests |

## 5.2.2. Preliminary Design Results

In the previous report, it was determined that to validate the positional accuracy of the SP a conventional CubeSat GNSS will be used. The main importance, as formulated in **STM-SYS-VP-1**, is that the output is more accurate than that of the SP. It furthermore, had to adhere to all the standard constraints that apply to CubeSat components. However, this is already accounted for by the designers of the COTS components. Furthermore, the option of SLR came in as a close second.

## 5.2.3. Detailed Design

Now that the groundwork has been laid, the detailed design can commence. First, the conventional receiver will be designed and picked in Subsection 5.2.3. Then a design iteration will occur to see whether SLR is a suitable redundant option for validation for this mission in Table 5.2.3.

### Conventional GNSS

As has been decided in the preliminary design, the conventional GNSS is used as the primary validation method. This is because it has the ability to validate the SP for the complete orbit. Furthermore, the same antennas and antenna configuration that the SP employs will be used. This is justified by the antenna's high reliability, resulting from its low complexity. This is further substantiated by them being a passive antennas. It then allows the VP to validate the antennas and broadcast data as well. Thus, if problems or errors occur it is easier to pinpoint where they arose.

The validation GNSS receiver, apart from adhering to the requirements, has a couple of preferred traits that will be looked for. The first is that it must minimize its power consumption due to the limited power budget available for this class size. The second is that it is PC/104 compatible. PC/104 is a family of embedded computer standards, having a receiver in this standard will reduce the amount of adaptation needed for integration. The standardized protocols for communication with the OBC are the main benefit. Lastly, due to the geopolitical developments in the United States, parts from the USA will not be chosen.

Now that these criteria are known, a part selection can be performed. Five options were found and shown in Table 5.2. Every receiver already complies with the specified dimensions as given in **VP-2** as to fit in a 1U CubeSat. The price is also an important parameter but only the piNAV-NG has a price listed of €7490. It is expected that the other receivers fall in the previously estimated price range of €6400 to €20 700 [46].

**Table 5.2:** Component selection for the validation GNSS receiver

| Part Name | Accuracy | Avg. power [W] | Communication protocols | Country |
|---|---|---|---|---|
| NanoSense GPS Kit[98] | 1.5 m | 0.9 | CAN, UART | DK |
| piNAV-NG[99] | 10 m, $2\sigma$ | 0.125 | UART | CZ |
| Celeste GNSS[100] | 2 m, CEP | 0.1 | I2C, RS485, UART, CAN, GPIO | CZ |
| ACC-GPS-NANO-NR[101] | 10 m, $1\sigma$ | <0.5 | UART (TX,RX), RS-232/RS-422 | IN |
| Hyperion GNSS200[102] | < 8 m | <0.15 | TTL UART | NL |

The accuracy is differently defined for each receiver. The NanoSense GPS Kit provides a horizontal accuracy of 1.5 m. The ACC-GPS-NANO-NR and piNAV-NG have its accuracies given in horizontal accuracy with a 1- and 2-$\sigma$ confidence level. It corresponds to the percent change that the satellite lies within a 1 or 2 standard deviation of the mean, guaranteeing a 65 % and 95 % chance respectively. The Celeste GNSS has its accuracy established as Circular Error Probable (CEP), which means that there is a 50 % chance that the satellite's position lies within a 2 m radius circle. This accuracy is based on a circular bivariate normal distribution and

can be adjusted to arrive at a value that guarantees a higher chance of detection. Taking a circle of '3n' or 6 m will provide a 99.8 % chance of the satellite being inside the circle.

The most suitable option is determined to be the Celeste GNSS from SpaceManic. It consumes the least amount of power and scores second in accuracy. The NanoSense is the winner in accuracy, but it consumes too much power to be considered. The Celeste also supports a broad range of communication protocols, which helps with its integration. The only downside is that it does not come in the standard PC/104 form factor. However, an adapter PCB board exists which can be utilized.

**Satellite Laser Ranging**

Satellite Laser Ranging remains an effective option in enhancing the redundancy of the validation system without contributing much to the mass and size budgets of the satellite due to the small form factor of retro-reflectors. Thus, a second design loop will be performed to see if integration is possible.

It was determined that for a tumbling satellite, a configuration with two retroreflectors with a diameter of 12.7 mm on each side would provide sufficient visibility if the SLR ground stations of Potsdam in Germany and Matera in Italy are used [103].

Two constraints need to be checked. The first constraint is if the inclusion of retroreflectors on the exterior of the CubeSat is possible, i.e. does it leave enough room for a sufficient solar cell and antenna area. The second constraint is if the S/C has a high enough visitation frequency and pass duration to justify using SLR.

**Retroreflector Integration Check**

The amount of space on each side of the S/C is 100 $cm^2$. The preliminary solar cell area required was 78 $cm^2$, as stated in Subsection 5.6.3. Furthermore, the patch antenna selected would take up another 2 $cm^2$ on two sides of the S/C. This leaves 16 $cm^2$ for the retroreflectors on the most constraint sides. The retroreflectors have a diameter of 12.7 mm resulting in around 1.27 $cm^2$ or 2.53 $cm^2$ in total. Therefore, the retroreflectors can be fitted on the exterior even when screws and fasteners are accounted for. The simplified calculation only proves that space should be available, however, due to the layout of the COTS solar panels, only one retroreflector is able to be placed on the +Z and -Z faces.

Not only available surface area is needed. Retroreflectors with a diameter of 12.7 mm have a depth of 10.16 mm when unmounted. Mounting on the surface is not possible due to the ESA CubeSat allowable protrusion specifications [10]. To paraphrase: *"No components shall protrude farther than* 6.5 mm *normal to the surface from the plane of the rail."* So, the retroreflectors have to intrude into the volume of the S/C. To achieve as little hindrance to the other systems, unmounted retroreflectors are preferred. This allows for less protrusion and intrusion but adds risk and cost due to custom cut-outs and fittings that need to be created. The standard housing of Edmund Optics adds 6 mm of extra depth since it also includes mounting holes. However, this would be an excessive amount of intrusion into the S/C. It was decided that a custom housing of around 2 mm would be sufficient to protect the retroreflectors from the vibrational loads, taking into account the adhesive clearance and thermal expansion.

The retroreflectors that were deemed most suitable were aluminum back-coated UV fused silica corner cube retroreflectors from Edmund Optics [103][(1)]. Concluding, it would be possible to fit the retroreflectors on the S/C.

**Ground Station Visibility**

Knowing that it is possible to fit the retroreflector on the S/C, the visibility to the ground station can be evaluated. The chosen ground station was TU Delft since it already possesses the required infrastructure. However, research determined that no link budget could be closed using 12.7 mm retroreflectors and TU Delft's station [103]. The other options that were considered are stations in Potsdam in Germany, Matera in Italy and lastly the TU Graz in Austria. All are part of the International Laser Ranging Service (ILRS) network. The ground stations were modeled in GMAT together with the chosen orbit to check the visitation frequency and duration of each pass for a month starting at 21st of March in 2029. The minimum elevation angle that was set for these stations was initially 20° [104] but was increased to 40° for Potsdam as to ensure that the link budget could be closed [103]. It also needs to be checked if the satellite is long enough in the visibility window to be found. The uncertainty of the position of the satellite requires a search to be performed in the area where it could be found. This size of the search area is either caused by the inherent TLE error of 1 to 2 kilometers or the propagation of the initial uncertainty of the S/C's position determined by the validation GNSS transmitted at last contact given.

[(1)]UV Fused Silica Corner Cube Retroreflectors, Edmund Optics, 2025, [Online]. DoLA: 4 June, 2025, Available: https://www.edmundoptics.com/f/uv-fused-silica-corner-cube-retroreflectors/13435/

The longest time without contact in one month was identified to be 16 hours, 56 minutes and 55 seconds and was rounded up to 17 hours by running GMAT simulations. The error after using propagation models after 24 hours differs a lot from source to source, some suggesting that it is only 30 meters of uncertainty[(1)], where other sources calculate the error range to be between 800 m and 1000 m [105]. To be conservative, 1 km was used as the search area diameter. So the search area in a worst case scenario is $3.14 \times 10^6$ m$^2$. It should be noted that the average contact time is 4 hours, which results in a much smaller search area.

The search area is scanned with the laser of the ground station. The amount of area the laser can cover when the S/C just enters the visibility is used. Starting with the station in Matera. The full-width beam divergence of the station is 218 µrad [103]. The maximum distance the S/C can be from the GS is calculated using trigonometry. For an altitude, $h$, of 500 km, a minimum elevation angle, $\delta$, of 20° and the Earth's radius, $R_E$, of 6371 km, the distance from S/C and GS, $d$, is 1193 km. The radius of the diverged beam at a certain distance is given by Equation 5.1.

$$r_{beam_{end}} = \frac{D_{beam}}{2} + d \cdot \theta_d \tag{5.1}$$

Where $r_{beam_{end}}$ is the radius of the diverged beam at final distance, $D_{beam}$ is the initial diameter of the beam, and $\theta_d$ is the full-width beam divergence. The resultant radius is 260 m which gives a laser area of $5.31 \times 10^4$ m$^2$. Since the laser radius is smaller than the search area a search needs to be performed. The smaller laser circle has to completely cover the search area with minimal overlap. For this, a tool was created in Python that fits tries to fit the smaller circles to completely cover the larger circle with minimum overlap and minimum amount of circles. The results are showcased in Figure 5.1

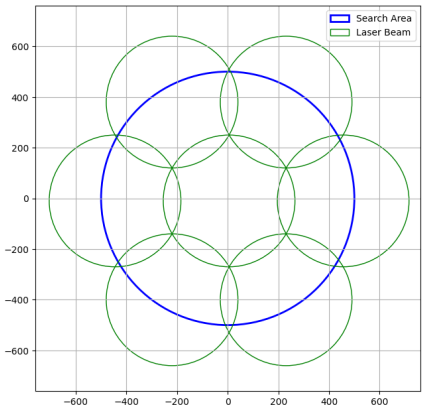


**Figure 5.1:** Optimally covered search area using the laser area for the scenario with the longest time without contact between ground station and satellite.

Since it is more likely that the satellite lies near the center of the predicted position a spiral search method is proposed to transfer from each circle to another. This is showcased in Figure 5.2 where the search begins in the center and follows the black arrows to cover the search area.

[(1)]Solving LEO Orbit Modeling Challenges, Spirent, 15 December, 2022, [Online]. DoLA: 6 June, 2025. Available: https://www.spirent.com/blogs/solving-leo-orbit-modelling-challenges

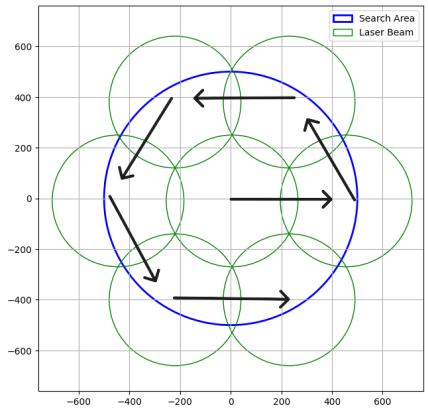


**Figure 5.2:** Proposed spiral search pattern for satellite acquisition using SLR for the scenario with longest time without contact between the ground station and satellite.

This only have to be implemented for the worst case. The average time between contact of the S/C and GS is around four hours. The search error would then be smaller than the area the laser covers. This would mean that it would lock-on the satellite significantly faster, negating the need for any search patterns. For Potsdam and TU Graz, the minimum elevation angles are 40° and 20° respectively and their full-width beam divergences are both 25 µrad[(1)(2)]. Using Equation 5.1, the areas that the laser covers for the stations are computed to be 1088 $m^2$ for Potsdam and 2801 $m^2$ for TU Graz. When trying to cover the worst case scenario search areas, it requires 1120 and 2900 smaller circles to completely cover. Assuming a dwell time of 1 s, it would not be possible to traverse the complete search area within a pass. So, using SLR would not be able justified for passes with a long time between last contact for the station of Potsdam and TU Graz.

It can be concluded that Matera would be advised to use as the main station, and the other station can be used when a short time between contacts are expected. Once again, the usual time between contact is 4 hours, which would provide ample SLR validation.

Now that it is determined that SLR can be used. It is useful to check the amount of passes and the duration of each pass. The averages for Potsdam, Graz, and Matera are 115, 233, and 230 seconds respectively. These times are all enough to acquire enough data points to generate normal points as long as the time between last contact is not an extreme. Simulations were run for a month starting from the 21st of March. The results are shown in Figure 5.3, Figure 5.4, and Figure 5.5.

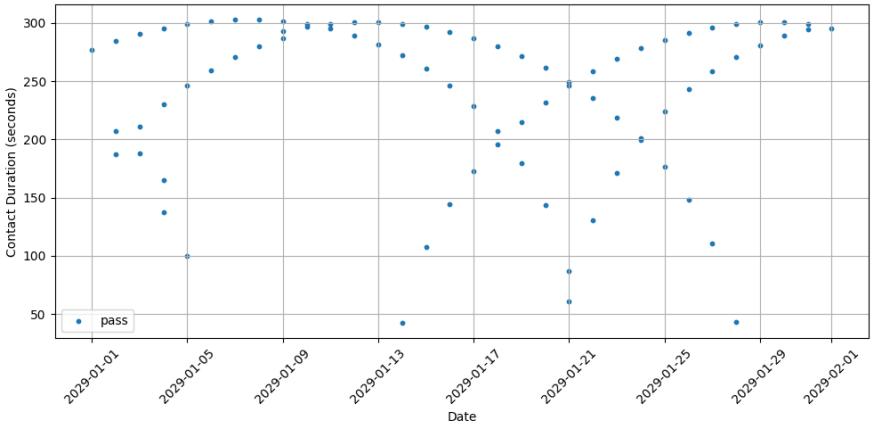


**Figure 5.3:** Duration of contact time between the Matera SLR station and a spacecraft in a 60°, 500 kilometer orbit.

(1) Graz, ILRS, [Online]. DoLA: 10 June, 2025. Available: https://ilrs.gsfc.nasa.gov/network/stations/active/GRZL_station_info.html?log
(2) Pot3 station info, ILRS. [Online]. DoLA: 3 June, 2025. Available: https://ilrs.gsfc.nasa.gov/network/stations/active/POT3_station_info.html

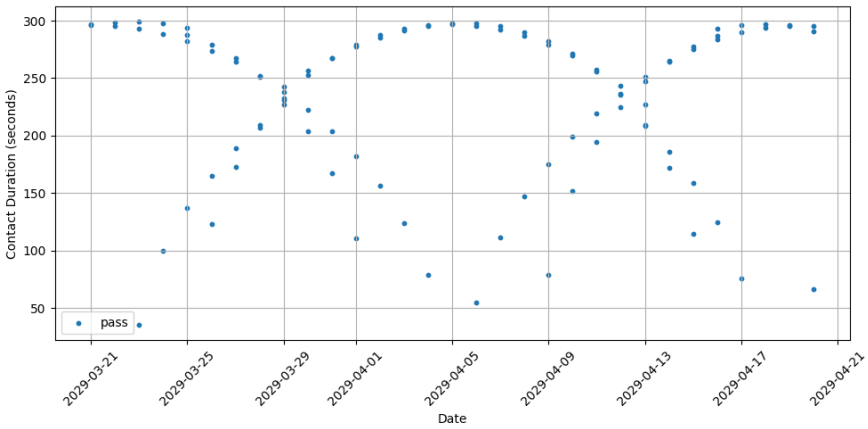


**Figure 5.4:** Duration of contact time between the TU Graz SLR station and a spacecraft in a 60°, 500 kilometer orbit.

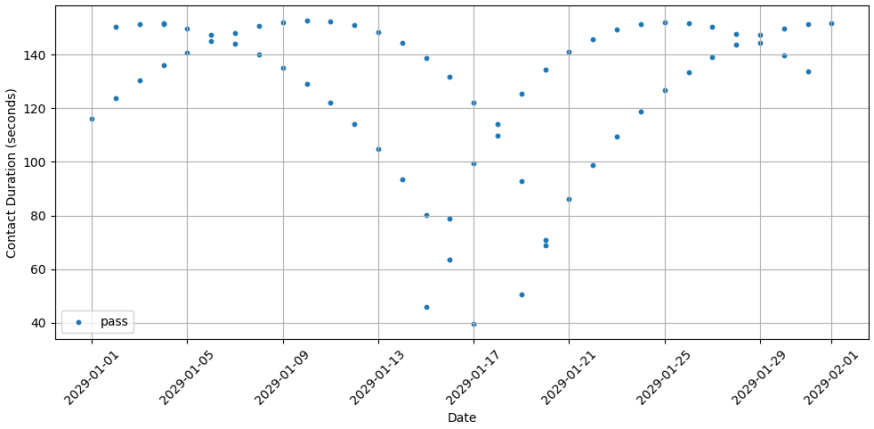


**Figure 5.5:** Duration of contact time between the Potsdam SLR station and a spacecraft in a 60°, 500 kilometer orbit

Thus, the inclusion of SLR for validating the payload is chosen together with the conventional GNSS receiver. The component characteristics of both systems are shown in Table 5.3.

**Table 5.3:** Validation components characteristics.

| Component | Amount | Margin [%] | Mass [g] | Size [mm] | Cost [€] | Power [mW] | Operational Temperature [°C] |
|---|---|---|---|---|---|---|---|
| Celeste GNSS receiver [100] | 1 | 5 | 74* | 67 × 42 × 7** | TBD [(1)] | 100 | -40 to +85 |
| UV Fused Silica Corner Cube Retroreflectors [106] | 10 | 10 | 5.6 | ∅12.7 × 10.16 | 2700 | N/A | −120 to 200 |
| **Total** | N/A | N/A | **84.8** | **N/A** | **TBD**[(2)] | **110** | **−40 to 85** |

*The mass is that of the Celeste, 24 g, and the adapter board, 50 g **The dimensions given are of the GNSS, it has to be mounted on a PCB so that it adheres to the PC/104 standard

The margin of 5 % is applied since the Celeste GNSS receiver is COTS [107]. The retroreflectors are also COTS, however, due to the custom fittings created a larger margin is added to account for the modifications that will be made by the team [107].

### 5.2.4. Next Steps

To conclude, the S/C will have a second conventional GNSS, the Celeste GNSS, as a validation system for the SP. Another validation system used is retroreflectors on the exterior of the S/C. This can be used by the ILRS

[(1)]Cost of receiver is approximated as €7.5 k based on piNAV-NG, SkyFoxLabs. [Online]. DoLA: 6 June, 2025. Available: https://www.skyfoxlabs.com/product/30-pinav-ng

[(2)]Based on the component cost estimations, VP is expected to cost €10.7 k

station situated in Matera for the whole mission. The stations at Potsdam and Graz can also be used if the time between contacts is not too large. The station at the TU Graz has the added benefit of being a university facility.

For further research and realizing the validation subsystem into a flight-ready system, the following steps need to be taken:

1. **Order parts:** Place purchasing orders through SpaceManic and Edmund Optics for the Celeste GNSS and retroreflectors.
2. **Reach out to ILRS stations:** Contact the ILRS stations of Matera, Potsdam, and Graz to inquire about the use of their facilities.
3. **Test components:** Reserve the signal simulator and cleanroom, both located in the high-rise building at the TU Delft faculty of Aerospace Engineering, to test the GNSS receiver and visually inspect the retroreflectors respectively. Afterwards, send the retroreflectors to an external company for optical performance analysis of the retroreflectors.
4. **Integrate subsystem into CubeSat:** Create custom fittings for the retroreflectors. Mount the retroreflectors on the body of the CubeSat. Meanwhile, install the GNSS receiver on the PCB to be PC/104 compatible and wire the board to the other PCBs/EPS.
5. **Run system-level tests:** Verify that the whole system is in accordance with ECSS standards.

## 5.3. Structural Design

This section discusses the design of the satellite structure, ensuring the satellite structure can fit all subsystems and payloads while being able to survive launch, deployment and operations.

### 5.3.1. Requirements

This subsection lists the final requirements for the structural subsystem and gives the selected validation method. The structural requirements are based on requirements set by the CubeSat design specifications [10] and launch vehicle, for which the RocketLab Electron [(1)] has been chosen.

**Table 5.4:** Structural requirements.

| ID | Requirement | Verification Method |
|---|---|---|
| STM-SYS-STRUC-1 | The S/C shall withstand acceleration loads between −2 g and 7.5 g axially and between −2 g and 2 g laterally. | **T/A**: Structural analysis and static load testing |
| STM-SYS-STRUC-2 | The S/C shall exhibit a structural Quality Factor (Q) in the range of 20 to 50 during LEOP. | **A**: Modal analysis or sine burst testing to extract Q-factors from structural response. |
| STM-SYS-STRUC-3 | The S/C shall withstand shock loads to 700 g over the frequency range of 100 Hz to 10 000 Hz | **T/A**: Shock testing using a high-energy shock table or pyroshock simulator, with Shock Response Spectrum (SRS) measurement using accelerometers mounted at the spacecraft interface. |
| STM-SYS-STRUC-4 | The S/C shall adhere to the out-gassing standards set by ECSS-Q-ST-70-02C. | **T**: Thermal vacuum outgassing test (Total Mass Loss / Collected Volatile Condensable Material analysis) following ECSS-Q-ST-70-02C. |
| STM-SYS-STRUC-5 | The S/C structure shall have a mass of at most 0.3 kg. | **I**: Precision weighing using a calibrated scale. |
| STM-SYS-STRUC-6 | The S/C structure shall be able to house every subsystem. | **I**: Check if all the subsystem fit within the provided structure. |
| STM-SYS-STRUC-7 | The S/C structure shall comply to the CubeSat design specifications [10]. | **I**: Check against the CubeSat design specifications using precise measurement tools. |
| STM-SYS-STRUC-7A | The CubeSat center of gravity shall fall within ±2 cm from the geometric center in each major axis. | **T**: Test using a center of gravity test bench. |
| STM-SYS-STRUC-7B | The CubeSat structure should be made from aluminum alloy. | **I**: Ensure manufacturer uses aluminum alloy. |
| STM-SYS-STRUC-8 | The S/C shall survive vibration frequencies between 10 Hz and 2000 Hz. | **T**: Vibration testing using a shaker table. |

### 5.3.2. Preliminary Design Results

The technology demonstration satellite shall have a mass of at most 10 kg. This puts it in the nanosatellite category. Designing the satellite as a CubeSat [10] is the ideal way to efficiently come to a good standardized structural design that is certain to integrate with a deployer, thereby omitting the need for a design option tree

[(1)] RocketLab Electron, RocketLab, 2025. [Online]. DoLA: 3 June, 2025. Available: https://rocketlabcorp.com/launch/electron/

or trade-off. CubeSats are built out of "units" (U), each of these is a cube with a form factor of 10 cm and a mass of no more than 2 kg. Widely used standardized sizes are 1U, 2U, 3U and 6U. These would have maximum masses of 2 kg, 4 kg, 6 kg and 12 kg, respectively. Based on payload sizing, the 1U form factor is expected to be sufficient to fit all subsystems and provide enough surface area for solar power generation. Figure 5.6 shows a technical drawing of a standardized 1U CubeSat with the outer dimensions. Low-mass CubeSat structures can be bought off-the-shelf flight qualified and space proven at low cost (~120 g [108], ~ €1400 to 4800 [(1)] [(2)]). Following the technical design specifications [10] ensures the satellite integrates seamlessly with the deployer, these deployers are also standardized and made to integrate smoothly into launch vehicles.

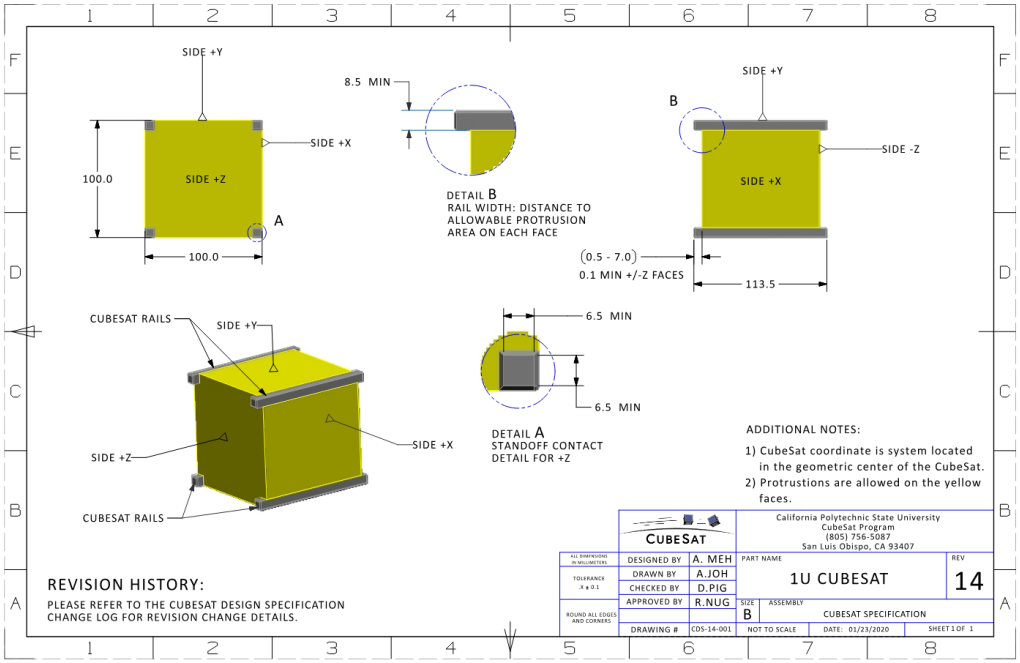


**Figure 5.6:** 1U CubeSat design specification technical drawing. [10]

### Spacecraft Axis System

For reference in the design of the other subsystems and the placement of components into or onto the spacecraft structure, an axis system must be defined. Figure 5.7 shows the defined right-hand axis system, centered in the geometric center of the CubeSat. The Z-axis system is aligned with the CubeSat rails, with the positive side pointing in the direction of the separation springs. The positive direction of the X-axis points in the direction of the PC/104 bus side as shown in Figure 4.3b. The Y axis completes the right-hand axis system.

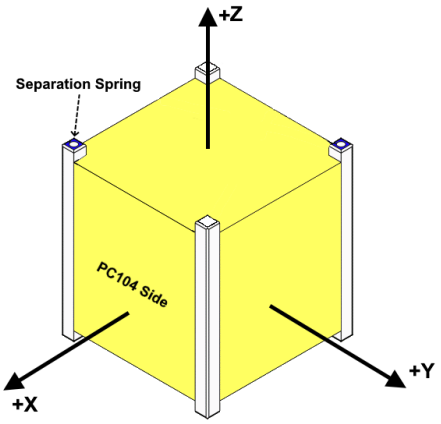


**Figure 5.7:** Technology demonstration satellite axis system.

[(1)] 1U CubeSat Bus, Endurosat. [Online]. DoLA: 20 May, 2025. Available: https://www.endurosat.com/products/1u-platform/
[(2)] CubeSat Kit Structures, Pumpkin Space. [Online]. DoLA: 20 May, 2025. Available: https://www.pumpkinspace.com

### 5.3.3. Material Characteristics

As stated in the CubeSat design specifications: materials used in the satellite structure must feature the same thermal expansion coefficient as the deployer to prevent deployment obstruction. Specifically, the CubeSat should be made from aluminum, specifically Aluminum Alloy (AA) 7075, 6061, 6082, 5005, and/or 5052 are used [36, 108]. The aluminum used on the structure which comes into contact with the deployer must be anodized to prevent cold welding. Table 5.5 shows the material properties of the possible CubeSat structure materials [(1)]. For each alloy a specific reference is chosen, then the following is given: the density $\rho$, the modulus of elasticity $E$, the yield strength $\sigma_y$, the ultimate strength $\sigma_{ult}$, the fatigue strength $\sigma_f$ and the melting temperature $T_{melt}$.

**Table 5.5:** Possible materials for CubeSat structures.

| Material | Reference | $\rho$ [g/cm$^3$] | $E$ [GPa] | $\sigma_y$ [MPa] | $\sigma_{ult}$ [MPa] | $\sigma_f$ [MPa] (@# of cycles 5.00e+8) | $T_{melt}$ [°C] |
|---|---|---|---|---|---|---|---|
| AA7075 | 7075-T6 | 2.81 | 71.7 | 503 | 572 | 159 | 477 - 635 |
| AA6061 | 6061-T6(51) | 2.70 | 68.9 | 276 | 310 | 96.5 | 582 - 651.7 |
| AA6082 | 6082-T6 | 2.70 | 71.0 | 250 | 300 | 95 | 585 - 650 |
| AA5005 | 5005-H38 | 2.70 | 68.9 | 186 | 200 | 84 | 632 - 654 |
| AA5052 | 5052-H38 | 2.68 | 70.3 | 255 | 290 | 140 | 607.2 - 649 |

### 5.3.4. Structure Selection

The CubeSat structure will be bought commercially off-the-shelf. Table 5.6 lists commercially available 1U CubeSat structures, with their masses, materials, cost and included services where applicable. When information is not publicly available, it is left blank. Eight different structures are considered, their suppliers are 2NDSpace[(2)], AAC Clyde Space[(3)], EnduroSat[(4)], German Orbital Systems[(5)], Gumush[(6)], Ishitoshi Machining[(7)], ISISpace[(8)] and NPC Spacemind[(9)].

**Table 5.6:** Considered commercially available 1U CubeSat structures.

| Supplier | Mass [g] | Material | Cost [€] | Included |
|---|---|---|---|---|
| 2NDSpace | 94 | - | - | - |
| AAC Clyde Space | 155 | AA7075 and AA6082 | - | - |
| EnduroSat | 120 | AA6061-T651 or AA6082-T6 | 1700 | 1 h engineering support, Delivery costs, Handling and administration costs |
| German Orbital Systems | 180 | - | - | - |
| Gumush | 100 | - | - | - |
| Ishitoshi Machining | 100 | AA7075 and AA6061 | - | - |
| ISISpace | 100 | - | 2200 | - |
| NPC Spacemind | 85 | - | 1350 | - |

The chosen CubeSat structure is the 1U CubeSat structure by EnduroSat[(10)], as it is the only option with all required parameters publicly available. As this structure adheres to the CubeSat design specifications and uses AA6061-T651 or AA6082-T6, it satisfies requirement STRUC-7. The material characteristics can be found in Table 5.5. Furthermore, at 120 g this structure also satisfies requirement STRUC-5. This structure also comes tested for thermal cycling, thermal vacuum, random vibrations, sine vibrations and shocks. Finally, the cost of the structure is very reasonable at €1700, especially when taking into account the included hour of engineering support and the delivery-, handling- and administration costs.

### Natural Frequency Estimation

This subsection presents an estimation for the minimum natural frequency of the technology demonstration satellite following the approach given in [109]. The minimum longitudinal natural frequency $f_{n,longitudinal}$

[(1)] MatWeb material property data, MatWeb, 2025. [Online]. DoLA: 19 May, 2025. Available: https://www.matweb.com
[(2)] 2NDSpace, 2025. [Online]. DoLA: 10 June, 2025. Available: https://www.2ndspace.eu/
[(3)] AAC Clyde Space, 2025. [Online]. DoLA: 10 June, 2025. Available: https://www.aac-clyde.space
[(4)] EnduroSat, 2025. [Online]. DoLA: 10 June, 2025. Available: https://www.endurosat.com/
[(5)] German Orbital Systems, 2025. [Online]. DoLA: 10 June, 2025. Available: https://www.orbitalsystems.de/
[(6)] Gumush, 2025. [Online]. DoLA: 10 June, 2025. Available: https://gumush.com.tr/
[(7)] Ishitoshi Machining, 2025. [Online]. DoLA: 10 June, 2025. Available: https://www.ishitoshi.co.jp/en/
[(8)] ISISpace, 2025. [Online]. DoLA: 10 June, 2025. Available: https://www.isispace.nl/
[(9)] NPC Spacemind, 2025. [Online]. DoLA: 10 June, 2025. Available: https://www.npcspacemind.com/
[(10)] 1U CubeSat Structure, EnduroSat, 2025. [Online]. DoLA: 10 June, 2025. Available: https://www.endurosat.com/products/1u-cubesat-structure/

is calculated using Equation 5.2 and the minimum lateral natural frequency $f_{n,lateral}$ is calculated using Equation 5.3.

$$f_{n,longitudinal} = \frac{1}{2\pi}\sqrt{\frac{E_S A_{lateral}}{m_S L}} \tag{5.2}$$

$$f_{n,lateral} = \frac{1}{2\pi}\sqrt{\frac{3E_S I}{m_S L^3}} \tag{5.3}$$

$$E_S = E_m \frac{A_S}{A_{lateral}} \tag{5.4}$$

$$I = \frac{L^4 - (L-2t)^4}{12} \tag{5.5}$$

Here $E_S$ is the Young's modulus of the entire satellite, calculated using Equation 5.4, assuming the Young's modulus of the components is much smaller than that of the structure. $A_{lateral}$ and $A_S$ are the lateral surface areas of the satellite and the lateral surface areas of the monocoque structure as shown in Figure 5.8, respectively. In order to calculate $A_S$, the thickness of the monocoque version of the structure must be calculated by assuming the satellite structure is a hollow beam with all the mass concentrated in a shell with a uniform thickness, this is done using a structural mass of 120 g and a density of 2.70 g cm$^{-3}$. The moment of inertia of the monocoque structure $I$ is calculated using Equation 5.5 as it is essentially a hollow beam. The length of a side of the CubeSat $L$ is 0.1 m and the mass of the satellite $m_S$ is taken to be 1.2 kg.

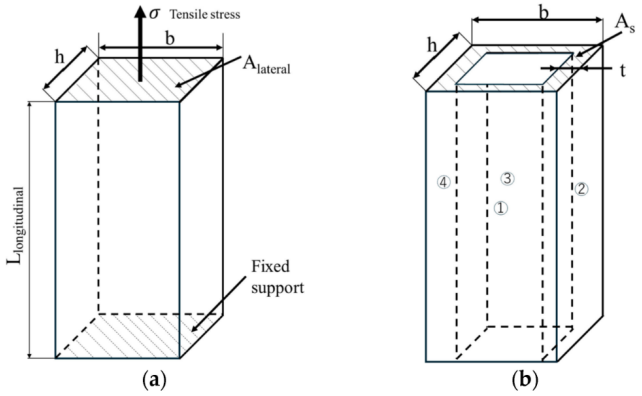


**Figure 5.8:** Satellite structure that looks like a rigidly clamped cantilever rod. **(a)** Structure in which tensile stress is applied in the launch direction (longitudinal direction). **(b)** Monocoque structure formed only by shells. [109]

Performing the calculations yields a minimum natural frequency of 820 Hz in longitudinal (launch) direction, and 38.8 Hz in lateral direction. As the method provided in [109] yields results with errors of 2 % to 5 %, these estimates are relatively accurate and can later be verified by vibration testing the satellite. Table 5.7 gives the estimated natural frequencies as well as the variables used in calculating them.

**Table 5.7:** Estimated minimum natural frequencies of the satellite and necessary variables.

| $\rho$ [g cm$^{-3}$] | $E_m$ [GPa] | $m_S$ [kg] | $L$ [mm] | $t$ [mm] | $A_{lateral}$ [m$^2$] | $A_S$ [m$^2$] | $E_S$ [GPa] | $I$ [kg m$^2$] | $f_{n,longitudinal}$ [Hz] | $f_{n,lateral}$ [Hz] |
|---|---|---|---|---|---|---|---|---|---|---|
| 2.70 | 71.0 | 1.20 | 100 | 0.112 | 0.01 | $4.49 \times 10^{-5}$ | 0.319 | $7.47 \times 10^{-8}$ | 820 | 38.8 |

## 5.3.5. Subsystem Budgets

Table 5.8 presents the final budgets for the satellite structure. The mass and power values include a 5 % margin as suggested by ESA for COTS components [107]. The structure is expected to have a mass around 126 g, a size of 100 mm × 100 mm × 113.5 mm, a cost of €1700 and a power usage of 0 mW.

**Table 5.8:** Structures final budgets.

| Component | Amount | Margin [%] | Mass [g] | Size [mm] | Cost [€] | Power [mW] | Operational Temp. [°C] |
|---|---|---|---|---|---|---|---|
| Structure | 1 | 5 | 120 | 100 × 100 × 113.5 | 1700 | 0 | −40 to 80 |
| **Total** | **N/A** | **N/A** | 126 | **N/A** | **1700** | **0** | **−40 to 80** |

## 5.3.6. Next Steps

With the structural design complete, a look towards the future can be taken. The list below shows the next steps to be taken for the satellite structure.

- **Perform Procurement** - Acquire the satellite structure.
- **Perform Verification** - Verify that the structure meets the requirements as given in Table 5.4.
- **Assembly** - Integrate the subsystems into the satellite structure.
- **Integration Testing** - Test the satellite once it is fully assembled with all subsystems integrated.

## 5.4. Command and Data Handling Subsystem Design

The C&DH Subsystem manages the data flow of the spacecraft. For this project, this entails both the communication subsystem, also known as Tracking Telemetry & Control subsystem, as well as the OBC subsystem. The communication subsystem design is the main subject of this section. The requirements for the C&DH subsystem are shown in Subsection 5.4.1. From the communication requirements, and preliminary design described in Subsection 5.4.2 a selection of component concepts were generated. This is reported on in Subsection 5.4.3. These design concepts entered the trade-off. The trade-off is reported on in Figure 5.4.3. Finally, with the chosen design, the overarching architecture will be explained in Figure 5.4.3. The finalized requirements and updated subsystem budgets and the system characteristics are determined. These are reported on in Subsection 5.4.6 and Table 5.4.4, respectively. With the steps needed to be taken reported in Subsection 5.4.7.

### 5.4.1. Requirements

In this section, the requirements for the C&DH subsystem are further derived and/or changed from the following high-level system requirements:

- STM-SYS-SC-5 The S/C shall have a mass of at most 10 kg.
- STM-SYS-SC-7 The S/C shall comply with international laws and regulations.
- STM-SYS-SC-8 The S/C shall be able to transmit all the on-board generated data to the ground station.
- STM-SYS-SC-9 The S/C shall support the reception of telecommand from ground stations.
- STM-SYS-SC-10 The S/C shall operate within radio frequency bands allocated by the ITU and relevant national regulatory bodies
- STM-SYS-M-8 The Technology Demonstration Mission shall cost no more than €10 M.

The subsystem requirements for the C&DH are summarized in Table 5.9. To demonstrate compliance, each requirement has its method of verification written after it. The way of verification is one of four; Testing, Analysis, Demonstration and Inspection (TADI).

**Table 5.9:** Verification methods for final requirements.

| ID | Requirement | Verification Method (TADI) |
|---|---|---|
| STM-SYS-CDH-1 | The C&DH subsystem shall have a mass of less than 200 g | T/I: Check against part specifications; put the parts on a scale. |
| STM-SYS-CDH-OBC-1 | The OBC shall be able to store S/C data for a period of at least 17 h.(1) | T: Test if S/C data is available for at least 17 h in replicated operational conditions. |
| STM-SYS-CDH-OBC-2 | The OBC shall be able to store a S/C data amount of at least 175 MB. (2) | T: Test if S/C data amount is able to be stored in replicated operational conditions. |
| STM-SYS-CDH-OBC-5 | The OBC shall have a memory size of at least 5 MB. | I: Check against OBC COTS part specification. |
| STM-SYS-CDH-OBC-6 | The OBC shall have a CPU capacity of at least 10 MHz. | I: Check against OBC COTS part specification. |
| STM-SYS-CDH-OBC-7 | The OBC shall be able to communicate to other subsystems. | I: Check against OBC COTS part specification. |
| STM-SYS-CDH-OBC-9 | The OBC shall have a peak power demand of less than 1 W. | T/I: If peak power complies to the requirement in replicated operational conditions. |
| STM-SYS-CDH-OBC-10 | The OBC shall have an average power demand of less than 0.5 W. | T/I: If average power complies to the requirement in replicated operational conditions. |
| STM-SYS-CDH-OBC-12 | The OBC shall have a cost of less than €15.0 k. | I: The cost of the OBC is estimated and checked with COTS part specification. |
| STM-SYS-CDH-OBC-13 | The OBC shall be compatible with the PC/104 connection standard | I: Check against OBC COTS part specification. |
| STM-SYS-CDH-OBC-14 | The OBC shall be able to use the I2C connection protocol | I: Check against OBC COTS part specification. |
| STM-SYS-CDH-COMM-1 | The Communication Subsystem shall provide a data rate of at least 9.6 kbit $s^{-1}$. | T/I: Test if the subsystem can deliver a data rate of 9.2 kbit $s^{-1}$ in replicated operational conditions. |

*Continued on next page.*

(1) This was found to be the maximum time between ground passes from the GMAT simulation in Section 3.3
(2) This was the highest storage found in the data rate simulation in Subsection 5.4.5

| ID | Requirement | Verification Method (TADI) |
|---|---|---|
| STM-SYS-CDH-COMM-2 | The Communication Subsystem shall operate within radio frequency bands allocated by the ITU and relevant national regulatory bodies | I: The chosen radio frequency band is checked if it falls within the regulations and licensing. |
| STM-SYS-CDH-COMM-3 | The Communication Subsystem shall support the reception of telecommand from ground stations. | T/I:Check against COTS part specification. Perform an integration test, replicating operational conditions. |
| STM-SYS-CDH-COMM-5 | The Communication Subsystem shall have a peak power demand of less than 4 W | T/I: Check if peak power complies to the requirement in replicated operational conditions. |
| STM-SYS-CDH-COMM-6 | The Communication Subsystem shall have an average power demand of less than 0.2 W. | T/I: Check if average power complies to the requirement in replicated operational conditions. |
| STM-SYS-CDH-COMM-7 | The Communication Subsystem shall have a cost of less than €50 k | I:The cost of the communication subsystem is estimated and checked with COTS part specification. |

## 5.4.2. Preliminary Design Results

From the mission description, the design of the antenna is selected based on preliminary trade-off. For the directional antenna, the operating frequency bands VHF and UHF are unfeasible. These frequency bands for directional antennas are eliminated due to antenna size being inversely proportional to frequency ($f$). High gain antennas rely on the wavelength ($\lambda$) of the signal and light speed ($c$) as shown in Equation 5.6:

$$\lambda = c/f \tag{5.6}$$

For UHF, the frequency is around 400 MHz, using Equation 5.6 results in a wavelength of 0.75 m. To demonstrate, using a low signal gain of 10 dB, the dish diameter needs to be multiple wavelengths wide; this points to 1 m in diameter, which is too large for a 1U CubeSat. The combination of omnidirectional antenna and X-band defeats the purpose of high-throughput communication, where the increase in high path loss is not compensated with high antenna gain.

Without any onboard optical equipment, the amount of data required for downlink is minimal. The goal for the S/C is to provide a reliable host to demonstrate the snapshot GNSS in a space environment, thus lowering the pointing accuracy and power requirement benefits the complexity of the S/C. The final design being the COTS omnidirectional antenna operating in the UHF.

## 5.4.3. Component Selection

For the C&DH subsystem, the components to select are the OBC, the transceiver, and the antenna. Notable items that have been omitted are the Analog to Digital (AD), the Digital to Analog (DA), modulation hardware, and other communication parts, since these are handled by the transceiver.

Components were searched that are heritage flight parts, i.e. with a Technology Readiness Level (TRL) of 9, that fit within the size, and average power requirements. From the components, 4 different concepts have been generated, as shown in Figure 5.9. The concepts then entered a trade-off, with criteria shown in Figure 5.10 and trade-off table in Figure 5.11. With the components chosen, a detailed budget could be created, and other detailing, such as layout and OBC Operating System (OS) could be looked at.

### Design Concepts

From the three C&DH components selection, four concepts are decided and shown in Figure 5.9. As the technology demonstration satellite desires high reliability and flight heritage, only COTS are considered. The concepts are grouped by company for ease of integration and compatibility, with flight heritage for the integrated system. One concept is composed of the best performing components on paper. Other components that are not considered are dropped due to not having publicly available data sheets or violating the C&DH allocated power budget of nominal usage of 850 mW.

| Component / Concept | Antenna | Transceiver | On Board Computer |
|---|---|---|---|
| ISISpace C1 | Cubesat Antenna System for 1U | VHF uplink/UHF donwlink Full Duplex Transceiver | ISISPACE On-Board COmputer (IOBC) |
| Gomspace C2 | NanoCom ANT430 | NanoCom AX100 | NanoMind A3200 NanoDock DMC-3 |
| Spacemanic C3 | SAM Small Antenna Module UHF/VHF | Murgas The UHF / VHF Transceiver | Deep Thought On-board Computer |
| Multiple Brands C4 | UHF Antenna III + Solar Panel | NanoCom AX100 | NST OBC |

**Figure 5.9:** Design concepts for the C&DH subsystem from commercial of the shelf component.

### Criteria

The trade-off evaluates each C&DH concept against four criteria:

1. **Average Power** : Different concepts have a different power consumption and lower power consumption is desired for the S/C. Average power is considered, as there is a battery on board. The consumption rate shall not exceed the limit the battery can provide. The system has a safe mode, this will activate the transceiver in receiving mode till the next window to enable contact the S/C. The C&DH needs to account for this procedure.
2. **Operating Temperature** : The spacecraft will operate under a certain temperature range, the components selected need to be operable within this defined range. The concepts will have a lower bound and upper bound temperature range derived from the critical components.
3. **Peak Power** : Different concepts have a different power consumption and lower power consumption is desired for S/C. Peak power is considered, as antenna deployment activation mechanisms require power that could deplete the battery faster or overload the components.
4. **Size, Mass, Cost** : Mass is always a constraint in S/C. With 1U CubeSat the dimension of the components need to fit inside the spacecraft. Reducing the cost of the components benefits the stakeholder.

Each criteria has the same weight and needs to comply with the C&DH budget. Violating the budget will eliminate the option. The four criteria are judged based on a 1-4 scoring scale, these are explained in Figure 5.10.

| Criteria / Score | Avg Power | Operating Temperature | Peak Power | SWaC |
|---|---|---|---|---|
| 1 | Exceeds subsytem power budget | Exceeds the temperature range | Exceeds subsytem power budget | SWaC exceeds budget |
| 2 | Exceeds subsytem power budget, but can be salvaged | Exceeds the temperature range, but can be salvaged | Exceeds subsytem power budget, but can be salvaged | Compliant to SWaC, but heavier than most options |
| 3 | Conforms to the subsystem power budget with small margin | Conforms to temperature range margin with small margin | Conforms to the subsystem power budget with small margin | Compliant SWaC, but same mass as other options |
| 4 | Conforms to the subsystem power budget | Conforms to temperature range margin | Conforms to the subsystem power budget | Lower SWaC than most options |

**Figure 5.10:** Trade criteria for the C&DH subsystem concept selection.

### Trade-Off Table

Figure 5.11 presents the weighted trade-off matrix. Each design concept is shown in the rows, where the criteria are shown in the columns. The column width shows the weight and explanation of each criterion. The subsystem concept that won is the C2 concept with components from Gomspace. The Spacemanic concept is a close second in terms of scoring, but the provided datasheet of Spacemanic is not detailed compared to Gomspace, with miscellaneous information not provided.

| Criteria / Concepts | Average Power | Temperature compliance | Peak Power | Size Weight & Cost | Total |
|---|---|---|---|---|---|
| ISISpace C1 | 0.44 W is lower than the budget average power (3) | Temperature of -20 exceeds the limit temperature (1) | 4.48 W is lower than budget peak power (3) | With 270 grams, heavier than most concepts, larger than most concepts (2) | 0.563 |
| Gomspace C2 | 0.17 W is significantly lower than the budget average power (4) | Temperature of -30 is close to the limit temperature (3) | 4.9 W is lower than budget peak power (3) | 150.5 grams is average mass compared to other concepts, size is small compared to other concepts (4) | 0.875 |
| Spacemanic C3 | 0.1 W is significantly lower than the budget average power (4) | Temperature of -40 is conforms to the limit temperature with a large margin (4) | Peak power of OBC is unknown (1) | 160 grams is average mass compared to other concepts, size is small compared to other concepts (4) | 0.813 |
| Multiple Brands C4 | 0.642 W is lower than the budget average power (3) | Temperature of -30 is close to the limit temperature (3) | 5 W is lower than budget peak power (3) | 169.5 grams is average mass compared to other concepts, size is small compared to other concepts (4) | 0.813 |

**Figure 5.11:** Trade-off table for the C&DH subsystem concept selection.

### Chosen Parts

For the chosen concept shown in Figure 5.11,the chosen parts are as follows:

- **Antenna** : NanoCom ANT430 [110]
- **Transceiver** : NanoCom AX100 [111]
- **On Board Computer** : NanoMind A3200 [112]
- **Motherboard** : NanoDock DMC-3 [113]

The NanoCom ANT430 is a deployable omnidirectional rigid antenna system with an insertion loss of $-1.6$ dB. The system supports 400 or 435 MHz. The antenna has a circular polarization, with torsion-spring loaded hinges for the deploying mechanism. The NanoCom AX100 is a half-duplex software configurable VHF/UHF transceiver.half-duplex is bidirectional communication but limited to only one direction, transmitting or receiving. The transceiver supports in orbit reconfiguration of the frequency, bitrate up to 38.4 kbit $s^{-1}$, filter bandwidth, and modulation type: GMSK and GFSK. The NanoMind A3200 contains a 3-axis magnetometer and a 3-axis gyroscope both for attitude control, real time clock, temperature sensor, and watchdog. NanoDock DMC-3 supports 4 daughterboards, providing communication interfaces I2C and CAN.

### Chosen Architecture

The main communication between the OBC and any other subsystem will be through the I2C bus. The I2C bus shall be operated in multi-master mode, meaning that not only the OBC is the owner of the bus, but that there are multiple masters, as the name suggests. The other masters are the transceivers. The reasoning behind setting the the I2C bus in multi-master mode, is simply that it is required by the transceiver spec [111]. All other subsystems will operate in slave mode.

For the data downlink, the following parameters are assumed: As modulation, GMSK is used, achieving a symbol rate of 9600[(1)]. For data compression, encryption, and Forward Error Correction (FEC) the standards set by CCSDS are followed [114–116]: For encryption the Space Data Link Security (SDLS) protocol is used, and for compression the POCKET+ algorithm is used. Finally, an FEC scheme of "conv r=1/2 k=7 + rs(223,255)" is

[(1)]This modulation was advised by Stefano Speretta, e-mail conversation 23-05-2025. "GMSK would be my recommendation as it has a constant envelope (while BPSK / QPSK does not) so it works very well with a non-linear amplifier (which has a DC ro RF efficiency of 50-60%)"

chosen. This is based on recommendations in the transceiver manual [117], and is approved by the CCSDS standard.

The encryption is used to ensure the communication data is only available to the ground station operator, and that the S/C cannot be controlled by unauthorized users. The compression algorithm is used to increase the effective data rate. The effective data rate is increased by a factor of at least 4, thanks to the compression algorithm [118]. Finally, the FEC scheme is used to improve the data link reliability, at a penalty of the data rate. Because the perceived gain on the ground can become very close to the noise floor, error correction is deemed essential. The chosen FEC scheme has a data rate penalty factor of 0.4, which is explained in more detail Figure 5.4.4.

To ensure the two transceivers are able to command the antenna independently, an Single Poly Dual Throw (SPDT) is used[(1)].

Once the spacecraft is fully assembled and especially after environment testing, where one can no longer open the spacecraft, one would still want to be able to communicate with the spacecraft, especially with the OBC. Therefore, a debug port is needed. For this spacecraft the debug port will serve two purposes. The first is creating a communication channel between the outside of the spacecraft and the OBC. The second purpose is that it will serve as the Apply Before Flight (ABF) port. In addition to the the separation springs on the structure of the satellite, the ABF acts as a second safety mechanism where the EPS will only start once the ABF is applied and the separation springs are unloaded (i.e. the spacecraft has left the launcher). The debug port on the OBC is called P1 and has a Molex PicoBlade 53261-0471 connector [119]. Ultimately, two cables that originate from the EPS (for the ABF) and OBC (for debugging) will have to merge into one cable and into one connector. The chosen connector will be from the Hirose DF52 series due to their small size, their temperature range and out-gassing properties. Lastly, one would have to determine the position of the connector on the exterior of the satellite, and ensure that the wiring path works and one does not bend the wire more than the allowable bending radius. The same methodology as for the GNSS antenna placement as seen in Section 4.7 can be applied.

### 5.4.4. Performance Analysis

A performance analysis is a crucial aspect of understanding the efficiency and effectiveness of communication systems. It involves evaluating various parameters that determine how well a system performs under different conditions.

#### Data Generation of the System

The data generation is one of the driving requirements for the C&DH subsystem. It comprises of two parts: The Housekeeping (HK) data, and the payload data. In the midterm report [46], the data generation was calculated based on assumptions on the amount of sensors, the size of each sensor snapshot, and the size of the payload measurements. For the detailed design this has been refined. For the HK data, the amount of sensors, and HK snapshot data size per subsystem was either looked up from datasheets, or estimated. This data is shown in Table 5.10. Due to the large HK data size, a HK period of **10 s** is chosen.

For the standardized-, and validation payload, a size of 1000 bit is assumed. Reasoning for this is that GNSS receivers generate not only position data, but other information such as perceived signal strength, what satellites are in view, or pseudoranges. The payload snapshot period for this analysis is chosen to be **60 s**. The complete data generation rates are shown in Table 5.11.

Any changes in data generation, and its impact on the C&DH subsystem will be discussed in Subsection 5.4.5

**Table 5.10:** HK data generation per snapshot per subsystem. If no information was found, an estimate was used.

| Subsystem | Amount of Sensors | HK data size [b] | Source |
|---|---|---|---|
| Transceiver | 18 | 424 | Manual [117] |
| OBC | 30 | 600 | Assumption |
| ADCS | 12 | 200 | Assumption |
| EPS | 60 | 1000 | Similar Model [120] |
| SP | 10 | 200 | Assumption |
| VPSP | 10 | 200 | Assumption |
| **Total** | **120** | **2624** | **N/A** |

[(1)] Low power SPDT, Radiall, 2025.[Online]. Date of last access: June 15, 2025. Available: https://www.radiall.com/products/space-qualified-components/space-coaxial-switches/low-power-spdt.html

**Table 5.11:** Data generation per second per subsystem, combining both HK data and payload data.

| Subsystem | Data generation HK [bps] | Data generation PL [bps] | Data generation combined [bps] |
|---|---|---|---|
| Transceiver | 42.4 | 0 | 42.4 |
| OBC | 60 | 0 | 60 |
| ADCS | 20 | 0 | 20 |
| EPS | 100 | 0 | 100 |
| SP | 20 | 16.7 | 36.7 |
| VPSP | 20 | 16.7 | 36.7 |
| **Total** | **262.5** | **33.3** | **295.8** |

### Link Budget

With the components selected mentioned in Figure 5.4.3, the transceiver can operate in a specific frequency; 437.5 MHz. The link budget is calculated to investigate if the signal gain is strong enough relative to the noise. The input values for the calculation are in Table 5.12. These values are used and derived from the mission parameters to determine the link budget shown in Table 5.13 for both uplink and downlink.

**Table 5.12:** Input values for the link budget.

| Variable | Symbol | Unit | Value |
|---|---|---|---|
| Frequency | f | Hz | $4.375 \times 10^8$ |
| Bandwidth | b | Hz | 25000 |
| S/C System Temperature | T | K | 400 |
| G/S System Temperature | T | K | 1003 |
| Distance | d | m | $2 \times 10^6$ |
| Data Rate | dr | bps | $9.6 \times 10^3$ |
| Bit Error Rate | BER | - | $1 \times 10^{-5}$ |
| Receiver Efficiency | $\eta_{rx}$ | - | 0.6 |
| Boltzmann constant | k | J/K | $1.38 \times 10^{-23}$ |

**Table 5.13:** Downlink & Uplink budgets using UHF with their respective signal to noise ratios (SNR).

| Parameter | Unit | Downlink | Uplink |
|---|---|---|---|
| Transmission power | dBm | 30.00 | 44 |
| Transmit antenna gain | dB | -5.00 | 15 [121] |
| Gain receiver antenna | dB | 23.04 | 0 |
| **Total Gain** | dB | **48.04** | **59** |
| Free space path losses | dB | -151.28 | -151.28 |
| Atmospheric losses | dB | -5 | -5 |
| miscellaneous losses | dB | -5 | -5 |
| **Path Loss** | dB | **-161.28** | **-161.28** |
| **Received Power** | dBm | **-113.24** | **-102.28** |
| **Noise Floor** | dBm | **-124.61** | **-130.93** |
| **SNR** | dB | **11.37** | **28.65** |
| Eb/N0 | dB | 15.53 | 32.80 |
| Required Eb/N0 GMSK | dB | 10.50 | 10.50 |
| Required Eb/N0 GFSK | dB | 12.00 | 12.00 |
| **Link Margin GMSK** | dB | **5.03** | **22.30** |
| **Link Margin GFSK** | dB | **3.03** | **20.80** |

The free space path loss $P_{loss}$ is calculated using Equation 5.7:

$$P_{loss} = 20 \log(4\pi \cdot d/\lambda). \tag{5.7}$$

The antenna gain $A_G$ is calculated using Equation (5.8):

$$A_G = 10 \log \left( \eta_{rx} \cdot \pi \cdot d \cdot \frac{1}{\lambda} \right)^2 \tag{5.8}$$

where $\eta_{rx}$ is the receiver antenna efficiency, d is the antenna diameter, and $\lambda$ is the wavelength.

The noise floor $NF$ in dBW is computed according to Equation (5.9):

$$NF = 10 \log (k \cdot T \cdot b) \tag{5.9}$$

where $k$ is Boltzmann's constant, $T$ is the system noise temperature in kelvin, and $b$ is the bandwidth in hertz.

The Signal to Noise Ratio (SNR) is obtained as the difference between the received signal power and the noise floor, both expressed in dBm.

For the UHF downlink band, an SNR of 11.37 dB was computed for uplink and 28.65 dB for the downlink, as shown in Table 5.13. From the SNR the carrier to noise spectral density ratio ($C/N_0$) can be determined using Equation 5.10. Using ($C/N_0$) and ($dr$) the data rate, ($E_b/N_0$) the energy per bit to noise power spectral density ratio can be calculated using Equation 5.11.

$$C/N_0 = SNR + 10 \log(b). \tag{5.10}$$

$$E_b/N_o = C/N_0 - 10\log 10(dr). \tag{5.11}$$

The determined $(E_b/N_0)$ is derived for an elevation angle of 90°. To determine the link budget for the entire contact window, the effective distance with the ground station for 500 km orbit is shown in Figure 5.12 for all elevation angles.

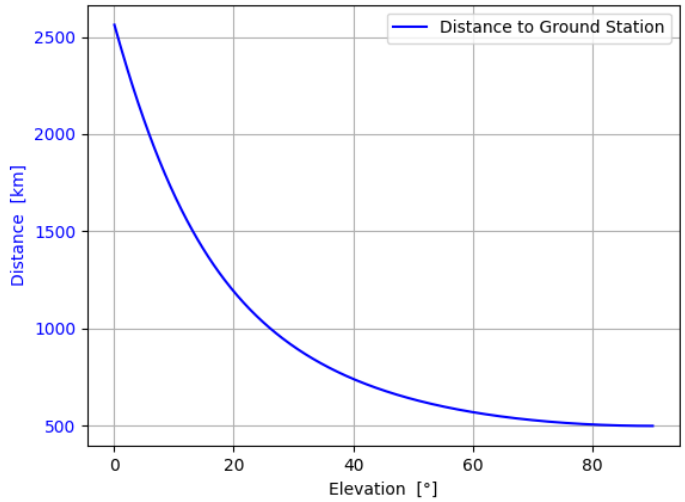


**Figure 5.12:** Elevation angle from 0 to 90 degrees plotted against distance to the ground station for 500 km orbit.

From Figure 5.12 the distance is 2500 km. From the 2500 km distance, the link budget is estimated using that distance range shown in Figure 5.13.

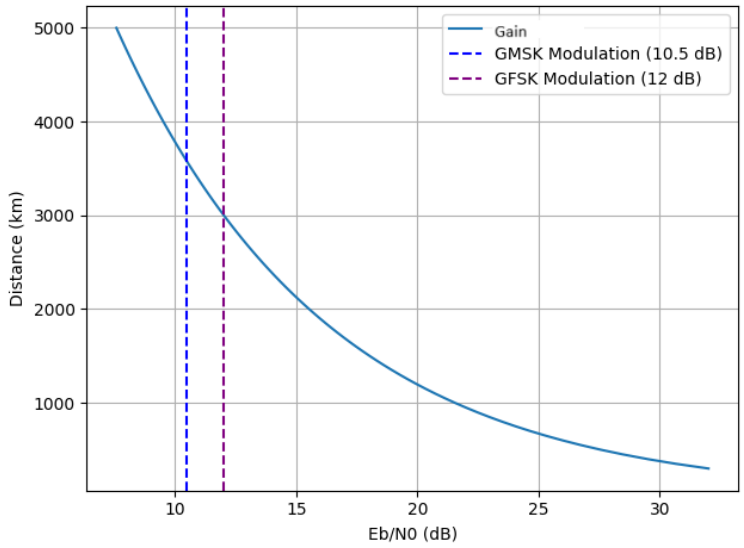


**Figure 5.13:** $(E_b/N_0)$ plotted against ground station to spacecraft distance range to ensure the link budget closes.

Seen in Figure 5.13 the worst case scenario for Gaussian Minimum Shift Keying (GMSK) leaves a conservative margin of 3 dB, with overestimated atmospheric losses and disregarding 3 dB gain using FEC with the modulation.

### Data Rate Simulation

With the data generation known, and with the updated mission simulation from Subsection 3.3.3 a more detailed analysis can be made to check whether the data generated on the S/C can be downlinked. The uplink

data rate is assumed not to be critical in the design; the commands sent to the spacecraft are not data intensive, and in the case of a software update, this can happen over multiple passes.

Using GMAT, the overpass timestamps of the S/C could be generated. With this data, the simulation could be created. The simulation logic is as follows: The simulation is moving in time, constantly increasing the data amount counter based on the data generation numbers in Subsection 5.4.4. Whenever the simulation time enters an overpass state from the GMAT data, decrease the data amount counter by the data downlink rate. At the end of the simulation, the storage size can be assessed, and checked if the storage size simulation is not divergent.

The only information that is not known yet is the downlink data rate. This can be calculated with Equation 5.12, where $B_r$ is the baud rate, $C_f$, the compression factor, $C_{ec}$, the FEC factor, $C_{FEC}$, and the safety factor, $SF$. The chosen values are based on the parameters chosen in Figure 5.4.3. The baud rate is 9600, the compression factor is 4, the FEC factor 0.4, and the safety factor 0.9. The effective downlink data rate could be determined to be $\mathbf{3.8\,kbit\,s^{-1}}$.

$$R_{eff} = B_r \cdot C_f \cdot C_{en} \cdot C_{FEC} \cdot SF \tag{5.12}$$

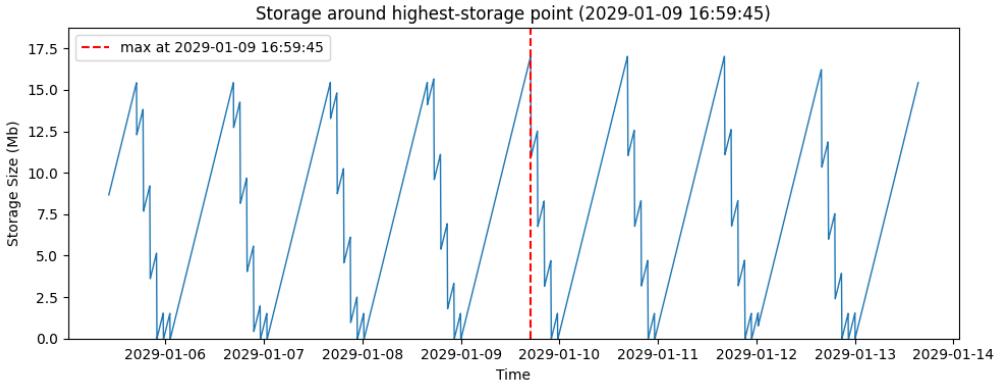


**Figure 5.14:** Result plot of the data rate simulation. Since the storage is emptied on the worst case, the chosen parameters are found satisfactory.

With the chosen parameters the simulation was performed, as shown in Figure 5.14. Since the storage could be emptied in the worst case, the chosen parameters were found to be satisfactory. The driving requirement for the data rate is the HK data. As shown in Subsection 5.4.4, the HK data accounts for over 85 % of the total data. If it was found that the data could not be downlinked, a lower HK snapshot frequency can be considered. A more detailed analysis on this will be discussed in Subsection 5.4.5.

### 5.4.5. Sensitivity Analysis

In this subsection, the sensitivity of the chosen parameters are discussed. The parameters to be taken into account for the sensitivity analysis are data generation, orbit altitude, orbit inclination, and modulation choice.

#### Data Generation

Data generation is the driving requirement for the communication link. With more data being generated, more data needs to be sent down. In this part of the sensitivity analysis, the system sensitivity will be analyzed based on the HK snapshot rate, the HK snapshot size, the PL snapshot rate, and the PL snapshot size. Especially the analysis on the PL is important, as that gives an upper bound on how many times the payload can be activated, an important parameter for the stakeholders. These parameters will be entering the same data rate simulation as in Figure 5.4.4, and will be individually increased until it is found that the data could not be fully down linked anymore. This essentially means the storage size is divergent in the simulation, as shown in Figure 5.15.

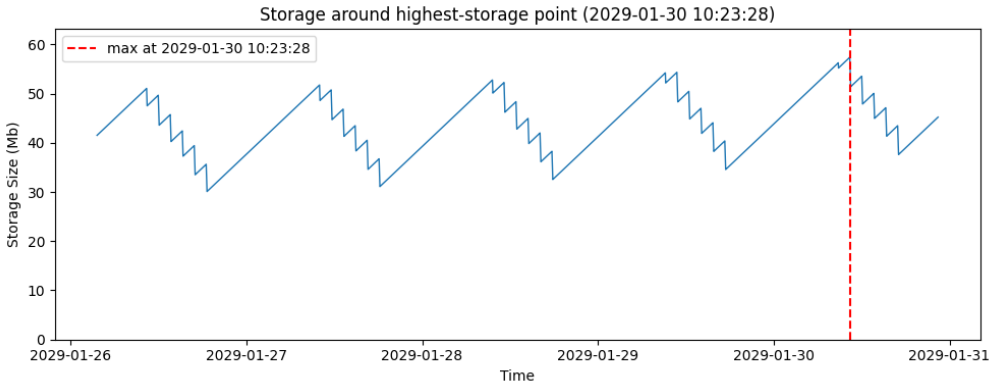


**Figure 5.15:** Example plot of a data rate simulation, where the chosen parameters were not found satisfactory, as the storage size is increasing.

The limit cases are shown in table Table 5.14. It is obvious that the snapshot size and snapshot rate are inversely related. This is because the simulation is built on the total data generation, which is a multiplication of the two parameters. Secondly it can be noted that the HK data generation is more sensitive than the PL data generation. This makes sense, as the HK data is the majority of the data being generated. With all parameters staying equal, the PL snapshot rate can be increased to once every 12 s, with an even higher limit, if a lower HK frequency is considered.

**Table 5.14:** Considering all parameters staying the same, the variables from the first column were increased until the data rate downlink wasn't possible anymore.

| Parameter | Original Value | Limit Value |
|---|---|---|
| HK snapshot size | 2624 b | 3250 b |
| HK snapshot rate | $\frac{1}{10}$ Hz | $\frac{1}{8}$ Hz |
| PL snapshot size | 1000 b | 5000 b |
| PL snapshot rate | $\frac{1}{60}$ Hz | $\frac{1}{12}$ Hz |

### Orbit Altitude

The sensitivity of the orbit altitude for the C&DH subsystem lies mainly in the link budget. With a higher altitude, the path loss is larger, and the link margin may not be reached. In Table 5.4.4 link budget is determined for 500 km orbit, the distance that still returns a positive link budget seen in Figure 5.13 is at 3700 km. The orbit altitude is 1000 km shown in Figure 5.16 due to the slant resulting in 3700 km.

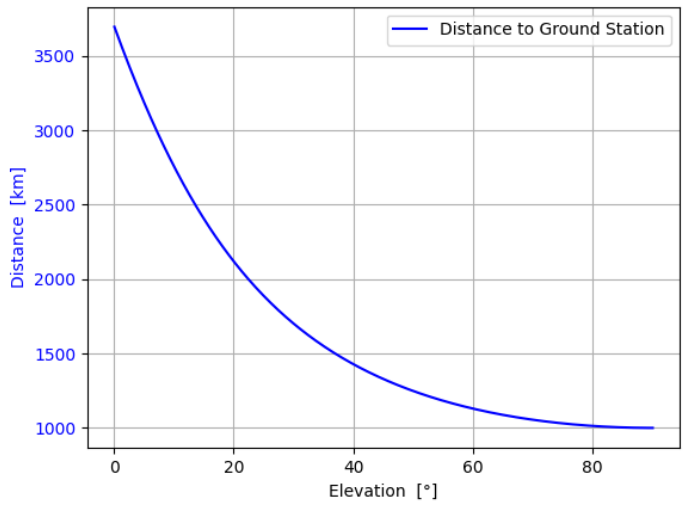


**Figure 5.16:** Elevation angle from 0 to 90 degrees plotted against distance to the ground station for 1000 km orbit.

**Orbit Inclination**
Currently the orbit inclination in the mission design is chosen such that ground contact time is optimized. Since the S/C will be launched piggyback, it might not end up in this inclination. Rather, the inclination will be similar to the main customer of the launcher. Most of the sensitivity analysis has already been performed in Subsection 3.3.3: The total duration of ground contact time versus multiple inclinations was analyzed. When comparing this data against the data generated, it was found that the inclination must be between 55° and 65°, if all other parameters stay the same. This is quite sensitive, so to comply with the data downlink, the data generation may need to be turned down after the final launch inclination is known.

**Modulation Choice**
The chosen transceiver has only two modulation options: Gaussian Frequency-Shift Keying (GFSK) and GMSK. As shown in Subsection 5.4.5, the GMSK option complies to the data downlink constraint. For the case of GFSK, the baud rate would be cut in half, to 4800. With this baud rate, the data downlink constraint will **not** be met without changing other parameters. While the modulation choice of GMSK is unlikely to change, if this is changed, the data generation needs to be lowered.

Each modulation type requires a certain threshold for the noise, depending on the desired Bit Error Rate (BER). The desired BER is $1 \times 10^{-5}$. The available transceiver modulation, GFSK and GMSK, are simulated to determine the optimal type to be used. Different modulations have different spectral efficiencies, which lower the data rate across the bandwidth. Link budget is sensitive to modulation type with a required $(Eb/No)$ impacting the link budget, for GMSK it ranges from 9.6 to 12 dB and GFSK it ranges from 11 to 13 dB.

**Sensitivity Takeaways**
The most sensitive parameters are found to be the data generation and the orbit inclination. If the orbit inclination is changed, the total ground pass time is changed, and the HK snapshot rate should be reduced to keep the data generation low enough such that all data can be sent down. In general, if parameters were to change such that the downlink data rate is limiting, the HK rate can be reduced, making the C&DH subsystem resilient to any changes in driving parameters.

## 5.4.6. Subsystem Budgets
For the chosen components shown in Figure 5.11, final sizing is put in the bill of material table shown in Table 5.15. With an additional 5 % margin for reliability.

**Table 5.15:** Subsystem final budgets for C&DH.

| Components | Amount | Margin [%] | Mass [g] | Size [mm] | Cost [€] | Power [mW] | Operational Temp. [°C] |
|---|---|---|---|---|---|---|---|
| NanoCom ANT430 | 1 | 5 | 30.00 | 65 × 40 × 7.1 | 8800 | - | −40 to 85 |
| NanoCom AX100 | 2 | 5 | 50.00 | 65 × 40 × 6.5 | 16 500 | 409 | −30 to 85 |
| NanoMind A3200 | 1 | 5 | 30.00 | 98 × 98 × 110 | 15 000 | 228 | −40 to 85 |
| NanoDock DMC-3 | 1 | 5 | 53.00 | 91.9 × 88.7 × 8.6 | 3200 | - | −40 to 85 |
| **Total** | **N/A** | **N/A** | **169.05** | **N/A** | **43 500** | **737**[(1)] | **−30 to 85** |

## 5.4.7. Next Steps
In this section, the detailed design for the C&DH subsystem has been discussed. A specific part selection has been made using a trade-off, an architecture has been chosen, and key parameters have been chosen as well. For the key parameters a sensitivity analysis was performed, and the subsystem was shown not sensitive to change in constraints.

If the project were to continue, there are things still needing to be developed, or tasks to be performed for the C&DH subsystem. Where other subsystems are relatively finished with the technical tasks, there are some still left for this subsystem, mostly in simulating the different parts, to verify their functionality. Other tasks include procurement, manufacturing and testing. The full list of tasks to be done for the C&DH subsystem can be found below.

- **OS Development** - While the software diagram has been created, this only is a high level description of what functions the OS needs to achieve. In the next steps, the OS shall have to be developed. The strategy for this is going to be the same as outlined in Autonomous Formation Flying for the PRISMA Mission [122]: Create a Matlab simulation for the chosen hardware, that can be iterated and tested quickly, whereafter this can be exported to C and implemented into the chosen OBC.

[(1)] During a ground pass, only one transceiver is using peak power and the other one is using idle power.

- **Simulate Antenna** - The antenna properties currently are taken from the provided data sheet [110]. In the data sheet there is a simulation present for a 1U CubeSat, but for the next steps a Matlab simulation [(1)] needs to be made to more accurately predict the radiation pattern of our integrated system, finding and fixing problems along the way.
- **Develop more accurate Communication Simulation** - The current simulations for the link budget and data rate are good, but still make simplifying assumptions. Along with a better antenna model, the simplifications should be changed for the actual mission parameters. For example, the full set of sensors should be included, with the full snapshot rate.
- **Iterate Performance Analysis** - As the subsystem and mission design have more detailed information, the performance analysis needs to be iterated to ensure the C&DH subsystem can perform what is requested.
- **Perform Procurement** - Acquire the parts as shown in the BOM at Table 5.15
- **Perform Verification** - The verification methods shown in Subsection 5.4.1 have to be performed.
- **Partial Testing** - The individual components can be tested separately. I.e. there is a debug port present on the OBC which can be used to prematurely check the part.
- **Apply for frequency license** - The specific frequency band that is going to be used for communication needs to be requested at the RDI, as mentioned in 2.2.
- **Assembly** - The C&DH subsystem parts need to be assembled into the S/C.
- **Integration Testing** - When the S/C has been fully manufactured, it needs to be tested. More information on this can be found in Section 7.3.

# 5.5. Attitude Determination and Control System Design

This chapter presents the design of the ADCS. First, the requirements are listed in Subsection 5.5.1, followed by an explanation of the design changes and the updates to the requirements. From this, a passive magnetic attitude control system is sized and designed. Furthermore, the chapter details the methods for attitude determination, incorporating sun sensors, gyroscopes, and magnetometers. Additionally, it analyzes the stability characteristics of the system and presents the final ADCS budgets, ensuring the design meets the mission's requirements for mass, power, and cost.

## 5.5.1. Requirements

This section lists the system requirements for the ADCS in Table 5.16. Significant changes to the scope of the ADCS design were made going into the detailed design, which led to some requirements no longer being applicable. The requirements which were discarded in the detailed design are shown in gray, but remain in the table for clarity as they served as the basis for design choices made during the preliminary design.

**Table 5.16:** Attitude determination and control system requirements. Requirements that were applicable in the preliminary design, but not in the final design are marked grey.

| ID | Requirement | Verification Method (TADI) |
|---|---|---|
| STM-SYS-ADCS-1 | The S/C shall have a pointing accuracy of ±70°. | |
| STM-SYS-ADCS-2 | The S/C shall be able to determine its attitude from all orientations. | **T:** Place the ADCS on a 3-axis air-bearing table and rotate through all axes to verify sensor readings remain valid. **A:** Simulate attitude determination using various sensor input combinations in software (e.g., magnetometer + sun sensor) over different attitudes and lighting conditions. |
| STM-SYS-ADCS-3 | The S/C shall be able to control its attitude in all orientations. | **A:** Model the magnetic torque. Simulate attitude convergence from multiple initial conditions. **T:** Use a torsional pendulum or air-bearing test platform to demonstrate that the permanent magnet aligns with Earth's field vector in a scaled Helmholtz cage setup. |
| STM-SYS-ADCS-4 | The S/C shall be able to initiate and halt tumbles from 0 to 5 revolutions per minute. | |
| STM-SYS-ADCS-5 | The S/C shall have a settling time of less than 21 days. | **T:** Simulate the nonlinear attitude dynamics under real orbital magnetic field data (e.g., IGRF model). Start from random attitude, model magnet torque + hysteresis damping, and determine time to convergence. |
| STM-SYS-ADCS-6 | The S/C shall limit its drift to <TBD>. | |

*Continued on next page.*

[(1)] Antenna Toolbox - Benchmarking and Verification, Mathworks [Online]. DoLA: June 6, 2025. Available: https://nl.mathworks.com/help/antenna/benchmarking-and-verification.html

| ID | Requirement | Verification Method (TADI) |
|---|---|---|
| STM-SYS-ADCS-8 | The ADCS shall have a mass less than **8 %** [41] of the total S/C mass. | **I:** Physically weigh the permanent magnet, damping material (e.g., hysteresis rods), and supporting structure. Check against CAD assembly mass breakdown. |
| STM-SYS-ADCS-9 | The ADCS shall cost less than **€20 k**. | **I:** Review procurement costs of permanent magnets, hysteresis rods, and sensor boards. Validate against total ADCS budget. |
| STM-SYS-ADCS-10 | The ADCS shall consume less than **0.1 W**. | **I:** Measure attitude determination power consumption for various cases. |
| STM-SYS-ADCS-11 | The ADCS shall keep the S/C pointed within **15°** of the Earth's magnetic field. | **A:** Simulate steady-state attitude deviation with modeled magnetic dipole, orbit propagation, and external disturbances (gravity gradient, drag torque). **A:** Use air-bearing or pendulum experiments in a Helmholtz cage to observe equilibrium alignment angle and oscillation amplitude. |

## 5.5.2. Preliminary Design Results

This section outlines the results of the preliminary design for the ADCS. Various design options were made, ranging from having no ADCS to having dual method active attitude control. High-accuracy pointing was not a requirement, as the mission only necessitates sufficiently low rotational velocities. This ensures that the payloads can receive GNSS signals for adequate durations and that the downlink antenna can transmit the required data during ground station passes. A key addition was the requirement that the ADCS should be able to change the tumbling rate such that the standardized payload could be tested for various tumbling rates. It must be noted that this tumbling requirement was removed in the detailed design after consulting with an expert.

In the preliminary design, the final concept chosen through the ADCS trade-off was passive attitude control with active damping. In LEO there are three main methods for passive attitude control: magnetic, gravity gradient and aerodynamic. The latter two were considered unfeasible because of the cube shape of the spacecraft. Thus, passive magnetic stabilization was chosen. A fully passive system using hysteresis rods for damping was considered, but this wouldn't allow testing the payload under different tumbling rates. Thus for the attitude control the design was chosen to be a permanent magnet in conjunction with magnetorquers.

For attitude determination it was decided that an attitude acquisition would be done during the sunlit period of the orbit using sun sensors and then during eclipse an attitude estimation could be done using gyroscopes. Finally, a magnetometer could be used to run the magnetorquers more precisely. Depending on the size of the permanent magnet, however, a magnetometer could be unfeasible. In that case the direction of the magnetic field of the earth could be derived from the position of the spacecraft using a model.

## 5.5.3. Attitude Control System Design

During the preliminary design a passive attitude control system using active damping was chosen. This was preferred over a fully passive system as it would allow testing the payload at different tumbling rates. Based on feedback and the fact that the vast majority of satellites are attitude stabilized, the importance of having tumbling initiation was previously overestimated and will not be needed. By using a fully passive attitude control system, the reliability of the mission can be increased while reducing the power consumption. Thus the design changes to a fully passive attitude control system. As explained in [46], a passive magnetic attitude control system allows for coarse attitude control using no power making it the most suited for this mission.

### Attitude Control Modes

SMAD [41] describes six typical attitude control modes, as shown in Table 5.17.

**Table 5.17:** Typical attitude control modes. [41]

| Mode | Description |
|---|---|
| Acquisition | Initial determination of attitude and stabilization of vehicle for communication with ground and power generation just after launch. Also may be used to recover from power upsets or emergencies. |
| Orbit Insertion | Period during and after boost while spacecraft is brought to final orbit. Options include no spacecraft control, simple spin stabilization of solid rocket motor, and full spacecraft control using liquid propulsion system. May drive certain aspects of ADCS design. |
| Normal/Mission, On-Station | Used for the vast majority of the mission. Requirements for this mode should drive system design. |
| Slew | Reorienting the vehicle when required. |
| Contingency or Safe | Used in emergencies if regular mode fails or is disabled. Will generally use less power or fewer components to meet minimal power and thermal needs. |
| Special | Requirements may be different for special targets or time periods, such as when the satellite passes through a celestial body's shadow, or umbra. |

However, seeing as the attitude control system is passive these do not apply.

### Disturbance Environment

Before sizing and selecting the components, an assessment of the disturbance environment must be carried out. At altitudes of 500 km and below, [41] states the driving disturbance torques are solar radiation pressure torque, gravity gradient torque and aerodynamic torque. Below, an analysis of each was performed.

#### Solar Radiation Pressure Torque

Solar radiation pressure is not expected to be a dominant source of external torque, as it is generally said to become significant only above altitudes of ~700 km [123, p.292]. For the sake of completeness, the worst-case disturbance torque due to solar radiation pressure is still estimated using Equation 5.13 [41, p.571].

$$T_S = \frac{\Phi}{c} A_S (1+q)(cp_s - cm)\cos(\phi) \tag{5.13}$$

In this equation $\Phi$ is the solar constant adjusted for distance from the Sun (1366 $\mathrm{W/m^2}$ [41, p.572]), $c$ is the speed of light, $A_S$ is the sunlit surface area, a conservative estimate 0.02 $\mathrm{m^2}$ is taken. $q$ is the unitless reflectance factor, a worst-case of value 1 is taken. $cp_s$ and $cm$ are the centers of solar radiation pressure and mass, respectively. A very conservative worst-case distance $cp_s - cm$ of 0.02 m [124] is taken. Finally, for the angle of incidence $\phi$ the worst-case value of 0° is taken. This then results in a disturbance torque $T_S$ of $2.19 \times 10^{-9}$ N m.

#### Gravity Gradient Torque

A worst-case gravity gradient disturbance torque can be estimated using Equation 5.14 [41, p.573]. $\mu$ is the Earth's gravitational constant ($3.986 \times 10^{14}\ \mathrm{m^3/s^2}$), $R$ is the distance from the center of the Earth ($6778.137 \times 10^3$ m), $I_z$ and $I_y$ are the moments of inertia about Z and Y, the difference between them is taken to be a very conservative worst-case of 0.02 $\mathrm{kgm^2}$ assuming a mass of 2 kg placed at 10 cm from the center of mass. Finally, $\theta$ is the angle between the local vertical and the Z principal axis. A worst-case scenario is taken where $\sin(2\theta)$ is equal to 1. This then leads to a torque $T_g$ of $9.60 \times 10^{-9}$ N m

$$T_g = \frac{3\mu}{2R^3} |I_z - I_y| \sin(2\theta) \tag{5.14}$$

#### Atmospheric Drag Torque

$$T_a = \frac{1}{2} \rho C_d A_r V^2 (cp_a - cm) \tag{5.15}$$

Using Equation 5.15 [41, p.573], the disturbance torque due to atmospheric drag can be estimated. Here $\rho$ is the atmospheric density, using the MSISE-90 model [125] at an altitude of 360 km gives a conservative estimate of $1.51 \times 10^{-12}\ \mathrm{kg/m^3}$ for $\rho$. This altitude was chosen because it is below the ~370 km [126] perigee after 1 year. This is larger than the new 6 month but since it is a conservative it was determined this could be changed in a subsequent design iteration. $C_d$ is the drag coefficient, a conservative value of 2.5 [41] is taken. For the ram area $A_r$ a conservative area of 0.02 $\mathrm{m^2}$ is used. $V$ is the orbital velocity (7691.29 $\mathrm{m\,s^{-1}}$). Finally, it was assumed that the center of pressure $cp_a$ and the center of mass $cm$ are on opposite sides of the spacecraft, leading to a $cp_a - cm$ of 0.02 m [124]. This then yields an estimate of $4.47 \times 10^{-8}$ N m.

**Summary**
In order to assist in later design stages the root mean squared sum of the independent disturbance torques must be calculated, Table 5.18 provides a summary and shows the Root Mean Square (RMS) value.

**Table 5.18:** Final calculated disturbance torques.

| Disturbance Torque | Value [N m] |
|---|---|
| $T_s$ | $2.19 \times 10^{-9}$ |
| $T_g$ | $9.60 \times 10^{-9}$ |
| $T_a$ | $4.47 \times 10^{-8}$ |
| $T_{RMS}$ | $4.57 \times 10^{-8}$ |

### Attitude Control System Sizing

In this section, a Passive Magnetic Attitude Control (PMAC) system will be designed and sized for the S/C. It will be composed of a permanent magnet and a set of hysteresis rods. The permanent magnet will align the S/C with the magnetic field lines of the earth. And the hysteresis rods aim to dampen the rotational motion of the S/C. The design of this system is mainly based on a conference paper detailing the design of a PMAC system for the Quetzal-1 CubeSat [11]. Since this was a successful 1U CubeSat mission, it was determined that this paper could be used as a starting point for the design. The first step of this process is to size the permanent magnet as can be seen below.

#### Permanent Magnet Sizing

The principal variable when sizing the permanent magnet is its magnetic dipole moment ($m$). A lower bound for the magnetic dipole moment can be found using Equation 5.16 [11].

$$m \geq 15 \frac{T_{RMS}}{B_{min} \sin(\beta_{max})} \tag{5.16}$$

Here, $T_{RMS}$ is the is the root mean squared sum of independent environmental torques and it was calculated to be $2.24 \times 10^{-7}$ N m from the disturbance torques calculated in Table 5.18. $B_{min}$ is the minimum magnetic field strength encountered during the mission. This is $2.44 \times 10^{-5}$ T for an altitude of 500 km as stated in the design of UNISAT-4 [13]. $\beta_{min}$ is the desired pointing accuracy for this, a value of $10^\circ$ was chosen as was done in [12] and [13]. This value is conservative since there are no specific requirements on the pointing accuracy. The final aspect that must be discussed, is the factor of 15 present in Equation 5.16. This factor was chosen in [11] to ensure that the control torque would be well above all possible disturbance torques for a 1U CubeSat. In [13], a factor of 30 was used. A risk of CubeSat design having the hysteresis rods saturated by the permanent magnet. For this reason, it is important the permanent magnet is not over-sized. This was not a problem for [13] as UNISAT-4 is was substantialy larger than a 1U CubeSat. This is also corroborated by the fact that [11] presents a S/C much closer in mass to this demonstration mission. From this computation a minimum magnetic dipole moment value of 0.162 $Am^2$ is obtained. This value 5 % smaller than the value used by [11] where a magnet was sized for the Quetzal-1 1 U CubeSat. This is acceptable as the the required pointing accuracy is lower for the mission in this report. It is important that the magnet is not over-sized as this could compromise the performance of the hysteresis rods.

#### Permanent Magnet Selection

The magnetic dipole moment ($m$) is given in Equation 5.17 by the residual flux density ($B_r$) in T, the volume of the magnet ($V$) and the vacuum magnetic permeability ($\mu_0$)

$$m = \frac{B_r V}{\mu_0}. \tag{5.17}$$

To achieve this a COTS magnet will be selected. The N52 grade has been chosen for its operating temperature of up to 80 °C and its high residual flux density of 1.45 T. This means the magnet should have a volume above $8.67 \times 10^{-7}$ $m^3$. A magnet from MagnetStore [(1)] has the following properties:

[(1)] 8 mm x 6 mm Neodymium Disc Magnet (N52, 2.82 kg pull), Magnet Store UK, 2025. [Online]. DoLA: April 30, 2025. Available: https://magnetstore.co.uk/disc-magnets/8mm-x-6mm-neodymium-disc-magnet-n52-2-82kg-pull/

**Table 5.19:** Selected permanent magnet properties.

| Property | Value |
|---|---|
| Diameter | 8 mm |
| Length | 6 mm |
| Grade | N52 |
| Residual Flux Density | 1.45 T |
| Magnetic Dipole Moment | 0.348 $Am^2$ |
| Cost | €9 |
| Operating Temperature | <80 °C |
| Mass | 2.26 g |

As can be seen in Table 5.19 the magnetic dipole moment is higher than the minimum required. This is because a COTS part had to be chosen. When building the spacecraft, the magnet can be tested and cut to obtain the needed magnetic dipole moment. In the case this larger magnet is kept, this would increase the control torque leading to greater pointing accuracy. In contrast, an over-sized magnet could lead to the hysteresis rods being saturated, thereby decreasing their performance.

**Hysteresis Rod Design**

Before sizing the hysteresis rods, an explanation of the theory of hysteresis rods must be given. This is explained in [127]. Magnetic hysteresis refers to the tendency of the atomic dipoles within a ferromagnetic material to align with an externally applied magnetic field. This can be visualized in Figure 5.17 where H is the magnetic field strength and B is the magnetic flux density in the material. When the material is shaped into a thin rod, the material is only affected by the component of the external magnetic field parallel to the rod, as stated in [127]. This is useful because when the spacecraft and its magnet are aligned with the magnetic field of the Earth, the hysteresis rods are demagnetized. As the spacecraft moves further out of alignment, the hysteresis rods become increasingly magnetized. The energy required to align the atomic dipoles is dissipated as heat, thereby damping the motion.

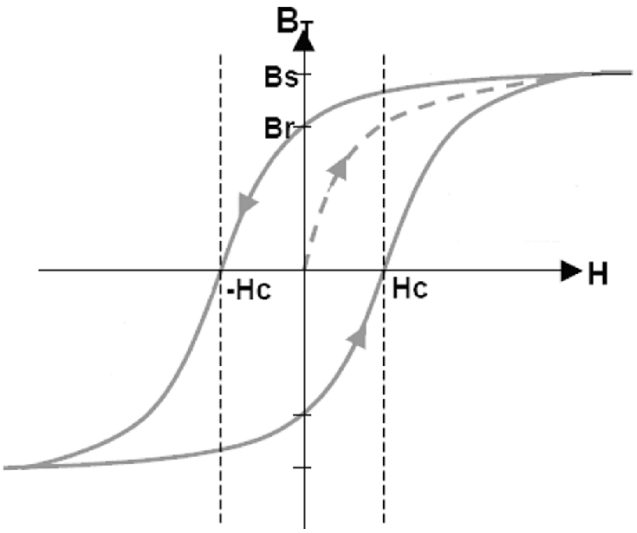


**Figure 5.17:** Hysteresis loop diagram. [128]

**Hysteresis Rod Sizing**

In order to maximize the performance of the hysteresis rods [12] states that slenderness of the rods $L/D$ (length / diameter) has to be maximized. For this reason, the value of $L$ must be maximized and is limited by the size of the spacecraft and has been chosen to be 8.5 cm this is smaller than the the side length of the spacecraft because the space might be take up by various wires. The diameter of the rods must be minimized but is also limited by manufacturing capabilities. It has been chosen to be 0.85 mm to stay within the slenderness values of 100 - 300 given by [12]. In case additional hysteresis rod volume ($V_{hyst}$) is needed, it is better to increase the number of rods rather than increasing the diameter as they will retain the efficiency associated with their slenderness. For this mission a single set of rods will be used as done on the the Quetzal-1 1U CubeSat [11]. One set of rods is comprised of two rods each placed on an axis perpendicular to the axis of the of magnetization of the permanent magnet.

**Hysteresis Rod Material**

Because of technology readiness level and available data, an alloy called HyMu-80 was chosen for the hysteresis rods. This is an 80 % Nickel alloy with high magnetic permeability which is also used by [11–13]

**Hysteresis Rod Effectiveness**
A good measure for effectiveness is the settling time of the spacecraft. In other words, how long it would take for the spacecraft to stop tumbling and align itself with the Earth's magnetic field. According to [129], the settling time can be estimated with

$$t_d = \frac{2\pi I}{W_h}(\omega_0 - \omega) \tag{5.18}$$

where $t_d$ is the settling time, $I$ is the mass moment of inertia, $\omega_0$ is the initial tumbling rate and $\omega$ is the final desired tumbling rate. $W_h$ is the energy dissipated in the hysteresis rods and is given by the equation below. The results are summarized in Table 5.20, with the additional constants in Table 5.21.

$$W_h = \kappa_w W_{h_m} V. \tag{5.19}$$

Here, $\kappa_w$ is a constant depending on the material and a mean value of 0.6 is used by [129], $V$ is the volume of the hysteresis rod and $W_{h_m}$ is the hysteresis loss in the center of the rod which depends on the equation below,

$$W_{h_m} = \eta B_{max}^m \tag{5.20}$$

where $\eta$ and $m$ are material properties equal to $12\,\mathrm{J/T^m}$ and 1.97 respectively for HyMu-80. $B_{max}$ is the maximum flux density induced in the rod and can be obtained by solving for the intersection of the curves shown below,

$$B(H) = B_s(1 - a_0 H^{-1}) + \kappa_0 H \tag{5.21a}$$

$$B(H_{in}) = (H_a - H_{in})\mu_0 N_d^{-1} \tag{5.21b}$$

where $B_s$ is the saturation flux density which is 0.45 T for HyMu-80, $a_0$ and $\kappa_0$ are the flux density constants which are $1.02\,\mathrm{A\,m^{-1}}$ and $5.0 \times 10^3\,\mathrm{T\,m\,A^{-1}}$ respectively for HyMu-80. In Equation 5.21b, $H_a$ is the maximum external magnetic field which is around $39.8\,\mathrm{A\,m^{-1}}$ according to [130] for a 60° inclination orbit. $\mu_0$ is the vacuum magnetic permeability which is $1.26 \times 10^{-6}\,\mathrm{T\,m\,A^{-1}}$. Finally, $N_d$ is the demagnetization factor of the rod which is given by its geometry. For this case it can be calculated using Equation 5.22a

$$N_d = \frac{4.02\log_{10}(e) - 0.185}{2e^2} \tag{5.22a}$$

$$e = \frac{L}{D} \tag{5.22b}$$

where $e$ is the elongation which is equivalent to slenderness of the rod. A value of 100 was chosen for this design as was done by [12]. Now solving for the intersection of Equation 5.21a and Equation 5.21b we find the point where $H = H_{max}$ and $B = B_{max}$ and we obtain the following:

$$H_{max} = \frac{\left(-(B_s - \mu_0 N_d^{-1} H_a) + \sqrt{(B_s - \mu_0 N_d^{-1} H_a)^2 + 4(\kappa_0 + \mu_0 N_d^{-1}) a_0 B_s}\right)}{2(\kappa_0 + \mu_0 N_d^{-1})}. \tag{5.23}$$

Now, $H_{max}$ can be calculated using Equation 5.23 and $B_{max}$ using Equation 5.21. Using Equation 5.20, $W_{h_m}$ is obtained and $W_h$ with Equation 5.19. The settling time $t_d$ can now be estimated using a value for $\omega_0$ taken from the flight data of Quetzal-1 [11]. The value for $\omega$ was chosen to be $0.1\,\mathrm{rad\,s^{-1}}$ because it was deemed sufficient for the technology demonstration mission needs. The value of $\omega$ is smaller for Quetzal-1 as the payload included a camera which had more stringent pointing needs. This yielded a settling time $t_d$ of 12.1 days. An overview of the results can be found in Table 5.20.This seems to be a conservative estimate when comapring with similar missions such as Colorado Student Space Weather Experiment (CSSWE) and Quetzal-1. This will be further elaborated in a subsequent section.

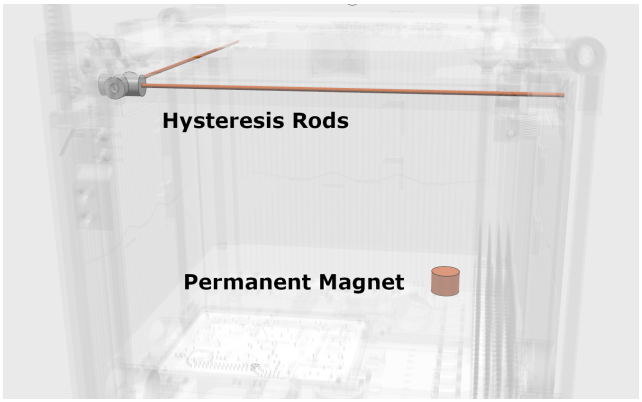


**Figure 5.18:** Placement of attitude control system components.

**Table 5.20:** Settling time estimation, necessary variables and their values.

| Variable | Value | Unit |
|---|---|---|
| $H_{max}$ | $9.55 \times 10^{-3}$ | $\mathrm{A\,m^{-1}}$ |
| $B_{max}$ | $1.04 \times 10^{-1}$ | T |
| $W_{h_m}$ | $1.40 \times 10^{-1}$ | $\mathrm{J\,m^{-3}}$ |
| $W_h$ | $4.05 \times 10^{-9}$ | J |
| $\omega_0$ | 0.436 | $\mathrm{rad\,s^{-1}}$ |
| $\omega$ | 0.1 | $\mathrm{rad\,s^{-1}}$ |
| $I$ | 0.002 | $\mathrm{kg\,m^2}$ |
| $t_d$ | 12.1 | days |

**Table 5.21:** Constants Value Summary.

| Variable | Value | Unit |
|---|---|---|
| $\kappa_w$ | 0.6 | |
| $V$ | $4.82 \times 10^{-8}$ | $\mathrm{m^3}$ |
| $\eta$ | 12 | $\mathrm{J/T^m}$ |
| $m$ | 1.97 | |
| $a_0$ | 1.02 | $\mathrm{A\,m^{-1}}$ |
| $\kappa_0$ | $5.0 \times 10^3$ | $\mathrm{m\,A^{-1}}$ |
| $H_a$ | 39.8 | $\mathrm{A\,m^{-1}}$ |
| $\mu_0$ | $1.26 \times 10^{-6}$ | $\mathrm{T\,m\,A^{-1}}$ |
| $N_d$ | $3.93 \times 10^{-4}$ | |
| $e$ | 100 | |

**Production of Hysteresis Rods**
In this design process, COTS components are generally favored. Unfortunately for the hysteresis rods, it was not possible to find HyMu-80 rods with the required dimensions. All material potions found had a diameter too large. This meant the elongation factor was so low it would have rendered the hysteresis rods ineffective. For this reason, it was decided to have these rods custom-made. In addition, testing of the properties of the rods needs to be done as described in [131].

**Negative Effects of the Permanent Magnet**
In all PMAC systems the permanent magnet has a negative effect on the performance of the hysteresis rods. For this reason, the settling time calculated above is shorter than the real settling time. Nevertheless, the permanent magnet chosen in this mission has a smaller magnetic dipole moment than CSSWE and Quitzal-1. This suggests that the discrepancy between the estimation and the real world performance fo the hysteresis rods will be smaller than the discrepancy in these other missions. Further testing will be needed to obtain concrete values. The permanent magnet could negatively affect other subsystems, since this was never considered in other successful missions this possibility was not considered as a risk. Nevertheless, this will be checked during integration testing of the spacecraft.

**Placement of Attitude Control Components**
According to [127] hysteresis rods must be placed perpendicular to the axis of magnetization of the permanent magnet. According to [12] the distance between the permanent magnet and the hysteresis rods must be maximize in order to minimize interference between the two. For ease of integration, it has been decided to place these components parallel with the axes of the body reference frame of the spacecraft. The permanent magnet is at one extremity and the hysteresis rods at the other extremity of the spacecraft.

### 5.5.4. Stability Characteristics

Due to the complex behavior of passive magnetic attitude control systems it was not possible to develop a full simulation within the given time frame. For this reason, a comparison was performed with two similar missions, namely, CSSWE and Quetzal-1. In the Table 5.22, the characteristics of each mission are listed as well as the settling time predicted by the method described previously.

**Table 5.22:** Settling time comparison.

| Variable | **Quetzal-1** [11] | **CSSWE** [12] | **Planned Mission** |
|---|---|---|---|
| $I^{(1)}$ [kg m$^2$] | 0.0018 | 0.019 | 0.002 |
| $W_h$ [J] | $5.23 \times 10^{-9}$ | $1.15 \times 10^{-8}$ | $4.05 \times 10^{-9}$ |
| $\omega_0$ [rad s$^{-1}$] | 0.44 | 0.218 | 0.44 |
| $\omega$ [rad s$^{-1}$] | 0.0320 | 0.0436 | 0.100 |
| Computed $t_d$ [days] | 10.1 | 21.0 | 12.1 |
| Simulated by [12] $t_d$ [days] | N/A | 6 to 7 | N/A |
| In orbit measured by [11] $t_d$ [days] | 5 to 6 | N/A | N/A |

As can be seen in the table above, the estimated settling time seems to be over-predicting the settling time when compared with the simulation done for CSSWE and the flight data of Quetzal-1. This over-prediction could be related to the average value used for the magnetic field strength of the Earth. The effect of different magnetic field strength on the results will be further explored in the sensitivity study. Since the planned mission has a larger mass moment of inertia compared to Quetzal-1, it can be expected that the in-orbit settling time of the technology demonstration mission will be larger than 5 to 6 days. This gives a final estimation for the settling time of the technology demonstration mission to be between 5 and 12 days. Regarding the alignment of the spacecraft, the z-axis of the spacecraft is expected to stay within 15 ° of the Earth's magnetic field with some expected oscillations.

**Sensitivity Analysis**

The design of this passive magnetic attitude control system was done using mostly linear relationships. This means that for many variables, a 10 % change would yield a 10 % change in the final value. For this reason, only a basic sensitivity analysis will be performed and the results can be found in Table 5.23. In the design of the permanent magnet, there are two variables which depend on the design of the spacecraft. These are the magnitude of the disturbance torque which will be increased by 10 % and the pointing accuracy angle which will be decreased by 10 %.

**Table 5.23:** Permanent magnet design sensitivity.

| Parameter | Max Disturbance Torque | Pointing Accuracy ($\beta_{max}$) |
|---|---|---|
| Change in Value | $+4.57 \times 10^{-9}$ N m | -0.0175 rad |
| Effect on Mass [g] | +0.105 | $\sim$ 0.00 |
| Affected Requirement | N/A | N/A |

In the table above, it can be seen that an increase in maximum disturbance torque does not significantly impact the mass of the system. Furthermore, the chosen permanent magnet is over-sized meaning that a larger magnet is already accounted for in the budget and is only expected to decrease as the during testing and manufacturing. Finally, the increase in pointing accuracy has a negligible effect on the design.

In the design of the hysteresis rods, the rod diameter, number of rods, and the spacecraft's mass moment of inertia were identified as driving variables. Other parameters, such as the rod length, were held constant due to geometric constraints within the spacecraft. Similarly, the choice of material was excluded from this analysis, as changing it would necessitate a full system redesign. However, in the next steps of this project a new design iteration could be considered, but it must be noted all the studies used in the design [11–13] used HyMu-80. For the purposes of the sensitivity study, the rod diameter and mass moment of inertia were each increased by 10 %, while the number of rods was increased by one. The most Important variable is the strength of the magnetic field of the earth which varies greatly depending on the position of the spacecraft. For this reason the value of $H_a$ was set to its maximum possible value at an altitude of 500 km [130].

**Table 5.24:** Hysteresis rod design sensitivity.

| Parameter | Rod Diameter | Nr of Rods | Mass Moment of Inertia | Max. External Magnetic Field $H_a$ |
|---|---|---|---|---|
| Change in Value | $+8.50 \times 10^{-2}$ mm | +1 | $+2 \times 10^{-4}$ N m$^2$ | +7.16 A m$^{-1}$ |
| Effect on Settling Time [days] | +3.13 | −10.2 | +2.04 | −3.91 |
| Affected Requirement | N/A | N/A | N/A | N/A |

In Table 5.24, an interesting behavior can be seen, as the hysteresis rod diameter is increased, the settling time also increases. This is because since the length of the rods is limited by the size of the spacecraft increasing the diameter reduces the slenderness of the rods thereby greatly decreasing their effectiveness. Increasing the

number of hysteria rods is the simplest way of decreasing the settling time but this also comes with challenges as adding more than two rods per axis will have diminishing returns due to their electromagnetic interactions. Furthermore, an increase in the mass moment of inertia has a linear effect on the settling time which will remain within an acceptable range. Finally, the increase in the magnetic field of the earth could suggests that the discrepancy between this model and the values obtained from flight data could be related to a difference in the magnetic field where the spacecraft was flying.

### 5.5.5. Attitude Determination System Design

The attitude determination will consist of sun sensors, a gyroscope and a magnetometer. The gyroscope and magnetometer are included in the OBC. When the spacecraft is in sunlight the sun sensors will perform the attitude acquisition, while in eclipse the gyroscope can estimate the attitude based on the last attitude determined by the sun sensors. The magnetometer provides redundancy and increases the reliability of the attitude determination.

#### Sun Sensors

A sun sensor will be included on every side of the spacecraft to ensure reliable attitude determination even in case the spacecraft is tumbling. This means six sun sensors will be included in the spacecraft. Table 5.25 lists commercially available sun sensors and their properties. If a property is not publicly available for a sun sensor then the cell is left empty in the table. The cost per sun sensor is based on a batch size of six, when available. Six different sun sensors from four suppliers are considered: AAC Clyde Space [(1)], needronix [(2)], Bradford Space [(3)] and NewSpace Systems [(4)].

**Table 5.25:** Commercially available sun sensors and their properties.

| Name | Supplier | Size [mm] | Mass [g] | Power [mW] | Cost [€] | Accuracy [°] | Update Rate [Hz] | FOV [°] |
|---|---|---|---|---|---|---|---|---|
| SS200 | AAC Clyde Space | 24.66 × 15.00 × 3.50 | 3 | 40 | | <0.3 | 100 | 110 |
| nanoSSOC-D60 | AAC Clyde Space | 43 × 14 × 5.9 | 6.5 | 2 | | <0.1 | | 60 |
| Eagle | needronix | 15 × 15.5 × 4.6 | 3 | 7 | 1615[(5)] | <0.15 | 10 | 110 |
| Eagle Plus | needronix | 29.5 × 11.5 × 6.5 | 5 | 15 | 1615[(6)] | <0.1 | 166 | 110 |
| Mini-FSS | Bradford Space | 50 × 46 × 17 | 50 | 0 | | <0.2 | | 128 |
| NFSS-411 | NewSpace Systems | 34 × 40 × 20 | 37 | 30 | | <0.2 | 5 | 140 |

The sun sensor chosen is the Eagle by needronix [(7)], its balance between small size, low mass, low power usage and high Field Of View make it ideal for the technology demonstration mission. It is one of the sun sensors mentioned in the 2024 NASA State-of-the-Art of small spacecraft technology report, with a technology readiness level of 7 to 9. These sensors can be mounted underneath the satellite surface, in between the solar panels. A small hole (<4 mm diameter) is sufficient to allow attitude acquisition. All six sun sensors connect directly to the OBC via a ribbon cable. The acquired sun vectors can then be sent to the ground station and combined with orbital knowledge into spacecraft attitude data relative to earth. While in eclipse sun sensors cannot acquire an attitude, therefore when the sun sensors can no longer sense the sun a gyroscope is used to estimate the spacecraft attitude based on the last attitude acquisition by the sun sensors.

#### Gyroscope

The gyroscope is included in the OBC, it is an MPU-3300 from InvenSense [119][(8)]. Table 5.26 shows the relevant budget values for the gyroscope. Its bias instability is 15 °/h, as the satellite is in eclipse for roughly 0.5 h this means the accuracy of the attitude determination is expected to drop to about 7.5°. This is acceptable, as there is no stringent accuracy requirement. When the satellite comes back into sunlight, the sun sensors can reacquire the sun vector and increase the accuracy again. Furthermore, the magnetometer could be used for a more accurate attitude estimation in eclipse if necessary.

[(1)] AAC Clyde Space, 2025. [Online]. DoLA: 6 June, 2025. Available: https://www.aac-clyde.space

[(2)] needronix, 2025. [Online]. DoLA: 6 June, 2025. Available: https://needronix.eu

[(3)] Bradford Space, 2025. [Online]. DoLA: 6 June, 2025. Available: https://www.bradford-space.com

[(4)] NewSpace Systems, 2025. [Online]. DoLA: 6 June, 2025. Available: https://www.newspacesystems.com

[(5)] Price based on cost when buying 6 to 8 units, and including the 15 % discount for universities and research institutes.

[(6)] Price based on cost when buying 6 to 8 units, and including the 15 % discount for universities and research institutes.

[(7)] Eagle, needronix, 2025. [Online]. DoLA: 6 June, 2025. Available: https://needronix.eu/products/sun-sensors/eagle-cubesat-sun-sensor

[(8)] MPU-3300, InvenSense, 2025. [Online]. DoLA: 6 June, 2025. Available: https://invensense.tdk.com/products/motion-tracking/3-axis/mpu-3300/

**Magnetometer**
The magnetometer is included in the OBC, it is an HMC5843 from Honeywell [119, 132]. Table 5.26 shows the relevant budget values for the magnetometer. Its field range is −4 G to 4 G, with a cross-axis sensitivity of ±0.2 %. The sun sensors and gyroscope are used as the main attitude determination methods rather than the magnetometer as the permanent magnet and hysteresis rods may interfere with the magnetometer.

### 5.5.6. Subsystem Budgets
Table 5.26 presents the final budgets for the ADCS. The mass and power values include a 5 % margin for COTS components and a 20 % margin for custom-designed components as suggested by ESA [107]. The ADCS is expected to have a mass around 25 g, a cost of about €12 300 and a power usage of 50 mW.

**Table 5.26:** Attitude determination and control system budgets.

| Component | Amount | Margin [%] | Size [mm] | Mass [g] | Power [mW] | Cost [€] | Operational Temp. [°C] |
|---|---|---|---|---|---|---|---|
| Permanent Magnet[(1)] | 1 | 20 | 8 × 8 × 6 | 2.26 | 0.00 | 9 | < 80 |
| Hysteresis Rods | 2 | 20 | 85 × 0.58 × 0.85 | 1.69 | 0.00 | [(2)]1300 | N/A |
| Sun sensor | 6 | 5 | 15 × 15.5 × 4.6 | 3.00 | 7.00 | 1615 | −40 to 85 |
| Gyroscope | 1 | 5 | 4 × 4 × 0.9 | ~0.00 | 11.88 | [(3)]0 | −40 to 105 |
| Magnetometer | 1 | 5 | 4.0 × 4.0 × 1.3 | ~0.00 | 2.64 | [(4)]0 | −30 to 85 |
| **Total** | **N/A** | **N/A** | **N/A** | **25.67** | **59.35** | **12 299** | **−30 to 80** |

### 5.5.7. Next Steps
- **Iterate** - Iterate the design using the final spacecraft budgets.
- **Perform Procurement** - Acquire the sun sensors.
- **Perform Manufacturing** - Manufacture the permanent magnet and hysteresis rods.
- **Perform Verification** - Verify that the ADCS satisfies all requirements as given in Table 5.16
- **Design Attitude Determination Algorithms** - Create methods to combine spacecraft attitude data relative to the sun from sun sensors and gyroscope with spacecraft positional data relative to earth from the payload to gain spacecraft attitude relative to earth.
- **Post-Mission Performance Evaluation** - Evaluate the performance of the ADCS after the mission.

## 5.6. Electrical Power Subsystem Design
In this section, the design of the EPS is presented. The subsystem-level requirements are derived from system-level requirements. The EPS architecture is selected through a trade-off study, followed by the preliminary sizing of its components. The design is then refined using COTS component selection to perform detailed sizing. Finally, the subsystem budgets, electrical block diagram, and future steps for the EPS are outlined.

### 5.6.1. Requirements
The EPS requirements are based on the key and deriving requirements outlined in the mid-term report. However, these have been adjusted to reflect changes in the needs of other subsystems identified during the detailed design phase. In addition, further requirements have been imposed on the EPS as a result of its preliminary sizing analysis. The subsystem requirements for the EPS are presented in Table 5.27.

**Table 5.27:** Electrical-power-subsystem requirements and their verification approaches.

| ID | Requirement | Verification Method (TADI) |
|---|---|---|
| STM-SYS-EPS-01 | The EPS shall supply a regulated 1 W average power to the spacecraft primary bus during all mission phases. | A/D: Power-budget analysis and bench demonstration with representative loads. |

*Continued on next page.*

[(1)] 8 mm x 6 mm Neodymium Disc Magnet (N52, 2.82 kg pull), Magnet Store UK, 2025. [Online]. Date of last access: April 30, 2025. Available: https://magnetstore.co.uk/disc-magnets/8mm-x-6mm-neodymium-disc-magnet-n52-2-82kg-pull/

[(2)] For 1 m of stock material: HyMu 80 Gelegeerd Staaf 6.6-63.5mm N-14080 Ronde Staaf, EVEKS. [Online]. DoLA: 18 June, 2025. Available: https://eveks.nl/nikkellegering/3406-348207-hymu-80-gelegeerd-staaf-66-635mm-n-14080-ronde-staaf.html#/12-lengte-1_meter/6159-diameter-66mm

[(3)] Included in cost of OBC.

[(4)] Included in cost of OBC.

| ID | Requirement | Verification Method (TADI) |
|---|---|---|
| STM-SYS-EPS-02a | The EPS shall be able to deliver 77 mW to the SP for 20 ms every minute throughout the mission, including eclipses. | T: Pulse-load testing. |
| STM-SYS-EPS-02b | The EPS shall deliver 32 mW to the SP for 50 s three times every orbit throughout the mission, including eclipses. | T: Pulse-load testing. |
| STM-SYS-EPS-03 | The EPS shall meet STM-SYS-EPS-01 through STM-SYS-EPS-02b for a nominal mission duration of 6 months. | A: Degradation, reliability and orbital energy-balance analysis. |
| STM-SYS-EPS-04 | The total EPS mass, including batteries and harness, shall not exceed 550 g. | I: Precision weighing with a calibrated scale. |
| STM-SYS-EPS-05 | The EPS shall not exceed a procurement cost of €25 000. | I: Detailed cost budget for EPS, including COTS component costs. |
| STM-SYS-EPS-06 | The EPS shall be capable of delivering a peak power of 6 W. | T: Peak-load bench test. |
| STM-SYS-EPS-07a | The payload shall be supplied with a regulated 5 V±5 % power line during all operational modes. | D: Multimeter verification during system-level power-on test. |
| STM-SYS-EPS-07a | The payload shall be supplied with a regulated 3.3 V±5 % power line during all operational modes. | D: Multimeter verification during system-level power-on test. |
| STM-SYS-EPS-08 | Battery depth-of-discharge shall not exceed 60 % in any orbit cycle. | A/T: Simulated mission profile analysis and discharge test with representative loads. |
| STM-SYS-EPS-09 | The EPS shall store a minimum usable energy of 1.08 W h at end-of-life. | D: Battery discharge test using calibrated load and energy logger. |

## 5.6.2. Design Options and Trade-Off

This subsection summarizes the Electrical Power Subsystem (EPS) architectures considered and the trade-off process that led to the baseline configuration.

### Candidate Architectures

Three feasible EPS concepts were identified:

- **Fuel Cells:** Devices that generate electricity from a chemical reaction.
- **Rigid Solar Panels:** Fixed, sturdy solar panels, typically mounted on spacecraft.
- **Deployable Solar Panels:** Compact solar panels that unfold in space to increase the surface area of energy generation.

All other unconventional sources (e.g. RTGs, solar concentrators, thermoelectric generators, beamed power) were discarded early because they violate CubeSat mass, safety, or cost constraints.

### Trade-Off Criteria and Weights

Each concept was evaluated on a 1–4 scale against four weighted criteria:

- **Reliability (30 %)**: Likelihood that the power system will perform without failure for the entire six-month mission. A high weight is justified because any EPS failure directly ends the technology demonstration.
- **SWaP-C (35 %)**: Combined size, weight, and life-cycle cost[(1)]. The EPS is the single biggest mass item on the spacecraft, so keeping its packed volume, mass budget, bus-power load, and hardware cost within launcher and program limits justifies the top weight.
- **Sustainability (15 %)**: Compliance with debris-mitigation policies, absence of consumables, and ease of disposal at end-of-life.
- **Other-Subsystem Effects (20 %)**: Impact on the rest of the spacecraft. Especially in the thermal subsystem, which requires radiating surfaces for heat dissipation, and the ADCS, as the EPS may impose pointing accuracy requirements on the ADCS.

Rigid, body-mounted solar panels outscored the other options in every weighted category, mainly due to their mechanical simplicity and heritage in CubeSat missions. They give a CubeSat reliable power with the least complexity. They are bolted to the spacecraft before launch, not requiring hinges or motors. They start producing power as soon as the satellite is in sunlight. This simplicity keeps mass, cost, and risk low. Power is available over a wide range of Sun angles, so attitude-control demands remain minimal [41]. The trade-off is that the panel area is limited to the surfaces of the CubeSat. However, since the mission involves a relatively simple payload with low power requirements, the total power budget remains low enough to be met by rigid panels. Fixed panels also cover free-radiating surfaces; thus, the thermal subsystem should handle more internal heat. However, with no moving parts, no consumables, and safe disposal of energy-loss fluids, rigid panels are the optimal way to meet the moderate power budget.

[(1)] Power does not apply to EPS as power is generated via EPS.

### 5.6.3. Preliminary Sizing

The sizing method, including both the key equations and the step-by-step process, follows the approach in the Spacecraft Design and Sizing Reader [133]. This approach provides a structured framework for sizing the EPS.

#### Solar Array Sizing

The power that the array must deliver is given in Equation 5.24.

$$P_{\text{SA}} = \frac{P_{\text{d}} \cdot \frac{t_{\text{d}}}{\eta_{\text{d}}} + P_{\text{e}} \cdot \frac{t_{\text{e}}}{\eta_{\text{e}}}}{t_{\text{d}}} \tag{5.24}$$

$$M_{\text{SA}} = \frac{P_{\text{SA}}}{P_{\text{sp,EOL}}} \tag{5.25}$$

$$A_{\text{SA}} = \frac{P_{\text{SA}}}{P_{\delta,\text{EOL}}} \tag{5.26}$$

where $P_{\text{SA}}$ is the power generated by the solar arrays, $P_{\text{d}}$ is the power required during the daylight, $P_{\text{e}}$ is the power required during the eclipse, $t_{\text{d}}$ is daylight time, $t_{\text{e}}$ is eclipse time, $\eta_{\text{d}}$ is daylight efficiency, and $\eta_{\text{e}}$ is eclipse efficiency. $\eta_{\text{d}}$ is approximated as 80 % for direct energy transfer and 85 % for peak power tracking [41]. $\eta_e$ is approximated as 60 % for direct energy transfer and 65 % for peak power tracking [41].

The mass and area of the solar array can be found from the electrical power to be delivered by the array through Equation 5.25 and Equation 5.26, where $M_{\text{SA}}$ is the mass, $A_{\text{SA}}$ is the area, $P_{\text{sp,EOL}}$ is the EOL specific power, and $P_{\delta,\text{EOL}}$ is the EOL power density of the solar array in orbit. As solar panels degrade over time, their EOL specific power and power density can be calculated using Equation 5.27 and Equation 5.28.

$$P_{\text{sp,EOL}} = P_{\text{sp,BOL}} \cdot \left(1 - \text{DF}\right)^{ML} \tag{5.27}$$

$$P_{\delta,\text{EOL}} = P_{\delta,\text{BOL}} \cdot \left(1 - \text{DF}\right)^{ML} \tag{5.28}$$

where $DF$ is the degradation per year and $ML$ is the duration of the mission, $P_{\text{sp}_{\text{BOL}}}$ is the specific power at the Beginning-of-Life (BOL) and $P_{\delta_{\text{BOL}}}$ is the power density at BOL of the solar array in orbit. The BOL specific power and power density can be calculated using Equation 5.29 and Equation 5.30.

$$P_{\text{sp,BOL}} = P_{\text{sp,ideal}} \cdot \cos\theta \ \cdot I_{\text{d}} \tag{5.29}$$

$$P_{\delta,\text{BOL}} = P_{\odot} \cdot \eta_{\text{SC}} \cdot \cos\theta \ \cdot I_{\text{d}} \tag{5.30}$$

Here $P_{\text{sp,ideal}}$ is the ideal (laboratory) specific power at normal incidence, $\theta$ is the angle between the Sun vector and the panel normal, $I_{\text{d}}$ is the inherent degradation factor that accounts for cover-glass, wiring, and mismatch losses, $P_{\odot}$ is the solar constant at 1 au (1322 $\text{W/m}^{2(1)}$ [41]), and $\eta_{\text{SC}}$ is the solar cell efficiency.

Because rigid, body-mounted arrays are limited to the satellite's surface area, the cells must convert sunlight as efficiently as possible to meet the power budget. Triple-junction gallium-arsenide (TJ GaAs) solar cells offer the highest efficiency among COTS space-qualified cells and also have relatively high specific power. TJ GaAs cells are easy to mount and have high flight heritage, making them the chosen solar cells for the satellite. Data on TJ GaAs cells can be found in Table 5.28.

**Table 5.28:** Key parameters for TJ GaAs rigid solar panels.

| Parameter | Value | Reference |
|---|---|---|
| $\eta_{\text{SC,BOL}}$ [%] | 30 | [41] |
| $P_{\text{sp,ideal}}$ [$\text{W kg}^{-1}$] | 70[(2)] | [134] |
| $I_{\text{d}}$ [–] | 0.72 | [41] |
| $DF$ [$\%\,\text{yr}^{-1}$] | 0.5 | [41] |

**Table 5.29:** Key parameters for lithium-ion batteries.

| Parameter | Value | Reference |
|---|---|---|
| $\eta_{\text{bat}}$ [%] | 90 | [41] |
| $e_{\text{sp}}$ [$\text{W h kg}^{-1}$] | 133 | [135] |
| $e_{\delta}$ [$\text{Wh l}^{-1}$] | 321 | [135] |
| $DoD$ [%] | 60[(3)] | [41] |

#### Secondary Battery Sizing

The mass and the size of the spacecraft batteries can be found through Equation 5.31 and Equation 5.32 where $M_{\text{bat}}$ is the mass, $V_{\text{bat}}$ is the volume, $e_{sp}$ is the specific power, $e_{\delta}$ is the energy density of the battery. The total energy stored in the battery, represented by $E_{\text{bat}}$, is given via Equation 5.33 where $P_{\text{e}}$ is the power required during eclipse, $\eta_{\text{bat}}$ is the efficiency of the battery, and $DoD$ is the depth of discharge of the battery.

$$M_{\text{bat}} = \frac{E_{\text{bat}}}{e_{\text{sp}}} \tag{5.31}$$

$$V_{\text{bat}} = \frac{E_{\text{bat}}}{e_{\delta}} \tag{5.32}$$

$$E_{\text{bat}} = \frac{P_{\text{e}} \cdot t_{\text{e}}}{DoD \cdot \eta_{\text{bat}}} \tag{5.33}$$

For the satellite, Lithium-ion batteries are chosen because of their high specific energy, energy density, and flight heritage. Table 5.29 gives an overview of Lithium-ion batteries' properties.

(1) This value is the annual minimum of the solar constant, it is adopted for a conservative design.

(2) This value was taken for a TJ GaAs rigid panel with a 26.8 % BOL efficiency. Current solar cells likely have higher efficiency values; thus, this value was taken to have a conservative mass budget.

(3) In the source, it is provided that lithium ion batteries have a $DoD$ higher than 60 % for $\mathbf{10^4}$ cycles. The battery goes through fewer than 6000 life cycles in a 12-month orbit. However, to have a conservative design, $DoD$ is taken to be 60 %.

### Power Conditioning and Distribution Unit Sizing

For the power conditioning and distribution, a light Power Conditioning & Distribution Unit (PCDU) with flight heritage should be selected. For these reasons, for the preliminary design, the AAC Clyde Space Starbuck Nano-Pico PCDU was selected, which is commonly used in 1U satellites [14]. Table 5.30 gives an overview of the AAC Clyde Space Starbuck Nano-Pico PCDU's properties.

**Table 5.30:** Key parameters for AAC Clyde Space Starbuck Nano-Pico PCDU [14].

| Parameter | Value |
|---|---|
| Mass, $M_{\text{PCDU}}$ [g] | 86.0 |
| Volume, $V_{\text{PCDU}}$ (L × W × H) [cm$^3$] | 140.0 (95.89 mm × 90.17 mm × 16.20 mm) |

### Harness

Based on literature, Raychem Spec44 AWG26 cables are commonly used in CubeSat EPS harnessing(1). Again based on literature, the solar arrays include pre-attached wiring(2). Thus, only an additional 1 m of Spec44 is assumed to connect the sun sensors and antennas. The cables have a mass of approximately 5 g [16] and a €7(3) cost.

For external ground interfacing, a charging port is included in the EPS layout. The selected connector is the Glenair M32139 Nano Miniature connector. Based on supplier data, this port has an estimated length of 6 mm and a width of 0.6 mm [17] and a unit cost of €807(4). The small size(5) of the charging port, allows it to be mounted on one of the side surfaces of CubeSat without requiring cutouts from the solar panels. This placement enables external access for ground testing of the EPS and supports pre-launch battery charging.

In total, the cable harness subsystem—including internal wiring and the charging port an estimated mass of 5 g and a combined cost of €812. In order to ensure that the connector fits on the outside of the satellite and that there are no issue with wire path and wire bending radius the same methodology that was used to find the antenna placement in Section 4.7 can be applied.

## 5.6.4. EPS Preliminary Subsystem Budgets

In this section, the EPS will be sized for the worst-case scenario to meet the power requirements of the subsystems with the method explained in Subsection 5.6.3. For the mission, the longest eclipse time is 35.7 min and the shortest daylight time is 58.8 min, as given in Section 3.3. $\theta$ is taken as 0° to estimate the effective area required. The peak power and the average power of the subsystems for the worst-case scenario are presented in Table 5.31 (6).

**Table 5.31:** Power budget of the subsystems.

| Subsystem | Avg. Power [mW] | Peak Power [mW] |
|---|---|---|
| SP | < 1 | 77 |
| VP | 110 | 110 |
| C&DH | 737 | 5000 |
| ADCS(7) | 59 | 59 |
| Thermal(8) | 25 | 25 |
| Structures | 0 | 0 |
| Margin | 10% | 10% |
| **Total** | **982** | **5849** |

**Table 5.32:** Electrical power component sizing.

| Component | Type | Mass [g] | Size |
|---|---|---|---|
| Solar Arrays | TJ GaAs | 44.1 | 77.8 cm$^2$ |
| Battery | Lithium Ion | 8.1 | 3.4 cm$^3$ |
| PCDU | AAC Clyde Space Starbuck Nano-Pico PCDU | 86.0 | 140.0 cm$^3$ |
| Harness | - | 9.2 | 1 m |

Based on the values given in Table 5.31, peak power tracking (also known as maximum power tracking) is the preferred technique for power regulation. The total power that EPS will supply was determined to be

(1)Small Satellite Solar Panels, ISISpace. [Online]. DoLA: 5 June, 2025. Available: https://www.isispace.nl/product/isis-cubesat-solar-panels

(2)Small Satellite Solar Panels, ISISpace. [Online]. DoLA: 5 June, 2025. Available: https://www.isispace.nl/product/isis-cubesat-solar-panels

(3)Small Satellite TE Connectivity SPEC44 Series Data Cable, 1 Pairs, 2 Cores, 0.6 mm², Screened, 20 AWG, 100m, Screened Shield, Type 44, RS. [Online]. DoLA: 11 June, 2025. Available: https://nl.rs-online.com/web/p/twisted-pair-multicore-data-cable/0362601?gb=s

(4)Mouser Electronics, M32139/04-B08TN. [Online]. DoLA: 11 June 2025. Available: https://mou.sr/4eiX5gK

(5)The mass of the connector is deemed negligible due to its size.

(6)The daylight and eclipse power of the subsystems were equal to each other.

(7)The power required for the magnetometer and gyroscope is not included in the total as the power consumption of these components is already accounted for in the OBC's power budget.

(8)Thermal subsystem is not included in the total as the components requiring power for the thermal subsystem are already accounted for in other subsystems' budgets.

**0.98 W**. The preliminary estimates of the mass and volume of the EPS components based on Subsection 5.6.3 are presented in Table 5.32. To ensure conservative design, a 10 % system-level margin was applied to the power budget in addition to the margins in the subsystem-level power budget.

A 1U CubeSat can meet the power budget with one face pointed normal to the Sun (most restrictive case), providing an effective illuminated area of 100 $cm^2$, exceeding the minimum surface area requirement based on the preliminary sizing (78.0 $cm^2$) by more than 28 %. Rigid solar panels will be mounted on all six surfaces of the satellite to eliminate dependence on satellite orientation for power generation. This design also reduces the pointing accuracy requirements imposed on the ADCS. With this redundant structure, EPS will be able to generate power in case of an ADCS malfunction and would have a higher tolerance to solar array failures. While covering all six surfaces with solar panels increases cost and mass, the gains in reliability and resilience outweigh the trade-offs. Full coverage ensures consistent power generation across various attitudes and orbital conditions. Also, a 1.08 W h battery is required to provide enough power to S/C during eclipse.

## 5.6.5. Detailed Design

This section presents a comparison, evaluation and selection of the COTS options for EPS. Following the selection, the EPS architecture will be demonstrated, including its connections to other subsystems within the satellite.

### Battery and PCDU Selection

The initial sizing in Subsection 5.6.3 was performed assuming that the PCDU and battery would be implemented as separate units. However, upon further investigation of COTS solutions, it was concluded that combining the battery and the PCDU into a single integrated unit is a more common, compact, and cost-effective approach for state-of-the-art small satellites. Most COTS PCDUs for 1U satellites contain an embedded battery of at least 10 W h, exceeding the mission's modest battery capacity requirement of 1.08 W h. Table 5.33 lists four COTS options for battery-integrated PCDUs.

**Table 5.33:** Key characteristics of four battery-integrated PCDUs.

| **Parameter** | **CubeSat Kit Linear EPS** [136] | **Compact EPS 2 (Type A)**[(1)] | **Starbuck Nano-Pico**[14] | **EPS I**[(2)] |
|---|---|---|---|---|
| Company | Pumpkin Space | ISISPACE | AAC Clyde Space | EnduroSat |
| Mass [g] | 155 | 184 | 86 | 230 |
| Height[(3)] | 15.60 | 26.45 | 16.20 | N/A |
| Cost [€] | 860[(4)] | On request | On request | 4200 |
| Battery capacity [Wh] | 11 | 22.5 | 10 | 10.2 |
| Number of cells in battery | 2 | 2 | 2 | 2 |
| Regulated voltage lines | +5 V, +3.3 V | +5 V, +3.3 V | +12 V, +5 V, +3.3 V | +5 V, +3.3 V |
| Operational temperature [°C] | -40 to +85 | -20 to +70 | -40 to +85 | N/A |
| Country | USA | Netherlands | Sweden | Bulgaria |

Among the four listed products, the Starbuck Nano-Pico has the lowest mass with 86 g and it is more than 40 % lighter than the Pumpkin Space's Linear EPS, the next-best candidate. Its integrated 10 W h lithium polymer battery exceeds the 1.08 W h battery energy capacity requirement [14]. The presence of two cells in the battery improves the reliability of the PCDU, as the battery would still be operational in the case of a single cell failure. The Starbuck Nano-Pico also provides three regulated outputs (+12 V, +5 V, +3.3 V), covering both the payload's and the S/C's voltage needs without the need for converters. It should be noted that, Pumpkin's Linear EPS is also a technically attractive and well-proven option. However, prioritizing a European supplier directly aligns with the "**STM-SH-ML-3:** *The SP shall contribute to reducing reliance on foreign-operated space-based navigation services*" requirement.

The selection of the Starbuck Nano-Pico implicitly fixes the mission to a centralized EPS architecture. In a centralized EPS architecture, a single unit (PCDU) conditions and distributes power to every subsystem, whereas in a decentralized EPS architecture, power conditioning and distribution are handled by two different units: Power Conditioning Unit (PCU) and Power Distribution Unit (PDU). Decentralized EPS architecture eliminates the single-point-failure risk associated with the centralized EPS architecture and results in less wiring harness [137]. However, the overall mass of the EPS is increased as splitting PCU and PDU results in

(1) Compact Electrical Power System 2, ISISpace. [Online]. DoLA: 5 June 2025. Available: https://www.isispace.nl/product/compact-eps/

(2) EPS I, EnduroSat. [Online]. DoLA: 5 June 2025. Available: https://www.endurosat.com/products/eps-i/

(3) Length and width are standardized to 95.89 mm × 90.17 mm.

(4) CubeSat Kit Linear EPS, Pumpkin Space. [Online]. DoLA: 5 June 2025. Available: https://www.pumpkinspace.com/store/p51/Linear_EPS_Module_%28LEPSM1%29.html

more hardware mass. For the 1U technology demonstration mission, the reliability of the PCDU was deemed sufficient. Thus, a centralized EPS architecture was selected for its simplicity in design and operation.

### Solar Array Selection

The characteristics of four commercial CubeSat solar-panel candidates are summarized in Table 5.34.

**Table 5.34:** Key characteristics of commercial CubeSat solar panels.

| Parameter | CubeSat Kit Fixed Solar Panels [136] | Small Satellite Solar Panels[1] | PHOTON [15] | 1U Solar Panel [138] |
|---|---|---|---|---|
| Company | Pumpkin Space | ISISPACE | AAC Clyde Space | EnduroSat |
| Mass per 1U [g] | 35 | 50 | 45 | 48 |
| Cost per 1U Surface [€] | 2500[2] | On request | On request | 2500[3] |
| Cell type | Spectrolab XTJ-Prime | GaAs triple-junction | Spectrolab XTJ-Prime | Azur Space 3G30A TJ |
| Cell BOL efficiency [%] | 30.7 | 30 | 30.7 | >29.5 |
| Cell EOL efficiency [%] | NA | NA | | |
| Operational temperature [°C] | –40 to +85 | –40 to +125 | –40 to +80 | –40 to +80 |
| Country | USA | Netherlands | Sweden | Bulgaria |

The AAC Clyde Space PHOTON panel emerges as the preferred option because it is compatible with the Starbuck Nano-Pico PCDU, simplifying the integration of EPS. It has the smallest mass among European options, weighing 45 g per 1U surface. Based on the procedure described in Subsection 5.6.3, solar arrays need to generate more than 1.75 W at their EOL, to provide sufficient power to the S/C. PHOTON generates around 3 W perpendicular to the Sun in BOL[4] per 1U surface [15] by using Spectrolab XTJ-Prime cells, comfortably surpassing the S/C's power demand.

### EPS Final Subsytem Budgets

The mass, size, and cost budget of the EPS components, along with their estimated costs and operational temperature ranges, are summarized in Table 5.35 for the described configuration.

**Table 5.35:** Subsystem final budgets for EPS.

| Component | Amount | Margin [%] | Mass [g] | Size [mm] | Cost [k€] | Power [mW] | Operational Temp. [°C] |
|---|---|---|---|---|---|---|---|
| Solar arrays [15] | 6 | 5 | 45 | 100 × 100 × 3.5[5] | TBD [6] | N/A | −40 to 80 |
| Battery & PCDU [14] | 1 | 5 | 86 | 95.89 × 90.17 × 16.20 | TBD [7] | N/A | −40 to 85 |
| Harness [16, 17] | 1 | 5 | 5 | ∅0.4 × 1000 | 0.80 | N/A | −65 to 150 |
| **Total** | **N/A** | **N/A** | **379** | **N/A** | **TBD**[8] | **N/A** | **−40 to 80** |

As it can be seen in Table 5.35, the EPS is expected to have a mass around **379 g**, and it takes up approximately **140 cm$^3$** of the S/C bus volume. The expected cost of EPS is **€20.9 k**. A 5 % margin is applied to the power and mass budget as suggested by ESA for COTS components [107].

### EPS Sensitivity Analysis

The key sizing parameters for the EPS are the eclipse fraction (dependent on both orbital altitude and inclination), eclipse duration (dependent on both orbital altitude and inclination), the average power requirement of the S/C, and mission duration. The EPS has already been sized for the worst-case scenario, incorporating both subsystem-level and system-level safety margins. In the sensitivity analysis, the relationship between the EPS and these parameters will be scrutinized by exploring the extreme cases that the current design can accommodate[9] All calculations will be performed using the methodology detailed in Subsection 5.6.3.

[1] Small Satellite Solar Panels, ISISpace. [Online]. DoLA: 5 June 2025. Available: https://www.isispace.nl/product/isis-cubesat-solar-panels/

[2] CubeSat Kit Fixed Solar Panels, Pumpkin Space. [Online]. DoLA: 5 June, 2025. Available: https://www.pumpkinspace.com/store/p154/CubeSat_Kit%E2%84%A2_Fixed_Solar_Panels.html

[3] 1U Solar Panel, EnduroSat. [Online]. DoLA: 5 June, 2025. Available: https://www.endurosat.com/products/1u-solar-panel-x-y/

[4] At EOL of the 6-month mission, PHOTON would generate 2.99 W and an EOL $P_{SA}$ of 2.22 W is required for the mission.

[5] The area required for antennas was deemed negligible.

[6] Cost of solar panels is approximated as €3200 based on EnduroSat's solar panels. Solar Panels, EnduroSat. [Online]. DoLA: 20 May, 2025. Available: https://www.endurosat.com/products-category/solar-panels/

[7] The cost of the Battery & PCDU is approximated to cost €867.3 based on Pumpkin Space's Linear EPS Module [136]

[8] Based on the component cost estimations, EPS is expected to cost €20.9 k.

[9] Only the explored parameter will be varied by keeping the rest of the parameters constant.

- **Eclipse Fraction:** This parameter is the proportion of each orbit spent in the shadow of the Earth, and it is a key driver for solar panel sizing. The eclipse fraction varies with orbital altitude, inclination, and orientation of the Earth relative to the Sun. The present solar panels can handle up to a 51.9 % eclipse fraction, 37.3 % more than the current eclipse fraction of 37.8 %.
- **Eclipse Duration:** This parameter is the time that the S/C spends in Earth's shadow in each orbit. Like the eclipse fraction, it varies with orbital altitude, inclination, and orientation of the Earth relative to the Sun. Because the power is provided to the S/C by the battery in eclipse, the eclipse duration is the dominant driver for battery sizing. The current battery system can sustain up to a 329.9 min eclipse duration while keeping the $DoD$ above the 60 % limit, which is more than 9 times longer than the current eclipse duration of 35.7 min.
- **S/C Average Power Requirement:** The average power requirement of the S/C directly drives solar panel sizing, since the arrays must generate enough power to meet the requirement. The current solar array design can sustain up to 1322 mW of average S/C power, which is 34.6 % more than the current 982 mW power budget.
- **Mission Duration:** The mission duration affects both the solar panel and the battery size. Solar cells degrade over time, while the $DoD$ decreases with increased duty cycles. The current EPS design can meet mission requirements for up to 18 years[(1)], which is 36 times longer than the current mission duration of 6 months.

The sensitivity study demonstrates that the EPS design is highly robust and capable of accommodating significant variations in the mission profile.

### EPS Architecture

The electrical block diagram of S/C is presented in Figure 5.19. The electrical power architecture of the spacecraft is a centralized system built around the PCDU integrated with the Starbuck Nano-Pico battery. The solar arrays act as the primary power source during daylight to provide power to the S/C. The integrated battery is charged during daylight and is discharged during the eclipse to provide power to the S/C as a secondary power source. The PCDU conditions and distributes the power provided by the solar arrays and the battery to the necessary components through its regulated +3.3 V, +5 V, and +12 V power busses. The SP uses the +5 V line, and all other subsystems draw power from the +3.3 V line.

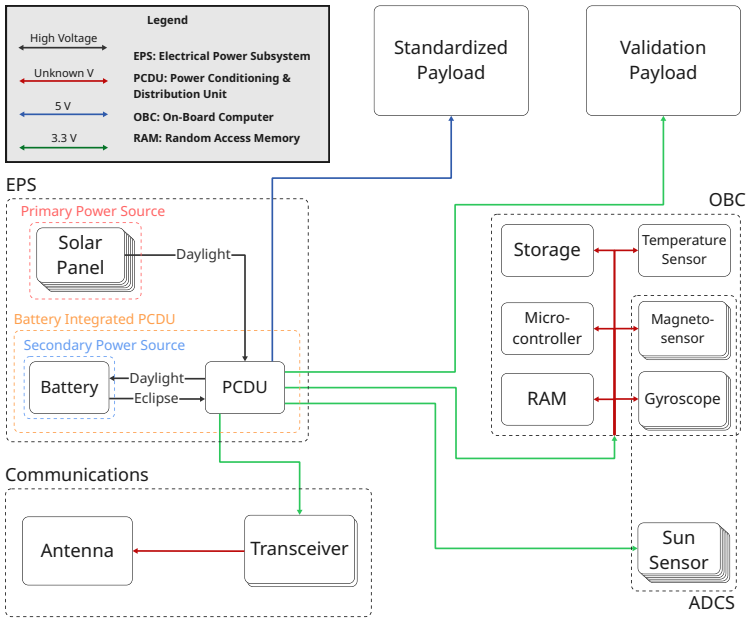


**Figure 5.19:** Electric block diagram of the S/C.

## 5.6.6. Next Steps

After the DSE, the design of the EPS will turn into a flight-ready hardware through the following steps:

[(1)] Limiting factor for the mission duration is the $DoD$ of the battery.

1. **Order parts:** Finalize the bill of materials for the EPS: solar panels, wires, charge port. Then, place purchase orders for the aforementioned components.
2. **Test individual components:** When parts arrive, inspect them for damage and asses their performance via the requirement verification methods outlined in Table 5.27 and detailed in Section 7.3.
3. **Install and hook up the EPS:** Attach the battery-integrated PCDU to the S/C through stacking PC/104 boards. Then run cables to the solar panels, sun sensors, antenna, and the charging port.
4. **Run system-level tests:** Use the external charge port to charge the battery. Then, put the S/C through the test campaign outlined in Table 5.27 and detailed in Section 7.3.
5. **Document:** Update drawings, harness diagrams, bill of materials, test reports, cabling diagrams.

## 5.7. Thermal Design

The following section presents the thermal analysis conducted to verify the adequacy of the thermal control system. It begins with the definition of key requirements, followed by insights gained during the preliminary design phase. Next, the methods used in the detailed design process and the rationale behind component selection are discussed. Finally, the impact of these design choices on the overall thermal budget is evaluated.

### 5.7.1. Requirements

The thermal subsystem has one major requirement, essentially stating that the thermal subsystem must keep the S/C components within their respective temperature ranges. Thus, the first step in creating requirements was to gather this information for each subsystem and turn them into requirements. Some requirements have been merged as they mandated similar results. The final list of requirements is given in Table 5.36.

**Table 5.36:** Thermal requirements.

| ID | Requirement | Verification Method (TADI) |
|---|---|---|
| STM-SYS-THERM-01 | The S/C shall keep all the components within their respective operational temperature ranges. | **T**: Thermal vacuum test under controlled conditions replicating LEOP. |
| STM-SYS-THERM-01A | The S/C shall keep the sub components of the Antenna, SP and VP within a temperature range of $-40\,°C$ to $85\,°C$ | **A** : Analysis of thermal ranges through a thermal model. |
| STM-SYS-THERM-01B | The S/C shall keep the sub components of the Structural, ADCS and EPS, within a temperature range of $-40\,°C$ to $80\,°C$ | **A** : Analysis of thermal ranges through a thermal model. |
| STM-SYS-THERM-01C | The S/C shall keep the transceiver and OBC within a temperature range of $-30\,°C$ to $85\,°C$ | **A** : Analysis of thermal ranges through a thermal model. |

### 5.7.2. Preliminary Design Results

The preliminary analysis made it clear that no active thermal control was necessary and no alterations needed to be made to the design to complete the set requirements [46]. However this conclusion was made with a slim margin build upon the assumption that the satellite was a cube of uniform mass and temperature. Thus if the heat transfer between components is too low, it may still fail to achieve its obligations.

For most components, thermal conditions are not expected to pose a significant issue, as their operational limits lie well beyond the spacecraft's anticipated temperature range. However, two subsystems have been identified as potential concerns: the antenna and the solar panels. During eclipse periods, these components will experience rapid cooling and may approach their lower operational limits. In the case of the solar panels, this is less critical, as they remain inactive during eclipses and will quickly reheat once exposed to sunlight again, minimizing any impact on performance. The antenna, however, is more critical, as communication capabilities may be required during eclipse periods. Therefore, while an active thermal management is not expected to be necessary, it cannot be entirely ruled out.

The specified operational temperature range for the spacecraft is from $-23\,°C$ to $25\,°C$, which includes a $15\,°C$ design margin. If the satellite remains in orbit beyond its intended mission lifetime, it is expected to encounter a broader range of temperatures from $-32\,°C$ to $50\,°C$, again including the same margin. This extended range is expected to be narrower for most subsystems, except for those directly exposed to the vacuum of space.

### 5.7.3. Detailed Thermal Model

In the detailed design phase the assumption that the S/C is a cube of uniform mass and temperature is no longer assumed valid. Instead, a more realistic model is developed, which considers the nature of the thermal connections between subsystems, the locations of power generation, and the pathways of heat transfer between them.

This shift in modeling approach necessitates the creation of a multi-node thermal model, where in each subsystem is represented by its own node. This transition significantly increases the complexity of the model, not only in terms of managing multiple nodes and their interconnections, but also in accounting for which surfaces are exposed to solar radiation, albedo reflection, and Infrared Radiation (IR) emissions.

## Model Definition

The first step in developing this multi-node thermal model is to note down which assumptions are taken in the establishing of this model, define its relationship with the environment and the interaction between the nodes.

#### Model Assumptions

The spacecraft is modeled as a network of discrete thermal nodes. Each node represents a lumped mass with uniform temperature and homogeneous material properties. Temperature gradients within individual nodes are neglected.

The thermal model consists of a total of 16 nodes: six nodes represent the solar panels, five represent structural components, and five represent internal subsystems. It is assumed that only the solar panels and the antenna are directly exposed to space and are therefore capable of radiating heat away.

A closely related assumption is that the solar panels cover the entire exposed side of the S/C. To maintain the validity of this assumption, the exposed areas of the structural frame must closely match the thermal properties, specifically the emissivity and absorptivity of the solar panels. If not, the assumption would no longer hold.

According to a material properties index[(1)], the material with properties closest to those selected for the solar panels is black anodized aluminum. Fortunately, this surface finish is also used on the EnduroSat structural frame selected for the mission[(2)], thus this assumption is valid.

After defining the stacking order and spatial arrangement of the nodes, their thermal connections to neighboring nodes are established. These connections are illustrated in Figure 5.20.

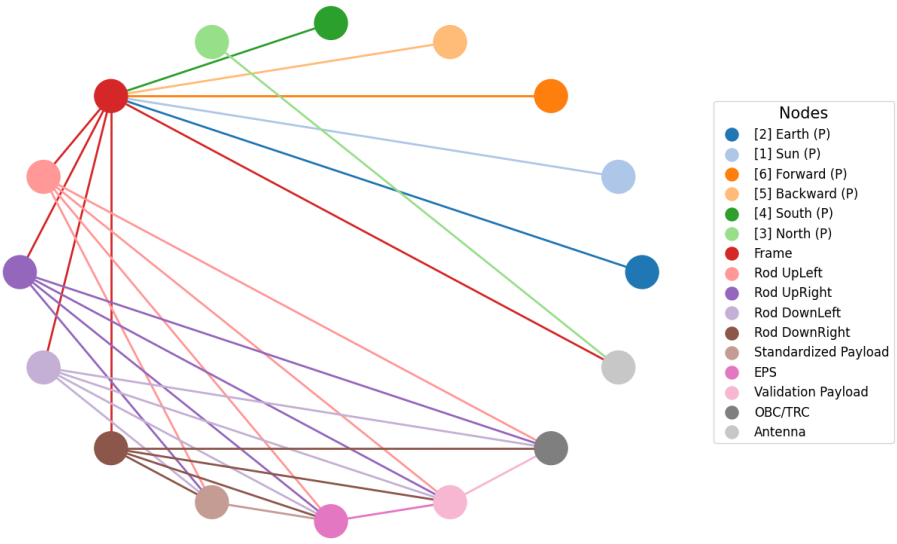


**Figure 5.20:** Visualization of the network used in the final model.

All nodes, expect the ones that represent PCB's, are assumed to have thermal properties close to those of

[(1)]Heliostat Design Concept, RedRok, 2009. [Online]. DoLA: 16 June, 2025. Available: `https://www.redrok.com/concept.htm#emissivity`

[(2)]1U CubeSat Bus, EnduroSat. [Online]. DoLA: 20 May, 2025. Available: `https://www.endurosat.com/products/1u-platform/`

aluminum alloy 6061 – $T651$. This material has a specific heat capacity of 896 J kg$^{-1}$ K$^{-1}$[(1)]. For the PCB's an estimation was made as no values could be found. As PCB's are mostly made out of copper and epoxy a weighing of their properties was used instead. Copper has a specific heat capacitance of 385 J kg$^{-1}$ K$^{-1}$ and was assumed to make up 21 % of the PCB. Epoxy has a heat capacitance of 1000 J kg$^{-1}$ K$^{-1}$ [(2)] and accounts for 79 %, resulting in a total heat capacitance of 867 J kg$^{-1}$ K$^{-1}$.

The thermal conductance of a material is influenced by numerous factors, including pressure, environment, surface finish, and more. Due to these varying conditions, conservative estimations were made for the contact conductance values. Two types of connections were identified: one between aluminum and aluminum, with a contact conductance of approximately 400 W m$^{-2}$ K$^{-1}$ [139], and the other between copper and aluminum, with an estimated contact conductance of around 666 W m$^{-2}$ K$^{-1}$ [139].

### Model Orientation

Using the preliminary thermal analysis as a baseline, the orientations of the S/C that require evaluation can be identified. From this analysis, a key conclusion emerges: the primary thermal concern is preventing the S/C from dropping below the lower limit of the operational temperature range. The upper limit is less critical, as the most extreme expected value remains approximately 20 °C below the maximum allowable temperature.

To address this, the thermal model is configured such that one side of the spacecraft consistently experiences minimal incident heat flux. This surface will receive most of its thermal energy through conduction from other subsystems rather than direct radiation. The antenna, identified as a thermally sensitive component due to its high minimum operational temperature and its exposure to space, is positioned behind this cold-facing panel. By making sure that the S/C can operate in this worst case scenario, one can assure that even if the spacecraft were to be tumbling it would still be able to operate.

For modeling purposes, this configuration implies that one surface of the spacecraft will always face Earth, while several other surfaces will alternately be exposed to solar radiation, depending on orbital position. This orientation is illustrated in Figure 5.21.

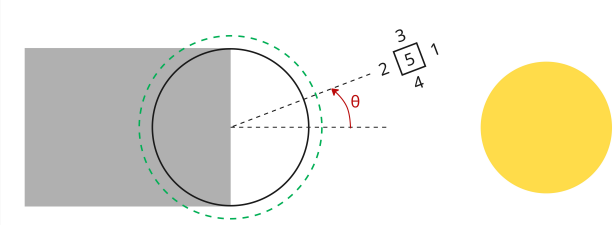


**Figure 5.21:** Orientation of spacecraft with respect to the Sun and Earth.

## Thermal Radiation

Having defined the workspace and assumption made for the basis of the model, the next step in the process is to identify the types of incoming and outgoing thermal radiation. Below a detailed overview is given for each form of relevant thermal radiation. These are defined in such a way they are applicable for all nodes present in the model.

### Solar Irradiance

The primary source of heat considered is solar irradiance. The amount of radiation received by the spacecraft ($Q_{P_\odot}$) can be calculated using Equation 5.34 [52], where $\alpha_i$ is the solar absorptivity, $A_i$ is the receiving area, $P_\odot$ is the solar irradiance at the spacecraft's location and $F_{S\to i}$ is a view factor accounting for the relative orientation of the Sun and the chosen node's surface area.

$$Q_{P_\odot} = \alpha_i A_i P_\odot F_{S\to i} \tag{5.34}$$

$P_\odot$ is a value that will change depending on position of earth along its orbit and can be approximated using Equation 5.35 [52], where r is the distance from the sun in Astronomical Unit (AU) and $(P_\odot)_{r=1}$ is taken to be 1367 [41].

[(1)] Al 6061-T6, World Material , 2025. [Online]. DoLA: 19 May, 2025. Available: https://www.theworldmaterial.com

[(2)] Specific Heat of Common Materials – Engineering Reference, Engineering ToolBox, 2025. [Online]. DoLA: 16 June, 2025. Available: https://www.engineeringtoolbox.com/specific-heat-capacity-d_391.html

$$P_{\odot} = \frac{(P_{\odot})_{r=1}}{r^2} \tag{5.35}$$

**Albedo Factor**
An other indirect contribution of the sun to the heat balance is the Albedo effect ($Q_a$), which can be quantized with Equation 5.36 [52], where $a$ is the Earth's Albedo coefficient and $F_{E\rightarrow i}$ is a view factor accounting for the relative orientation of the Earth and the chosen node's surface area.

$$Q_{\mathrm{a}} = a\alpha_i A_i P_{\odot} F_{E\rightarrow i} \tag{5.36}$$

The albedo factor is typically kept constant throughout a simulation. However, in reality, the intensity of albedo dimmers as the satellite moves away from orbital noon,the point at which the Sun directly illuminates the Earth [52]. To account for this variation, one can use the correction provided in Equation 5.37 [52], where $\xi$ is the solar zenith angle. This angle, in turn, can be calculated using Equation 5.38 [52].

$$a(\xi) = a_{\xi=0} + 4.9115 \times 10^{-9}\xi^4 + 6.0372 \times 10^{-8}\xi^3 - 2.1793 \times 10^{-5}\xi^2 + 1.3798 \times 10^{-3}\xi \tag{5.37}$$

$$\xi = \cos^{-1}\left(\cos(\beta)\cos(\theta)\right) \tag{5.38}$$

**Infrared Radiation**
The last form of incoming thermal radiation is IR received by the spacecraft from Earth ($Q_{IR}$) given by Equation 5.39 [52], where $\epsilon_i$ is the emissivity.

$$Q_{IR} = \epsilon_i \frac{P_{\odot}(1 - a(\xi))}{4} A_i F_{E\rightarrow i} \tag{5.39}$$

**Heat Transfer**
The heat a node transfers to or receives from its neighbors can be quantified using Equation 5.40 [140], where $k_i$ is the contact conductance, $n$ is its number of neighbors, $T_i$ their temperature , $T_j$ its own and $(A_i)_c$ the contact area.

$$Q_{transfer} = k_i \sum_{i=0}^{n} (T_i - T_j)(A_i)_c \tag{5.40}$$

**Stefan–Boltzmann Law**
The final form of thermal radiation considered is black body radiation ($Q_{rad}$) which is described by the Stefan–Boltzmann law, with $\sigma$ the Stefan–Boltzmann constant, given by Equation 5.41 [141].

$$Q_{rad} = A_i \sigma \epsilon_i T_i^4 \tag{5.41}$$

## Correction Factors

To model at which time and how intensely a certain node/ area was exposed to the different forms of radiation, view factors and step functions were used.

**View Factors**
The View factor is a factor which takes into account the fact that not all of the radiation leaving a certain surface will strike another, due to normal vector misalignment. These view factors are unique per pair of emitting and receiving surfaces and are therefore presented in Table 5.37 for the relevant nodes/areas. Here $F_1$ is given by Equation 5.42 and $F_2$ is given Equation 5.43 [142].

**Table 5.37:** View factors w.r.t the Sun and the Earth for each node exposed to them.

| View Factor | Sun (2) | Earth (1) | V+ (6) | V- (5) | North (3) | South (4) |
|---|---|---|---|---|---|---|
| $F_{E\rightarrow i}$ | 0 | $F_1 \cos\theta \cos\beta$ | $F_2 \cos\theta \cos\beta$ | $F_2 \cos\theta \cos\beta$ | $F_2 \cos\theta \cos\beta$ | $F_2 \cos\theta \cos\beta$ |
| $F_{S\rightarrow i}$ | $\cos\theta \cos\beta$ | $\cos\theta \cos\beta$ | $\sin\theta$ | $\sin\theta$ | $\cos\theta \sin\beta$ | 0 |

$$F_1 = \frac{R_e^2}{(R_e + h)^2} \tag{5.42}$$

$$F_2 = \frac{1}{2\pi}\left(\pi - 2\arcsin\sqrt{1 - F_1} - \sin 2\arcsin\sqrt{1 - F_1}\right) \tag{5.43}$$

### Step Functions

Step functions are employed in two manners, one to model the beginning and ending of the eclipse and the other to indicate when a panel is exposed to solar irradiance and albedo of the Earth. The step function describing the eclipse period of the S/C is given by Equation 5.44 [53]. Where $\tau$ is the orbital period and $f_E$ is the eclipse fraction calculated by Equation 3.3 [53].

$$\hat{s}(t) = \begin{cases} 1 & \frac{\tau}{2}(1 - f_E) < t < \frac{\tau}{2}(1 + f_E) \\ 0 & \text{otherwise} \end{cases} \tag{5.44}$$

The second step function is embedded more directly into the thermal model. Every 90° of the true anomaly, the sun-exposed panels are reassessed, panels that are no longer illuminated are turned off and those that become illuminated are turned on accordingly. Albedo radiation is considered negligible beyond 90° and is thus turned off between 90° and 180° of the true anomaly. This behavior is illustrated in Figure 5.22, which shows at which time in the orbit a certain node is exposed to the Sun.

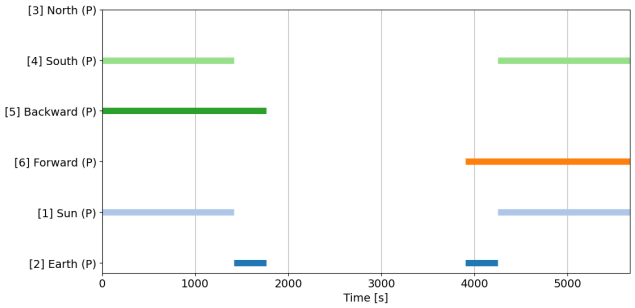


**Figure 5.22:** Graph showing which node/surface is exposed to sunlight over one orbit.

## Thermal Balance

All these forms of radiation are than added up to obtain the change in thermal energy for a certain node in the model using Equation 5.45.

$$\Delta Q = k_i \sum_{i=0}^{n} (T_i - T_j)(A_i)_c + Q_{IR} + Q_{P_\odot} + Q_A + Q_{gen} - A_i \sigma \epsilon_i T^4 \tag{5.45}$$

Here, $Q_{gen}$ is internally generated heat, $A_i$ and $\epsilon_i$ represent the surface areas and corresponding emissivities and $T$ is the current temperature.

This energy variation can then be related to the change in temperature over a certain timestep with Equation 5.46 [53], where $c_p$ is the specific heat capacity of the spacecraft, $m$ its mass and $\Delta t$ the time step. Rearranging yields an equation that expresses the temperature as a function of the change in thermal energy and the previous temperature value, as shown in Equation 5.47. Having established these relations, one can now determine the temperature at a given time step by simply incrementing the time.

$$\Delta Q = c_p m \frac{dT}{dt} \approx c_p m \frac{\Delta T}{\Delta t} \tag{5.46}$$

$$T_{i+1} = T_i + \frac{\Delta t}{c_p m} \Delta Q_i \tag{5.47}$$

## Model Verification

Verification was carried out through unit tests, where the model's calculations were compared to hand calculations. Additionally, extreme scenarios were tested to assess the robustness of the model. The model's accuracy was validated by comparing its results to those presented in 'Preliminary Thermal Analysis of Small Satellites' Structures' [53] and 'Introduction to On-Orbit Thermal' [52]. When tuned to the parameters described in those reports, the model produced similar outcomes. However, to ensure the validity of the results, they should ultimately be compared to the actual temperatures experienced by the S/C during its mission.

### Sensitivity Analysis

The model includes a multitude of parameters, many of which are open variables that must be either assumed or calculated. However, most of these ultimately depend on the assumptions made regarding the material properties and their geometries. Consequently, all parameter values were either sourced from existing literature or, when unavailable, conservatively estimated.

For this analysis, the thermal properties that were varied include thermal conductivity and specific heat. It was found that increasing thermal conductivity consistently improved performance. And on the other hand halving the value, the system still operated within acceptable limits.

Regarding specific heat, only the value for the PCB was adjusted. The specific heat of aluminum is well-documented and relatively consistent across the materials considered, so it was left unchanged. Since the PCBs make up a minor part of the system, any inaccuracy in their specific heat was found to have a negligible impact on the model's overall compliance.

Additionally, mass variations would only enhance the system's heat retention capabilities. Deviations in orbital altitude, due to launcher inaccuracy, would also not push the system beyond its operational boundaries.

## 5.7.4. Model Initialization

With the inner workings of the model clearly defined, the simulation can be ran and the result presented. To reduce the amount of computational time necessary to get to an answer, the most restricting scenario can be identified first. It is assumed that surviving this scenario, means it can survive any other that is thrown at it. Like alluded to in Subsection 5.7.2 , the most restricting configuration was identified to be a 'cold' scenario, in which the incoming heat to the spacecraft is minimal and worst case environmental conditions are expected. This would mean the S/C is in a mode where only the OBC is still functioning in idle mode, while also in an orbit with the longest eclipse period at the aphelion. From Figure 3.4a it is observed that the longest eclipse period will be when $\beta$ equals to zero. A peculiarity of this scenario is that the Albedo factor is the highest possible, as then less heat can get absorbed and later rejected as infrared form the Earth.

The described scenario is then ran for a full day to give the model the opportunity to stabilize and reach steady-state. The temperature is then plotted over time for each node in Figure 5.23 from which each component is then separately assessed if compliant with their respective requirements.

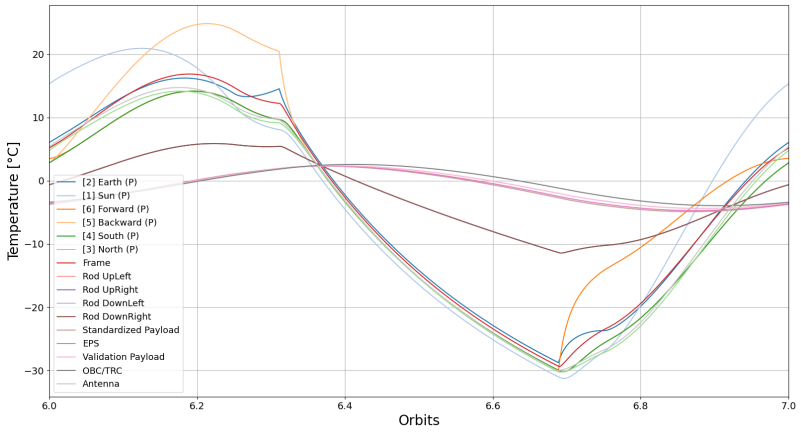


**Figure 5.23:** Temperatures range experienced by the S/C over a full orbit, for the final configuration.

As the surfaces available to conduct thermal energy generated by the subsystems are relatively limited, a significant portion of this energy remains trapped within the spacecraft core. Another observable effect is the time delay between the external subsystems heating up and the internal subsystems subsequently receiving this heat. This delay further indicates that the conductive area between them is small.

This leads to a notable difference in operating temperatures between the internal and external subsystems. The internal subsystems are expected to oscillate between $-5.4\,°C$ to $3.0\,°C$, whereas the external subsystems can experience a broader range from $-31.25\,°C$ to $24.8\,°C$. The structural frame is an exception to all, with a range of $-11.65\,°C$ to $6.20\,°C$.

Special attention must now be given to the antenna to ensure it meets the specified thermal requirements. As part of the external subsystem, it is expected to reach a minimum temperature of −31.25 °C. However, this value must be adjusted by applying a design margin to account for uncertainties in the thermal model. According to European Cooperation for Space Standardization (ECSS) guidelines, a margin of ± 8 °C is recommended. This adjustment results in a conservative minimum temperature of −39.25 °C.

Although this value is near the acceptable threshold, it still satisfies the design requirements. Furthermore, since the actual simulated temperature is around −30 °C for the antenna, the effective thermal margin increases to approximately 2 °C.

Table 5.38 presents the final expected temperature ranges for all subsystems, which all comply with their set ranges.

**Table 5.38:** Predicted temperature ranges for worst case scenario.

| Subsystems | Predicted Temperature [°C] | Including Margin [°C] |
|---|---|---|
| EPS, SP,VP, C&DH | −5.4 to 3.0 | −13.4 to 11.0 |
| Structural Rods | −11.7 to 6.2 | −19.7 to 14.2 |
| Antenna | −30 to 14.8 | −38 to 22.8 |
| Solar Panels, Frame | −31.25 to 24.8 | −39.25 to 32.8 |

### 5.7.5. Part selection

After a brief literature review, it was concluded that no dedicated components needed to be selected for the thermal subsystem. Most PCBs commonly used in CubeSat design already include integrated temperature sensors, which can be accessed to obtain temperature readings. This leaves only the structural subsystem to consider. However, since thermocouples can be fragile and introduce unnecessary complexity to the internal layout and given that structural temperature monitoring is not mission critical, a less accurate but simpler approach was chosen. Structural temperatures can be estimated based on the known temperatures of adjacent subsystems and the thermal properties of their connections.

To provide a clear overview of how much of the budget is allocated to the thermal subsystem, Table 5.39 shows the portion dedicated to temperature sensing, but this will not contribute to budgets as they are part of the components selected in other subsystems. The budget accounts for ten sensors in total.

**Table 5.39:** Theoretical budget of the thermal subsystem.

| Component | Amount | Mass [g] | Size [mm] | Cost [€] | Power [mW] | Operational Temperature [°C] |
|---|---|---|---|---|---|---|
| *TMP*100 [143] | 10 | ~0 | 8.12 × 2.9 × 2.8 | 1.2 | 2.5 | −55 to 125 |
| **Total** | **N/A** | **~0** | **N/A** | **12** | **25** | **−55 to 125** |

### 5.7.6. Next Steps

The actions required to prepare the thermal subsystem for its operational responsibilities can vary significantly depending on the outcomes of certain tests. In the best-case scenario, only minimal effort may be needed; however, in other cases, additional steps could be necessary. Since a passive thermal system has been chosen, no specific thermal control components have been selected. As a result, only system-level testing is required.

A thermal vacuum test can be conducted on the fully assembled system, replicating specific environmental conditions. If the test results align with those predicted by the thermal model, the model can be considered validated. In that case, no further action is needed, and the system is deemed ready for launch.

However, if discrepancies arise, the assumptions made in the thermal model must be revisited or the model itself expanded for a more detailed analysis. This refinement may involve accounting for internal heat gradients, improving the estimation of component material properties, including internal radiative heat transfer, and considering other relevant thermal effects.

## 5.8. Conclusion

In this chapter, the detailed design decisions of the subsystem were shown. First, in Section 5.2, the systems to validate the accuracy of the SP were established. These are a conventional CubeSat GNSS receiver, the Celeste GNSS from SpaceManic, and SLR. SLR functions by emitting a laser pulse to the satellite where it is reflected by retroreflectors fitted on the exterior of the S/C. The stations used for SLR are located in Potsdam (Germany), Matera (Italy) and the facilities of the TU Graz in Austria. Then in Section 5.3, it is motivated

that all the subsystems will be able to be fitted in the standardized 1U CubeSat, which has a form factor of 10 mm × 10 mm × 10 mm. The chosen material is either AA6061-T651 or AA6082-T6 which are both variants of aluminum.

Next, the Command and Data Handling subsystem was designed. C&DH is divided into two parts, the first is the OBC and the second the TT&C. After a trade-off, the Nanocom product line was chosen as they are require the least power and weigh the least. For the antenna, an omni-directional UHF antenna was selected as to limit the pointing and power constraint posed on the SP. The pointing constraints posed are handled by the ADCS subsystem. It consists of a passive system using a permanent magnet and hysteresis rods and its design is found in Section 5.5. The permanent magnet creates a control torque with the hysteresis rods functioning as dampeners. It was calculated that the time to reach a stable tumbling rate would be within 5 to 12 days. The attitude determination was subsequently designed, it focused on redundancy and simplicity. It consists of six sun sensors on each side and one gyroscope as to keep attitude determination during eclipse. Additionally, a magnetometer is present on the OBC which can function as a back-up and adds further redundancy.

Moreover, the EPS subsystem was designed in Section 5.6. It was intentionally designed later since it is sized based on the power requirements of the other subsystems. For power generation, six rigid solar panels mounted on the sides of the S/C were chosen as this is a mission critical system extra redundancy is preferred. This option is also less complex than foldable solar panels. The PCDU works on peak power tracking since there is a large difference between its average and peak power. Included in the PCDU is also the battery which has sufficient storage and can supply the S/C for 330 minutes without sunlight. Lastly, the thermal system was designed to regulate the temperature and ensures that the range falls inside all the extrema for nominally operating. After making a multi-node thermal model of the whole satellite in its orbit, it was found that the final configuration was thermally compliant. In the next chapter, the integration of the subsystems will be elaborated on.

# 6. Final Design of the Technology Demonstration Satellite

The technology demonstration satellite is a combination of all the subsystems which were designed in the previous chapter. This chapter aims to outline the interfaces between the subsystems, evaluate the design and quantify the environmental impact of this project. First, an overview is given of the S/C lay-out and its power, mass and data rate budgets. This is followed by a cost breakdown for the project. These will be useful when evaluating the feasibility of the project. After this the Hardware, Software and Data Handling diagrams are shown. This outlines the physical and digital interfaces between all components of the S/C. The communication flow diagram outlines the interface between the S/C and the ground segment. The last diagram is the mode transition diagram. This shows how the S/C should act once its mission has started. Finally, the project is evaluated through three lenses. The risk assessment addresses possible failure points and how to avoid them. The sustainable development strategy assesses the environmental impact of this project and how it can be minimized. The last part evaluates the project by checking its compliance with the stakeholder requirements which the design is based.

## 6.1. Configuration/Layout

As the structure of the technology demonstration satellite is a CubeSat, the configuration design ultimately concerns the stacking order. To reduce the amount of cabeling, the systems which need a connection to the antenna's are placed at the top of the CubeSat frame , as close as possible to the antenna's. The stacking orders is thus as follows going from top to bottom : The OBC and Transceiver combination, the VP, the SP and then finally the EPS. The ADCS system is spread out over the whole spacecraft, with the permanent magnet placed on the adapter plate for the SP and the hysteresis rods in the space between the OBC and the upper solar panel. Finally the space below the subsystem stack is taken up by the retro reflectors and the sun sensor, for which special holes are made into the solar panels. An exploded overview is given in Figure 6.1

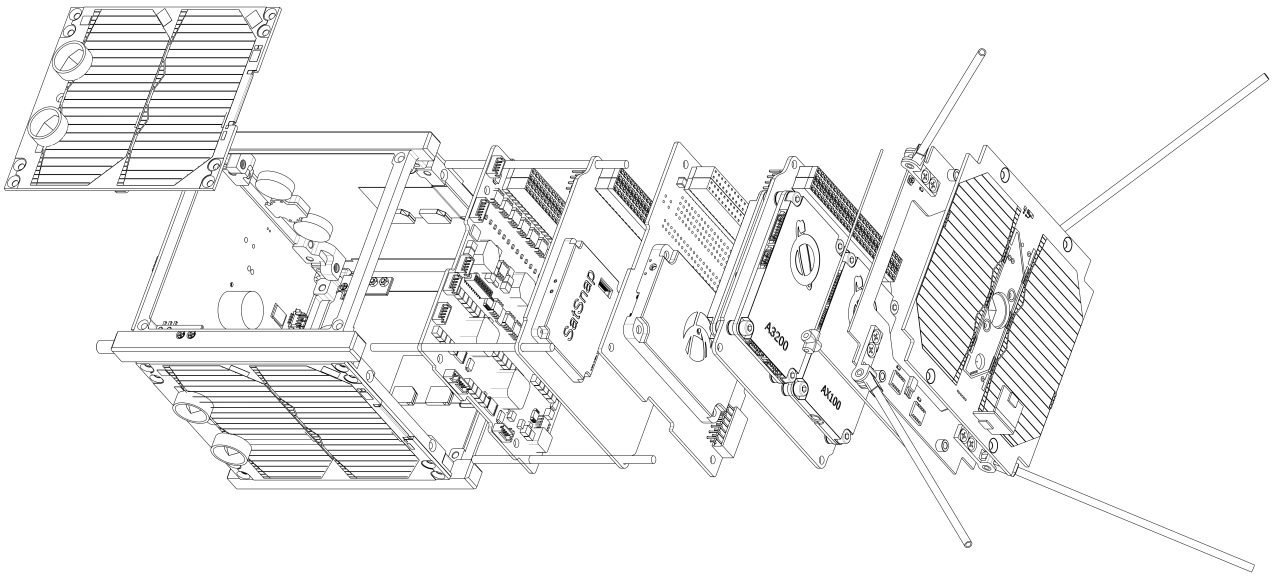


**Figure 6.1:** Final Satellite Stacking Order.

## 6.2. Budgets

This section presents the finalized subsystem budgets and cost breakdown for the technology demonstration mission. Engineering budgets cover power, mass, and data rate allocations across all subsystems. The cost breakdown accounts for COTS components, testing, labor, transport, GS, launch, and other mission costs.

### 6.2.1. Engineering Budgets

Table 6.1 presents a summary of the power, mass, and data rate budgets allocated to each subsystem of the spacecraft. To ensure conservative design, a 10 % system-level margin was applied to the overall budgets in addition to the margins already included in the subsystem-level budgets. With the system-level margins, the final spacecraft engineering budgets are 982 mW for average power, 900 g for mass, and 325.4 bit $s^{-1}$ for data rate.

**Table 6.1:** Subsystem power, mass, and data rate budgets.

| Subsystem | Average Power [mW] | Mass [g] | Data Rate [bps] |
|---|---|---|---|
| SP | < 1 | 33 | 36.7 |
| Validation Payload | 110 | 85 | 36.7 |
| C&DH | 737 | 169 | 102.4 |
| ADCS [(1)] | 59 | 26 | 20.0 |
| Thermal [(2)] | 25 | 0 | 0 |
| Structures | 0 | 126 | 0 |
| EPS | 0 | 379 | 100.0 |
| Margin | 10% | 10% | 10% |
| **Total** | **982** | **900** | **325.4** |

### 6.2.2. Cost Breakdown

The final high-level cost breakdown is provided in Figure 6.2. Firstly, since the team is a student group of the Aerospace Engineering faculty of the TU Delft, certain costs are assumed to be zero. As has been the case in previous TU Delft missions, the testing and assembly are assumed to have no cost due to the connections of the faculty with partners in this sector. The cost of the last acceptance testing done at the launch complex is included in the launch cost. Furthermore, the student team has no hourly wage; thus, the personnel cost has no cost as well. Then the ground segment is also assumed to have no cost since the needed infrastructure is already present on university premises, and the use of ILRS stations is also provided free of charge. Lastly, the satellite is able to perform without a thermal system. Each step in the gradient in Figure 6.2 from dark gray to white indicates a hierarchical relationship; lighter elements are subcategories of the darker parent category.

Now that the individual segments are identified a total cost can be determined. These are shown in Table 6.2. The values of the components were determined in each respective section and already include the margins that are applicable for each component. It should be mentioned that C&DH is split up into Telemetry, Tracking and Command (TT&C) and the OBC.

The satellite's small size allows for personal transport to the launch site. So it is mainly the plane tickets and accommodation costs. The considered launch sites are in New Zealand and The USA. This is estimated by use of `www.Skyscanner.nl` and `www.Booking.com` for two people including carry-on baggage for the 1U CubeSat. The insurance is commonly included in the launch cost. Also, since an Engineering Qualification Model and a Flight model will be created, the component cost is doubled compared to the values given in the budget section of each component. Due to all the components specifically being chosen to be COTS, the availability should not be a problem.

**Table 6.2:** Cost breakdown of each segment and system for the demonstration mission.

| Cost Segment | Price (Y25) [k€] |
|---|---|
| **Travel expenses** | [(3)]8.2 |
| **Launch** | 82.5 |
| **TT&C** | *50.6 |
| **ADCS** | 5.8 |
| **OBC** | *36.4 |
| **Structure** | 3.4 |
| **EPS** | 41.8 |
| **VP** | *21.8 |
| **SP** | 0.4 |
| **Total** | 251.9 |

Values indicated by an asterisk, *, are estimates based on prices of similar products.

[(1)]The power and mass budgets for the magnetometer and gyroscope are not included in the total; the budgets for these components are already accounted for in the OBC's budgets.

[(2)]The power and mass budgets for the thermal subsystem are not included in the total; the budgets for thermal are already accounted for in other subsystems' budgets.

[(3)]New Zealand Travel Cost, BudgetYourTrip, [Online]. DoLA: 13 June, 2025. Available:https://www.budgetyourtrip.com/new-zealand

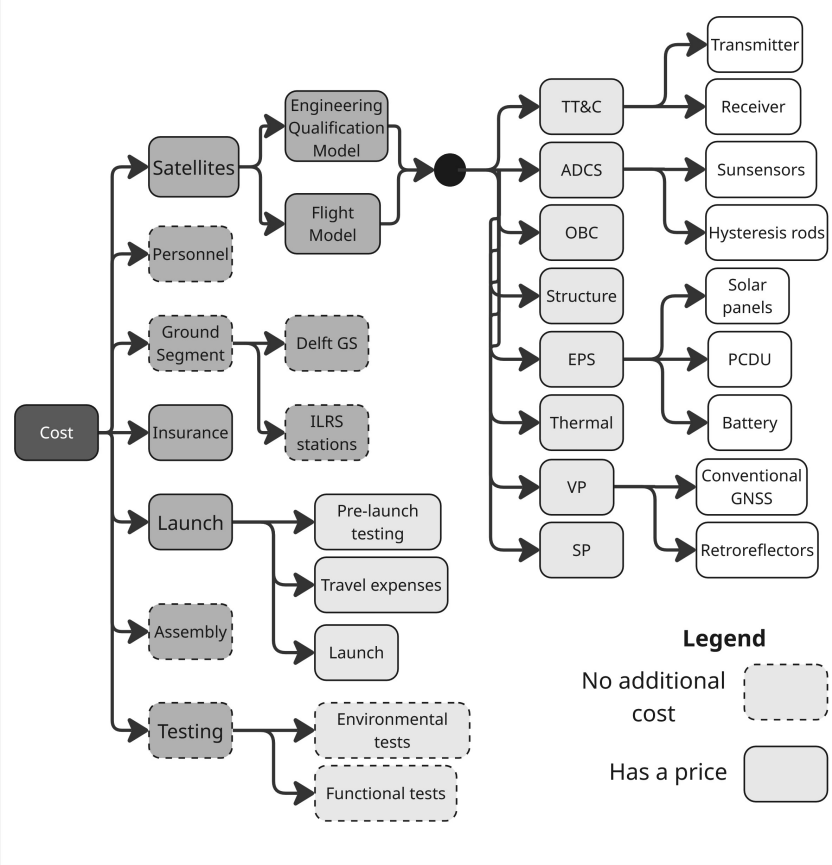


**Figure 6.2:** Cost Breakdown Structure for the technology demonstration mission.

## 6.3. Diagrams

This section accumulates all the main visuals to show physical, electrical and data subsystem inter-dependencies, like the hardware block diagram, the data handling block diagram and the communication flow diagram. Additional diagram showing software inter-dependencies and mode transitions are also presented.

### Hardware Diagram

Figure 6.3 primarily shows the physical connections between the different subsystems of the satellite, in addition to the power (shown in red) and the communication/data bus (shown in blue). Important to note is that the PC/104 connections in black (the pins that run through the side of satellite connection most subsystems with each other) indicate subsystem that are located either directly above or below each other. The CubeSat Kit Bus (CSKB) shows units that are within the rails of the satellite whereas all other structural connections (indicated by the orange lines) are either integrated into other units in the CSKB or attached to the housing of the satellite (i.e. the solar panels) through mounting holes or space epoxy.

### Software Diagram

The software block diagram for S/C is shown in Figure 6.4. The diagram portrays how the hardware interactions between different subsystems can be accomplished from software. The legend categorizes 2 types of blocks: the orange attribute points towards the input or output of a function, and the blue software action is the function being executed within the subsystem. The dashed blocks demonstrate the main subsystem of the S/C, the black outlined block within each subsystem groups the action into a top level for overview. The interaction between each subsystem is denoted by the attribute block at the end of the flow of each system, from event logs as output to system logs for storage and command execution. Based on SMAD table 11-6 [41], the amount of source lines of code for spacecraft control is estimated to be 10000. For ground operation 15000 lines of code and 7500 lines for controlling the sensor, using 50 man-months and 25 man-months.

### Data Handling Block Diagram

In Figure 6.5 the data handling block diagram is shown. The different communication protocols are highlighted by the different colors. The data generation rates are taken from Subsection 5.4.4. As up- and downlink data

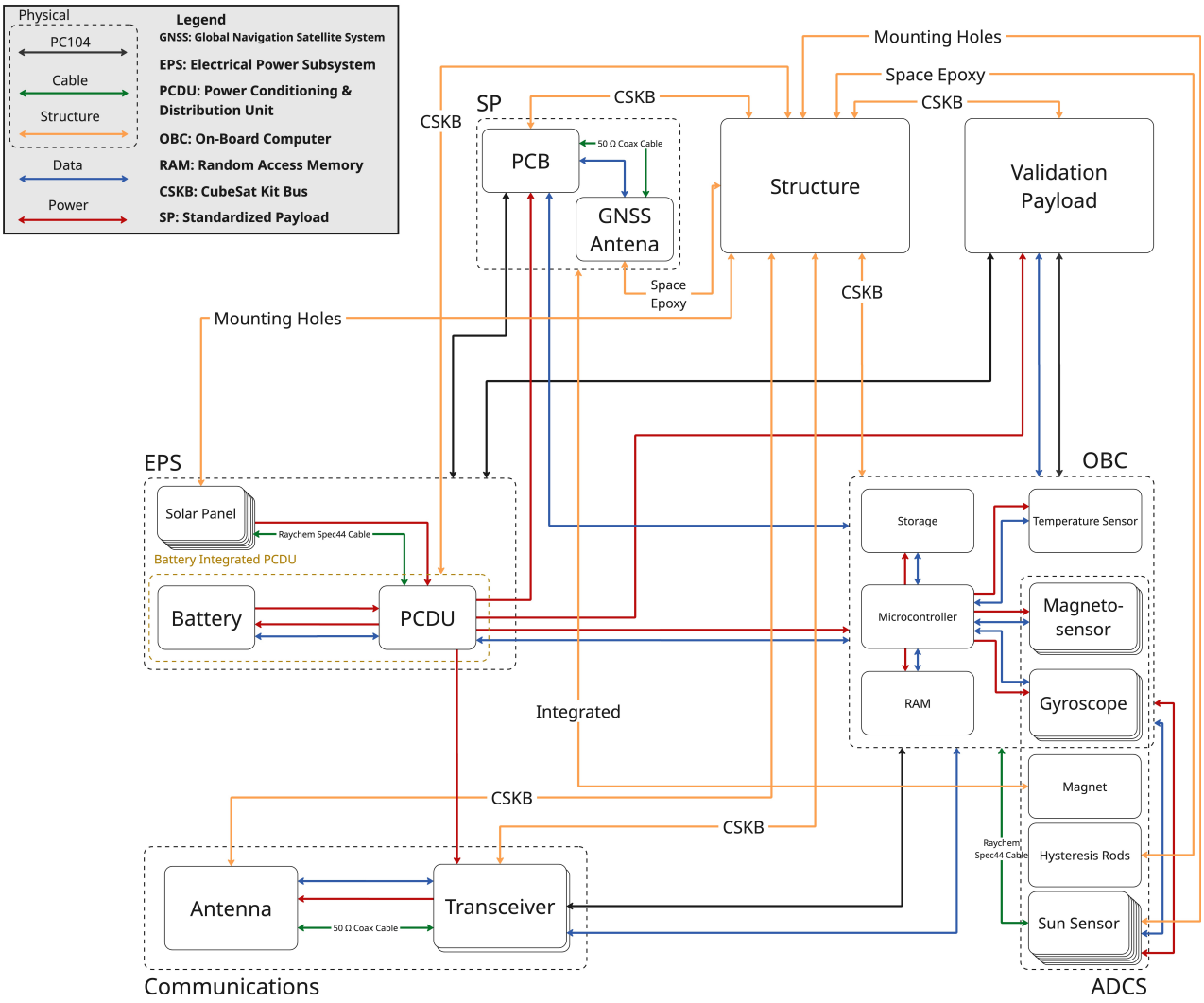


**Figure 6.3:** Hardware block diagram for the finalized spacecraft.

rates, the baud rate is shown. In reality, the data rates between the transceiver and the OBC will be lower, to account for encryption and FEC.

## Communication Flow Diagram

In Figure 6.6 the communication flow diagram is shown. It outlines the way the S/C interacts with its environment. In the case of this mission this is only due to contact with the ground system. The ground system functions are shown in detail; where the S/C functions can be seen more in detail in software diagram in Figure 6.3. The payload validation is shown on the ground segment. The SP will be validated with the data of the VP on board of the spacecraft. The validation itself will happen on the ground however. In a similar way, the density model and orbit determination will happen on the ground only.

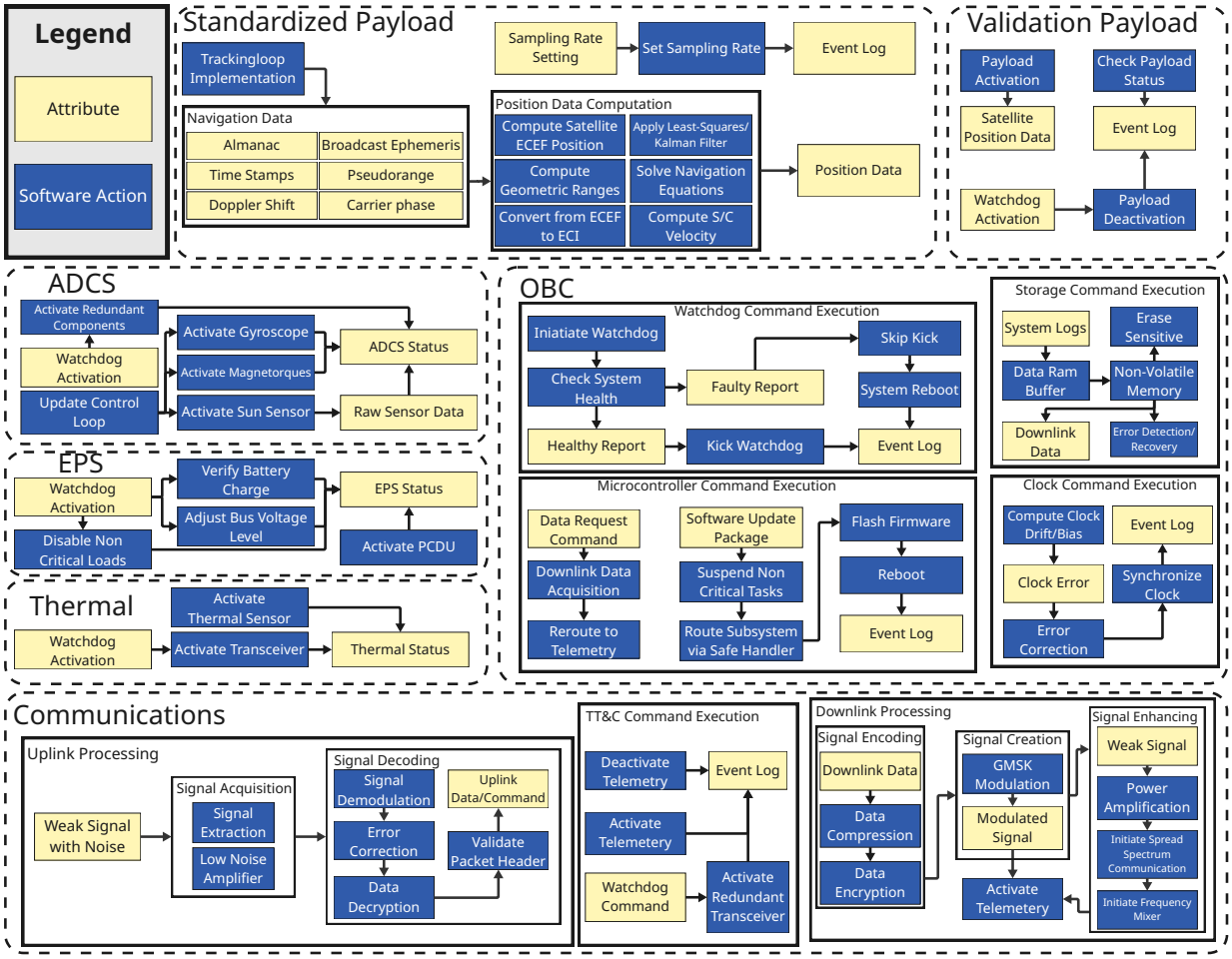


**Figure 6.4:** Software block diagram for the finalized spacecraft.

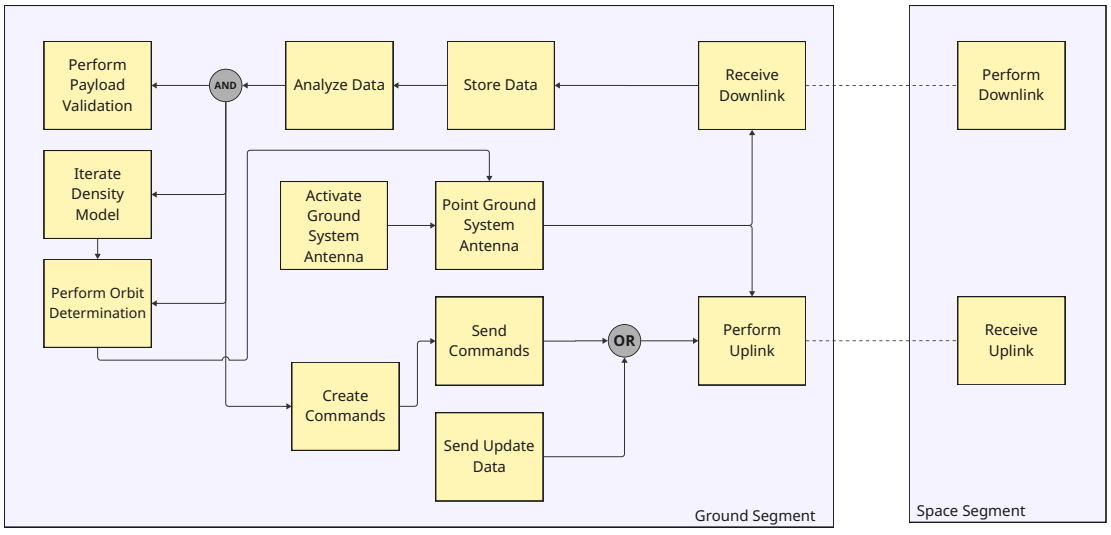


**Figure 6.6:** Communication flow diagram for the mission.

## Mode Transition Diagram

In Figure 6.7 the mode transition diagram is shown. It outlines how different operating modes of the S/C interact with the internal system. Software update and end-of-life mode are activated through the telecommand. The other modes: Idle, safe, and communication mode are activated either through system clock timing or

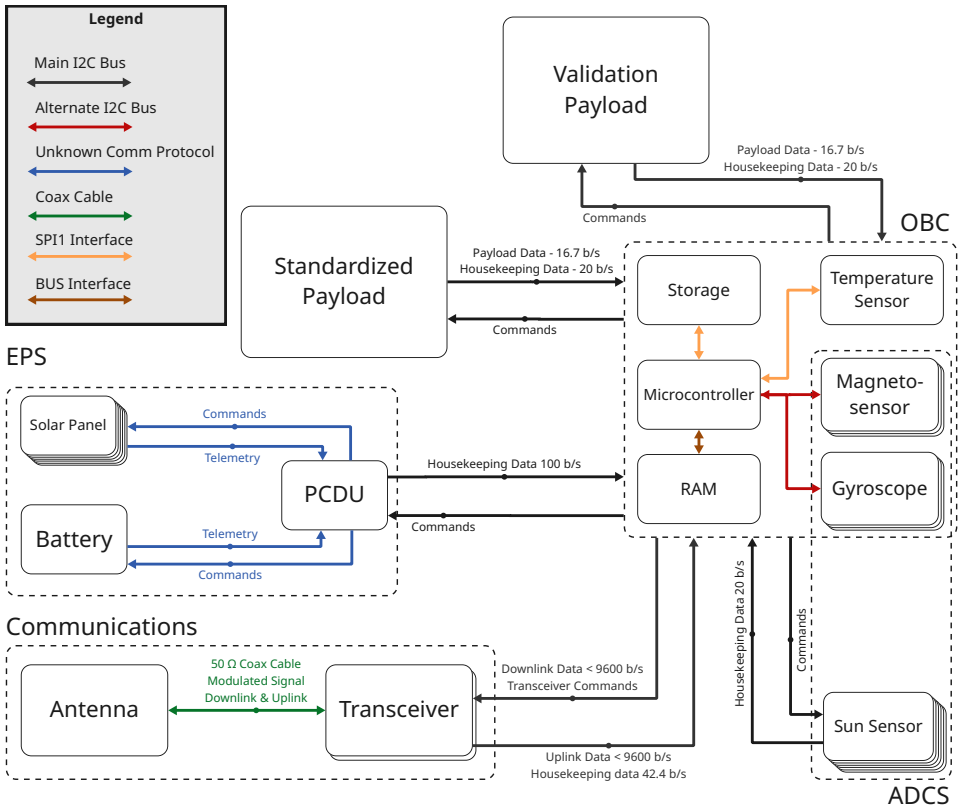


**Figure 6.5:** Data Handling Block diagram for the finalized spacecraft.

error response by the watchdog. Boot up happens automatically when it is deployed by the S/C, after the communication mode is initiated to activate the entire C&DH system. Save mode is only initiated if the system reports a failure.

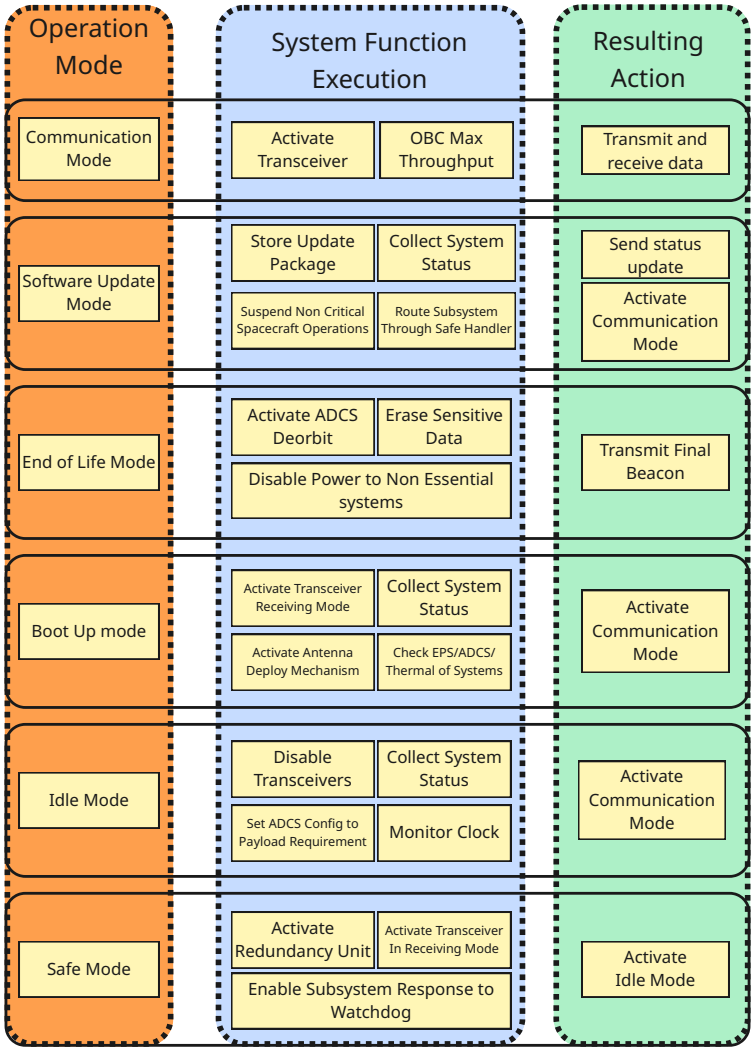


**Figure 6.7:** Mode transition diagram for the spacecraft.

## 6.4. Technical Risk Assessment

In any collaborative engineering project, the early identification and mitigation of technical risks is essential to achieving reliable system performance and mission success. This chapter focuses on the evaluation of technical risks that arose throughout the design, development, and integration phases of the project.

The evaluation of the technical risk assessment is done by identifying the uncertainties in development or production tasks, with the aim to meet project objectives. These risks originate from the launch conditions and the environmental aspects in space, for spacecraft and payload; the design, testing, and verification, and the mission of the project.

### Risk Determination

A structured risk assessment process was employed, beginning with a detailed analysis of potential failure points across subsystems: mechanical, electrical, thermal, and software. The identification process is carried out by all team personnel tracking mission critical parameters and requirements with large variances and potentially serious consequences. These were expanded via Technical Performance Measures standard parameters as seen in Table 6.3. Each risk was assessed in terms of its likelihood of occurrence seen in Table 6.4 and the severity of its impact on system functionality seen in Table 6.5.

### Mitigation

The technical risks are given an identifier to relate them to their associated project phase and these risk identifiers are used in Table 6.6: R-LXX for Launch Risks, R-EVXX for Environmental Risks, R-EXX for

**Table 6.3:** Technical performance measurement parameters.

| Spacecraft |
|---|
| Mass |
| On-board computer capacity |
| Electrical power |
| Structural stiffness |
| Pointing (error) |
| Delta V |
| Propellant mass |
| Communication link |
| Envelope / size |
| (Series) production cost |

**Table 6.4:** Likelihoods.

| Likelihood | Probability |
|---|---|
| Very low | $p < 1\%$ |
| Low | $1\% < p < 30\%$ |
| Moderate | $30\% < p < 50\%$ |
| High | $50\% < p < 70\%$ |
| Very high | $p > 70\%$ |

**Table 6.5:** Consequence levels.

| Consequence level | Definition |
|---|---|
| Negligible | inconvenience or non-operational impact |
| Marginal | degradation of secondary mission or small reduction in technical performance |
| Critical | mission's success is questionable or some reduction in technical performance |
| Catastrophic | mission failure or significant non-achievement of performance |

Engineering Risks, R-DXX for Design Risks, R-TXX for Testing Risks, R-SXX for Software Risks, and R-MXX for Mission Risks. This enabled the creation of a ranked list of critical technical risks as shown in Table 6.6. For each identified risk, targeted mitigation strategies and engineering safeguards were defined, including design redundancies, component qualification procedures, and fault-tolerant architectures. The impact of these mitigations were illustrated using pre-mitigation and post-mitigation risk matrices, clearly showing a measurable reduction in system-level vulnerability.

**Table 6.6:** Pre-mitigation and post-mitigation technical risks table .

| ID | Risk | Pre Prob | Pre Sev | Probability Mitigation | Severity Mitigation | Post Prob | Post Sev |
|---|---|---|---|---|---|---|---|
| R-L01 | Launch Vehicle Explodes | 2 | 3 | Use Flight Proven Launch Vehicles | Replacement Agreement | 1 | 2 |
| R-L02 | Inadequate orbit injection | 2 | 3 | Use Flight Proven Launch Vehicles | - | 1 | 3 |
| R-L03 | Launch load/vibration damage toS/C | 1 | 3 | - | Vibration pads, NRCDS compliance, vibrational testing | 1 | 1 |
| R-L04 | Poor weather conditions | 3 | 4 | Relocation, Weather Monitoring, Back-up Window | Lightning rods, storm-proof building procedures | 2 | 2 |
| R-L05 | Shock Loads During Deployments | 2 | 3 | Use Flight Proven Launch Vehicles | Shock Load Testing | 1 | 1 |
| R-EV01 | Coronal Mass Ejection | 4 | 4 | Space weather monitoring, Orbit and trajectory planning | Hardening Electronics, Operational Response Planning | 2 | 1 |
| R-EV02 | Corrosion Due to Space Environment | 4 | 3 | Use of Coatings, Use of non galvanic pairs,Isolation | Healing Agents | 1 | 2 |
| R-EV03 | Space Exposure to Internal Systems | 2 | 4 | Increased protection against punctures | Extra Protection around critical parts | 1 | 3 |
| R-EV04 | Radiation Exposure | 5 | 3 | Avoid High Radiation Orbits | Radiation Shielding | 3 | 2 |
| R-EV05 | Thermal Cycling | 5 | 4 | Thermal Management System | Verify Operational Range | 3 | 2 |
| R-EV06 | Non Compliance with CP-CDS-R14.1 | 4 | 3 | Audits, Interface Testing and Certification | Use of Verified Deployments Simulation Models | 3 | 1 |
| R-E01 | Thermal Leakage | 2 | 4 | Insulation Process Verification | Better Insulation Material | 1 | 2 |
| R-E02 | Faulty Thermal Regulation | 3 | 4 | Passive Thermal Regulation | Isolate Critical System From Thermal Concentration Spots | 2 | 1 |
| R-E03 | Electrical Leakage | 3 | 4 | Electrical System Testing | Redundancy to Electrical System | 1 | 1 |
| R-E04 | Electrical Short Circuit | 2 | 4 | Conformal Coating, Circuit Simulation | Protective Circuit Breakers | 1 | 3 |
| R-E05 | EMI/EMC Issues On Cross-system | 3 | 4 | EMI Shielding, Cable Routing | Isolation of Sensitive Systems, Shielding | 1 | 3 |
| R-E06 | Faulty Power Transmission to Subsystems | 1 | 4 | Power Bus Testing, Redundancy in Power Lines, Validation Under Load | Backup Power Paths, Fault Isolation Switching | 1 | 2 |
| R-E07 | Battery Failure | 2 | 4 | Battery Qualification Testing, Temperature Regulation | Parallel Battery Strings, Battery Protection System | 1 | 2 |
| R-E08 | Battery Over-Discharge | 2 | 4 | Low-voltage Cut-off Controls, Charge Monitoring Software | Load Shedding Protocol | 1 | 2 |
| R-E09 | Battery Degradation | 4 | 3 | Battery Aging Modeling, Cycle Optimization, | Design for End-of-Life Capacity | 2 | 1 |
| R-E10 | Faulty Stabilization | 3 | 4 | Closed-Loop Control Testing | Safe Mode Fallback | 2 | 2 |
| R-E11 | Part Failure | 3 | 4 | Space Grade Components, Stress Testing | Redundant Components, Fail-Safe System | 2 | 3 |
| R-E12 | Part Degradation | 4 | 4 | Material Aging Analysis, Thermal Cycling Tests | Redundant Components, Fail-Safe System | 2 | 3 |

*Continued on next page.*

| ID | Risk | Pre Prob | Pre Sev | Probability Mitigation | Severity Mitigation | Post Prob | Post Sev |
|---|---|---|---|---|---|---|---|
| R-D01 | Patented Critical System | 1 | 3 | Ensure planned technologies are not patented, patent newly developed technologies so they cannot be stolen | Have backups in mind for patent pending technologies | 1 | 2 |
| R-D02 | Design Noncompliance to Requirements | 1 | 4 | Verify and validate requirement compliance | Verify and validate requirement compliance | 1 | 3 |
| R-D03 | Design Noncompliance to Regulations | 1 | 4 | Verify and validate regulation compliance | Verify and validate regulation compliance | 1 | 3 |
| R-D04 | Undeployed Antenna | 2 | 4 | Verify and validate antenna deployment mechanism | Add redundancy, perhaps a secondary fixed antenna | 1 | 3 |
| R-D05 | Design Noncompliance to Budget | 2 | 3 | Ensure proper budget management | Have margins in the budgets such that worst-case scenarios are accounted for | 1 | 2 |
| R-D06 | Single Points of Failure Component | 2 | 4 | Ensure reliability of components | Have redundancy for single points of failure components | 1 | 3 |
| R-D07 | Incorrect Thermal Coating Application | 2 | 3 | Verify and validate thermal coating reliability | Verify and validate thermal coating reliability | 1 | 2 |
| R-T01 | Faulty Testing Equipment | 4 | 4 | Regular Maintenance | Redundant Testing | 2 | 3 |
| R-T02 | Calibration Errors | 3 | 3 | Traceability of Calibration, Pretest calibrations | - | 1 | 3 |
| R-T03 | In-Adequate Test Environment | 2 | 3 | Validate Test Environment, Monitor Environment | - | 1 | 3 |
| R-T04 | Bad Quality Testing | 4 | 3 | Standardized Test Procedures,Test Engineers, Audits | - | 2 | 3 |
| R-S01 | Runaway Code | 3 | 4 | Verify and validate code | Ensure code can be updated | 2 | 2 |
| R-S02 | Overfull RAM & RoM | 3 | 3 | Verify and validate hardware, simulate usage | Have redundant RAM and RoM | 2 | 1 |
| R-S03 | Data Corruption | 3 | 4 | Verify and validate hardware and connections | Redundant, partitioned storage and End-to-end error-detection and correction | 2 | 3 |
| R-S04 | Unit Conversion Error | 3 | 4 | Verify and validate code | Ensure code can be updated | 2 | 2 |
| R-S05 | Floating Point error | 3 | 3 | Verify and validate code | Ensure code can be updated | 2 | 1 |
| R-S06 | Commanding Error | 3 | 3 | Verify and validate all commands before they are sent | - | 1 | 3 |
| R-S07 | Bit Flip | 2 | 3 | Error corrected memory algorithms | Resetting system via Watchdog service | 1 | 1 |
| R-M01 | Failure to Meet Data Resolution | 3 | 3 | Validate Sensor Capabilities | - | 1 | 3 |
| R-M02 | Failure to Meet Latency Requirements | 3 | 3 | Data Compression, Validate Bandwidth | - | 1 | 3 |
| R-M03 | Inadequate Coverage | 3 | 4 | Ground Station Back-up Locations | Autonomous Operations | 2 | 3 |
| R-M04 | Orbital Trajectory Dispute | 3 | 3 | Legal Agreements | Emergency Repositioning Capabilities | 2 | 1 |
| R-M06 | De-Orbit Failure | 1 | 3 | - | Make Cross-section As Big as Possible to be tracked | 1 | 1 |

## Reliability

Table 6.6 was generated during the Midterm Report and is specifically made to be broad as to include all the subsystems. However, specific mitigation plans and redundant options have been implemented in the subsystems. It must be noted that improved testing results in a higher reliability than redundant systems [144]. Most redundant systems that are used came about due to surplus budget availability or the part was already integrated in another part. Since the mission duration is only 6 months, most systems function nominal without the need for much redundancy as degradation due to radiation or thermal cycling will not have effected the subsystems. Still, the need for redundancy and contingency plans remains present and is always good practice to include if possible. The technology demonstration satellite uses the following:

- **SP:** Included into the design are a voltage regulator and capacitors to ensure that no current surges or short circuits occur.
- **VP:** Two different systems are used to validate the SP, a conventional GNSS and SLR. The SLR has the added benefit that it requires no power thus can not experience power issues.
- **C&DH:** The S/C has two transceivers so that the system is redundant and communication between GS and S/C is assured.

- **ADCS:** The attitude determination has multiple redundant systems. The first is a magnetometer integrated in the OBC. The six sun sensors also offer redundancy, the system can still perform with two sensors. The only issue is that more blind spots exist which increases the chance of the sun sensors not being able to determine it.
- **OBC:** Due to the size constraint, a second OBC could not be implemented. However, the system has watchdog coded in which reboots the system if errors like overflows or infinite recursion loops occur
- **Thermal:** The contingency plan that is put in place is when the S/C's internal temperature drops too much. For this one or two transceivers can be turned on which in turn will increase the temperature back to a nominal operational temperature range.
- **EPS:** The power system has an 28% amount of extra solar array on the exterior. Furthermore, the batterypack is split into two cells of 5 W h whilst the system only needs 2 Wh of capacity.

Furthermore, the software running on the S/C shall have a safe mode programmed in that would only let the radio reception and attitude control active. Usually this mode is also active during launch.

## Risk Map

Technical risks are evaluated in Table 6.4 and the critical risks are placed into a risk map in Figure 6.8 to visualize the overall risk that the project experiences. From the pre-Mitigation risk map, risks that are catastrophic or very high probability are carefully considered. For example, for R-E12, Part Degradation, the probability mitigation strategy is to perform material aging analysis and thermal cycling tests. The risk mitigation strategy, on the other hand, is having redundant components and a fail-safe system. These are viable methods that will allow the operators to reduce the risk from a high probability catastrophic risk to a low probability critical level. Similar methods utilized to mitigate other risks are provided in Table 6.6, and the improvements made by these mitigation measures are shown in Figure 6.8 and Figure 6.9. Ultimately, all risks that have been determined to be on the critical parts of the pre-mitigation risk map have been moved to regions where they are considerably more tolerable.

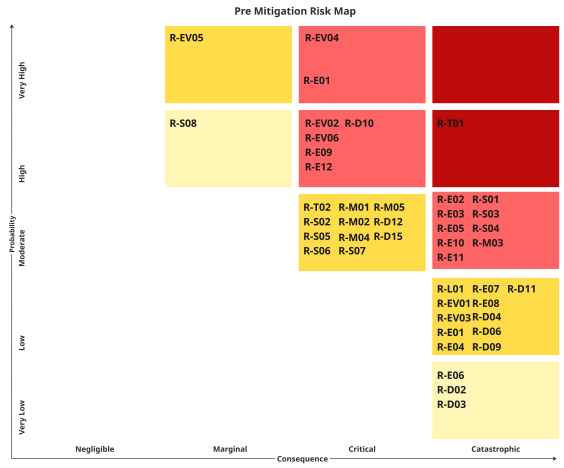


**Figure 6.8:** Risk map pre-mitigation and pre-contingency.

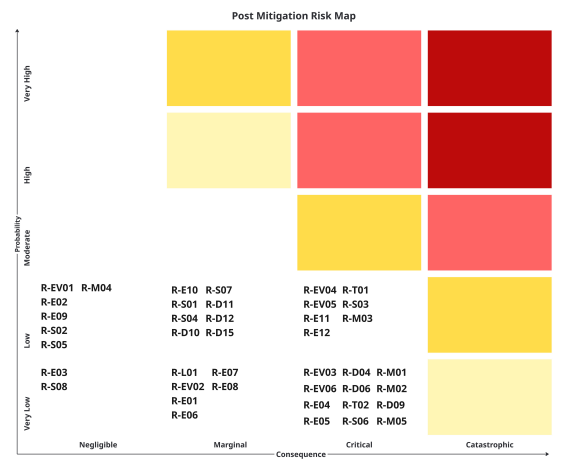


**Figure 6.9:** Risk map post-mitigation and post-contingency.

The risk mitigation measures and the final risk map show that all possible risks have been reduced to a non-critical level. However, this result is unrealistic and optimistic. When the risk mitigation measures are applied after the design is complete, it is likely that certain risks will have a larger probability than expected or still have a higher severity than anticipated. This requires additional iterations on the risk measures as more detail is added to the subsystems and the mission.

## Maintainability

Due to the mission consisting of a S/C, maintenance can only occur in the form of updates that are provided by the GS. The S/C runs periodic system diagnostics that is downlinked as housekeeping data. This data is then used to update the software so that missed errors or system limitations can be resolved. This approach is constraint by the time between contact which can be up to 17 hours.

## 6.5. Sustainable Development Strategy

It is clear that there are concerns regarding space traffic and space debris. This is in fact one of the major markers the team looked for regarding sustainability in the project. However, minimizing space traffic and space debris is only part of the sustainability equation. This section outlines the challenges in designing sustainably for a space mission, the main driving criteria in the design process and quantifying the sustainability impact of the project.

### Contribution to Space Sustainability

An important factor to take into account when evaluating the sustainability of the project is that, by its very nature, the standardized payload would contribute to space sustainability. Having frequent and accurate knowledge of the position of LEO satellites allows to predict their future positions much more precisely, thus being able to determine whether satellites are in danger of colliding with other satellites or known space debris alike. Being able to maneuver satellites to avoid collisions ensures less space debris is created and the LEO environment and its critical infrastructure is protected for the future.

### Driving Parameters

Assessing sustainability for a space mission can be split up into two parts: Impact on the earth environment, and impact on the space environment. For each environment, different parameters are driving for sustainability.

#### Earth Environment

When assessing aircraft sustainability, the operations part needs to be minimized, since this is easily the largest contributor. For space missions there is a large contributor as well: The launch vehicle. This is expected to have the majority impact on the earth environment. Because of this, minimizing mass and volume will be key. Other, less critical sustainability parameters are shown below.

- Pollution of the atmosphere: How much greenhouse gasses are released throughout the manufacturing processes, including the transport of various parts to be integrated. How much damage to the atmosphere does the launch vehicle do?
- Natural resource usage: materials such as lithium and gold are non-renewable and there are legitimate concerns about their future availability.
- Material toxicity: will the burning up of the standardized payload or technology demonstration satellite after end-of-life lead to the release of toxic substances in the earth atmosphere?
- Energy usage: How much energy is used in the manufacturing processes of both the technology demonstration satellite, the standardized payload and their individual parts? Furthermore, is the energy used in manufacturing green or non-renewable?
- Human sustainability: to what degree do the various manufacturers of the off-the-shelf standardized payload parts value and respect their employees. Are the materials they use obtained without the abuse of laborers?

#### Space Environment

For the space environment, the three aspects to minimize are space debris, RF congestion and RF pollution [(1)].

### Industry standard to assess sustainability

Looking at the aerospace industry, it is common to perform a Life Cycle Assessment (LCA) to assess the environmental impact of products and services [145]. The use of a LCA has been standardized since 2006, and has been documented in ISO 14040 and ISO 14044 [146].

For space missions, general theory for performing a Life Cycle Assessment may not always be sufficient. The main challenges with regards to regular Lice Cycle Assessments are defining functional units, low production volumes, long testing cycles, and the impact of long R&D [147]. To address these issues, the European Space Agency (ESA) have developed their own framework to perform LCA's with regards to space applications. This consists of an LCA handbook, a LCA database, and an ecodesign tool [148]. Of these, only the LCA handbook is freely available upon request.

ESA has been working extensively on sustainable space engineering since 2012, when they launched the clean space initiative [(2)]. Within the clean space initiative, ESA have developed multiple methods to quantify

[(1)] Communication with Petra Wijnja, dd. 01-05-2025

[(2)] Clean Space Projects and Core Activities - CM22, ESA, 2025.[Online]. DoLA: April 30, 2025. Available: https://www.esa.int/Space_Safety/Clean_Space_Projects_and_Core_Activities_-_CM22

sustainability for space missions. Moreover, Space Situational Awareness, one of the driving goals of this project, is actively researched within the clean space initiative.

## Preliminary Design Strategy

When performing early design trade-offs, generating an ISO 14040 and ISO 14044 compliant LCA for each design option was found not to be practical, or feasible. For this reason, for the early design options, a qualitative approach was done, based on the driving parameters.

## Detailed Design Strategy

For the detailed design, with subsystem concepts locked in, a Life Cycle Assessment (LCA) is possible. While this is not required by regulations, assessing the sustainability impact of any mission is of ever increasing importance. Because of this, the team would like to perform this as well. The approach taken, is to look at the parts used in the mission, and to attempt to compare them against the TU Delft LCA Database [(1)]. With this database, the earth impact of the spacecraft can be assessed. For the launch vehicle environmental impact, an emission calculation was performed.

The space impact was found hard to assess, unfortunately. The spacecraft is designed to burn up in the atmosphere in the end-of-life, so space debris won't be an issue, but the RF pollution and RF congestion impact are hard to quantify. In the end these values were not quantified. For future missions more research should be done into these aspects of space sustainability to quantify and predict its impact. One positive aspect is that the mission is relatively short, and with that the contribution to the RF congestion and pollution is acting for a short time as well. The standardized payload uses a receiving antenna only, and is not contributing to the RF congestion and pollution.

## Sustainability Results

As mentioned in Section 6.5, a LCA is the chosen approach to assess the projects' sustainability. First, all processes and materials used in the S/C, and its environmental impact are identified in Section 6.5. From there the environmental is assessed from small to large: First the environmental impact of the SP was analyzed in Table 6.5. Then the environmental impact of all subsystems are looked at in Figure 6.5. The environmental impact of the Launch Vehicle (LV) is shown in Figure 6.5, and other environmental contributors are highlighted in Equation 6.5. Finally the missions' environmental impact is summarized in Equation 6.5.

### Environmental impact of subsystems at a high-level

Before looking at the Life Cycle Assessment results, the subsystems can be looked at holistically whether they are sustainable, or if there's improvements to be made. While environmental improvements will be highlighted by the LCA, some aspects regarding sustainability can be clearly identified. On top of that, the LCA currently doesn't take into account the space sustainability, making the high-level observations even more important.

- **SP** - The SP design itself didn't take sustainability into account directly. Rather, the power and mass requirements made it such that it is sustainable: With a low mass, size and power footprint, little additional environmental impact is expected, as most environmental impact will arrive from additional mass on the launcher. The SP will in general be a positive sustainability contribution to any mission; any size, mass and power will be offset by its reduction to space debris.
- **VP** - The VP has multiple systems on board, driving up mass and power requirements. While this could be reduced, having multiple systems also increases reliability. If the VP subsystem were to fail, the SP cannot be verified, requiring a second mission to be launched. With this in mind, the redundant systems are favorable for sustainability.
- **C&DH** - For the C&DH subsystem, a UHF omni-directional communications architecture was selected. Although unfavorable for space sustainability due to RF congestion, it minimizes power usage and mass. Alternatives like higher frequency directional antennas have a higher mass and power draw, and a more complex ADCS is needed as well. The C&DH subsystem prioritizes Earth sustainability over space sustainability. Future missions may reverse this trade-off if RF pollution becomes more critical, or if higher frequency communication options gain a better SWaP-C value.
- **ADCS** - ADCS is not an active system. This is a benefit for sustainability: An active system requires more power, by definition, has a higher complexity, and a higher mass.
- **EPS** - The EPS design favors space sustainability: Rigid solar panels pose minimal risk of detachment and creating space debris when compared to deployable solar panels. The rigid solar panel design is

[(1)] Idemat and Ecoinvent and eco-costs midpoint tables, TU Delft, 2025.[Online]. DoLA: May 21, 2025. Available: https://www.ecocostsvalue.com/data-tools-books/

also more reliable: With 6 panels, a panel failure is unlikely to result in losing the S/C. The drawback to the design is that it requires more solar panels, increasing the mass of the S/C. This means space sustainability is traded for earth sustainability.

- **Structures** - Structures doesn't have sustainability options to assess: It simply needs to house the S/C, and is subject to the Cubesat standard. Because of the Cubesat standard, the structure is locked in, and there are no (sustainability) gains to be made.
- **Thermal** - Similar to the ADCS system, it is a passive system. This is more sustainable than an active system.

### Life Cycle Inventory

In Table 6.7 processes or materials that are used in the S/C are shown. Manufacturing is notably missing. This was omitted for simplicity: Manufacturing was assumed to contribute relatively little to the environmental impact. Using these values, the environmental impact was able to be assessed. The Eco Cost column represents an abstract value to environmental impact, taking carbon footprint, material scarcity, human harm and material toxicity into account. The Carbon Footprint column represents exactly that: how much CO2 is emitted due to using this material or process. Not all values are direct matches to parts in the S/C, but closest match was chosen instead in that case. For the LCA tables, the processes mentioned match the process names in the LCI table.

**Table 6.7:** Life Cycle Inventory of processes and materials used in the LCA for the S/C. All values, including LCI Number and Process name, are taken from the database. Not all values are direct matches to parts in the S/C, but the closest match known in the databases was chosen.

| LCI Database | LCI Number | Process | Eco Cost [€/kg] | Carbon Footprint (CF) [kg/kg] |
|---|---|---|---|---|
| EcoInvent | A.050.01.264 | Electronic component, active, unspecified | 745.19 | 1312.82 |
| EcoInvent | A.050.01.266 | Electronic component, passive, unspecified | 74.68 | 65.84 |
| EcoInvent | A.050.01.278 | Integrated circuit, logic type | 1136.54 | 1667.24 |
| EcoInvent | A.050.01.307 | Resistor, wirewound, through-hole mounting | 9.29 | 32.00 |
| EcoInvent | A.050.01.310 | Transformer, low voltage use | 6.63 | 5.65 |
| EcoInvent | A.050.06.215 | Printed wiring board, through-hole mounted, unspecified | 50.50 | 77.11 |
| EcoInvent | A.050.01.241 | Capacitor, electrolyte type, < 2cm height | 38.86 | 66.29 |
| EcoInvent | A.050.01.274 | Inductor, low value multilayer chip | 14.18 | 43.60 |
| EcoInvent | A.050.01.307 | Resistor, wirewound, through-hole mounting | 9.29 | 32.00 |
| Idemat | A.100.28.108 | AlMgSi0.5 (6060 and 6063) | 2.18 | 8.16 |
| Idemat | A.050.06.401 | PCB of average laptop (including ICs) | 41.14 | 42.26 |
| Idemat | A.080.02.105 | Silica glass | 0.53 | 2.89 |
| Idemat | A.050.06.301 | PCB = Printed Circuit Board (empty) | 10.02 | 7.08 |
| Idemat | A.050.06.301 | CuZn37 (Brass) | 3.10 | 3.01 |
| Idemat | A.100.40.102 | Neodymium magnet (NdFeB) 50 MGOe | 83.37 | 18.30 |
| Idemat | A.100.34.104 | Nickel (primary) | 30.12 | 13.10 |
| Idemat | A.100.24.125 | Molybdenum (EoL-RIR = 9%)e | 62.22 | 15.52 |
| Idemat | A.100.40.102 | GG15 | 0.25 | 1.22 |
| Idemat | A.100.40.102 | Lithium LiFePO4 (145 Wh per kg incl packaging excl electronics) | 2.86 | 8.86 |
| Idemat | A.100.40.102 | PV cell (Mono-Si) per m2 in Rotterdam [(1)] | 18.07 | 60.77 |

### SP LCA Results

In Table 6.8, the environmental impact per part of the SP is identified. Each part is known for the SP, which makes analyzing the environmental impact in detail more feasible than for other subsystems. As shown in Figure 6.10 and Figure 6.11, it is clear the EAR and PCB are the largest contributors to the environmental impact. In future design iterations, a different part selection for the EAR could be investigated to reduce the environmental impact.

[(1)] The database specifically mentions Rotterdam as the process value.

**Table 6.8:** Life Cycle Analysis of the SP. Base values for both the CF and Eco Cost can be found in Table 6.7.

| Part | Amount | Mass | Process | Eco Cost [€] | CF [kg CO2] |
|---|---|---|---|---|---|
| Voltage Regulator | 1 | 12 mg | Electronic component, passive, unspecified | $8.96 \times 10^{-4}$ | $7.90 \times 10^{-4}$ |
| EAR | 1 | 0.8 g | Electronic component, active, unspecified | $5.96 \times 10^{-1}$ | 1.05 |
| SR | 1 | 63 mg | Electronic component, active, unspecified | $4.96 \times 10^{-2}$ | $8.27 \times 10^{-2}$ |
| RF Switch | 1 | 0.75 g | Electronic component, passive, unspecified | $5.60 \times 10^{-2}$ | $4.94 \times 10^{-2}$ |
| MCU | 1 | 49 mg | Integrated circuit, logic type | $5.57 \times 10^{-2}$ | $8.17 \times 10^{-2}$ |
| Antenna Connector | 1 | 0.3 g | Electronic component, passive, unspecified | $2.24 \times 10^{-2}$ | $1.98 \times 10^{-2}$ |
| SP Connector | 1 | 2 g | Electronic component, passive, unspecified | $1.49 \times 10^{-1}$ | $1.32 \times 10^{-1}$ |
| PCB | 1 | 5 g | Printed wiring board, through-hole mounted, unspecified | $2.53 \times 10^{-1}$ | $3.86 \times 10^{-1}$ |
| Capacitor | 24 | 1.5 mg | Capacitor, electrolyte type, < 2cm height | $1.30 \times 10^{-3}$ | $2.39 \times 10^{-3}$ |
| Capacitor | 1 | 7 mg | Capacitor, electrolyte type, < 2cm height | $2.72 \times 10^{-4}$ | $4.64 \times 10^{-4}$ |
| Capacitor | 1 | 20 mg | Capacitor, electrolyte type, < 2cm height | $7.77 \times 10^{-4}$ | $1.33 \times 10^{-3}$ |
| Inductor | 3 | 4 mg | Inductor, low value multilayer chip | $1.70 \times 10^{-4}$ | $5.23 \times 10^{-4}$ |
| Resistor | 1 | 0.7 mg | Resistor, wirewound, through-hole mounting | $6.50 \times 10^{-6}$ | $2.24 \times 10^{-5}$ |
| Housing | 1 | 8 g | AlMgSi0.5 (6060 and 6063) | $1.74 \times 10^{-2}$ | $6.53 \times 10^{-2}$ |
| **Total** | | | | **1.28** | **1.95** |

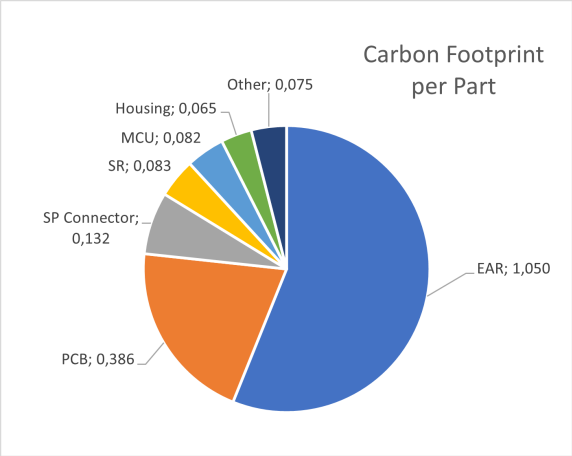


**Figure 6.10:** Carbon Footprint of the SP per part. For each part the KG CO2 value is shown.

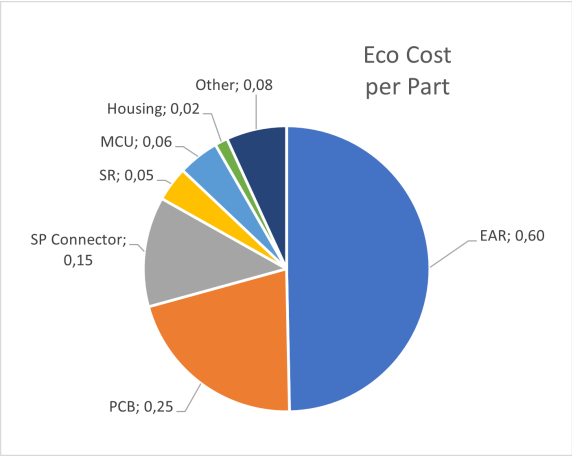


**Figure 6.11:** Eco Cost of the SP per part. For each part the euro eco cost is shown.

### Subsystem LCA Results

For each subsystem, the parts have been identified. With these parts, a Life Cycle Inventory (LCI) value can be assigned and an LCA can be performed. The results of the LCA is shown in Table 6.9. Some things to note are that not everything was found the LCI databases. In that case, a substitute database item was used that was found appropriate. Examples of this are the multiple usages of the "PCB of average laptop (including ICs)", when an electronic part is used, or the "PV cell (Mono-Si) per m2 in Rotterdam", for the solar cells. The rationale behind the change in database values, is that the value is probably close, and with a close value, an environmental analysis was still possible.

The results per subsystem are summarized in Figure 6.12 and Figure 6.13. Compared to the similar figures in the SP section, a clear difference between the CF and Eco Cost can be seen. The EPS and C&DH subsystem are the largest contributors to the environmental impact. To reduce the EPS environmental impact, a choice could be made to use a directional solar panel system instead of an omnidirectional system, where each side of the cubesat has a solar panel. Reducing the amount of solar panels directly reduces the environmental impact of the EPS subsystem, trading more control requirements in the ADCS subsystem. For the C&DH subsystem, a large contributor to the environmental impact is the second transceiver. Assessing the risk of losing the mission to the environmental impact of a second transceiver hasn't been done, but due to the large environmental impact of the launch, using redundant systems is likely to be the better options regarding sustainability.

The EPS subsystem is notably less contributing to the environmental impact in the Eco Cost graph compared to the Carbon Footprint graph. At the same time, the C&DH subsystem is contributing more to the environmental impact in the Eco Cost graph compared to the Carbon Footprint graph. This may be an error due to the assumptions made. The "PCB of average laptop (including ICs)" has a high resource scarcity penalty, where the

"PV cell (Mono-Si) per m2 in Rotterdam" has a low penalty. In reality, the solar panels are made in part with Gallium, one of the scarcer materials. This illustrates that the LCA is inaccurate at times. However, having a first order estimate of the environmental impact of a design is invaluable in designing for sustainability. Large environmental impacts will be highlighted through the LCA process, even if the intermediate values are slightly off. With this a sustainability can be taken into account in further design iterations.

**Table 6.9:** Life Cycle Analysis of the subsystems. Base values for both the CF and Eco Cost can be found in Table 6.7.

| Subsystem | Part | Amount | Part Unit | Process | Eco Cost [euro] | CF [kg CO2] |
|---|---|---|---|---|---|---|
| **SP** | **Total** | | | | **1.95** | **1.28** |
| **VP** | **Total** | | | | **3.07** | **3.29** |
| | GNSS Receiver | 1 | 74 g | PCB of average laptop (including ICs) | 3.04 | 3.13 |
| | SLR Reflector | 10 | 5.6 g | Silica Glass | $2.97 \times 10^{-2}$ | $1.62 \times 10^{-1}$ |
| **C&DH** | **Total** | | | | **5.32** | **5.29** |
| | OBC | 1 | 30 g | PCB of average laptop (including ICs) | 1.23 | 1.27 |
| | Transceiver | 2 | 30 g | PCB of average laptop (including ICs) | 2.47 | 2.54 |
| | Daughterboard | 1 | 53 g | PCB = Printed Circuit Board (empty) | $5.31 \times 10^{-1}$ | $3.75 \times 10^{-1}$ |
| | Antenna, Rod | 4 | 1 g | CuZn37 (Brass) | $1.24 \times 10^{-2}$ | $1.20 \times 10^{-2}$ |
| | Antenna, PCB | 1 | 26 g | PCB of average laptop (including ICs) | 1.07 | 1.10 |
| **ADCS** | **Total** | | | | **1.02** | **$8.41 \times 10^{-1}$** |
| | Permanent Magnet | 1 | 2.26 g | Neodymium magnet (NdFeB) 50 MGOe | $1.88 \times 10^{-1}$ | $4.14 \times 10^{-2}$ |
| | Hysteresis Rods, Nickel[(1)] | 2 | 1.352 g | Nickel (primary) | $8.14 \times 10^{-2}$ | $3.54 \times 10^{-2}$ |
| | Hysteresis Rods, Molybdenum[(1)] | 2 | 0.085 g | Molybdenum (EoL-RIR = 9%)e | $1.06 \times 10^{-2}$ | $2.64 \times 10^{-3}$ |
| | Hysteresis Rods, Iron[(1)] | 2 | 0.254 g | GG15 | $1.27 \times 10^{-4}$ | $6.20 \times 10^{-4}$ |
| | Sun Sensor | 6 | 3 g | PCB of average laptop (including ICs) | $7.41 \times 10^{-1}$ | $7.61 \times 10^{-1}$ |
| **EPS** | **Total** | | | | **3.02** | **5.99** |
| | PCDU | 1 | 43 g[(2)] | PCB of average laptop (including ICs) | 1.77 | 1.82 |
| | Battery | 1 | 43 g[(2)] | ithium LiFePO4 (145 Wh per kg incl packaging excl electronics) | $1.23 \times 10^{-1}$ | $3.81 \times 10^{-1}$ |
| | Solar Panel | 6 | 0.01 $m^2$ | PV cell (Mono-Si) per m2 in Rotterdam | 1.08 | 3.65 |
| | Harness | 6 | 3 g | AlMgSi0.5 (6060 and 6063) | $3.92 \times 10^{-2}$ | $1.47 \times 10^{-1}$ |
| **Structures** | **Total** | | | | **$2.62 \times 10^{-1}$** | $9.79 \times 10^{-1}$ |
| | Skeleton | 1 | 120 g | AlMgSi0.5 (6060 and 6063) | $2.62 \times 10^{-1}$ | $9.79 \times 10^{-1}$ |
| Thermal | Total | | | | 0 | 0 |
| **Total** | | | | **$1.46 \times 10^{1}$** | $1.77 \times 10^{1}$ | |

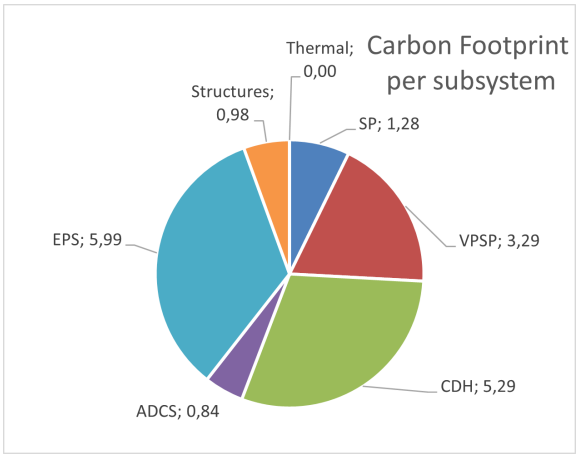


**Figure 6.12:** Carbon Footprint of the subsystems. For each subsystem the KG CO2 value is shown.

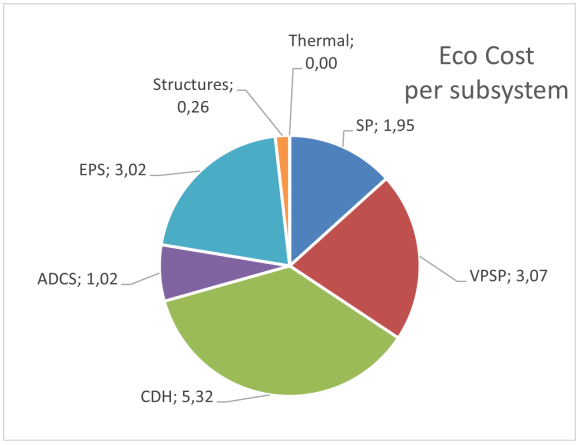


**Figure 6.13:** Eco Cost of the subsystems. For each subsystem the euro eco cost is shown.

[(1)]For the hysteresis rods, the alloy "HyMu" of 80% nickel, 15% iron and 5% molybdenum is used
[(2)]PCDU data sheet doesn't show battery data, it is assumed half of that amounts to the PCDU itself, and the other half to the battery

**Environmental Impact Analysis of the launch vehicle**
The original approach to assess the launcher environmental impact, was to use the Launch Emission Assessment Tool (LEAT) emission calculator [(1)]. This was unfortunately found not to be possible. To accurately use the LEAT emission calculator, the thruster specifications need to be entered, which are unknown. Falcon 9 information is available, but this will not result in an accurate prediction of the emissions.

A different approach was used instead, by estimating the amount of propellant used, and estimate the total carbon emission from that. From the launcher information, it is known that the lift-off mass is $1.3 \times 10^4$ kg. Kerosene burns with oxidizer ratio of 2.56 [(3)], and a CO2 emission per kilo of kerosene is 3.15 [149]. If assumed the propellent mass is $1 \times 10^4$ kg, the CO2 emissions for the entire launch can be calculated with Equation 6.1, where $R_{ox}$ is the oxidizer ratio, $E_{CO2}$ is the CO2 emissions per kilo kerosine and $m_{pr}$ is the propellent mass. An emission value for the launch can be found of $8.85 \times 10^3$ kg CO2.

$$E_L = \frac{1}{1 + R_{ox}} \cdot E_{CO2} \cdot m_{pr} \tag{6.1}$$

The launch is only a single aspect of the environmental impact. Large impacts include propellant production, manufacturing, logistics, assembly and launch facilities. In Impact of Life Cycle Assessment Considerations on Launch Vehicle Design [150], an analysis was made for a launcher similar to this projects': a 2-stage RP-1 expendable launcher. In the analysis, the launch itself attributed 23.9% of the total carbon footprint. Using this same value, a launch carbon footprint of $3.5 \times 10^4$ kg CO2 can be found.

Finally, the launch will not only be for this project's S/C, but for multiple S/C. Assuming the emissions will be proportional to the S/C mass, and a S/C mass of 1 kg, a launcher emission value for this project of $1.85 \times 10^2$ kg CO2 can be found. This emission value per kg CO2 is similar to the result found in Impact of Life Cycle Assessment Considerations on Launch Vehicle Design, which improves the confidence in the result.

**Environment Impact Analysis Other Sources**
It is not clear what falls under the environmental analysis scope of this project and what doesn't. For example, do the test facilities need to be assessed, or does the R&D of the project need to be given an environmental score? For a full environmental impact assessment, these can be assessed. However, for this project, it is assumed that those processes have a small environmental impact. Instead the only other assessment will be done on the travel to the launch site. As mentioned in Subsection 6.2.2, travel to the launch site is planned with 2 persons. This travel can be assessed using the Idemat LCI Database: Idemat LCI C.010.01.106 outlines the environmental impact for an air passenger for intercontinental travel. For every kilometer per passenger, a carbon emission of $5.78 \times 10^{-2}$ kg is emitted. A round trip to new zealand has a flight length of two times $1.81 \times 10^4$ km. In total this results in a carbon emission of $4.19 \times 10^3$ kg CO2.

**Sustainability Results Summarized**
From previous sections it can be concluded that the S/C manufacturing has little impact on sustainability. However, because the launch environmental impact is related to the mass of the spacecraft, a general goal should be to minimize the mass of the S/C. This was already a goal though, and the design should be designed with striving for low mass in mind. The sustainability results are summarized in Figure 6.14. The human transport segment takes up 95% of the missions' carbon footprint. In a following iteration, a choice could be made to either travel by boat, or to outsource the launch to a different party, as also highlighted in the next section.

## Mission improvements to sustainability

Previous sections mostly focused on subsystem or S/C improvements to sustainability. Larger sustainability improvements could be reached by considering to outsource the satellite design and launch to a third party. In the end the goal is to have the SP validated. For that a mission needs to be flown. Nowadays however, there are service providers that will launch 3U cubesats, where multiple payloads are present [(2)]

When a third party cubesat provider is chosen, not only will the launch environmental impact be offset, but also the human transport environmental impact: The payload can be simply sent via mail to the third party cubesat provider, avoiding the intercontinental travel environmental impact. For the DSE this was not possible

[(1)] Launch Emission Assessment Tool (LEAT), Jan-Steffen Fischer, Sebastian Winterhoff and Stefanos Fasoulas, University of Stuttgart, 2025 [Online]. DoLA: 20/05/2025. Available: https://github.com/lcasts/LEAT

[(3)] RP-1, ChemEurope, 2025 [Online]. DoLA: 16 June, 2025. Available: https://www.chemeurope.com/en/encyclopedia/RP-1.html

[(2)] Rideshare on a CubeSat - Smallsat Catalog, 2025.[Online]. Date of last access: June 17th, 2025. Available: https://catalog.orbitaltransports.com/rideshare-on-a-cubesat

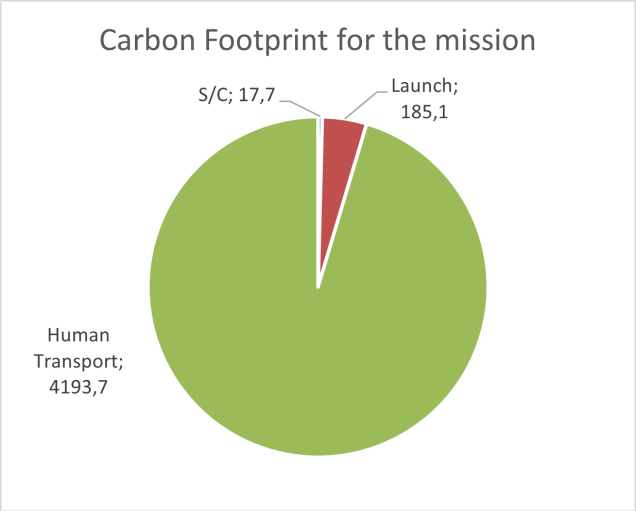


**Figure 6.14:** Carbon Footprint of the entire mission. For each segment, the KG CO2 value is shown.

of course; designing a S/C is part of the learning experience. Even in real missions, integrating payloads into existing missions poses challenges: There may be constraints on data rate, or there may be lack of a validation option. With these risks, and the added benefit of the SP, designing our own S/C may be the better option; the space sustainability contributions are simply worth it.

### Reflection & Conclusion

To take sustainability into account for a space mission was an interesting challenge. First of all, it was not clear at all what sustainability meant in the context of a space mission. Thanks to the consultation with experts such as Petra Wijnja and Irene Fernandez Villegas, a better idea was gained on the different aspects and goals regarding sustainability.

In the early stages of the design a qualitative approach was taken, to attempt to take sustainability into account in early design decisions. In the detailed design, with the parts known for each subsystem, and a launch vehicle locked in, a Life Cycle Assessment could be performed. Following this, it became clear that the launch had a far greater impact than the spacecraft itself. But surprisingly, the travel to the launch site had an even greater impact still.

For future cubesat missions, the advice would be to not weigh earth sustainability too heavily in the trade-off. While this is always important, due to the more efficient launch vehicles, the environmental impact is minimal compared to other contributions. Instead, the focus should lie on space sustainability. One of the challenges in the project was assessing the space sustainability. This can be greatly eased, if access is gained to the ESA LCI Database. The other advice is therefore to request access to this database.

If the design were to happen again with the lessons learned, sustainability would probably have been weighted more heavily in the early trade-offs. Using an X-band transmitter would have been more sustainable than a UHF transmitter, simply due to the non-conflict in the frequency bands, even if it requires higher power and higher mass. In the analysis in the later stages of the design, power and mass turned out to be not a large factor in the earth environmental impact, in part thanks to the efficient launch vehicles.

Finally, a great deal has been learned regarding sustainability in the DSE. Not only was the opportunity given to get expert opinions, first-hand experience was gained by actually creating a Life Cycle Assessment for the project. As sustainability is of ever increasing importance, the lessons learned will be used hopefully in many years to come.

## 6.6. Stakeholder Requirement Compliance Matrix

Having completed the detailed design of the SP and S/C, one can now revisit the stakeholder requirements to ensure all are still upheld. Table 6.10 displays the compliance status, where a cross (×) indicates non-compliance, a checkmark (✓) indicates compliance.

**Table 6.10:** Stakeholder requirements compliance.

| ID | Requirement | Compliance |
|---|---|---|
| | **Royal Netherlands Air Force** | |
| **STM-SH-ML-1** | The SP shall provide accurate data for space threat monitoring. | ✓ |
| **STM-SH-ML-2** | The SP shall provide reliable data transfer. | ✓ |
| **STM-SH-ML-3** | The SP shall contribute to reducing reliance on foreign space navigation services. | ✓ |
| **STM-SH-ML-4** | The SP shall provide accurate data that can improve SSA. | ✓ |
| **STM-SH-ML-5** | The operation of the SP shall require minimal personnel involvement. | ✓ |
| | **Scientific Community** | |
| **STM-SH-SCC-1** | The SP shall provide data to improve atmospheric density models. | ✓ |
| | **Space Agencies** | |
| **STM-SH-SA-1** | The SP shall aid in SSA and collision avoidance. | ✓ |
| **STM-SH-SA-2** | The Technology Demonstration Mission shall comply with applicable international space debris mitigation guidelines. | ✓ |
| | **Regulatory Agencies** | |
| **STM-SH-RA-1** | The S/C shall have an EOL disposal procedure. | ✓ |
| **STM-SH-RA-2** | The SP and S/C shall comply with the ITU-R legal regulations. | ✓ |
| **STM-SH-RA-3** | The SP and S/C shall operate within allocated frequency bands to avoid interference. | ✓ |
| | **Manufacturers** | |
| **STM-SH-MF-1** | Both the SP and the S/C design shall follow standard mechanical interface requirements. | ✓ |
| **STM-SH-MF-2** | Both the SP and the S/C design shall follow standard electrical interface requirements. | ✓ |
| **STM-SH-MF-3** | Both the SP and the S/C shall be designed to meet all applicable safety requirements. | ✓ |
| **STM-SH-MF-4** | The SP shall be mass manufacturable. | ✓ |
| **STM-SH-MF-5** | The S/C and SP shall come with complete documentation for manufacturing. | × |
| | **Launch Brokers** | |
| **STM-SH-LB-1** | The S/C shall fit within the predetermined mass budget. | ✓ |
| **STM-SH-LB-2** | The S/C shall fit within the predetermined volume budget. | ✓ |
| **STM-SH-LB-3** | The S/C shall comply with safety requirements during LEOP. | ✓ |
| | **Launch Vehicle Providers** | |
| **STM-SH-LVP-1** | The S/C shall be compatible with standard launch interfaces. | ✓ |
| **STM-SH-LVP-2** | The S/C shall comply with LEOP safety requirements as defined by the launch vehicle. | ✓ |
| | **Satellite Developers** | |
| **STM-SH-SD-1** | The SP shall be easy to integrate as a plug-and-play module. | ✓ |
| **STM-SH-SD-2** | The SP shall have low power consumption. | ✓ |
| **STM-SH-SD-3** | The SP shall have low mass. | ✓ |
| **STM-SH-SD-4** | The SP shall have a low volume envelope. | ✓ |
| **STM-SH-SD-5** | The SP shall come with complete documentation for operation. | × |
| **STM-SH-SD-6** | The SP shall interface with the other satellite system. | ✓ |
| **STM-SH-SD-7** | The SP shall not interfere with the other satellite operations. | ✓ |
| **STM-SH-SD-8** | The SP shall be safe to handle during assembly, integration, and testing. | ✓ |
| **STM-SH-SD-9** | The SP shall come with complete documentation for integration and testing. | × |
| | **Satellite Operators** | |
| **STM-SH-SO-1** | The S/C shall be able to send telemetry to ground stations. | ✓ |
| **STM-SH-SO-2** | The S/C shall be able to receive telecommands from ground stations. | ✓ |
| | **TU Delft College van Bestuur** | |
| **STM-SH-TUD-1** | The SP and S/C shall be developed at TU Delft. | ✓ |

The justification for the non-compliance of each stakeholder requirement is as follows:

- **STM-SH-MF-5** A general manufacturing plan has been established to outline the steps and facilities necessary to manage the construction and assembly of the SP. However, since the majority of the S/C consists of COTS components, a traditional manufacturing plan is not applicable. Instead, the process is better characterized as an integration plan. Despite this approach, the absence of a detailed, system-wide plan results in this requirement being considered not fully compliant.
- **STM-SH-SD-5** Similarly, while most of the internal components of the SP have been developed and placed, only a general idea of its functionality can be derived at this stage. A comprehensive understanding depends on the development of the controlling software, which has not yet been completed. As a result, the system definition remains incomplete, and this requirement must also be marked as non-compliant.
- **STM-SH-SD-9** In line with the limitations noted above, only a high-level overview of the required testing and integration steps has been provided. However, the lack of sufficient technical detail prevents this plan from satisfying the requirement. Consequently, this item is also deemed non-compliant.

# 7. Next Steps

The next steps chapter provides an overview of the necessary tasks and plans to manufacture, assemble, integrate, and verify all subsystems as well as the complete system. Additionally, detailed explanations of testing and modeling methods are provided in this section. Section 7.1 presents the phases and the project Gantt chart, Section 7.2 explains the manufacturing, assembly, and integration steps, Section 7.3 provides the verification and validation methods used on the system level, and in Section 7.4, the next operational steps are explained upon.

## 7.1. Post DSE plan

The post-DSE plan presents the next steps that will be taken to fully develop, test, and integrate all subsystems, including the SP, after the DSE concludes. Furthermore, it provides additional tasks related to external communications and the technology demonstration mission, including launch preparations and post-launch checks.

ESA and many other space agencies utilize a "phase" structure to classify the current state of the design [(1)]. Table 7.1 provides the structure utilized by ESA. Based on these definitions and the level of detail of the current design concerning industry standards rather than DSE phases, it can be concluded that the payload is close to completing phase C, whereas the majority of the remaining subsystems are at the initial stages of phase C. This is expected as the main focus of this mission is to demonstrate the SP; therefore, more resources were allocated to payload development.

Ultimately, the post-DSE plan presents the steps that will take the design to phase E, which can be classified as the start of the technology demonstration mission in orbit. The timelines are placed as overall time windows with a sufficient buffer. However, as the expected members of the team after the planned expansion is currently unknown, several tasks that are planned to be tackled simultaneously as shown in the Gantt chart in Appendix C, might experience delays due to a lack of available work hours. However, as the launch date is set at 21st of March 2028, there is a large buffer to accommodate such delays.

**Table 7.1:** Satellite Development Phases According to ESA

| Phase | Description |
|---|---|
| Phase 0 | Mission analysis and identification |
| Phase A | Feasibility |
| Phase B | Preliminary Definition |
| Phase C | Detailed Definition |
| Phase D | Qualification and Production |
| Phase E | Utilisation |
| Phase F | Disposal |

## 7.2. Manufacturing, Assembly and Integration

The Manufacturing, Assembly, Integration (MAI) plan is an essential step in the realization of the project. It establishes a road map that can be followed to end up at a flight-ready S/C. Before the MAI can begin, certain regulatory licensing as seen in Section 2.2 must be completed. Additionally, legal and regulatory steps need to be followed when procuring parts and system. Afterwards, flight-specific documentation must be developed and submitted to the appropriate bodies.

[(1)] Building and Testing Spacecraft - ESA, 2025. [Online]. DoLA: June 18, 2025. Available: https://www.esa.int/Science_Exploration/Space_Science/Building_and_testing_spacecraft

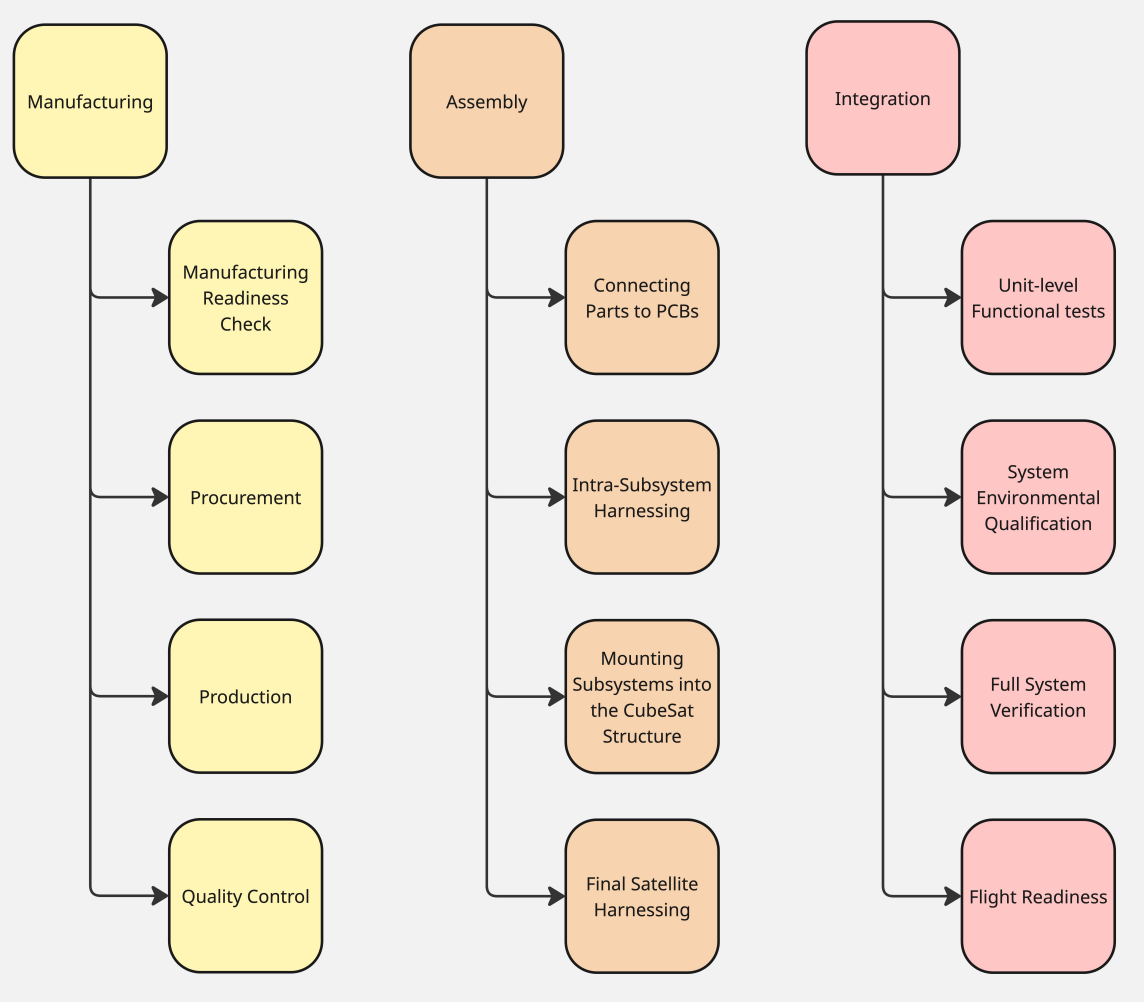


**Figure 7.1:** Manufacturing, assembly and integration plan visual.

The S/C consists of COTS components as to reduce the cost and ease integration, thus manufacturing is the selection and ordering process of each subsystem. Some parts need to be altered in order to accommodate for the specific needs of this mission. For example, the solar panel sides have to be drilled as to accommodate the retro-reflectors.

The first phase of the MAI is that of Manufacturing. Manufacturing consists of laying the ground work for assembly. It is the acquisition of the components and validation of the tools. The following steps encapsulate the manufacturing phase:

1. **Manufacturing Readiness Check:** Establish the design stability as to verify that no big changes or redesigns will occur. Ensure the availability of parts, materials and tools. Validate the manufacturing processes and confirm that quality control measures are in place, in addition to selecting and confirming manufacturing facilities. Lastly, identify and mitigate possible manufacturing risks.
2. **Procurement:** Purchase all the materials and parts necessary for manufacturing through vendors.
3. **Production:** Create the parts and components needed for assembly.
4. **Quality Control:** Perform and verify that the quality control measures were executed correctly and that all parts passed.

Now, that all the components and parts are present at the TU Delft the assembly phase can begin. In this phase all the parts are combined and mounted to create the final complete S/C. For this the following steps need to be taken:

1. **Connecting Parts to PCBs:** Mount the parts on their respective PCBs to ensure PC/104 compliancy, for example.
2. **Intra-subsystem Harnessing:** Create the electrical and communicating connections which cannot run via the PC/104, like the wire between the solar panels and PCDU and the wire between the GNSS antenna

and the SP PCB.

3. **Mounting Subsystems into CubeSat Structure:** Ensure proper integration, alignment and mechanical stability as to survive the launch loads.
4. **Final Satellite Harnessing:** Route and connect all electrical connections of the subsystems for reliable power and signal transmission, i.e. conduct a fit-check for the PC/104 and connect the transceiver and antenna via the 50 Ω coaxial cable.

The whole S/C is assembled thus, the integration stage then can begin. In this stage, system environmental qualification and full system verification occur. These are described in more detail in the next section, Section 7.3. During integration the system as a whole is tested and qualified as to end up at a flight ready S/C via the following steps:

1. **Unit-level Functional Tests:** Perform tests on unit level so that the components all perform their function according to the specified requirements.
2. **System Environmental Qualification:** Described in Section 7.3
3. **Full System Verification:** Described in Section 7.3
4. **Flight Readiness:** Provide all the paperwork summarizing compliance with all the requirements of the regulatory bodies and those of the S/C itself. This includes: Orbital Debris Mitigation Compliance, Transmitter surveys, Materials list, Mass Properties Report, Battery Report, Dimensional Verifications, Eletrical Report, Venting analysis, Testing Procedures, Compliance letter and Safety Package Inputs[151].

Now that the MAI road map has been presented, the integration phase is described in more detail in the next section.

## 7.3. System Verification and Validation

As seen in Section 7.2 under the integration branch system environmental qualification and full system verification are required in the MAI plan. The aforementioned qualification and verification, in addition to the model philosophy will be discussed in this section using the ECSS as guidance and inspiration[152]. Both the environmental qualification and system verification will need test plans which shall abide by the following standard:

1. Describe and sequence all the tests.
2. State the objectives and the scope of the tests.
3. Specify the test facilities.
4. Govern the execution of all tests.

However, the number and type of satellite models need to be determined in order to know which model to choose for which test.

### Model Philosophy

In Table 7.2 one can see that there are multiple models for various use-cases. Due to the fact that the SP is designed in-house, it will require more design iterations. Thus, more models of the SP are needed in comparison to the COTS parts that have already undergone the development and testing process.

**Table 7.2:** Overview of satellite model types, their objectives, representativeness, and applicability [152].

| Model | Objectives | Representativeness | Applicability / Remarks |
|---|---|---|---|
| Mock-Up (MU) | Layout optimization, procedure validation | Geometrical config., interfaces | System/element level. Classified as low or high fidelity. |
| Development Model (DM) | Design feasibility confirmation | Functional, not necessarily full-size or interfaces | All levels. Also called breadboard. |
| Integration Model (IM) | Functional and S/W development | Functionality, with simulators for missing parts | All levels. Between MU and EM. |
| Suitcase | RF and functional simulation | Functional, using flight and commercial parts | Equipment/System level. Used in qualification. |
| Structural Model (SM) | Structural validation | Flight structure | Subsystem level (structure). For qualification. |
| Thermal Model (TM) | Thermal design validation | Thermal dummies, temperature behavior | Subsystem level. Can merge into STM. |
| Structural-Thermal Model (STM) | Combined thermal and structural tests | Structural + thermal reps. | System level. For qualification. |

*Continued on next page.*

| Model | Objectives | Representativeness | Applicability / Remarks |
|---|---|---|---|
| Engineering Model (EM) | Functional demonstration | Functional without hi-rel parts | All levels. Partial qualification. |
| Engineering Qualification Model (EQM) | Qualification of design and interfaces | Full flight design with MIL-grade parts | All levels. For Qualification Testing. |
| Qualification Model (QM) | Design qualification | Flight design + standards | Subsystem/Equipment level. |
| Flight Model (FM) | Flight use | Fully qualified hardware | All levels. Acceptance tested. |
| Protoflight Model (PFM) | Combined qual. + flight use | Flight-standard hardware | All levels. For Protoflight Testing. |
| Flight Spare (FS) | Flight-ready backup | Same as FM | Equipment level. For redundancy. |
| Function-Oriented Models | Qual. for function-specific reqs | Only necessary subsystems included | Qualification Testing for special functions. |
| Training Model | Ops training / handling | Simplified to match baseline ops | All levels. Used in operations prep. |
| Simulators | Concept or ops validation | As needed for functional use | Qualification for ops or software. |
| Other Human-Oriented Models | HFE requirement testing | Human-centered representativeness | Qualification for handling/user interaction. |

For the SP the following models have been chosen:

- Development Model
- Integration Model
- Engineering Qualification Model
- Flight Model.

Multiple Development Models will be needed for testing. These models will have different architectures compared to the final design in order to ease testing and accelerate the iteration of designs. For example, larger connectors with more mating cycles or various and multiple testing pins will be implemented. The Integration Model will have all the right hardware and will mainly be used for software development. The Engineering Qualification Model will be used for all final system testing (including lifetime testing) and environmental testing. Finally, the Flight Model will be identical to the Engineering Qualification Model and will undergo all the Acceptance Testing before being integrated into the launcher.

For the technology demonstration spacecraft the prototype approach has been selected which means the following models have been chosen [152]:

- Engineering Qualification Model
- Flight Model.

This approach was chosen because apart from the SP all other components are COTS, therefore requiring less testing as this was done by the manufacturer. The Engineering Qualification Model will be used for various kinds of testing but Acceptance Testing, this includes Electromagnetic compatibility (EMC), functional, flatsat, lifetime and environmental testing. Moreover, other CubeSat, student-led missions, like EIRSAT1 had an Engineering Qualification Model and a Flight Model [153].

## Testing

According to the ECSS Testing standards, there are 6 general branches of testing:

1. Development Testing
2. Qualification Testing
3. Acceptance Testing
4. Protoflight Testing
5. Pre-launch Testing
6. In-orbit Testing
7. Post-landing Testing.

Only Development, Qualification, Acceptance Testing and Pre-launch are considered for this mission. Pre-launch Testing are tests to ensure the system did not break post-transportation and handling. Protoflight Testing which combines qualification and acceptance on a single unit is not necessary as this mission has an Engineering Qualification Model and a separate Flight Model. In-orbit Testing is done implicitly in the LEOP phase. Post-landing Testing does not apply to this CubeSat as it will burn up in the atmosphere. The following sections detail Development, Qualification and Acceptance Testing. Note that Qualification Testing and Acceptance Testing are almost identical; the only differences are that Qualification Testing is done on the

Engineering Qualification Model and Acceptance Testing is done on the Flight Model. Additionally, Acceptance Testing (especially the environmental testing) is usually less invasive as it is done on the model that goes to space, and one wants to minimize damage and use.

**Development Testing**
According to the ECSS testing standards [152]:

a. "The objective of Development Testing is to support the design feasibility and to assist in the evolution of the design.
b. Development tests are used to validate new design concepts and the application of proven concepts and techniques to a new configuration".

This only applies to the SP as the development tests shall be used to confirm [152]:

1. Performance margins
2. Manufacturability
3. Testability
4. Maintainability
5. Reliability
6. Life expectancy
7. Failure modes
8. Compatibility with safety requirements.

This does not apply to the rest of the satellite as one does not consider manufacturability or the design of failure modes when purchasing the COTS component, for example.

**Qualification Testing**
The qualification tests will be performed on both the Standardized Payload and the Technology Demonstration Satellite. "The purpose of Qualification Testing shall be to demonstrate that the items perform satisfactorily in the intended environments with sufficient margin[152]."

These tests will be done on the Engineering Qualification Models and includes:

- Single-unit Testing
- FlatSat Testing
- Integrated Testing
- Day-in-the-life Tests
- Environmental Testing.

**Single-unit Functional Testing** concerns checking the electrical performance, unit software and firmware validation, communication integrity, autonomous behavior, redundancy checks, and fallback checks. **FlatSat and Integrated Testing** concerns all the tests done with the subsystems laid out on a test bench and connected to each other using an Electrical Ground Support Equipment (EGSE), as opposed to the vertical assembly in a stack. This creates a better testing environment as it makes connecting and troubleshooting a lot easier due to easier access to the various subsystems. One performs the same tests as in single-unit testing to see if it still performs as intended when connected to other subsystems or when it draws power from other sources. Additionally, interface compatibility and inter-subsystem communication is tested as well. Figure 7.2 shows an example of what a FlatSat testbed would look like.

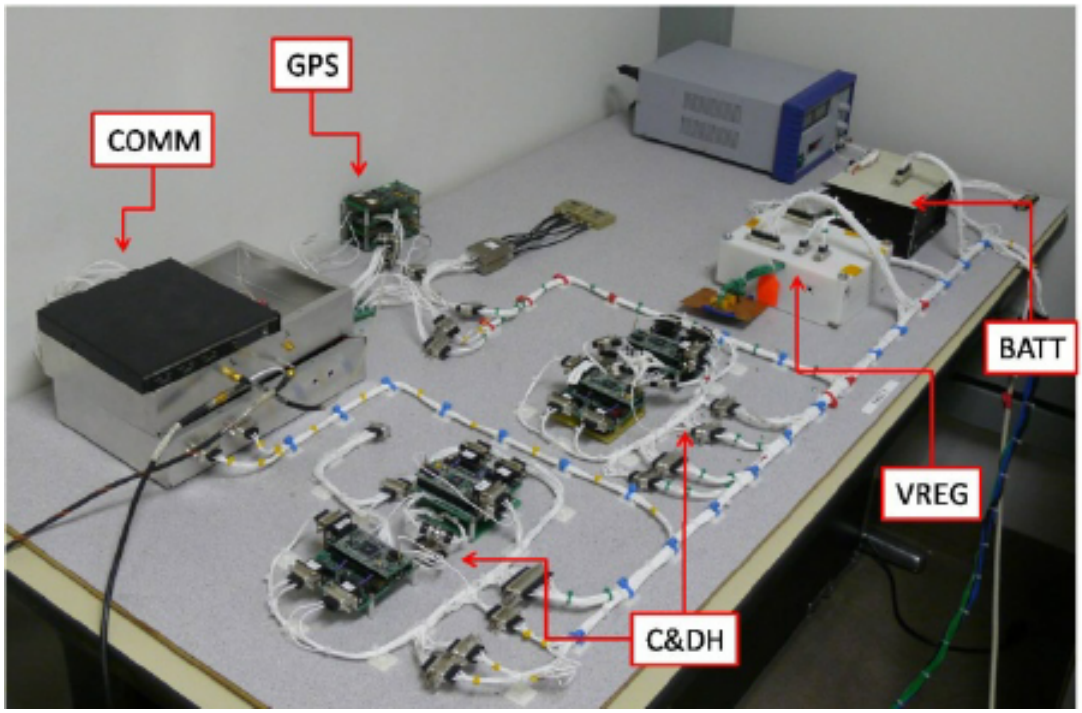


**Figure 7.2:** Example of FlatSat testing [154].

The following combination of subsystems shall be tested for communication and general functionality while being connected to each other:

- OBC + EPS
- OBC + transceiver
- OBC + transceiver + antenna
- OBC + SP
- OBC + VP
- OBC + ADCS
- EPS + transceiver
- EPS + transceiver + antenna
- EPS + SP
- EPS + VP
- EPS + VP + SP
- EPS + ADCS
- EPS + OBC + transceiver + antenna
- EPS + OBC + transceiver + antenna + VP + SP + ADCS.

At first, pairs of subsystem including the OBC are connected to each other ensuring communication compatibility. Then, subsystem pairs with EPS are tested in order to check if the EPS can properly power every subsystem without any issues. Next, various combinations leading up to the final test setup with all subsystems are connected to check for any malfunctions or inconsistencies. Lastly, all systems are put into a stack and all the aforementioned tests are repeated. This is called integrated testing.

**Day-in-the-life Testing**

In Day-in-the-life (DITL) tests, the S/C is simulated to check if all electronics and flight software are working nominally. Once this test is completed, no changes to the code are allowed. If the code is changed, the tests have to be run again to renew the verification [151]. These tests may take up multiple days to ensure the satellite can function continuously in all modes without any issues.

After the tests, reports are drafted that have to, at minimum, contain the following content:

- As-run procedures with all steps time-stamped
- Proof that the separation switches function as required
- Proof that timers function as required
- Simulation of flight-like release of deployables
- Time of deployment
- Time of first transmission.

**Environmental tests**

Environmental tests are performed as part of the verification testing. This proves to the regulatory bodies and launch provider that the S/C functions as required. There are two main places where it is advised to perform these tests. The first is the European Space Research and Technology Center (ESTEC) located in Noordwijk, the Netherlands. It is convenient due to the close proximity to TU Delft and its long-standing partnership. The second location is the CubeSat Support Facility in Transinne, Belgium. It is provided by ESA as well, but as part of its Fly Your Satellite! program[(1)]. This is an educational program for university student teams from an eligible state that are developing CubeSats or PocketQubes with mainly educational purposes. Both host the necessary facilities for the environmental tests that need to be performed. These include: Dynamic Environment Testing and Thermal-Vacuum bakeout (TVAC). These tests are described in the next section, including the minimum report content after the tests.

**Dynamic Environment Testing**

During launch the S/C will experience large vibrational and shock loads. These loads are determined by the choice of launch vehicle. During the dynamic environment test, the same loads are applied to the S/C to verify that it can handle these stresses. A constraint is placed after it passes the test. After dynamic environment testing, it is not allowed to alter or make any physical changes, i.e. remove a panel or tighten bolts, for any reason to the S/C. The following specifications have to be followed as to comply with ECSS standards [155].

For vibration tests, a resonance search test is performed for all axes for frequencies ranging from 5-2000 Hz with a level of 0.5 g with a sweep rate of 2 octaves per minute. This happens during Qualification Testing as well as Acceptance Testing.

For Qualification Testing, a sinusoidal test and a random vibration test are done with the parameters given in Table 7.3. For Acceptance Testing, only a random vibration test is done with the parameters in Table 7.4. The parameters are specifically tailored for smaller satellites, <50 kg [155].

**Table 7.3:** Vibration test parameters for Qualification Testing.

| Test | Duration | Frequency [Hz] | Level |
|---|---|---|---|
| **Sinusoidal** | 2 octaves/min | 5-21 | 11 mm (0-peak) |
| | 2 octaves/min | 21-60 | 20 g (0-peak) |
| | 2 octaves/min | 60-100 | 6 g (0-peak) |
| **Random** | 2.5 min/axis | 20-100 | 3 dB/octave |
| | 2.5 min/axis | 100-300 | $2.4\,g^2\,Hz^{-1}$ |
| | 2.5 min/axis | 300-2000 | −5 dB/octave |

**Table 7.4:** Vibration test parameters for Acceptance Testing.

| Test | Duration | Frequency [Hz] | Level | Remark |
|---|---|---|---|---|
| **Random** | 2 min/axis | 20-80 | 3 dB/octave | |
| | 2 min/axis | 80-350 | $0.04\,g^2\,Hz^{-1}$ | 6.06 $g_{RMS}$ |
| | 2 min/axis | 350-2000 | −3 dB/octave | |

For shock testing, it is best described by the ECSS itself:

> "The shock spectrum in each direction of the three orthogonal axes shall be equivalent to a half sinusoidal pulse of 0,5 ms duration and 200 g (0-peak) amplitude."

After the tests are completed, reports must be drafted that include the following content:

- As-run procedures with all steps time-stamped
- Photos of the test setup, including accelerometer locations
- Plots of the test data showing the test durations and levels
- Proof that the CubeSat survived testing.

[(1)]ESA - About Fly Your Satellite!, ESA. [Online]. DoLA: 13 June, 2025. Available: https://www.esa.int/Education/CubeSats_-_Fly_Your_Satellite/About_Fly_Your_Satellite!

### Thermal-Vacuum

As the satellite will cycle through large temperature differences due to continuously alternating between being exposed to sunlight and the cold empty space, one has to test and ensure that the system can endure these conditions in a vacuum.

Qualification temperatures used for testing are the predicted flight temperatures with a margin ±10 °C. Using the values found in Subsection 5.7.4, the temperatures that will be used for testing are −41.55 °C and 37 °C. The pressure created in the test chamber must be $10 \times 10^{-5}$ hPa or less [155]. Throughout the cycling, small functional tests like communication verification and health checks are made to ensure the system works, in addition to seeing the possible effects of cold/hot cases over time. Figure 7.3 shows an example of a Thermal Vacuum (TVAC) Chamber at ESA.

After the tests are completed, reports must be drafted that include the following content:

- Time-stamped logs to show that proper temperature and vacuum levels were maintained
- Photos of the test setup, including thermocouple locations
- Plots of the test data showing the temperature levels and durations
- Plots of the test data showing the vacuum levels and durations
- Proof that the CubeSat survived testing.

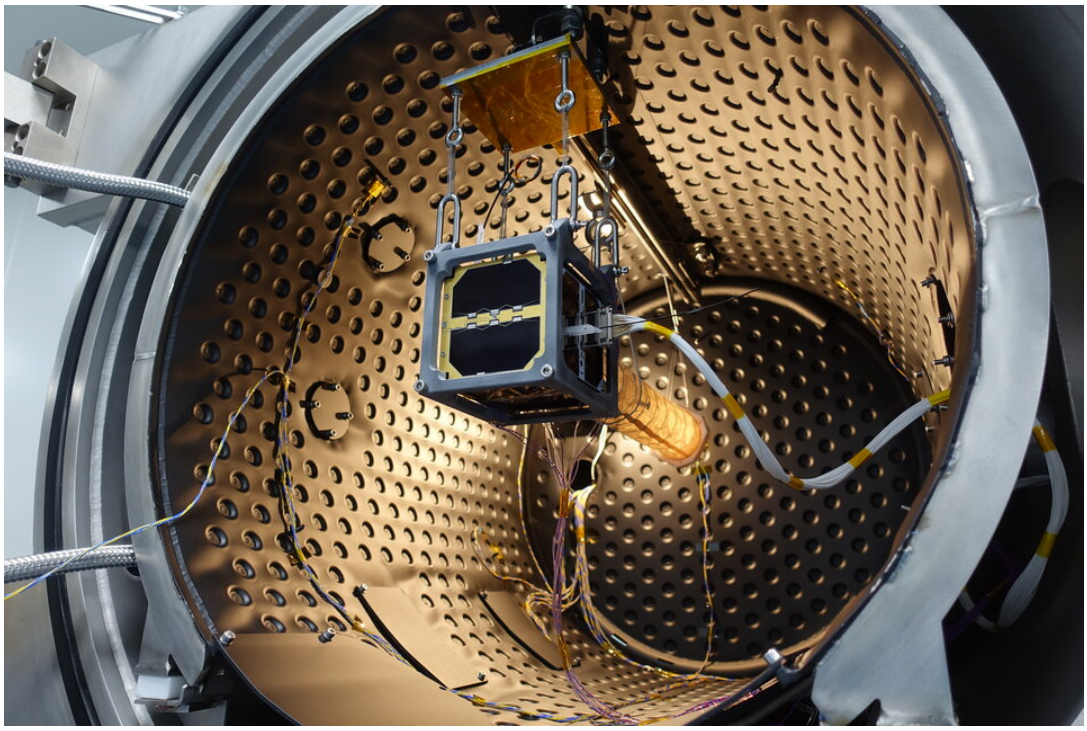

**Figure 7.3:** ESA TVAC chamber.
(1)

### Radiation Testing

One constituent of the harsh space environment is cosmic radiation which can create latch-up and single event upsets within electronic components. Therefore one needs to test if shielding on these components is necessary. If it is necessary one also needs to check if it properly protects the components from radiation. The ECSS-Q-ST-60-15C standard on Radiation Hardness Assurance states that the following tests need to be conducted for certain electrical, electronic, and electromechanical components:

- Total Ionizing Dose
- Total Non-Ionizing Dose
- Single Event Effects.

The Total Ionizing Dose tests check how components perform and react to long exposure to radiation, like gamma rays or high-energy electrons. Total Non-Ionizing Dose tests check how the components perform and react when exposed to large doses of neutrons and protons. Lastly, Single Event Effects tests measure the effect of components being hit by single high-energy particles which may lead to Single Event Upsets, Latch-ups or Burnout.

**Acceptance Testing**
Successful Acceptance Testing proves that the current Flight Model is ready for launch, as opposed to Qualification Testing, which proves that the design works and passes all the requirements. Acceptance Testing shows that there are no production and workmanship errors and is normally less invasive than Qualification Testing in order not to harm the Flight Model.

## 7.4. Logistics and Operations

The first critical step in preparing for the mission is to initiate contact with the selected launch provider. This will bring more clarity to the launch path taken and will also give an initial indication of the amount of ground stations needed to remain in contact with the spacecraft in the crucial LEOP phase. Furthermore these discussion will indicate what kind of acceptance test that will need to be passed by the CubeSat to be allowed on the launcher. With this information in hand, a comprehensive test plan can be formulated. Based on the test plan, the appropriate facilities can be identified and then contacted to gauge their availability and if possible to reserve or rent them.

In parallel, it is important to establish a communication channel with the TU Delft Space Institute to explore the possibility of utilizing their ground station infrastructure for spacecraft operations. This inquiry will serve two purposes: first, to understand the technical and logistical feasibility of using their assets; second, to clarify any data handling protocols or formatting requirements that must be adhered to. These interactions will collectively inform the development of a more detailed mission operations plan. This plan must align the ground station's availability and technical capabilities with the specific communication and control needs of the mission, including downlink bandwidth, uplink command structures, and operational cadence.

Next, it will be necessary to either develop or acquire ground segment software that serves as an interface between mission operators and the spacecraft. This software should support telemetry visualization, command uplink capabilities, fault detection, and possibly mission reconfiguration functionalities. The goal is to ensure intuitive and reliable interaction with the satellite, minimizing operational complexity while maximizing mission flexibility and responsiveness.

Finally, once the launch date has been firmly established and a clearer picture emerges of the timeline leading up to it, a detailed logistical plan can be developed to coordinate the final pre-launch activities. This plan will outline how the critical final weeks will unfold, including the scheduling and deployment of the integration team. Key aspects such as when the team needs to be present at the processing facility, the duration of their stay, and the specific roles they will fulfill during the spacecraft integration and verification phases must be clearly defined.

In addition, practical arrangements, such as accommodation, local transportation, and access to site facilities will need to be organized to ensure the team's effectiveness and well-being on site. Equally important is establishing robust communication channels with the support team remaining in Delft. These channels must ensure real-time coordination, status reporting, and the ability to troubleshoot or approve changes remotely, if required. The logistical plan should also include contingencies for potential delays or technical issues, ensuring that the team is prepared to adapt without compromising mission readiness.

# 8. Conclusions

## 8.1. Summary

This project set out to design a standardized payload for Low-Earth Orbit (LEO) satellites, incorporating a snapshot Global Navigation Satellite System (GNSS) receiver, and to develop a technology demonstration mission for this payload. The final report documents the detailed design of the standardized payload and its dedicated technology demonstration mission, building on the midterm report.

The mission will demonstrate the innovative snapshot GNSS receiver technology and validate its accuracy. The spacecraft (S/C) will be launched to a **500 km** circular orbit at **60°** inclination from Rocket Lab's Launch Complex 1 in Mahia, New Zealand. The S/C will have, on average, five ground station passes per day over TU Delft, enabling the transmission of both housekeeping and payload data. The mission will have a duration of **6 months** and will be followed by a natural deorbit phase of approximately 2 years, ensuring compliance with ESA and ISO 24113 debris mitigation guidelines.

The mission is centered around the ultra-low SWaP-C snapshot GNSS standardized payload. The standardized payload is implemented on a 37 mm × 44 mm six-layer PCB, and offers support for a variety of communication protocols. The standardized payload has an adjustable snapshot frequency. For the technology demonstration mission it will operate at different snapshot frequencies ranging from one snapshot per orbit to one snapshot per minute, with each snapshot lasting approximately 20 ms. In order to compute accurate positions, ephemeris data must be acquired periodically. This data is obtained in 50 s acquisition windows and is collected three times per orbit, remaining valid for up to three hours—roughly two orbital periods. The standardized payload receives the GNSS signals required for snapshot and ephemerides data acquisition through two passive patch antennas. An onboard correlator processes each snapshot to compute a position fix in under 1 s. Internally, the standardized payload features a dual-channel RF front-end, a low-power microcontroller, 4 GB of RAM, and 8 GB of non-volatile flash memory. To validate its positioning accuracy, the spacecraft includes a **SpaceManic CELESTE GNSS module**, drawing **110 mW**, along with ten 12.7 mm fused-silica corner-cube retro-reflectors for centimeter-level satellite laser ranging. The standardized payload's position fixes will be verified on the ground by comparing them against the data provided by these validation systems. The system is designed to achieve a positioning accuracy better than **20 m 3D rms**. The standardized payload averages **0.94 mW** in power consumption, has a total mass of **33 g**, and is built entirely from COTS components, keeping the unit cost around **€250** with appropriate margins.

The S/C bus integrates all supporting subsystems required for the mission. A **1U** CubeSat form factor is utilized, employing an **AA6061-T651** or **AA6082-T6** frame structure. This standardized format enables seamless integration with launchers and simplifies mechanical and electrical interfacing between subsystems. A detailed thermal model was developed to evaluate the S/C's temperature change throughout the orbit, considering worst-case scenarios. The analysis confirmed that all components remain within operational limits without the need for active thermal control. Attitude determination is performed using coarse sun sensors on all six faces, along with a gyroscope and magnetometer integrated in the onboard computer. Attitude control is achieved passively through the use of a permanent magnet and hysteresis rods, which provide alignment and damping relative to the Earth's magnetic field. The power requirement of the S/C is met using body-mounted solar panels. The solar panels are mounted on all six external surfaces to increase the reliability of power generation. The power generated by the solar cells is conditioned and stored for eclipse periods by a **10 W h** battery-integrated Power Conditioning & Distribution Unit (PCDU). The PCDU distributes power to respective subsystems through regulated +3.3 V, +5 V, and +12 V power lines. The Command and Data Handling (C&DH) system enables data exchange with the TU Delft ground station during ground passes, using a UHF transceiver and antenna. It transmits housekeeping and payload data and receives telecommands from the ground. A dedicated On-Board Computer (OBC) on a motherboard manages internal communication, schedules payload operations, and stores data. The average power requirement of the S/C is **982 mW**, its total mass is **900 g**, and the total downlink data rate is **325.4 bit s$^{-1}$**. These values include a 10 % system-level margin on top of the individual subsystem margins applied to the mass and power budgets. The total cost of the mission is estimated at **€251.9 k**.

The principal project risk identified prior to mitigation is faulty testing equipment. This is addressed through regular maintenance and redundant test set-ups to ensure measurement accuracy. For Earth sustainability, pollution of the atmosphere, material toxicity, natural resource use, energy use, and human sustainability

were considered, while RF congestion and pollution are considered for space sustainability. Component and system-level environmental and functional tests are planned post Design Synthesis Exercise (DSE), to verify the mission requirements.

By establishing a technical baseline for the snapshot GNSS standardized payload and its dedicated technology demonstration mission, this report paves the way for future developments in autonomous space traffic management systems.

## 8.2. Recommendations

Several improvements and future steps can enhance the development of the standardized payload and improve the mission's success. Developing a unified system-level model for the sizing of the subsystems would enable quick sizing iterations, and accelerate the design process. Comprehensive thermal vacuum, vibration, and radiation tests, with redundant setups, are recommended to mitigate risks and improve the reliability of the verification procedure. Currently, TU Delft is the selected ground station, due to cost efficiency and accessibility for the described technology demonstration mission. However, future teams are encouraged to explore other ground stations with wider coverage or higher performance equipment. This could relax the link budget requirements, potentially lead to a redesign of C&DH subsystem and reduce the power budget. With a smaller power budget, the same mission can be accommodated by using smaller shape platforms, such as PocketQubes. Conducting the mission with a PocketQube would validating the payload's compatibility with this form factor, and also is expected to lower both development and launch costs. Furthermore, alternative launch sites, launch providers and orbits can be considered to accommodate the mission's timeline and also to reduce the mission's carbon footprint. Future missions could also run the snapshot GNNS receiver at different snapshot frequencies depending on the specific objectives. Lastly, precisely calculating the microcontroller's computation time for position fixing would significantly improve the accuracy of the standardized payload's power budget.

## 8.3. Reflection

Performing the system engineering and project management tasks, such as the work breakdown, planning, requirement analysis, and functional analysis, was not easy in the beginning. For the most part, only theoretical knowledge about these steps was known. The first iterations of each of these were not perfect. Luckily, with the project plan report, the baseline report, the midterm report, and the final report, multiple chances were given to iterate on these. Entering the final stages of the DSE, the team has a good grasp on how to perform the system engineering and project management tasks. The tasks were perceived as tedious at times, but the team recognizes its value: If the project were to be done again, these tools could be used more effectively to deliver a higher quality design in less time.

Moreover, the team could have used the extensive network of TU Delft researchers and professors more. For example, Şevket Uludağ, a researcher at the TU Delft, was only contacted during the detailed design phase for advice on PCB design. In hindsight, multiple meetings with Şevket Uludağ would have been very beneficial with design iterations.

Lastly, while the subsystems were individually parameterized via scripts, this was not done at the system level. The design iteration process could have been accelerated by having a central processing unit that performs all the calculations necessary in case certain parameters change.

Overall, the DSE has been one of the most valuable engineering learning experiences for the team, and the lessons learned will be used in the professional careers of the team for years to come.

## 8.4. Outlook

Following the completion of the DSE, the team intends to continue the development of the snapshot GNSS receiver and conduct a technology demonstration mission to validate its accuracy. In the near future, steps will be taken to apply for a patent as a group and to establish a spin-off company. The ultimate goal is to standardize the snapshot GNSS receiver and to contribute to the advancement of autonomous space traffic management systems.

# Bibliography


[1] Novaspace, "Satellites to be Built and Launched 27th edition," , 2024. Extract of analysis.

[2] Aida, S., Patzelt, T., Leushacke, L., Kirschner, M., and Kiehling, R., "Monitoring and Mitigation of Close Proximities in Low Earth Orbit," , 2009.

[3] Montenbruck, O., and Gill, E., *Satellite Orbits: Models, Methods and Applications*, Springer, Berlin, Heidelberg, 2000.
https://doi.org/10.1007/978-3-642-58351-3.

[4] Arnold, D., Montenbruck, O., Hackel, S., and Sosnica, K., "Satellite laser ranging to low Earth orbiters: orbit and network validation," *J. Geod.*, Vol. 93, No. 11, 2019, pp. 2315–2334.

[5] Gill, E., and Akos, D., "Snapshot GNSS receivers for low-effort, high-gain space situational awareness," *Advances in Space Research*, Vol. 73, No. 1, 2024, pp. 42–52.
https://doi.org/10.1016/j.asr.2023.11.041.

[6] European Union, "REGULATION (EU) 2021/821 OF THE EUROPEAN PARLIAMENT AND OF THE COUNCIL," , 5 2021. Control of dual-use items.

[7] Wassenaar Arrangement Secretariat, "List of Dual-Use Goods and Technologies and Munitions List 2024," , 12 2024. Updated December 2024.

[8] Battegazzore, A., and Phillips, A., "Tips & Tops PM/SE Tasks Baseline Report," , 2024.

[9] Rocket Lab USA, Inc., "Electron Payload User's Guide, Version 7.0 (v6)," Tech. Rep. –, Rocket Lab, 2022.

[10] Johnstone, A., "CubeSat Design Specification," Technical Report Revision 14.1, Cal Poly, 7 2022.

[11] Alvarez, J., Ordóñez, A., Lara, J., Pineda, J. C., Ramírez, A. I., Alvarado, P., Vásquez, M., and Martínez, E., "Design and On-Orbit Performance of the Attitude Determination and Passive Control System for the Quetzal-1 CubeSat," *Journal of Small Satellites*, Vol. 12, No. 2, 2023, pp. 137–152.

[12] Gerhardt, D. T., University of Colorado, B., and Foundation, T. N. S., "Passive magnetic Attitude Control for CubeSat spacecraft," Tech. rep., University of Colorado, Boulder, 2010.

[13] Santoni, F., and Zelli, M., "Passive magnetic attitude stabilization of the UNISAT-4 microsatellite," *Acta Astronautica*, Vol. 65, No. 5, 2009, pp. 792–803.
https://doi.org/10.1016/j.actaastro.2009.03.012.

[14] Space, A. C., "STARBUCK-NANO: Electrical Power Systems for CubeSats," Tech. rep., AAC Clyde Space, Glasgow, UK, 2020. Product Datasheet, Release Date: 28 July 2020.

[15] AAC Clyde Space, "PHOTON Solar Panels Datasheet," , 2020.

[16] Raychem Corporation, "Spec 44 Wire and Cable," , 1996. Printed in UK, Document WC 93330 8/96.

[17] Glenair, Inc., "MIL-DTL-32139 Nanominiature – Single and Dual Row Rectangular Connectors, Series 89 Catalogue," Datasheet, Series 89 Nanominiature Catalog, pp. E-2–E-3, 2024. CAGE 06324, document retrieved from Glenair catalogue.

[18] Kessler, D. J., and Cour-Palais, B. G., "Collision Frequency of Artificial Satellites: The Creation of a Debris Belt," *Journal of geophysical research*, Vol. 83, 1978.

[19] Yule, A., and Reigate, S., "EUROPEAN PATENT SPECIFICATION: Hybrid satellite positioning with prediction," , 2011.

[20] United Nations Office for Outer Space Affairs, "SPACE-TRACK.ORG DEMONSTRATION," , 2021.

[21] United Nations Office for Outer Space Affairs, "International Space Law: United Nations Instruments," , 5 2017. ST/SPACE/61/Rev.2.

[22] Michael P. Gleason, C. A. M., "Anticipating the New European Union Space Law," , 10 2024. Center for Space Policy and Strategy.

[23] NSO, "NSO Advies voor het ruimtevaartbeleid 2023-2025," , 2 2022.

[24] Kim, J. Y., "U.S. Export Controls on GPS/GNSS Equipment," , March 18, 2022.

[25] Deltek Inc, "US Munitions List Category XV," , 2025.

[26] European Commission, "DECISION No 1104/2011/EU OF THE EUROPEAN PARLIAMENT AND OF THE COUNCIL," , 11 2011.

[27] International Telecommunication Union, "Radio Regulations," , Edition of 2020.

[28] UNOOSA, "GUIDELINES FOR THE LONG-TERM SUSTAINABILITY OF OUTER SPACE ACTIVITIES OF THE COMMITTEE ON THE PEACEFUL USES OF OUTER SPACE," , 6 2021. Version June 2021.

[29] Inter-Agency Space Debris Coordination Committee, "IADC Space Debris Mitigation Guidelines," , 3 2022. Revision 2.

[30] ESA Space Debris Mitigation Working Group, "ESA Space Debris Mitigation Requirements," , 2023.

[31] Bureau of Industry and Security, "CATEGORY 5 TELECOMMUNICATIONS AND "INFORMATION SECURITY" Part 1 – TELECOMMUNICATIONS," , 3 2024. Export control list.

[32] New Zealand Government, "Outer Space and High-altitude Activities Act 2017," , 7 2017. Act No.29.

[33] Frandsen, H. O., "Looking for the Rules-of-the-Road of Outer Space: A search for basic traffic rules in treaties, guidelines and standards," *Journal of Space Safety Engineering*, Vol. 9, No. 2, 2022, pp. 231–238. https://doi.org/10.1016/j.jsse.2022.02.002.

[34] ICAO North American, Central American and Caribbean Office, "Seventh Meeting of the North American, Central American and Caribbean Directors of Civil Aviation," , 9 2017. Seventh DCA meeting, 2017.

[35] Gill, E., "Project Guide Design Synthesis Exercise - Autonomous Space Traffic Management," , 4 2025.

[36] The CubeSat Program, Cal Poly SLO, "CubeSat Design Specification," , 2022.

[37] ArianeGroup, "Ariane 6 MLSs User's Manual," , 2024. Edition 0.0.

[38] SpaceX, "Falcon User's Guide," Tech. rep., Space Exploration Technologies Corp. (SpaceX), Hawthorne, California, USA, 9 2021.

[39] GomSpace A/S, "NanoUtil Transport Box Datasheet," , 2024. Protective ESD-safe transport box for 1U–3U nanosatellites.

[40] Wertz, J. R., and Larson, W. J., *Space Mission Analysis and Design*, 3rd ed., Space Technology Library, Microcosm Press and Springer, El Segundo, California, USA, 1999.

[41] Wertz, J. R., Everett, D. F., and Puschell, J. J., *Space Mission Engineering: The New SMAD*, 1st ed., Space Technology Library, Microcosm Press, Hawthorne, California, USA, 2011.

[42] European Cooperation for Space Standardization (ECSS), "Space Engineering – System Engineering General Requirements," Tech. Rep. ECSS-E-ST-10C Rev.1, ECSS, 2009. Noordwijk, The Netherlands.

[43] NASA, "NASA Systems Engineering Handbook," Tech. Rep. NASA/SP-2007-6105 Rev.2, NASA Headquarters, 12 2007.

[44] Barrez, W., Hübner, M., Huson, T., Ilegitim, S., Tapiero, Y., Truyts, R., Uğurlu, E., van Mierlo, C., Xu, R., and Yazıcı, S., "Baseline Report Autonomous Space Traffic Management AE3200 Design Synthesis DSE Group 06," , 2025.

[45] Langer, M., and Bouwmeester, J., "Reliability of CubeSats – Statistical Data, Developers' Beliefs and the Way Forward," *Proceedings of the 30th Annual AIAA/USU Conference on Small Satellites*, 2016.

[46] Barrez, W., Hübner, M., Huson, T., Ilegitim, S., Tapiero, Y., Truyts, R., Uğurlu, E., van Mierlo, C., Xu, R., and Yazıcı, S., "Autonomous Space Traffic Management Midterm Report," Tech. rep., TU Delft, 2025.

[47] Suggs, R. J., "Future Solar Activity Estimates for Use in Prediction of Space Environmental Effects on Spacecraft Orbital Lifetime and Performance," , 2016.

[48] Cakaj, S., Kamo, B., Lala, A., and Rakipi, A., "The Coverage Analysis for Low Earth Orbiting Satellites at Low Elevation," *International Journal of Advanced Computer Science and Applications*, Vol. 5, No. 6, 2014. https://doi.org/10.14569/IJACSA.2014.050602.

[49] Gill, E., "Design status of the Delfi-Next Nanosatellite Project," *International Astronautical Congress*, 2010.

[50] Rocket Lab USA, I., "Payload User's Guide," , 2022.

[51] Brown, C. D., *Elements of Spacecraft Design*, 1st ed., AIAA Education Series, Reston, Virginia, 2002.

[52] Rickman, S. L., "Introduction to On-Orbit Thermal Environments," , 2014.

[53] Versteeg, C., and Cotten, D. L., "Preliminary Thermal Analysis of Small Satellites," , 2018.

[54] McDowell, J. C., "The Low Earth Orbit Satellite Population and Impacts of the SpaceX Starlink Constellation," *The Astrophysical Journal Letters*, 2020.

[55] Nanoracks, "Space Station Cubesat Deployment Services," , 2023.

[56] Beuchert, J., and Rogers, A., "SnapperGPS: Algorithms for Energy-Efficient Low-Cost Location Estimation Using GNSS Signal Snapshots," *SenSys '21: Proceedings of the 19th ACM Conference on Embedded Networked Sensor Syste*, Association for Computing Machinery, New York, NY, USA, 2021, p. 165–177. https://doi.org/10.1145/3485730.3485931.

[57] Antenova Ltd., "M20071 GNSS Receiver Module Datasheet," , 2020. Document Number: M20071-PS-1.02.

[58] u-blox AG, "Modern GNSS/GPS signals: moving from single-band to dual-band," , 2024.

[59] Kuwahara, T., "Introduction to CubeSat Command and Data Handling System," , 2021. KiboCUBE Academy Lecture 10, Tohoku University, Department of Aerospace Engineering.

[60] Speretta, S., Bouwmeester, J., Menicucci, A., Mascio, S. D., and Uludag, M., "Command and Data Handling Systems," *Next Generation CubeSats and SmallSats: Enabling Technologies, Missions, and Markets*, edited by F. Branz, C. Cappelletti, A. J. Ricco, and J. Hines, Elsevier, 2023, pp. 369–399. https://doi.org/10.1016/B978-0-12-824541-5.00012-1.

[61] Bouwmeester, J., "The Architecture of CubeSats and PocketQubes: Towards a Lean and Reliable Implementation of Subsystems and Their Interfaces," Ph.D. thesis, Delft University of Technology, 2021.

[62] STMicroelectronics, "STM32L452xx Ultra-low-power Arm® Cortex®-M4 32-bit MCU+FPU, 100DMIPS, up to 512KB Flash, 160KB SRAM, analog, audio, ext. SMPS," , 2020. Datasheet, October 2020, DS11912 Rev 7.

[63] GmbH, A., "Overview of MIL-STD-1553," , 2019. White Paper, AIM GmbH, 2019.

[64] Semiconductors, N., "UM10204: $I^2C$-bus Specification and User Manual," , 2014. User Manual, Rev. 6, April 2014.

[65] Instruments, T., "Basics of the SPI Communication Protocol," , 2011. Application Report SLYT441, September 2011.

[66] STMicroelectronics, "RM0351: STM32L4x2 Advanced ARM® 32-bit Cortex®-M4 MCUs," , 2018. Reference Manual, Rev. 4, March 2018.

[67] Software, E., "RS-485 Pinout: What is RS-485 and How Does It Work?" , n.d. Virtual Serial Port Organization.

[68] Group, D. C., "RS-232 Kabel Übersicht," , n.d. Technical Manual, Decision Computer Group.

[69] Inc., M. T., "AN713: Implementing RS-232 Communication on PIC Microcontrollers," , 1999. Application Note AN713, Rev. A.

[70] Analog Devices, "LTC3407-3 Dual Synchronous, 1.8V/0.8A and 3.3V/0.8A Step-Down DC/DC Regulator," , 2006.

[71] Analog Devices, "MAX2769C Universal GNSS Receiver Datasheet," , 2016.

[72] Skyworks Solutions, Inc., "SKY13351-378LF SPDT Reflective RF Switch Datasheet," , 2020.

[73] TTM Technologies, Inc., "*PD1722J5050S2HF – Ultra-Low-Profile 0805 Power Divider* (Datasheet, Rev. E)," , 2022.

[74] STMicroelectronics, "STM32L452xC STM32L452xE Advanced ARM Cortex-M4 32-bit MCU Datasheet," , 2021.

[75] 2J Antennas, "2JL67 GNSS Surface Mount Antenna Datasheet," , 2020.

[76] Amphenol RF, "*Ultraminiature Product Series – AMC, AMC4 and AMMC Micro Coaxial Products* (Cutsheet, Rev. 040621)," , 2021.

[77] Hirose Electric Co., Ltd., "DF17 Series 0.5 mm Pitch Board-to-Board Connector Datasheet (Includes DF17(3.0)-50DS-0.5V(57))," Hirose Electric Website (DF17 Series Catalog), 2025. See part DF17(3.0)-50DS-0.5V(57), published May 1, 2025.

[78] SiTime Corporation, "SiT8021 1 to 26 MHz, Ultra-Small µPower Oscillator Datasheet," , 2025. Rev. 2.0, March 2025.

[79] Lim, S., Rogers, R. L., and Ling, H., "Ground Plane Size Reduction in Monopole Antennas for Ground-Wave Transmission," *Proceedings of IEEE International Symposium on Antennas and Propagation*, 2005.

[80] Antenova Ltd., "Raptor GNSS Antenna Datasheet: A10340," , 2021. Covers L1, L2, and L5 bands for GPS, GLONASS, Galileo, and BeiDou.

[81] Hoover, M., Samim, M., Patel, J., Pitre, T., Evans, R., Yeh, T.-H., and Gregory, J. C., "Mission Radiation Modeling for Europa Clipper," Tech. Rep. NASA/TP–20220011775, NASA Jet Propulsion Laboratory, 2022.

[82] Gibelli, L., Ricciardi, M., Scibetta, M., Farina, B., and Apicella, A., "Tungsten polymer composites for radiation shielding applications," *Scientific Reports*, Vol. 11, No. 1, 2021, p. 19734. https://doi.org/10.1038/s41598-021-99739-2.

[83] Gorbunova, O., Salnikova, E., Larionov, A., Popov, A., Zuev, M., Kotov, Y., Blinov, A., and Yudintsev, S., "Radiation Shielding Properties of Polymer Composites for Spacecraft Applications," *Polymers*, Vol. 17, No. 1, 2023, p. 113. https://doi.org/10.3390/polym17010113.

[84] Li, F., Xu, Y., Zhang, X., Wang, Y., Chen, Z., Cao, H., Liu, F., Chen, J., Lu, Y., Liu, W., and Li, L., "Gamma-Ray-Induced Photoelectric Field Exacerbating Irradiation Damage in Ceramic Capacitors," *Journal of the American Ceramic Society*, 2024. https://doi.org/10.1111/jace.19594.

[85] AVX Corporation, "S311P838 Series – COTS-Plus SMT Tantalum Capacitors," , 2020. Datasheet.

[86] European Cooperation for Space Standardization (ECSS), "ECSS-Q-ST-70-12C Rev.1: Design rules for printed circuit boards," , 2025. Published by ECSS, 30 April 2025.

[87] National Instruments, "GPS Receiver Testing," , 2009.

[88] Peixeiro, C., "Small Ground-Plane Size Effects on Microstrip Patch Antennas Revisited," *IEEE AP-S/URSI Int. Symp.*, 2007, pp. 2821–2824. https://doi.org/10.1109/APS.2007.4396122.

[89] Liu, Z., He, Y., and Li, Y., "Beamwidth Enhancement of Microstrip Antennas Using Capacitive Via-Fence Loading," *IEEE Open Journal of Antennas and Propagation*, Vol. 4, 2023, pp. 1–10. https://doi.org/10.1109/OJAP.2023.3240850.

[90] Clemente, M., Lepage, A.-C., and Bégaud, X., "All Dielectric Superstrate to Control the Half-Power BeamWidth of a Dual-Polarized Patch Antenna," *Proc. 8th European Conference on Antennas and Propagation (EuCAP)*, 2014, pp. 1–5.

[91] 2J Antennas, "2JL67 GNSS Surface Mount Antenna – Product Datasheet," , 2023. Includes antenna specifications, electrical parameters, and radiation pattern data. The antenna exhibits a hemispherical radiation pattern, suitable for GNSS reception.

[92] VectorNav Technologies, "Inertial Navigation Primer," , 2025. Educational resource covering inertial navigation systems and RF hardware considerations.

[93] GradConn, "1.13mm Low Loss Coaxial Cable – Product Specification Sheet," , 2023. Specifies compact 1.13 mm outer diameter and low attenuation ( 2.2 dB/m at 2 GHz), making it suitable for spacecraft where weight and signal integrity are critical.

[94] Amphenol RF, "Ultraminiature Coaxial Product Series – Technical Datasheet," , 2023. Details the mechanical and RF characteristics of ultraminiature coaxial connectors, commonly used in compact RF applications such as aerospace systems.

[95] Raposo-Pulido, V., and Peláez, J., "Regular propagators and other techniques in orbit determination problems," Technical report, Universidad Politécnica de Madrid, Open Access Repository, 2019. Available at: `https://oa.upm.es/56455/1/VIRGINIA_RAPOSO_PULIDO.pdf`.

[96] "Digital Signal Processing for STM32 Microcontrollers Using CMSIS," Application note an4841, revision 2, STMicroelectronics, February 2018. Accessed 24 June 2025.

[97] Lorenser, T., "The DSP Capabilities of ARM Cortex®-M4 and Cortex-M7 Processors: DSP Feature Set and Benchmarks," White paper, Arm Limited, November 2016. Accessed 24 June 2025.

[98] GOMspace, "NanoSense GPS Kits," , 2025.

[99] SkyFoxLabs, "Space-Friendly CubeSat GPS Receiver/Next Generation with DROP (Dead Reckoning Orbital propagator) piNAV-NG Product Datasheet," , 2024.

[100] SpaceManic, "Celeste The GNSS receiver," , 2022. Consumer info sheet.

[101] Accord, "ACC-GPS-NANO-NR," , 2022. Consumer info sheet.

[102] Technologies, H., "GNSS200 Datasheet," , 2019.

[103] Giacomo, S., "Design and Optimization of a Retroreflector Array for Satellite Laser Ranging," Ph.D. thesis, TU Delft, 2024.

[104] Howard, D., "Reduction of the Minimum Elevation Angle for NASA Satellite Laser Ranging Tracking Operations," Tech. rep., Honeywell Technology Solutions Incorporated, 2001.

[105] Mesalles-Ripoll, P., Rositani, R., and Matthew, D., "Low-Earth Orbit Prediction Accuracy Review of Modern Empirical Atmospheric Models and Space Weather Data Sources," , 2023.

[106] Optics, E., "12.7mm Aluminum Coated, Fused Silica Corner Cube," , 2025.

[107] European Space Agency, "Margin Philosophy for Science Assessment Studies," Tech. Rep. SRE-PA/2011.097, ESA/ESTEC, Noordwijk, The Netherlands, 2012. Issue 1, Revision 3, 15 June 2012.

[108] Weston, S. V., Burkhard, C. D., Stupl, J. M., Ticknor, R. L., Yost, B. D., Austin, R. A., Galchenko, P., Newman, L. K., and Soto, L. S., "State-of-the-Art Small Spacecraft Technology report," Tech. rep., NASA, 2024.

[109] Okuyama, K.-i., Yoshikawa, K., and Oue, C., "A Simple Method for Identifying the Natural Frequency of a Micro Satellite with a Primary Structure Made of Aluminum Alloy," *Aerospace*, Vol. 11, No. 6, 2024. `https://doi.org/10.3390/aerospace11060436`.

[110] GomSpace, "NanoCom ANT430," , 2020. Communication System Antenna.

[111] GomSpace, "NanoCom AX100," , 2019. Communication System.

[112] GomSpace, "NanoMind A3200," , 2021. Command and Data Handling Subsystem.

[113] GomSpace, "NanoDock DMC-3," , 2021. Product page.

[114] Consultative Committee for Space Data Systems (CCSDS), "Space Data Link Security Protocol," , 2022. Recommendation for Space Data System Standards.

[115] Consultative Committee for Space Data Systems (CCSDS), "Robust Compression of Fixed-Length Housekeeping Data," , 2023. Recommended standard for telemetry compression with resiliency features.

[116] Consultative Committee for Space Data Systems (CCSDS), "TM Synchronization and Channel Coding," , 2023. CCSDS Recommended Standard for Telemetry Link Layer Coding.

[117] GomSpace, *AX100 Manual*, 2020.

[118] Trembly, J. P., "Why Make Spacecraft Operations Harder Than They Already Are?" , 2018. https://doi.org/10.2514/6.2018-2613, session: CAN - Communications Architectures and Spectrum.

[119] KERA, "NanoMind A3200 On-Board Computer," Tech. Rep. 1006901-117, GomSpace, 2019. Datasheet.

[120] GomSpace A/S, *P31u Manual*, 2023. Manual.

[121] ISIS, "ISIS-Ground-Stations-Brochure," , 2016.

[122] Gill, E., D'Amico, S., and Montenbruck, O., "Autonomous formation flying for the PRISMA mission," *AIAA Journal of Spacecraft and Rockets*, Vol. 44, 2007. https://doi.org/10.2514/1.23015.

[123] Fortescue, P., Swinderd, G., and Stark, J., *Spacecraft Systems Engineering*, Wiley, 2011.

[124] CalPoly, S. L. O., University, S., Puig-Suari, J., (SSDL), S. S. D. L., of Aeronautics, D., Astronautics, and Coakley, K., "CUBESAT Design Specifications Document," Tech. rep., CalPoly, 3 2001.

[125] Hedin, A. E., "Extension of the MSIS Thermosphere Model into the middle and lower atmosphere," *Journal of Geophysical Research: Space Physics*, Vol. 96, No. A2, 1991, pp. 1159–1172. https://doi.org/10.1029/90JA02125.

[126] Colombo, C., Trisolini, M., Scala, F., Brenna, M., Gonzalo, J. L., Antonetti, S., Tolle, F., Redaelli, R., Lisi, F., Luca, M., Alberti, M., Francesconi, A., Olivieri, L., and Tipaldi, M., "E.CUBE MISSION: THE ENVIRONMENTAL CUBESAT," Tech. rep., Politecnico di Milano, 05 2021.

[127] General Electric Spacecraft Department, "Magnetic Hysteresis Damping of Satellite Attitude Motion," Technical Report 64SD4252, U.S. Naval Weapons Laboratory, Dahlgren, Virginia, 11 1964.

[128] Shahmohamadi Ousaloo, H., "Hysteresis Nutation Damper for Spin Satellite," *The Open Aerospace Engineering Journal*, Vol. 6, 2013, pp. 1–5. https://doi.org/10.2174/1874146001306010001.

[129] Farrahi, A., and Sanz-Andrés, A., "Efficiency of Hysteresis Rods in Small Spacecraft Attitude Stabilization," *The Scientific World Journal*, Vol. 2013, No. 1, 2013, p. 459573. https://doi.org/10.1155/2013/459573.

[130] Saad, N., and Ismail, m., "Influence of geomagnetic field on the motion of low satellites," *Astrophysics and Space Science*, Vol. 325, 2010, pp. 177–184. https://doi.org/10.1007/s10509-009-0185-5.

[131] Battagliere, M., Santoni, F., Ovchinnikov, M., and Graziani, F., "Hysteresis rods in the passive magnetic stabilization system for university micro and nanosatellites," , 01 2008.

[132] Inc., H. I., "HMC5843 3-Axis Magnetoresistive Sensor Datasheet," Tech. Rep. HMC5843, Honeywell, 2009. Component Datasheet.

[133] instructors team, A.-I., "AE1222-II: Aerospace Design & Systems Engineering Elements I," , 2021.

[134] Luque, A., and Hegedus, S. (eds.), *Handbook of Photovoltaic Science and Engineering*, John Wiley & Sons, Chichester, UK, 2003.

[135] Surampudi, R., Bugga, R., Smart, M. C., Narayanan, S. R., Frank, H. A., and Halpert, G., "Overview of Energy Storage Technologies for Space Applications," Tech. rep., Jet Propulsion Laboratory, California Institute of Technology, Pasadena, CA, 2006. JPL Publication.

[136] Pumpkin, Inc., "CubeSat Kit Linear EPS," Data Sheet 711-00338-D, Rev. F, Pumpkin, Inc., San Francisco, CA, 7 2012.

[137] Faculty of Aerospace Engineering, Delft University of Technology, ""Generating Architectures."," PowerPoint presentation, Course AE4-S12-06, 10 2015. Version 1.2.

[138] Supply, A., "Solar Panel User Manual Rev1.4," , 2025.

[139] ido50, "Contact Conductance Estimator (CoCoE)," , 7 2006. Version 0.5 beta.

[140] Colorado State University, "Heat Transfer Mechanisms," , 9 2015. The College of Engineering at Colorado State University.

[141] Stefan, J., "Über die Beziehung zwischen der Wärmestrahlung und der Temperatur," *Sitzungsberichte der Mathematisch-naturwissenschaftlichen Classe der Kaiserlichen Akademie der Wissenschaften*, Vol. 79, 1879, pp. 391–428. [On the relationship between heat radiation and temperature].

[142] Incropera, F. P., DeWitt, D. P., Bergman, T. L., and Lavine, A. S., *Principles of Heat and Mass Transfer*, 7th ed., Wiley, Hoboken, New Jersey, 2013.

[143] Texas Instruments, "TMP100 Digital Temperature Sensor with SMBus and Two-Wire Serial Interface," , 2015. Datasheet.

[144] Bouwmeester, J., Menicucci, A., and Gill, E., "Improving CubeSat reliability: Subsystem redundancy or improved testing?" *Elsevier*, 2022.

[145] Haddad, Y., Jagtap, S., Pagone, E., and Salonitis, K., "Sustainability Assessment of Aerospace Manufacturing: An LCA-Based Framework," *Manufacturing Driving Circular Economy*, edited by H. Kohl, G. Seliger, and F. Dietrich, Springer International Publishing, Cham, 2023, pp. 712–720.

[146] ISO, "Environmental management — Life cycle assessment — Requirements and guidelines," , 2006. Confirmed 2022; Amendments 1 & 2: 2020.

[147] ESA Clean Space Team, "LCA & EcoDesign for space," , 2022.

[148] Wilson, A. R., Serrano, S. M., Baker, K. J., Oqab, H. B., Dietrich, G. B., Vasile, M., Soares, T., and Innocenti, L., "From life cycle assessment of space systems to environmental communication and reporting," *Journal of the British Interplanetary Society*, Vol. 75, No. 9, 2022, pp. 321–336.

[149] (ICAO), I. C. A. O., "ICAO Carbon Emissions Calculator Methodology, Version 10," , 2017. Open-source methodology for estimating passenger CO2 emissions; includes fuel-burn formula, load factors, cabin class, and equation model.

[150] Bellier, T., Urbano, A., Morlier, J., Bil, C., and Pudsey, A., "Impact of Life Cycle Assessment Considerations on Launch Vehicle Design," , 2022. Available at HAL Open Archive, version hal-03888108v1.

[151] NASA, *CubeSat101, Basic Concepts and Processes for First-Time CubeSat Developers*, 2017.

[152] Division, E. P., "Verification, Validation, and Testing in Satellite Missions," , 2002.

[153] Doyle, D., Thompson, C., Lawrence, L., Sheerin, C., Doyle, C., French, B., Garland, J., Murphy, R., Loughnane, R., Jordan, P., O'Cearbhaill, R., Ward, O., Knapp, M., O'Donnell, A., Somers, C., O'Cearbhaill, A., O'Callaghan, E., Azzam, N., O'Donnell, B., O'Donnell, E., Cody, J., Hanley, G., Murray, M., McEnery, F., Duffy, P., Corcoran, A., Farrell, E., Doyle, C., O'Donoghue, P., Kavanagh, C., Bracken, C., Fitzsimons, C., O'Cearbhaill, F., Murphy, L., D'Arcy, S., Duff, K., Arshak, K., McCarthy, B., Bowe, D., Mangan, D., Keating, A., Grimes, C., Shortt, B., Fitzpatrick, C., and Dennehy, C., "EIRSAT-1: The Educational Irish Research Satellite, Ireland's First Satellite," *MDPI, Aerospace*, Vol. 8, 2021. https://doi.org/10.3390/aerospace8090254.

[154] Muñoz Toro, S., Greenbaum, J., Campbell, T., Holt, G., and Lightsey, G., "The FASTRAC Experience: A Student Run Nanosatellite Program," *AIAA/USU Conference on Small Satellites*, 2010. Presented at the 24th Annual Conference, Logan, UT.

[155] European Cooperation for Space Standardization (ECSS), "Space Engineering - Testing," Tech. rep., ECSS, Noordwijk, The Netherlands, 2 2002.

# A. Functional Breakdown Structure

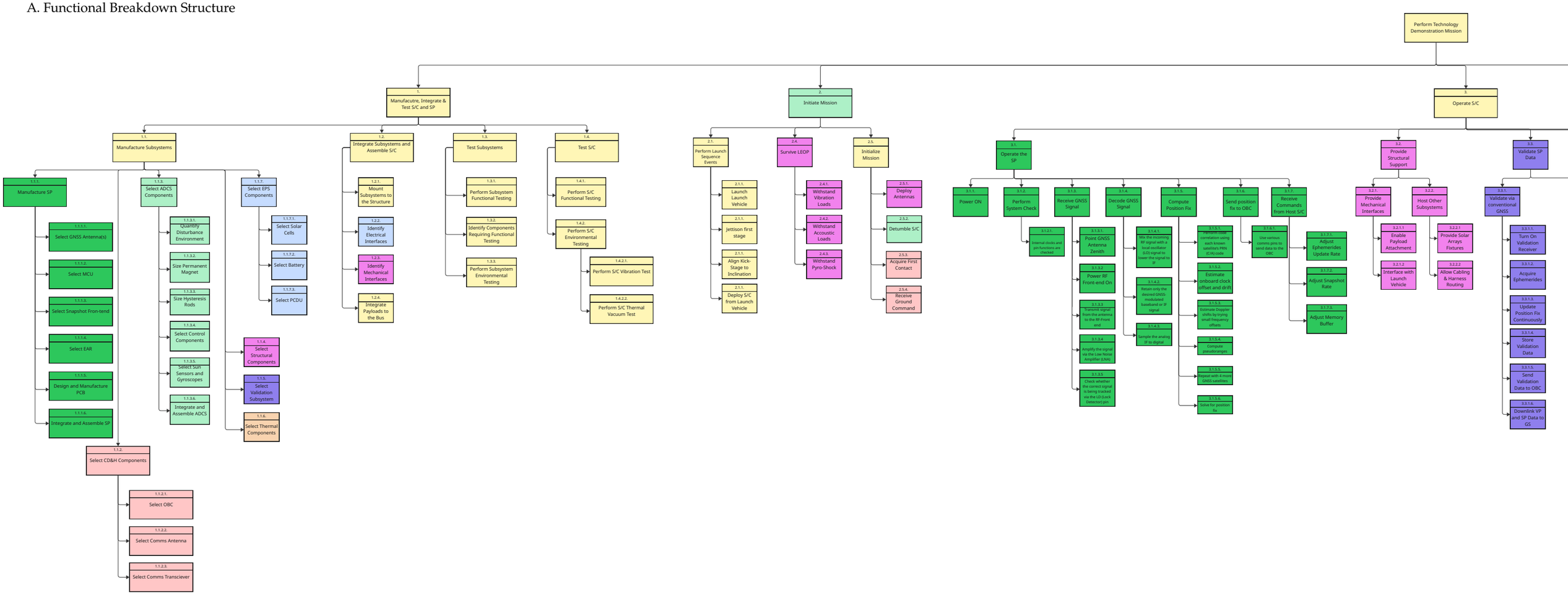


## Legend

All | EPS | C&DH
ADCS | Thermal | Structural
Ground Operation | SP | VP

**S/C: Spacecraft**
**SP: Standardized Payload**
**EPS: Electrical Power Subsystem**
**VP: Validation Payload**
**C&DH: Communication & Data Handling**
**ADCS: Attitude Determination & Control**

- 3.3.2. Validate via Satellite Laser Ranging
  - 3.3.2.1. Propagate Orbit for Visitation Window
  - 3.3.2.2. Perform Satellite Search
  - 3.3.2.3. Create Data Points using SLR station
  - 3.3.2.4. Generate Normal Points
  - 3.3.2.5. Compare Data of SLR to SP Data
- 3.4. Handle S/C Command & Data
  - 3.4.1. Perform Communication
    - 3.4.1.1. Perform Downlink
      - 3.4.1.1.1. Gather data for downlink
      - 3.4.1.1.2. Perform data compression
      - 3.4.1.1.3. Perform data encryption
      - 3.4.1.1.4. Create communication packets
      - 3.4.1.1.5. Perform digital to analog conversion
    - 3.4.1.2. Receive Uplink
      - 3.4.1.2.1. analog to digital conversion
      - 3.4.1.2.2. Perform communication packet error correction
      - 3.4.1.2.3. Decrypt data
      - 3.4.1.2.4. Decompress data
      - 3.4.1.2.5. Receive Commands
      - 3.4.1.2.6. Receive Update Data
      - 3.4.1.2.7. Validate Packet Header
  - 3.4.2. Board Computer Commands
    - 3.4.2.1. Update On Board Software
      - 3.4.2.1.1. Apply Update
      - 3.4.2.1.2. Apply Reboot
      - 3.4.2.1.3. Send Update Status
      - 3.4.2.1.4. Route Subsystem through Safe Handler
      - 3.4.2.1.5. Suspend Non Critical Systems
    - 3.4.2.2. Apply Data Request Command
      - 3.4.2.2.1. Synchronize Clock
      - 3.4.2.2.2. Extract Spacecraft Data
      - 3.4.2.2.3. Compress and Queue Transmission Data
    - 3.4.2.3. Apply Idle Command
      - 3.4.2.3.1. Suspend Non Critical Systems
      - 3.4.2.3.2. Activate Time Manager To Deactivate Idle Mode
    - 3.4.2.4. Apply Safe Command
      - 3.4.2.4.1. Activate Receiver
      - 3.4.2.4.2. Activate Subsystem in Safe Mode
    - 3.4.2.5. Apply End of Life Command
      - 3.4.2.5.1. Activate Transmission
      - 3.4.2.5.2. Deactivate Verification Payload
    - 3.4.2.6. Apply Start Command
      - 3.4.2.6.1. Activate Subsystem
      - 3.4.2.6.2. Subsystem Data and Status
      - 3.4.2.6.3. Activate Transmission
  - 3.4.3. Manage Subsystems
    - 3.4.3.1. Apply Subsystem Command
      - 3.4.3.1.1. Activate Subsystem
      - 3.4.3.1.2. Request Subsystem Data
      - 3.4.3.1.3. Update Subsystem Settings
      - 3.4.3.1.4. Confirm Subsystem Settings
    - 3.4.3.2. Perform ADCS calculation demands
      - 3.4.3.2.1. Update ADCS sensor data
      - 3.4.3.2.2. Attitude Determination Loop
      - 3.4.3.2.3. Calibrate Attitude Determination
    - 3.4.3.3. Thermal Safe Mode Commands
      - 3.4.3.3.1. Extract Subsystem Data
      - 3.4.3.3.2. Activate System Components for Thermal
    - 3.4.3.4. Perform EPS Safe Mode Commands
      - 3.4.3.4.1. Extract Subsystem Data
      - 3.4.3.4.2. Activate System Components for EPS
  - 3.4.4. Perform Watchdog
    - 3.4.4.1. Interpret Telemetry
    - 3.4.4.2. Enter safe mode if applicable
      - 3.4.4.2.1. Regulate Thermal Subsystem
      - 3.4.4.2.2. Regulate EPS Subsystem
      - 3.4.4.2.3. Regulate ADCS Subsystem
      - 3.4.4.2.4. Regulate C&DH Subsystem
    - 3.4.4.3. Reboot system if applicable
      - 3.4.4.3.1. Suspend Non Critical Systems
      - 3.4.4.3.2. Route with Safe Handler
      - 3.4.4.3.3. Apply Reboot
      - 3.4.4.3.4. Create Reboot Status Report
  - 3.4.5. Perform program loop
    - 3.4.5.1. Gather Telemetry
    - 3.4.5.2. Store Telemetry
- 3.5. Provide Electrical Power
  - 3.5.1. Generate Solar Power
  - 3.5.2. Charge Batteries (Daylight)
  - 3.5.3. Distribute Power
    - 3.5.3.1. Draw Power Directly from Solar Arrays (Daylight)
    - 3.5.3.2. Draw Power from Battery (Eclipse)
    - 3.5.3.3. Report Output Telemetry to the OBC
    - 3.5.3.4. Switch Power Lines on or off as Needed
  - 3.5.4. Condition Power
    - 3.5.4.1. Track Peak Power Point
    - 3.5.4.2. Regulate Voltage to Required Levels
  - 3.5.5. Provide Power to the SP and S/C
    - 3.5.5.1. Provide Power to ADCS
    - 3.5.5.2. Provide Power to OBC
    - 3.5.5.3. Provide Power to Validation Payload
    - 3.5.5.4. Provide Power to SP
    - 3.5.5.5. Provide Power to Transmitter
    - 3.5.5.6. Provide Power to Reciever
- 3.6. Point and Stabilize S/C
  - 3.6.1. Determine Attitude
    - 3.6.1.1. When in Sunlight use Sun Sensors
    - 3.6.1.2. In Eclipse use Gyro for Attitude Estimation
    - 3.6.1.2. In case of failure of other sensors use magnetometer
  - 3.6.2. Control Attitude
    - 3.6.2.1. Permanent Magnet Provides Control Torque
    - 3.6.2.2. Hysteresis Rods Damp Rotational Motion
- 3.7. Maintain Thermal Environment
  - 3.7.1. Regulate Temperatures Passively
  - 3.7.2. Ensure S/C Components are within Operational Temperature Ranges
    - 3.7.2.1. Monitor S/C Temperature
    - 3.7.2.2. Signal Exceedance to OBC
- 3.8. Handle Ground Operation
  - 3.8.1. Create Commands
  - 3.8.2. Perform Communication
    - 3.8.2.1. Ground System Antenna
      - 3.8.2.1.1. Ground System Antenna
      - 3.8.2.1.2. Point Ground System Antenna
    - 3.8.2.2. Receive Downlink
    - 3.8.2.3. Perform Uplink
      - 3.8.2.3.1. Send Commands
      - 3.8.2.3.2. Send Update Data
  - 3.8.3. Handle Data
    - 3.8.3.1. Analyze Data
      - 3.8.3.1.1. Compare VP and SP Data
      - 3.8.3.1.2. Iterate Density Model
      - 3.8.3.1.3. Perform Orbit Determination
    - 3.8.3.2. Store Data
- 4. Deorbit S/C at EOL
  - 4.1. Authorize EOL Procedure
  - 4.2. Secure Mission Data
  - 4.3. Configure High-Drag Attitude
  - 4.4. Monitor Orbital Decay
  - 4.5. Confirm Atmospheric Re-entry

## B. Functional Flow Diagram

### 3. Operate S/C

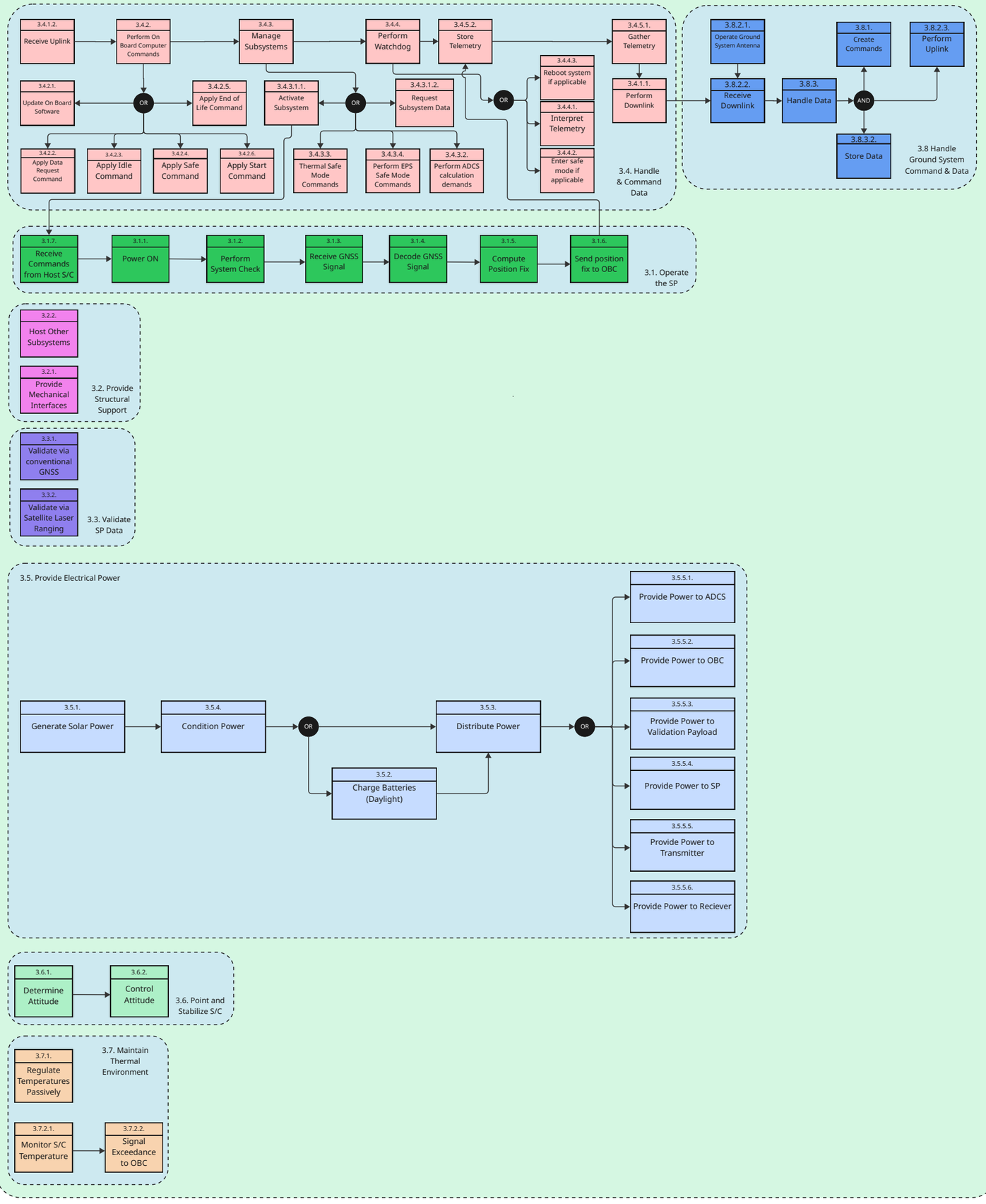


### 5. Deorbit S/C at EOL

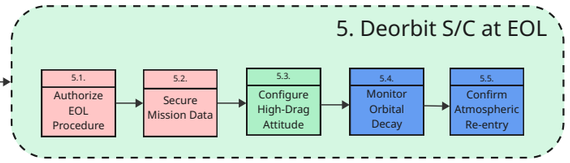

## C. Gantt Chart

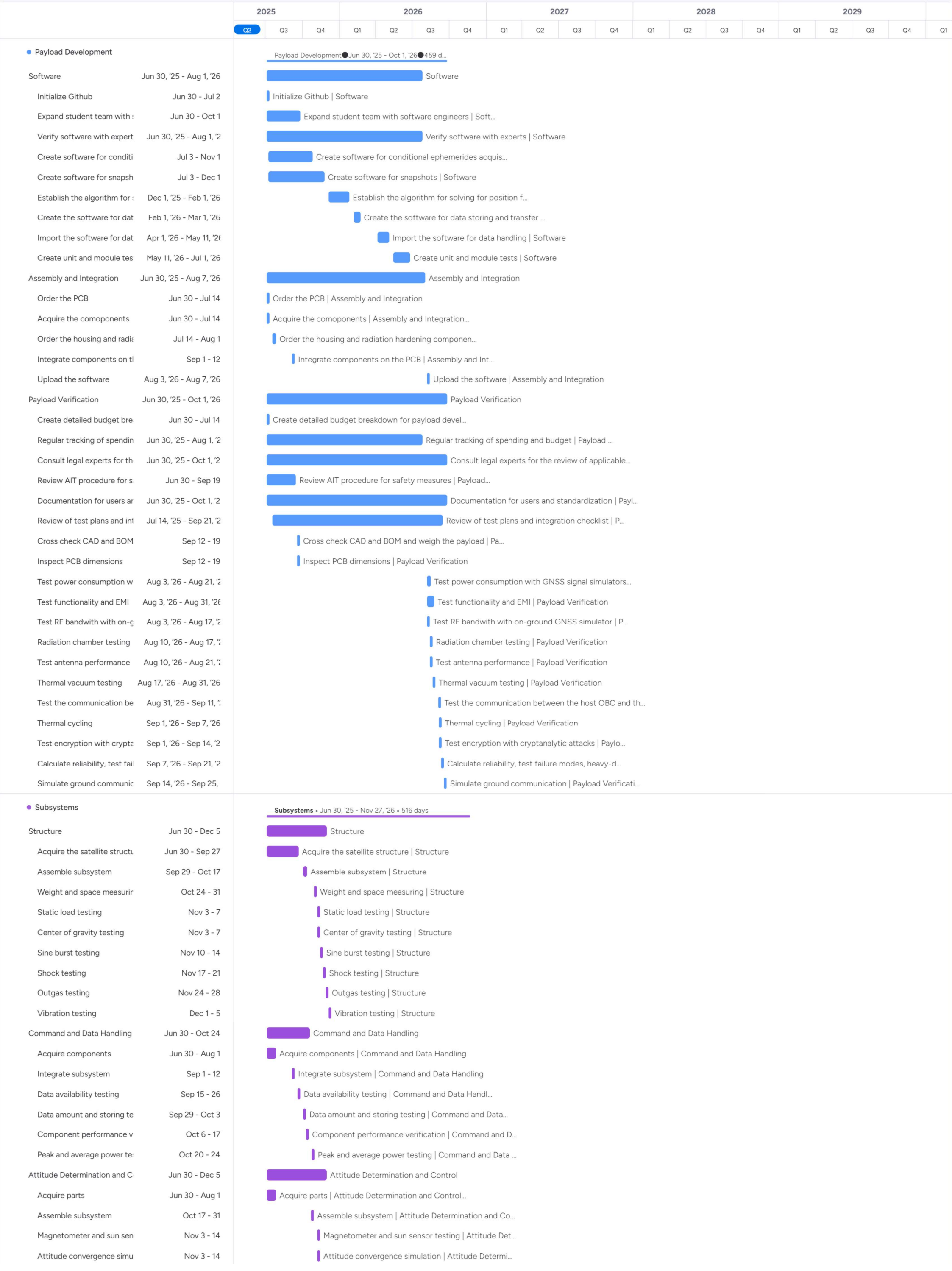

| | |
|---|---|
| Size and weight verificatior | Nov 3 - 7 |
| Magnet alignment verificati | Nov 17 - 21 |
| Non-lineaer attitude dynar | Nov 17 - 28 |
| Peak and average power te: | Dec 1 - 5 |
| EPS | Jun 30 - Dec 5 |
| Acquire parts | Jun 30 - Aug 1 |
| Assemble subsystem | Oct 20 - 31 |
| Bench demonstration | Nov 3 - 14 |
| Weight verification | Nov 3 - 7 |
| Degradation analysis | Nov 17 - 28 |
| Pulse load testing | Nov 21 |
| Battery discharge test | Dec 1 - 5 |
| Thermal Management | Jun 30, '25 - Oct 9, '26 |
| Acquire sensors | Jun 30 - Jul 11 |
| Thermal modelling | Jun 30, '25 - Oct 9, '26 |
| Connect sensors | Sep 14, '26 - Sep 18, '26 |
| Thermal vacuum test | Sep 21, '26 - Oct 2, '26 |
| Verification Payload | Jun 1, '26 - Nov 27, '26 |
| Contact ILRS Stations | Jun 1, '26 - Jun 26, '26 |
| Acquire parts | Oct 5, '26 - Oct 16, '26 |
| Assemble the subsystem | Oct 19, '26 - Oct 30, '26 |
| Test with signal simulator | Nov 2, '26 - Nov 13, '26 |
| Retroreflector optical perfc | Nov 16, '26 - Nov 27, |

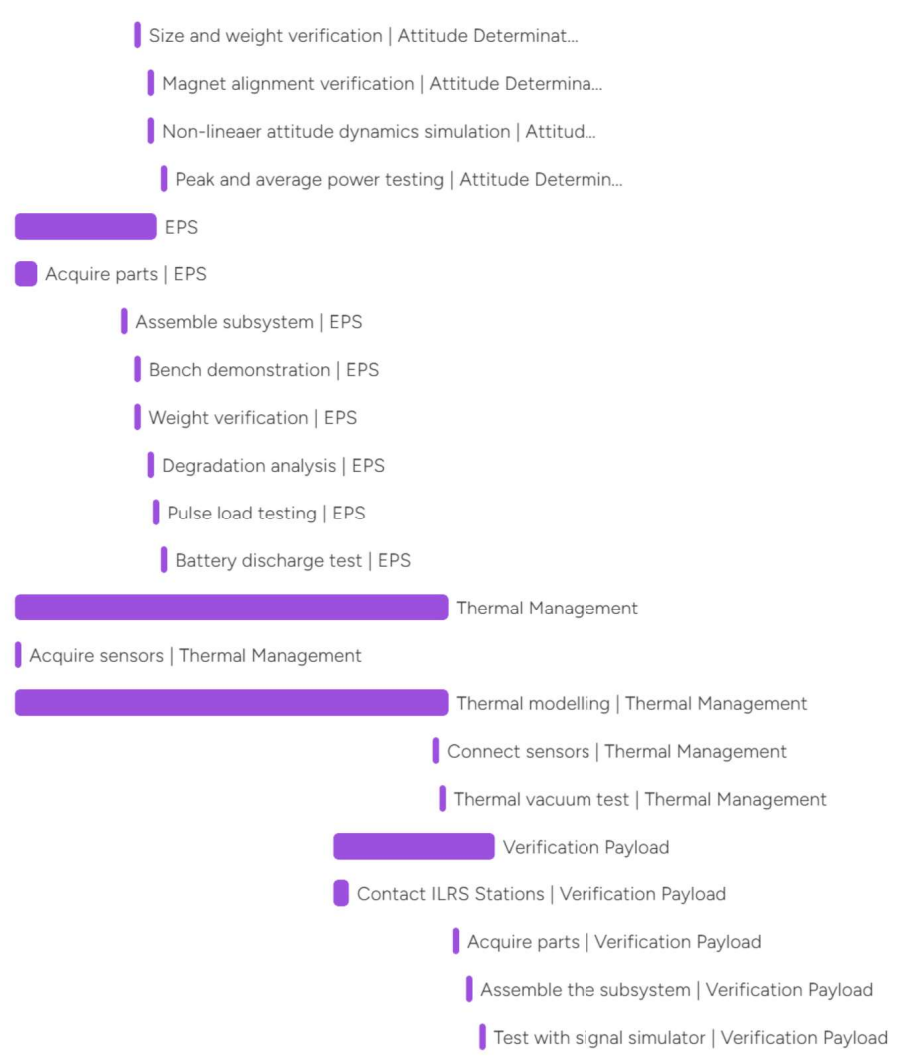


| | |
|---|---|
| **External Commincations** | |
| Contact stakeholders | Jun 30, '25 - Mar 21, '28 |
| Contact established stakeh | Jun 30, '25 - Mar 21, ' |
| Present final design and ne: | Jun 30 - Jul 18 |
| Contact possible new stake | Jul 3, '26 |
| Search for sponsorships | Jun 30, '25 - Jan 15, '27 |
| Present the design to parts | Jun 30 - Aug 1 |
| Search for logistics and ope | Jan 2, '26 - Jan 15, '2 |
| Consult with experts | Jun 30, '25 - Oct 9, '26 |
| Verify subsystem and syste | Jun 30, '25 - Oct 9, '2 |
| Verify tests and verificatior | Jun 30, '25 - Oct 9, '2 |
| Verify payload software wit | Jun 30, '25 - Aug 7, '2 |
| Verify PCB design with elec | Aug 10, '26 - Sep 4, '2 |
| Certification applications | Jun 30, '25 - Dec 31, '26 |
| Documentation | Jun 30, '25 - Dec 31, '26 |


| | |
|---|---|
| **System Assembly Integration and Testing** | |
| Integrate all subsystems on th | Oct 5, '26 - Oct 30, '2 |
| Verify the connections betwe | Nov 2, '26 - Nov 13, '2 |
| Perform structural tests | Nov 16, '26 - Dec 4, '26 |
| Vibration testing | Nov 16, '26 - Nov 20, '26 |
| Shock testing | Nov 23, '26 - Nov 27, '26 |
| Center of gravity testing | Nov 30, '26 - Dec 4, '26 |
| Perform ADCS tests | Dec 7, '26 - Dec 18, '26 |
| Perform EPS tests | Dec 21, '26 - Jan 1, '27 |
| Perform thermal tests | Jan 4, '27 - Jan 15, '27 |

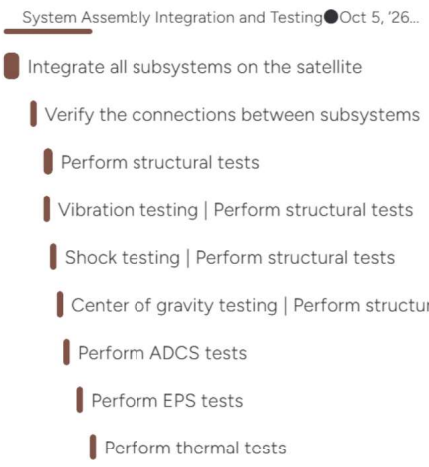


| | |
|---|---|
| **Demonstration Mission** | |
| Regulatory Licensing | Jun 30, '25 - Dec 31, '26 |
| Flight-Specific documentatio | Jun 30, '25 - Jan 15, ' |
| Securing funding | Jun 30 - Dec 31 |
| Finalize launch agreements | Jan 15, '27 - Mar 21, '28 |
| Transport the satellite to the l | Dec 21, '27 - Mar 7, '2 |
| Prepare for LEOP | Jan 31, '28 - Mar 21, '28 |
| Mission Reaediness Reviews | Jan 31, '28 - Feb 18, '28 |
| Secure the satellite inside the | Feb 28, '28 - Mar 10, |
| Cubesat to dispenser integrat | Mar 7, '28 - Mar 17, '2 |
| Verify system functions and d | Mar 21, '28 |
| Provide commands to the OB( | Mar 21, '28 |
| Begin the technology demons | Mar 21, '28 |
| Mission Coordination | Mar 21, '28 - Sep 21, '28 |


Demonstration Mission · External Commincations · Payload Development · Subsystems · System Assembly Integra